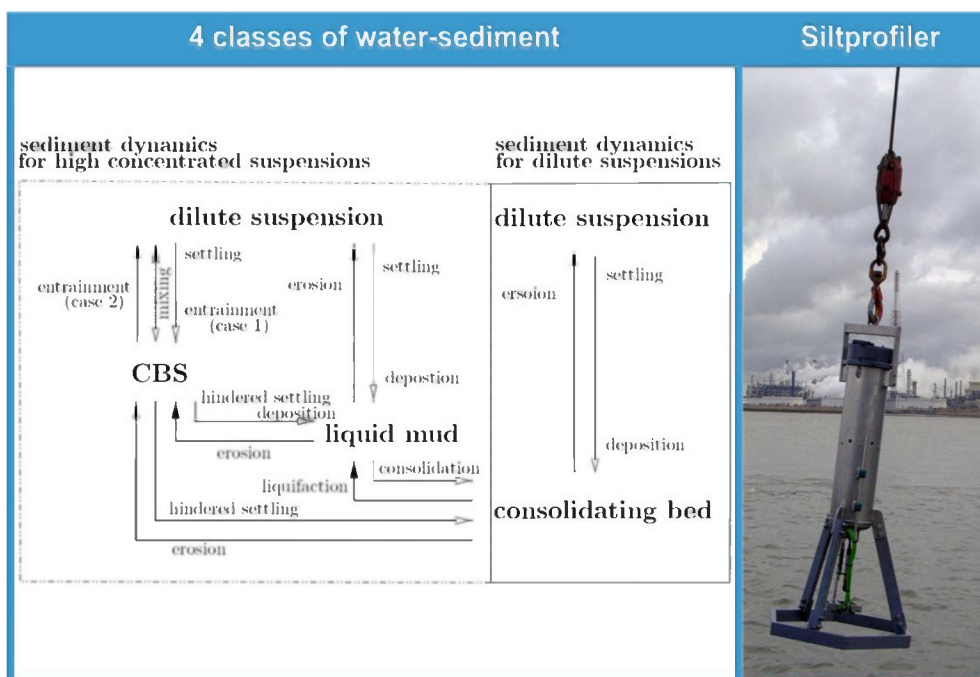# Uitbreiding studie densiteitsstromingen in de Beneden Zeeschelde in het kader van LTV Meetcampagne naar hooggeconcentreerde slibsuspensies

Bestek 16EB/04/13

Deelrapport 12 : Het voorkomen van HCBS lagen in de Beneden-Zeeschelde

Report 12 : Report concerning the presence of HCBS layers in the

09 mei 2011
I/RA/11291/06.109/MSA

i.s.m.   en

Document Control Sheet

Document Identification

Title:	Deelrapport 12 : Het voorkomen van HCBS lagen in de Beneden-Zeeschelde
Project:	Uitbreiding studie densiteitsstromingen in de Beneden Zeeschelde in het kader van LTV Meetcampagne naar hooggeconcentreerde slibsuspensies Field measurements : high-concentration benthic suspensions (HCBS 2)
Client	Waterbouwkundig Laboratorium
File reference:	I/RA/11291/06.109/MSA
File name	K:\PROJECTS\11\11291 - HCBS Meetcampagne 2\10-Rap\12_RA06109-voorkomen HCBS\RA06109_v2.docx

Revisions

Version	Date	Author	Description
1.0	07/02/2008	MSA/BVM	First draft
2.0	05/05/2011	MSA/BVM	Final Draft

Distribution List

Name	# ex.	Company/authorities	Position in reference to the project
Joris Vanlede	digitaal	Waterbouwkundig Laboratorium	client

Approval

Version	Date	Author	Project manager	Commissioner
2.0	05/05/2011	Bas van Maren, Marc Sas	Johan Melotte	Marc Sas

TABLE OF CONTENTS

APPENDICES

LIST OF TABLES

LIST OF FIGURES

1. INTRODUCTION

1.1. The assignment

This report is part of the set of reports describing the results of the extension of the study on density currents in the Lower Sea Scheldt (Beneden Zeeschelde) as part of the Long Term Vision for the Scheldt estuary – Field measurements high-concentration benthic suspensions (HCBS 2)[1]. It is complementary to the study 'Monitoring and analysis of silt accretion in Deurganckdok.

The terms of reference for this study were prepared by the 'Departement Mobiliteit en Openbare Werken van de Vlaamse Overheid, Waterbouwkundig Laboratorium' (16EB/04/13). The execution of this study was awarded to International Marine and Dredging Consultants NV in association with WL | Delft Hydraulics, dr. R. Kirby and Gems International on 09/12/2005.

'Waterbouwkundig Laboratorium – Cel Hydrometrie Schelde' provided data on discharge, tide, salinity and turbidity along the river Scheldt and provided survey vessels for the long term and through tide measurements.

The settling velocity measurements with INSSEV were subcontracted to the Coastal Processes Research Group (SEOES, University of Plymouth), with team leader Dr Andrew Manning.

1.2. Purpose of the study

The Lower Sea Scheldt is the stretch of the Scheldt estuary between the Belgium-Dutch border and Rupelmonde, where the entrance channels to the Antwerp sea locks are located. The navigation channel has a sandy bed, whereas the shallower areas (intertidal areas, mud flats, salt marshes) consist of sandy clay or even pure mud. This part of the Scheldt is characterized by large horizontal salinity gradients and the presence of a turbidity maximum with depth-averaged concentrations ranging from 50 to 500 mg/l at grain sizes of 60 - 100 μm. The salinity gradients generate significant density currents between the river and the entrance channels to the locks, causing large siltation rates. It is to be expected that in the near future also the Deurganckdok will suffer from such large siltation rates, which may double the amount of sediments to be dredged and relocated in the Lower Sea Scheldt.

Another observation is that the composition of the sediment dredged at the Sill of Zandvliet has become muddier during the last years, resulting in a strong increase in dredged material at the allocated relocation sites since 2002.

To deal with these problems, and to facilitate the management of the Lower Sea Scheldt, more knowledge on the fine sediment dynamics is required. This can be obtained from in-situ measurements and the development of an advanced numerical sediment transport model.

In the past, already many surveys have been carried out to increase the understanding of the dynamics of fine sediment in the Lower Sea Scheldt. Also, salinity and turbidity is measured

---

[1] Uitbreiding studie densiteitsstromingen in de Beneden Zeeschelde in het kader van LTV Meetcampagne naar hooggeconcentreerde slibsuspensies

continuously at Prosperpolder and Oosterweel. However, none of these measurements have been carried out in the lower 1 m of the water column.

It is expected that temporary layers of soft mud may be formed in this lower part of the water column, which may move independently of the tidal water movement, in particular during slack water. These layers may be remixed during accelerating tide, an indication for which is the observation of mud clouds at the water surface during maximum ebb and flood velocities. If such layers exist, they may contribute significantly to the siltation rate in the Deurganckdok. This would imply that measures (for instance passive constructions) to minimize siltation in the Deurganckdok can only be successful if the dynamics of these soft mud layers are also affected. Therefore it is important to establish the role of these soft mud layers on the sediment dynamics in the Lower Sea Scheldt, both from a qualitative and quantitative point of view.

The goal of the first HCBS study (2005) was threefold:

1.   The primary goal of the study (and the survey) is to investigate the occurrence of near-bed high-concentration mud suspensions (referred to as **high-concentration benthic suspensions - HCBS**), their dynamic behaviour and the conditions and locations of their occurrence,
2.   The second goal is to establish fluxes of fine sediment in the river with the purpose to calibrate a numerical 3D cohesive sediment transport model of the Lower Sea Scheldt,
3.   The third goal is to establish the sediment properties required for the cohesive sediment transport model.

The second HCBS survey aims to complete the same HCBS and flux measurements after the opening of Deurganckdok in July 2005. The measurements are repeated under the same (seasonal and tidal) conditions as the original HCBS survey. These are referred to as the winter campaign. Seasonal influences were examined in September 2006, when the survey was repeated in summer conditions, being the summer campaign.

1.3.   Overview of the study

1.3.1. HCBS1 reports

The HCBS1 campaign was carried out mainly in February 2005, before opening of the Deurganckdok. Reports of the first HCBS campaign are summarized in Table 1.1

Table 1.1: Overview of HCBS 1 Reports

Report	Description	
Test Survey		
1	Test survey 2-3 February 2005 (I/RA/11265/05.008/MSA)	IMDC (2005a)
Through tide and DON frame Measurements Winter 2005		
2.1	February survey – Deurganckdok 17 February 2005 (I/RA/11265/05.009/MSA)	IMDC (2005b)
2.2	February survey – Zandvliet 17 February 2005 (I/RA/11265/05.010/MSA)	IMDC (2005c)
2.3	February survey – Liefkenshoek 17 February 2005 (I/RA/11265/05.011/MSA)	IMDC (2005d)
2.4	February survey – Schelle 17 February 2005 (I/RA/11265/05.012/MSA)	IMDC (2005e)
2.5	February survey – Deurganckdok 16 February 2005 (I/RA/11265/05.013/MSA)	IMDC (2005f)
2.6	February survey – Kallosluis 18 February 2005 (I/RA/11265/05.014/MSA)	IMDC (2005g)
2.7	February survey – Near bed continuous monitoring (I/RA/11265/05.015/MSA)	IMDC (2005h)
INSSEV		
3	February survey – Settling velocity - INSSEV (I/RA/11265/05.016/MSA)	IMDC (2005i)
Cohesive Sediment		
4	February survey – Cohesive sediment properties (I/RA/11265/05.017/MSA)	IMDC (2005j)
Ambient Conditions Lower Sea Scheldt		
5.1	Overview of ambient conditions in the river Scheldt – January-June 2005 (I/RA/11265/05.018/MSA)	IMDC (2005k)
5.2	Overview of ambient conditions in the river Scheldt – July-December 2005 (I/RA/11265/05.019/MSA)	IMDC (2005l)
Analyse		
6.1	Analysis of ambient conditions in the river Scheldt: RCM-9 buoy 84 & 97 (21/09/05-1/10/06) (I/RA/11265.162/MSA)[2]	

1.3.2. HCBS2 reports

The HCBS2 campaign consists of two separate surveys. The first survey is a repetition of the first HCBS measurement campaign (winter campaign) and was conducted in March 2006. The second survey was held in September 2006. An overview of these reports is given in Table 1.2

---

[2] Has been integrated in HCBS Report 5.6 (see section 1.3.2)

Table 1.2: Overview of HCBS 2 Reports

Report	Description	
Ambient Conditions Lower Sea Scheldt		
5.3	Overview of ambient conditions in the river Scheldt – January-June 2006 (I/RA/11291/06.088/MSA)	IMDC (2006a)
5.4	Overview of ambient conditions in the river Scheldt – July-December 2006 (I/RA/11291/06.089/MSA)	IMDC (2007a)
5.5	Overview of ambient conditions in the river Scheldt : RCM-9 buoy 84 & 97 (1/1/2007 -31/3/2007) (I/RA/11291/06.090/MSA)[3]	IMDC (2007b)
5.6	Analysis of ambient conditions in the river Scheldt, September 2005 – March 2007 (I/RA/11291/06.091/MSA)	IMDC (2007c)
Calibration		
6.1	Winter Calibration (I/RA/11291/06.092/MSA)	IMDC (2006b)
6.2	Summer Calibration and Final Report (I/RA/11291/06.093/MSA)	IMDC (2007d)
Through tide Measurements Winter 2006		
7.1	21/3 Scheldewacht – Deurganckdok – Salinity Distribution (I/RA/11291/06.094/MSA)	IMDC (2006c)
7.2	22/3 Parel 2 – Deurganckdok (I/RA/11291/06.095/MSA)	IMDC (2006d)
7.3	22/3 Laure Marie – Liefkenshoek (I/RA/11291/06.096/MSA)	IMDC (2006e)
7.4	23/3 Parel 2 – Schelle (I/RA/11291/06.097/MSA)	IMDC (2006f)
7.5	23/3 Laure Marie – Deurganckdok (I/RA/11291/06.098/MSA)	IMDC (2006g)
7.6	23/3 Veremans Waarde (I/RA/11291/06.099/MSA)	IMDC (2006h)
HCBS Near bed continuous monitoring (Frames)		
8.1	Near bed continuous monitoring winter 2006 (I/RA/11291/06.100/MSA)	IMDC (2006i)
INSSEV		
9	Settling Velocity - INSSEV summer 2006 (I/RA/11291/06.102/MSA)	IMDC (2006j)
Cohesive Sediment		
10	Cohesive sediment properties summer 2006 (I/RA/11291/06.103/MSA)	IMDC (2007e)
Through tide Measurements Summer 2006		
11.1	Through Tide Measurement Sediview and SiltProfiler 27/9 Stream - Liefkenshoek (I/RA/11291/06.104/MSA)	IMDC (2007f)
11.2	Through Tide Measurement Sediview 27/9 Veremans - Raai K (I/RA/11291/06.105/MSA)	IMDC (2007g)

---

[3] Has been replaced by Deurganckdok Report 3.1 (see section 1.3.3)

11.3	Through Tide Measurement Sediview and SiltProfiler 28/9 Stream - Raai K (I/RA/11291/06.106/MSA)	IMDC (2007h)
11.4	Through Tide Measurement Sediview 28/9 Veremans – Waarde (I/RA/11291/06.107/MSA)	IMDC (2007i)
11.5	Through Tide Measurements Sediview 28/9 Parel 2 - Schelle (I/RA/11291/06.108/MSA)	IMDC (2007j)
11.6	Through Tide measurement Longitudinal Salinity Distribution 26/9 Scheldewacht – Deurganckdok (I/RA/11291/06.161/MSA)	IMDC (2007k)
Analysis		
12	Report concerning the presence of HCBS layers in the Scheldt river (I/RA/11291/06.109/MSA)	IMDC (2007l)

1.3.3. Monitoring siltation processes in Deurganckdok

Parallel with the HCBS study, measurement campaigns were conducted as a part of study to 'Monitoring and analysis of siltation in Deurganckdok'. These measurements (see IMDC, 2006l to 2006o & IMDC, 2007m to 2007w) add valuable information to understand the tidal dynamics within Deurganckdok and on the river Scheldt. The list of reports is given in Table 1.3. The measurements started in March 2006 and were completed in March 2009.

Table 1.3: Overview of Deurganckdok Reports

Report	Description	
Sediment Balance		
1.1	Sediment Balance: Three monthly report 1/4/2006 – 30/06/2006 (I/RA/11283/06.113/MSA)	IMDC (2007m)
1.2	Sediment Balance: Three monthly report 1/7/2006 – 30/09/2006 (I/RA/11283/06.114/MSA)	IMDC (2007n)
1.3	Sediment Balance: Three monthly report 1/10/2006 – 31/12/2006 (I/RA/11283/06.115/MSA)	IMDC (2007o)
1.4	Sediment Balance: Three monthly report 1/1/2007 – 31/03/2007 (I/RA/11283/06.116/MSA)	IMDC (2007p)
1.5	Annual Sediment Balance (I/RA/11283/06.117/MSA)	IMDC (2007q)
1.6	Sediment balance Bathymetry: 2005 – 3/2006 (I/RA/11283/06.118/MSA)	IMDC (2006l)
1.10	Sediment Balance: Three monthly report 1/4/2007 - 30/06/2007(I/RA/11283/07.081/MSA)	IMDC (2007w)
1.11	Sediment Balance: Two monthly report 1/7/2007 – 31/08/2007 (I/RA/11283/07.082/MSA)	IMDC (2007x)
1.12	Sediment Balance: Four monthly report 1/09/2007 – 31/12/2007 (I/RA/11283/07.083/MSA)	IMDC (2008b)
1.13	Sediment Balance: Three monthly report 1/1/2008 –	IMDC (2008c)

Report	Description	
	31/03/2008 (I/RA/11283/07.084/MSA)	
1.14	Annual Sediment Balance (I/RA/11283/07.085/MSA)	IMDC (2008d)
1.20	Sediment Balance: Three monthly report 1/4/2008 - 30/6/2008 (I/RA/11283/08.076/MSA)	IMDC (2008s)
1.21	Sediment Balance: Three monthly report 1/7/2008 – 30/9/2008 (I/RA/11283/08.077/MSA)	IMDC (2008v)
1.22	Sediment Balance: Three monthly report 1/10/2008 – 31/12/2008 (I/RA/11283/08.078/MSA)	IMDC (2009d)
1.23	Sediment Balance: Three monthly report 1/1/2009 – 31/03/2009 (I/RA/11283/08.079/MSA)	IMDC (2009g)
1.24	Annual Sediment Balance (I/RA/11283/08.080/MSA)	IMDC (2009h)
Through tide measurements, Salinity and silt distribution DeurganckdokBoundary Conditions: Upriver Discharge, Salt concentration Scheldt, Bathymetric evolution in access channels, dredging activities in Lower Sea Scheldt and access channels		
2.1	Through tide measurement SiltProfiler 21/03/2006 Laure Marie (I/RA/11283/06.087/WGO)	IMDC (2006m)
2.2	Through tide measurement SiltProfiler 26/09/2006 Stream (I/RA/11283/06.068/MSA)	IMDC (2007r)
2.3	Through tide measurement Sediview spring tide 22/03/2006 Veremans (I/RA/11283/06.110/BDC)	IMDC (2006n)
2.4	Through tide measurement Sediview average tide 27/09/2006 Parel 2 (I/RA/11283/06.119/MSA)	IMDC (2006o)
2.5	Through tide measurement Sediview average tide 24/10/2007 Parel 2 (I/RA/11283/06.120/MSA)	IMDC (2007s)
2.6	Salinity-Silt distribution & Frame Measurements Deurganckdok 17/3/2006 – 23/05/2006 (I/RA/11283/06.121/MSA)	IMDC (2006p)
2.7	Salinity-Silt distribution & Frame Measurements Deurganckdok 15/07/2006 – 31/10/2006 (I/RA/11283/06.122/MSA)	IMDC (2007t)
2.8	Salinity-Silt distribution & Frame Measurements Deurganckdok 15/01/2007 – 15/03/2007 (I/RA/11283/06.123/MSA)	IMDC (2007u)
2.9	Calibration stationary equipment autumn (I/RA/11283/07.095/MSA)	IMDC (2008e)
2.10	Through tide measurement SiltProfiler 23 October 2007 (I/RA/11283/07.086/MSA)	IMDC (2008f)
2.11	Through tide measurement Longitudinal Salinity distribution 12/3/2008 during springtide - Deurganckdo	IMDC (2008g)

Report	Description	
	(I/RA/11283/07.087/MSA)	
2.12	Through tide measurement Sediview winter 11 March 2008 during spring tide Transect I (I/RA/11283/07.088/MSA)	IMDC (2008h)
2.13	Through tide measurement Sediview winter 11 March 2008 during spring tide Transect K (I/RA/11283/07.089/MSA)	IMDC (2008i)
2.14	Through tide measurement Sediview winter 11 March 2008 during spring tide Transect DGD (I/RA/11283/07.090/MSA)	IMDC (2008j)
2.15	Through tide measurement SiltProfiler 12 March 2008 during spring tide (I/RA/11283/07.091/MSA)	IMDC (2008k)
2.16	Salinity-Silt distribution Deurganckdok summer (21/6/2007 – 30/07/2007) (I/RA/11283/07.092/MSA)	IMDC (2007y)
2.17	Salinity-Silt distribution & Frame Measurements Deurganckdok autumn (17/09/2007 - 10/12/2007) (I/RA/11283/07.093/MSA)	IMDC (2008l)
2.18	Salinity-Silt distribution & Frame Measurements Deurganckdok winter (18/02/2008 - 31/3/2008) (I/RA/11283/07.094/MSA)	IMDC (2008m)
2.19	Calibration stationary & mobile equipment winter (I/RA/11283/07.096/MSA)	IMDC (2008n)
2.20	Through tide measurement Sediview DGD during average tide Spring 2008 – 19 June 2008 (I/RA/11283/08.081/MSA)	IMDC (2008t)
2.21	Through tide measurement Sediview DGD during average tide Spring 2008 –26 June 2008 (I/RA/11283/08.082/MSA)	IMDC (2008u)
2.22	Through tide measurement Sediview DGD during neap tide Summer 2008 – 24 September 2008 (I/RA/11283/08.083/MSA)	IMDC (2008w)
2.23	Through tide measurement Sediview DGD during spring tide Summer 2008 – 30 September 2008 (I/RA/11283/08.084/MSA)	IMDC (2009a)
2.24	Through tide Measurement Sediview on 10/12/2008 during neap tide - Deurganckdok (transect DGD) (I/RA/11283/08.085/MSA)	IMDC (2009e)
2.25	Through tide Measurement Sediview on 02/12/2008 during spring tide - Deurganckdok (transect DGD) (I/RA/11283/08.086/MSA)	IMDC (2009f)
2.26	Through tide Measurement Sediview on 06/03/2009 during neap tide - Deurganckdok (transect DGD) (I/RA/11283/08.087/MSA)	IMDC (2009i)
2.27	Through tide Measurement Sediview on 12/03/2009 during neap tide - Deurganckdok (transect DGD)	IMDC (2009n)

Report	Description	
	(I/RA/11283/08.088/MSA)	
2.28	Through tide measurement ADCP eddy DGD Summer 2008 – 1 October 2008 (I/RA/11283/08.089/MSA)	IMDC (2008x)
2.29	Through tide measurement Siltprofiler DGD Summer 2008 – 29 September 2008 (I/RA/11283/08.090/MSA)	IMDC (2009b)
2.30	Through tide Measurement SiltProfiler 13 March 2009 at the entrance of Deurganckdok (I/RA/11283/08.091/MSA)	IMDC (2009j)
2.31	Through tide Measurement Longitudinal Salinity Distribution on 11/03/2009 during spring tide - Deurganckdok (I/RA/11283/08.092/MSA)	IMDC (2009k)
2.32	Salinity-Silt distribution Deurganckdok: Six monthly report 1/4/2008 - 30/9/2008 (I/RA/11283/08.093/MSA)	IMDC (2008y)
2.33	Salinity-Silt distribution Deurganckdok: Six monthly report 1/10/2008 – 31/3/2009 (I/RA/11283/08.094/MSA)	IMDC (2009l)
2.34	Calibration stationary & mobile equipment Autumn 2008 (I/RA/11283/08.095/MSA)	IMDC (2009c)
Boundary Conditions: Upriver Discharge, Salt concentration Scheldt, Bathymetric evolution in access channels, dredging activities in Lower Sea Scheldt and access channels		
3.1	Boundary conditions: Three monthly report 1/1/2007 – 31/03/2007 (I/RA/11283/06.127/MSA)	IMDC (2007v)
3.10	Boundary conditions: Three monthly report 1/4/2007 – 30/06/2007 (I/RA/11283/07.097/MSA)	IMDC (2007z)
3.11	Boundary conditions: Three monthly report 1/7/2007 – 30/09/2007 (I/RA/11283/07.098/MSA)	IMDC (2007aa)
3.12	Boundary conditions: Three monthly report 1/10/2007 – 31/12/2007 (I/RA/11283/07.099/MSA)	IMDC (2008o)
3.13	Boundary conditions: Three monthly report 1/1/2008 – 31/03/2008 (I/RA/11283/07.100/MSA)	IMDC (2008p)
3.14	Boundary conditions: Annual report (I/RA/11283/07.101/MSA)	IMDC (2008q)
3.20	Boundary conditions: Six monthly report 1/4/2008 – 30/09/2008 (I/RA/11283/08.096/MSA)	IMDC (2008z)
3.21	Boundary conditions: Six monthly report 1/10/2008 – 31/03/2009 (I/RA/11283/08.097/MSA)	IMDC (2009m)
Analysis		
4.1	Analysis of Siltation Processes and Factors April 2006 – March 2007 (I/RA/11283/06.129/MSA)	IMDC (2008a)
4.10	Analysis of Siltation Processes and Factors April 2007 – March 2008 (I/RA/11283/07.102/MSA)	IMDC (2008r)

Report	Description	
4.20	Analysis of Siltation Processes and Factors April 2006 – March 2009 (I/RA/11283/08.098/MSA)	IMDC (2009o)

1.4. Structure and content of the report

This report is the summary report on the behaviour of HCBS layers in the Beneden-Zeeschelde, aiming at summarising and interpreting the measurements and model results. The first chapter provides an introduction, followed by background information on HCBS (Chapter 2). An overview of previous studies, and measurements/studies carried out within the HCBS and Deurganckdok campaigns, is given in Chapter 3. The large scale sediment transport patterns and processes are analyzed in Chapter 4, followed by a more detailed analysis on the longitudinal and temporal variation of the mud concentration in the lower Sea Scheldt (Chapter 5). The exchange mechanisms of water and sediment between the Scheldt and the Kallo and Deurganckdok harbours are analysed in Chapter 6. Chapter 7 focuses on the near-bed sediment concentrations and the occurrence and dynamics of HCBS. The results are summarised in Chapter 8.

2. BACKGROUND INFORMATION

2.1. General introduction project density currents

In view of the development of the tidal dock (Deurganckdok) along the river Scheldt both numerical models and physical models have been used extensively for the design and optimization of the Deurganckdok

During the early feasibility study a coarse 4 layer 3D rectilinear grid model was used to estimate the mud deposition for different locations and different lengths of the tidal dock (IMDC-WLH, 1995), see Figure 2.1The model incorporated to a certain extent the simulation of the different mechanisms that contribute to the water exchange between river and dock : tidal filling, eddy currents and density currents (see further in chapter 6).

The final location was selected and further investigations started to optimize the global lay-out of the dock and the entrance configuration. A physical scale model was constructed at Flanders Hydraulics (steady state, no density differences) to analyze the flow pattern and the development of the entrance eddy revision of the edges of the dock and the first analysis of the effect of a Current Deflecting Wall (CDW) on the exchange mechanism (WLH, 1997)
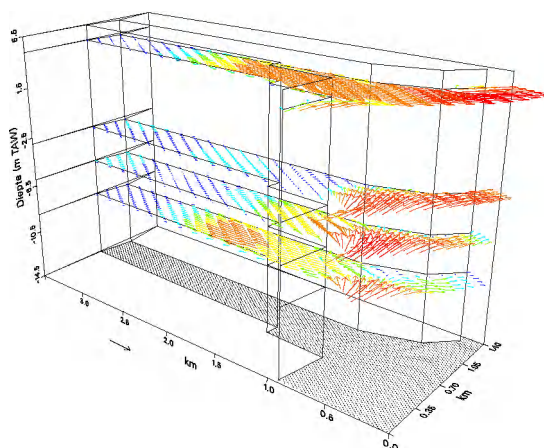
Figure 2.1: Flow pattern in 3D hydrodynamic model of Deurganckdok (IMDC-WLH, 1995).

In parallel, a new more detailed (5 layer) 3D rectilinear grid model was constructed; grid size 50 m and top layer of variable thickness (IMDC, 1998) and (Fettweis et al, 1999). The model was used to analyze the different exchange mechanisms between the river and the dock. By comparing the total amount of water leaving or entering the dock with the tidal volume, it was possible to identify that horizontal water exchange, due to density currents and eddy formation, is the dominant factor. The analysis led to the following conclusions :

- During a spring tide ebb or flood the water exchange due to tidal filling is 7×10^6 m3, due to eddy effects about $6\text{-}12 \times 10^6$ m3 depending on the section and due to density effects about

29x106 m3. With density currents the total water exchange is thus about 42-48x106 m3. Without density effects the exchange would reduce to about 13-19x106 m3.

- Density currents are responsible for ± 60-67% of the total water exchange.

Simulations were made to analyze the mud deposition in the dock. During a spring tide and considering a salinity gradient in the river, the siltation rate in the dock was simulated as ±1700 tonnes and during a neap tide as ±1200 tonnes. With density effects the mud was more equally distributed: a siltation of 0.6 kg/m2/tide (1 mm/tide) at the end of the dock increasing to about 2.1-2.2 kg/m2/tide (9 mm/tide) at the entrance was simulated (N.B. the mud layer thickness was obtained by assuming a bulk density of 1.15 kg/l). Without salinity gradients the mud was concentrated at the entrance of the dock (max deposition: 3.5 kg/m2/tide, 14.5 mm/tide), 750 m further inside the deposition was nearly zero. In Table 6.6 the distribution of mud deposition in the dock is shown for three different situations.

Table 2.1: Percentage distribution of mud deposition in tidal dock. Zones occupy an area ca.1/3 total dock surface.

	Entrance	Middle	End
Spring tide - salinity	40	36	24
Neap tide - salinity	47	36	17
Spring tide - no salinity	93	7	0

However, none of these models were able to study the effect of a CDW in detail. Therefore a physical scale model including density currents was constructed at WL-Delft Hydraulics (Van Kessel et al. 2003). The model was used to optimize the shape of the near-bank bottom configuration and the shape of the walls both up estuary and down estuary of the dock.

Furthermore, a field survey campaign was set up to determine the flow structure near Deurganckdok and at the access channel to Kallo lock (WL Delft-IMDC, 2002) (see also chapter 3) and a second set of surveys to investigate the presence of highly concentrated benthic suspensions (HCBS) in the river Scheldt in the vicinity of the dock as analyzed in this report. The results of the former survey were used to calibrate the physical scale model, the latter are used to calibrate a new very detailed 3D flow and cohesive sediment transport model with a horizontal resolution of approx 20 m in Deurganckdok and 40 layers of variable thickness to simulate the mud processes with enough accuracy (van Maren, 2006).

The new, very detailed, model led to the following results:

1. the high resolution model can reproduce the exchange mechanisms between the river and the dock, in terms of velocity patterns and suspended sediment concentration (Figure 2.2 and Figure 2.3)

2. the model can reproduce the total sedimentation in the dock

3. the model estimates a yearly sedimentation reduction in the order of 15% if a EFOS/CDW is installed, representing a 600,000m³/yr reduction.
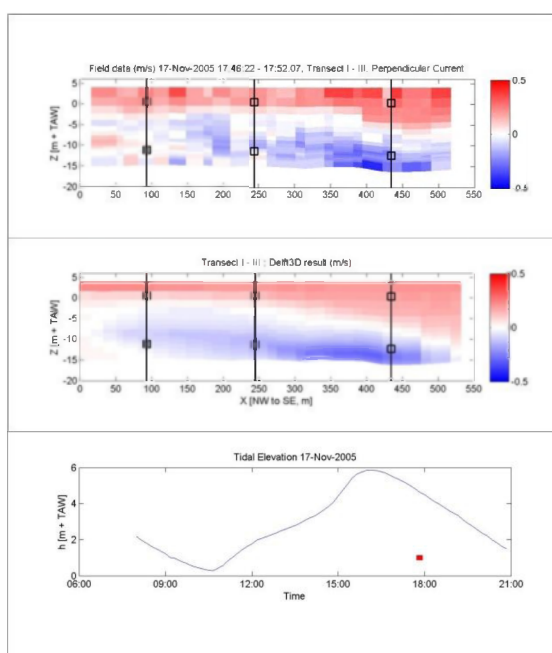
Figure 2.2: velocity pattern as measured (above) and modelled (below) (van Maren, 2006).
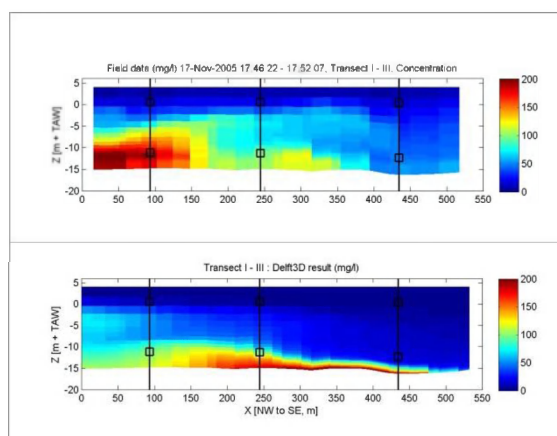
Figure 2.3: sediment concentration as measured (above) and modelled (below) (van Maren, 2006).

2.2.   Definition HCBS

The concentration of sediment suspensions may vary from several mg/l to several 100's of g/l. With increasing sediment concentration different processes become important, such as fluid-sediment interactions (from several 100's mg/l – several g/l), hindered settling (from several g/l - 10's g/l), non-Newtonian effects (from several 10's g/l), consolidation (from several 10's g/l – 100's g/l). As a result, the behaviour of sediment suspensions strongly varies. This has resulted in a wide range of definitions formulated to describe the behaviour of all the different types of sediment suspensions. Of particular interest for the Deurganckdok is the occurrence of highly dynamic, dense bottom currents which may propagate into the dock, and therefore the focus here is on the occurrence of this type of sediment suspensions, which are also known as high concentrated benthic suspensions (HCBS). A HCBS is defined as a highly concentrated near-bottom suspension with a notable interaction between the sediment and the turbulent flow through buoyancy effects. The interaction between the sediment and the turbulent flow results in the

formation of a pronounced lutocline (a sharp sediment-induced vertical density gradient). It is important to realize that turbulence in the water column is mainly generated near the bed, most of which is damped by a lutocline. Therefore HCBS also affects the turbulence in, and consequently also the flow dynamics of, the upper layer. Due to the decoupling of the HCBS layer from the overlying layer, HCBS has its own flow dynamics. This layer may be driven by gravity, or by the flow dynamics of the overlying layer.

HCBS often forms during slack tide conditions, when sediment settles from suspension and turbulent energy to mix sediment is low. With continuous settling from suspension, the vertical sediment concentration gradient near the bed increases. At a certain point, this vertical sediment concentration gradient is sufficiently high that sediment-induced density gradients are sufficiently strong to dampen turbulent mixing. At this point, sediment can no longer be held in suspension, and settling from suspension accelerates: the sediment concentration profile collapses. This results in the formation of a lutocline. If this highly concentrated near-bottom layer is generated near a harbour dock, it may then propagate into the dock by gravity affects. Alternatively, it may remain stationary and be fully mixed throughout the water column during the following tide. However, when a sufficient amount of sediment is available, or the flow velocity of the tidal currents following slack tide is too low, the HCBS layer may be more persistent. The sediment concentration will then increase from several 10's to several 100's g/l, the flow will become non-Newtonian, and consolidation processes will become important. This is generally known as a fluid mud (if mobile) or a consolidating mud (if stationary). Fluid mud is subject to consolidation, and therefore as no mechanisms exists top keep the particles in suspension, fluid mud is a transient state (Winterwerp and van Kesteren, 2004).
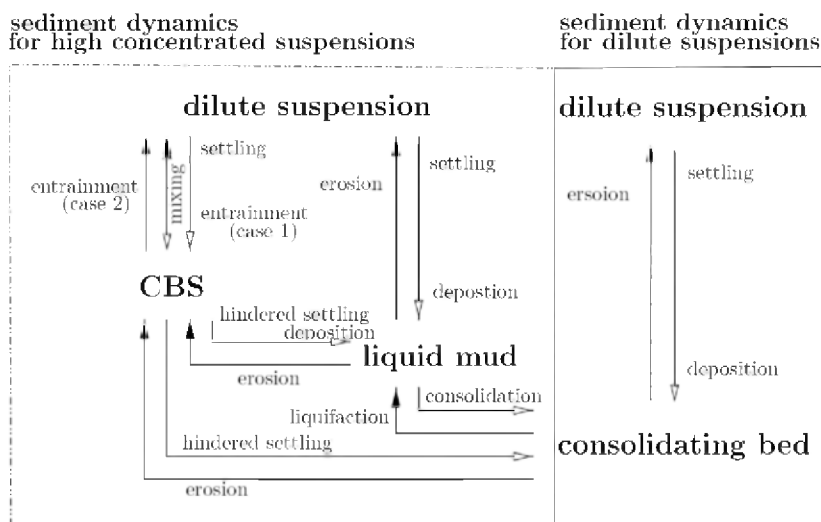
Figure 2.4: Diagram of the four classes of water-sediment mixtures as defined by Bruens (2003[4]), with the physical exchange processes.

The occurrence of HCBS, fluid mud, and /or consolidating muds depends on the ambient sediment concentrations. In low-concentrated mud suspensions, sediment settles from suspension, and forms a consolidating bed or fluid mud. However, in highly concentrated suspensions, HCBS is formed, which afterwards transforms into a liquid mud or a consolidating bed (see Figure 2.4 and Bruens, 2003). Note that Bruens used the term CBS instead of HCBS, distinguishing between high

---

[4] Bruens used CBS as a basic definition, further distinghuishing high concentrated CBS and low concentrated CBS. At low depth-averaged sediment concentrations, sediment settles from suspension onto a consolidating bed. For higher depth-averaged concentrations, a combination of CBS and/or mobile mud may occur.

concentrated CBS and low concentrated CBS. The formation of HCBS therefore requires that a sufficient amount of sediment is available. In time, the HCBS layer will become a liquid mud or a consolidating mud. Whether the consolidating mud is mobile or stationary depends on the degree of consolidation, the flow velocity in the upper layer, and the bed level gradient. A consolidating mud builds up yield strength, which increases with the degree of consolidation. The mud may become mobile when the shear stress exerted on the mud exceeds this yield strength. This shear stress may be driven by gravity (hence the importance of the bed level gradient) or by the water flow in the upper layer.

HCBS layers can achieve a state of equilibrium at which the suspended sediment is mixed only over a part of the water depth, where turbulence production and sediment-induced buoyancy are balanced. HCBS layers may be entrained in the upper layer, or water from the upper layer may be entrained in the HCBS layer, depending on which of the two layers is turbulent. If most turbulence is generated near the bed, then most of the turbulence will be dissipated on the lutocline, and the HCBS layer is more turbulent than the upper layer. In this case, water from the upper layer will be entrained by the HCBS layer. This will lead to a lowering of the sediment concentration in the HCBS layer, and an increase in the height of the lutocline. Alternatively, if the upper layer is more turbulent than the HCBS layer, the HCBS will be entrained by the upper layer. This will then lead to increasing sediment concentrations in the upper layer and a lowering of the lutocline while the HCBS concentration remains constant.

2.3. International context
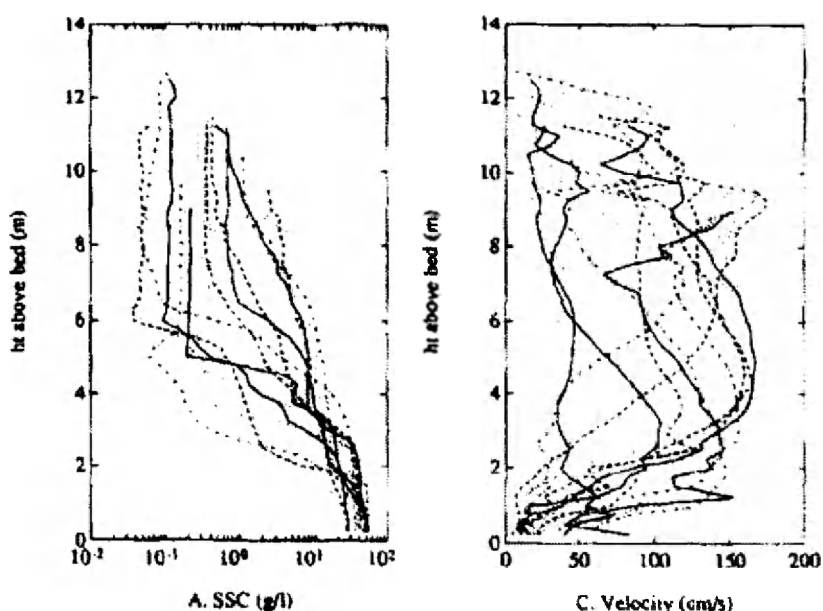
Figure 2.5: Sediment concentration SSC and flow velocity measured in the Amazon estuary

Bruens (2003) re-examined observations of some well-studied case-studies on the occurrence of CBS. In the Amazon, she concluded that active CBS forms during spring tides (Figure 2.5), when mixing and entrainment dominate over hindered settling effects. During neap tide conditions, a less active CBS forms which is more a transient state towards a mobile fluid mud. During high wave conditions, this fluid mud can be mobilized and transformed into a CBS. A CBS appears to form in the frontal zone of the Eel River plume, which evolves into a mobile fluid mud when sufficient sediment is available. In the Loire, for instance, the sediment concentration in the highly concentrated mud layers is close to 40 g/l, while the flow velocity is up to 1 m/s (Le Hir, 1997, see

Figure 2.6). In the Amazon, suspensions with concentrations over 10 g/l still remain highly mobile while simultaneously modifying the flow velocity profile (Figure 2.5). In the Humber tributary the Ouse River, sediment concentrations near the bed reach values close to 20 g/l during slack tide (Figure 2.7). The suspension becomes fully mixed again during maximum flow conditions. A collapse of the concentration profile at concentrations exceeding the saturation concentration does probably generate CBS in the Ems estuary. A re-analysis of the Van Leussen (1994) data in Winterwerp (2001) showed that the observed tidal variation in sediment concentration profiles is probably caused by damping of turbulence.

The examples presented above are only a fraction of highly concentrated near-bed suspensions presented in literature. However, all observations have in common that near-bed, highly concentrated, mobile layers may reach typical concentrations of several g/l to several tens of g/l.
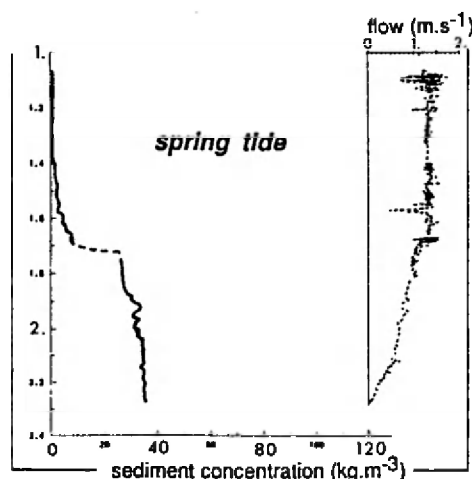
Figure 2.6: Suspended sediment concentration and flow velocity in the Loire estuary. From Le Hir, 1997.
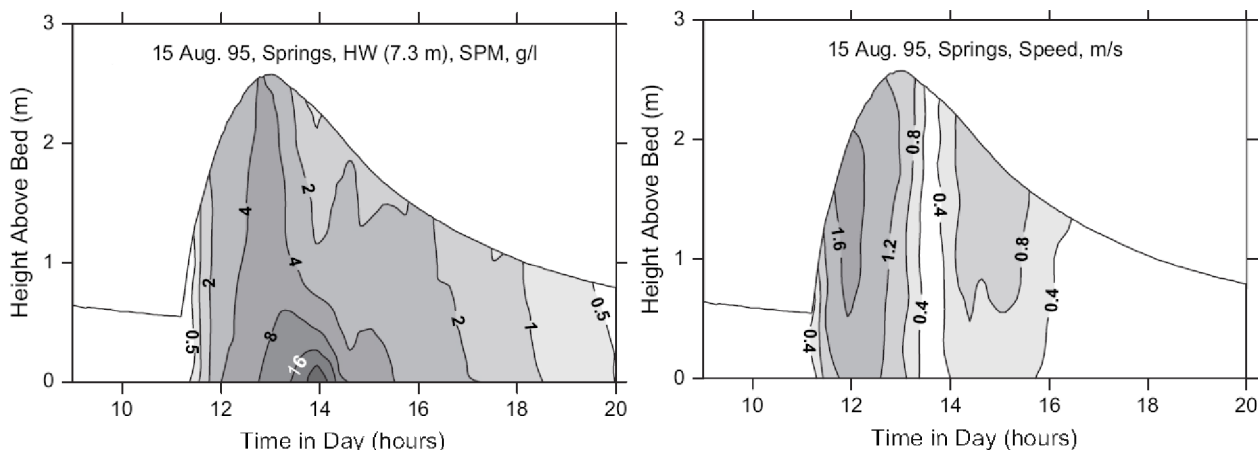
Figure 2.7: Sediment concentration and flow velocity measured in the Ouse River (tributary of the Humber River). From Uncles et al., 2006.

Of particular interest for the Deurganckdok is the HCBS formation in the Maasmond area (Rotterdam). This is one of the few harbour basins where the effect of highly concentrated bed suspensions on sedimentation has been thoroughly analysed. In the Euro-Maas channel and the Rotterdam Waterway, the increasing water depth in the landward direction result in decreasing

flow velocity, and therefore decreasing capacity conditions. Highly concentrated suspensions that are transported from the sea into the Rotterdam Waterway during storm conditions will, therefore, become saturated at a certain point. The concentration profile then collapses, and HCBS is formed (Winterwerp and van Kessel, 2003). This HCBS propagates into the harbour docks, after which it becomes immobile, and consolidates. This plays an important role for sedimentation in the docks close to the Calland-Beer channel. Further upstream, in the Rotterdam Waterway near the Botlek harbour, recent and detailed measurements (de Nijs et al., 2009) indicate that the concentrations are typically below capacity conditions. Therefore the role of sediment-induced density currents for sediment import into the dock is only minor: sediment is mainly transported into the dock by salinity-induced density currents. It does, however, probably play a role in the transport and deposition of sediment in the dock itself.

3. OVERVIEW MEASUREMENTS

3.1. Historical measurements

Before 2002, suspended sediment measurements in the lower Sea Scheldt were relatively fragmented and their results not widely disseminated, with the exception of the studies from 1991 to 1998 titled 'Sediment transport and sedimentation processes in the Scheldt' (Wartel and Francken 1995, 1997a, 1997b, 1998a-g) and (Wartel et al., 1998) and research by IMDC in Fettweis et al (1994) concerning sediment transort on the "Drempel van Zandvliet' a. Detailed analyses on measured datasets include the work of Verlaan (1998, 2000) on the sources of sediment in the Scheldt Estuary. The origin of the fluvial Scheldt sediments has been analysed in more detail in the PhD thesis of Wartel (1972) and in a report by IMDC (1993). The seasonal variation of Scheldt sediments in the main part of the river has been studied by IMDC in view of the construction of new port infrastructure along the river and was published by Fettweis et al. (1997 and 1998a) and was studied on the mud flats. by IMDC-IN (1998), Fettweis et al (1999b) , Temmerman et al. (2005) and Chen et al. (2005) The behaviour of the turbidity maximum in the Scheldt has been analysed by Peters (1972), Wartel and van Eck (2000). Additionally, dedicated studies have been carried out on sedimentation in some of the tidal harbour basins, such as the study by Sas and Claessens (1988) on sedimentation processes in the Kallo access channel, the access channel to Zandvliet-Berendrecht (Fettweis and Sas, 1994) and Deurganckdok (Fettweis et al 1999a).

3.2. New measurements

An extensive measurement campaign was carried out in 2002 for the study of density currents in the framework of LTV ('studie densiteitsstromingen in het kader van LTV') by IMDC (WL Delft-IMDC, 2002). These consisted of shipborne ADCP and CTD through-tide measurements on 5 June and 12 June 2002, near Waarde, Deurganckdok, Kallo, and Oosterweel. Additional long-term measurements near Lillo, Kallo, Oosterweel, Petroleum-steiger and Schelle, including water levels, flow velocity, salinity, and turbidity, were done in May and June 2002.

Table 3.1: survey of the measurement campaigns that have been conducted for the study on density currents in the river Scheldt.

Measurement Location	Measurement Period	Type of Measurement	Report number
Waarde	5/06/2002	Through tide current and salinity measurement (ADCP&CTD)	IMDC (2002b)
Waarde	12/06/2002	Through tide current and salinity measurement (ADCP&CTD)	IMDC (2002c)
Oosterweel	5/06/2002	Through tide current and salinity measurement (ADCP&CTD)	IMDC (2002d)
Oosterweel	12/06/2002	Through tide current and salinity measurement (ADCP&CTD)	IMDC (2002e)
Deurganckdok	5/06/2002	Through tide current and salinity measurement (ADCP&CTD)	IMDC (2002f)
Deurganckdok	12/06/2002	Through tide current and salinity measurement (ADCP&CTD)	IMDC (2002g)
Kallo	5/06/2002	Through tide current and salinity measurement (ADCP&CTD)	IMDC (2002h)
Kallo	12/06/2002	Through tide current and salinity measurement (ADCP&CTD)	IMDC (2002i)
Zandvliet	June 2002	Long term current and salinity measurement	IMDC (2002j)
Lillo-Ponton			
Deurganckdok			
Schelle			
Oosterweel			
Petroleum steiger			
Kallo	June 2002	Long term current and salinity measurement	IMDC (2002h)
Merelbeke	June 2002	Discharge measurement	IMDC (2002a)
Analysis of the data			IMDC (2002l)

The study on density currents in the framework of LTV was extended from 2005 onwards, with specific focus on the new container dock Deurganckdok. Large-scale measurement campaigns were carried out consisting of simultaneous through-tide ship borne ADCP and CTD measurements, long-term moorings, and deployment of measurement frames. The first campaign was the HCBS1 campaign, carried out in February 2005, to document the hydrodynamics and sediment dynamics in the lower Sea Scheldt before construction of the Deurganckdok. Simultaneous ship borne measurements were carried out near Schelle, Kallo, Liefkenshoek, Deurganckdok and Zandvliet (Table 3.2), and a frame was deployed near the Deurganckdok and Boei84 (Table 3.3), from February to June 2005. The second HCBS campaign, in 2006, aimed at documenting the hydrodynamics and sediment dynamics in the lower Sea Scheldt after opening of the Deurganckdok. Shipborne measurements were carried out in March and September near Schelle, Liefkenshoek, Deurganckdok and Waarde (Table 3.2). Two frames were deployed: one on the sill of the Deurganckdok and another on the location of the future CDW (Table 3.3). The HCBS3 campaign measured inside the Deurganckdok, and consisted of through-tide ship borne surveys (Table 3.2) and continuous salinity measurements (Table 3.3), between February 2006 and April 2007.

Throughout the different campaigns, from 2005 onwards, salinity, sediment concentration, flow velocity and water levels were continuously measured at several locations along the Scheldt.

Table 3.2: Through-tide HCBS measurements

Location	Date	Data	Report[5]	Remarks
Schelle	17-02-2005	ADCP	HCBS 2.4	
	23–03-2006	ADCP	HCBS 7.4	
	28-09-2006	ADCP	HCBS 11.5	
Kallo	18-02-2005	ADCP & SiltProfiler	HCBS 2.6	No complete tidal cycle SiltProfiler
Liefkenshoek	17-02-2005	ADCP	HCBS 2.3	
	22-03-2006	ADCP & SiltProfiler	HCBS 7.3	
	27-09-2006	ADCP & SiltProfiler	HCBS 11.1	
K-transect DGD	16-02-2005	ADCP & SiltProfiler	HCBS 2.5	
	17-02-2005	ADCP & SiltProfiler	HCBS 2.1	
	22-03-2006	ADCP	HCBS 7.2	
	23-03-2006	ADCP & SiltProfiler	HCBS 7.5	
	27-09-2006	ADCP	HCBS 11.2	
	28-09-2006	ADCP & SiltProfiler	HCBS 11.3	
Zandvliet	17-02-2005	ADCP	HCBS 2.2	
Waarde	23-03-2006	ADCP	HCBS 7.6	
	28-09-2006	ADCP	HCBS 11.4	
DGD	17-11-2005	ADCP	DGD_flux 1	IMDC(2006q)
	28-11-2005	ADCP	DGD_flux 2	IMDC(2006r)
	21-03-2006	SiltProfiler	DGD 2.1	
		salinity	HCBS 7.1	
	22-03-2006	ADCP	DGD 2.3	
	26-09-2006	SiltProfiler	DGD 2.2	
	27-09-2006	salinity	HCBS 11.6	
		ADCP	DGD 2.4	

---

[5] We refer to par. 1.3 for the overview of the reports

Table 3.3: Continous & INSSEV HCBS measurements

Location	Date	Data	Report	Remarks
DGD down	17-02 to 03-03-2005	Argus, Altus, OBS, EMC	HCBS 2.7	Malfunctioning OBS & EMC
Boei84	12-03 to 25-03-2005			
DGD-up	24-05 to 08-06-2005			Only first 4 days data
frame CDW	14-03 to 06-04-2006		HCBS 8.1	
	19-04 to 23-05-2006		DGD 2.6	
	18-07 to 11-10-2006		DGD 2.7	
	15-03 to 12-04-2007		DGD 2.8	No Argus & no data last week
frame sill	19-04 to 23-05-2006		DGD 2.6	Burial instruments
	19-07 to 11-10-2006		DGD 2.7	
	09-02 to 18-04-2007		DGD 2.8	No Argus 1st month
P&O1	17-03 to 28-04-2006	Salinity & silt	DGD 2.6	
	20-07 to 12-10-2006		DGD 2.7	
	12-02 to 27-03-2007		DGD 2.8	
P&O2	17-03 to 28-04-2006		DGD 2.6	
	20-07 to 12-10-2006		DGD 2.7	
	12-02 to 27-03-2007		DGD 2.8	
PSA	17-03 to 28-04-2006		DGD 2.6	
	20-07 to 12-10-2006		DGD 2.7	
	12-02 to 27-03-2007		DGD 2.8	
DGD-up	17-02 to 18-02-2005	INSSEV	HCBS 3	
Kallo	19-02-2005			
frame CDW	05-09-2006		HCBS 9	
frame sill	05-09-2006			
western quay	05-09-2006			

3.2.1. River surveys

Simultaneous ship borne measurements were carried out at several locations along the Scheldt. The ship borne measurements can be either ADCP tracks, or point measurements. ADCP tracks are continuously repeated (usually throughout a tidal cycle), where the flow velocity and backscatter is sampled approximately every 20 minutes. The backscatter is converted into sediment concentration using Sediview. The point measurements are repeated throughout a tidal cycle at a number of locations along a transect. At each location CTD and SiltProfiler measurements are carried out. The CTD records salinity and temperature profiles, and the attached OBS (Optical Backscatter Sensor) measures sediment concentration profiles. Additionally, the rapid SiltProfiler also measures the sediment concentration. The rapid SiltProfiler is especially accurate in high concentration areas such as near the bed.

Most ship borne surveys were carried out near the Deurganckdok. In 2002, as well as the HCBS1, and both HCBS2 campaigns, the flow velocity distribution was measured near the K-transect, just downstream of the Deurganckdok. During all surveys 2 tidal cycles were measured, with a one-week interval in 2002 but at two consecutive days in the HCBS1 and HCBS2 campaigns. Also, point measurements were obtained during the HCBS1 campaign as well as both HCBS2 campaigns. The location Liefkenshoek is just upstream of the Deurganckdok. Here, measurements were carried out in February 2005 (HCBS1), March 2006 and September 2006 (HCBS2). During the HCBS2 campaign, ADCP as well as SiltProfiler / CTD measurements were carried out, whereas only ADCP measurements were carried out during HCBS1.

Other measurements in the river are more fragmented and often without SiltProfiler/CTD. The most downstream location, Waarde, was surveyed in 2002 (with ADCP and CTD), and during HCBS2 (only ADCP). During HCBS1, the most downstream measurement location was Zandvliet, but this location was only measured during HCBS1 (ADCP only). Upstream of the Deurganckdok, several measurements were carried out near Kallo (see the next section), Oosterweel, and Schelle. ADCP and CTD measurements were carried out at Oosterweel in 2002 only. ADCP measurements were carried out near Schelle during the HCBS1 and both HCBS2 campaigns.

3.2.2. Measurements Kallosluice

Extensive measurements were carried out near the Kallosluice (in the access channel to the lock as well as on the adjacent Scheldt) in 2002 and during the HCBS1 campaign (2005) to determine exchange mechanisms and sediment transport. For this purpose transects were navigated in the Scheldt, and in the locks, supplemented with point measurements. The 2002 campaigns were carried out at 5 and 12 June, and cover a full tidal cycle. The salinity and temperature were measured using a CTD. Only velocity was measured with the ADCP; backscatter was not converted to sediment concentration. In the 2005 measurements, the SiltProfiler was also deployed, and ADCP backscatter was converted into sediment concentration. However, in 2005 no full tidal cycles were measured at one location or transect, because different transects were measured consecutively (with each transect being measured for several hours).

3.2.3. Measurements Deurganckdok

In addition to the DON frame measurements (next section), several long-term moorings have been deployed in the Deurganckdok, measuring the salinity and turbidity at several locations in the dock. Additional ship-based surveys were carried out, measuring the tidal variation of the longitudinal salinity distribution and the tidal variation of the cross-sectional flow velocity and sediment concentration patterns. Dedicated campaigns with the INSSEV device were carried out to establish the role of flocculation. SiltProfiler measurements were carried out throughout a tidal cycle at 15 locations at the entrance of the dock. The bed level of the Deurganckdok is regularly measured

with a dual-frequency echo sounder, occasionally supplemented with density measurements of the mud deposit in the Deurganckdok.

3.2.4. DON frame measurements

Two large measurement frames, each equipped with 2 EMC current meters, 2 OBS sensors, a pressure sensor, an ALTUS echo sounding device, and an ARGUS sediment concentration array, was deployed during several measurement campaigns in and in the vicinity of the Deurganckdok.

The ARGUS consists of 96 backscatter infrared laser sensors, embedded in a stainless steel rod, measure the vertical structure of the suspended sediment concentration. The ALTUS is a high frequency acoustic altimeter that precisely quantifies (with an accuracy of 2 mm) changes of bottom elevation.

The first campaign was the HCBS 1 campaign, during which one frame measured in February 2005 (downstream of the Deurganckdok) and March 2005 (near Buoy 84), reported in IMDC report 2.7 The frame also measured in March 2006, during the HCBS2 campaign, on the location of the envisaged CDW (IMDC report 8.1). During the Deurganckdok campaigns, two frames were deployed simultaneously: one on the location of the envisaged CDW, and one the sill of the Deurganckdok. Simultaneous surveys were carried out in April-May 2006 (IMDC report DGD 2.6), July-November 2006 (IMDC report DGD 2.7) and February – March 2007 (IMDC report DGD 2.8).

4. LARGE-SCALE SEDIMENT TRANSPORT PATTERNS IN THE SCHELDT ESTUARY

4.1. Introduction

One of the aims of the HCBS campaigns was to establish the sediment fluxes through the Lower Sea Scheldt. Therefore, the sediment transport patterns and processes are analysed in this chapter.

Sediment is transported upstream in the lower reaches of the lower Sea Scheldt (i.e. Verlaan (1998, 2000) and sediment is transported downstream at Schelle. As a result, sediment converges somewhere between Antwerpen and Boei84 (see for example the sediment fluxes computed with the 3D mud model in (Figure 4.1). This large-scale transport of sediment is probably the result of

- Tidal asymmetry

- Gravitation circulation

- Residual flow

On a smaller time- and spatial scale, the sediment transport is additionally influenced by

- Wind-generated water level setup and setdown

- Secondary flow patterns

- Local wind- and ship-generated waves

- Relocation of dredged material

In this chapter, the relative contribution of these processes will be determined using the measurement results of the HCBS field campaign, and using numerical models developed for the 3D mud project. First, the source and composition of sediment is reviewed (section 4.2). The effect of tidal asymmetry on sediment transport is determined based an analysis of water levels, currents, and sediment concentrations, in section 4.3. The effect of gravitational circulation and residual flow is analysed in section 4.4. The more local contribution of water level setup and setdown, secondary flow, and local waves are described in sections 4.5-4.7. Effects of dredging and relocation are analysed in section 4.8, and a summary of the main processes is given in section 4.9.
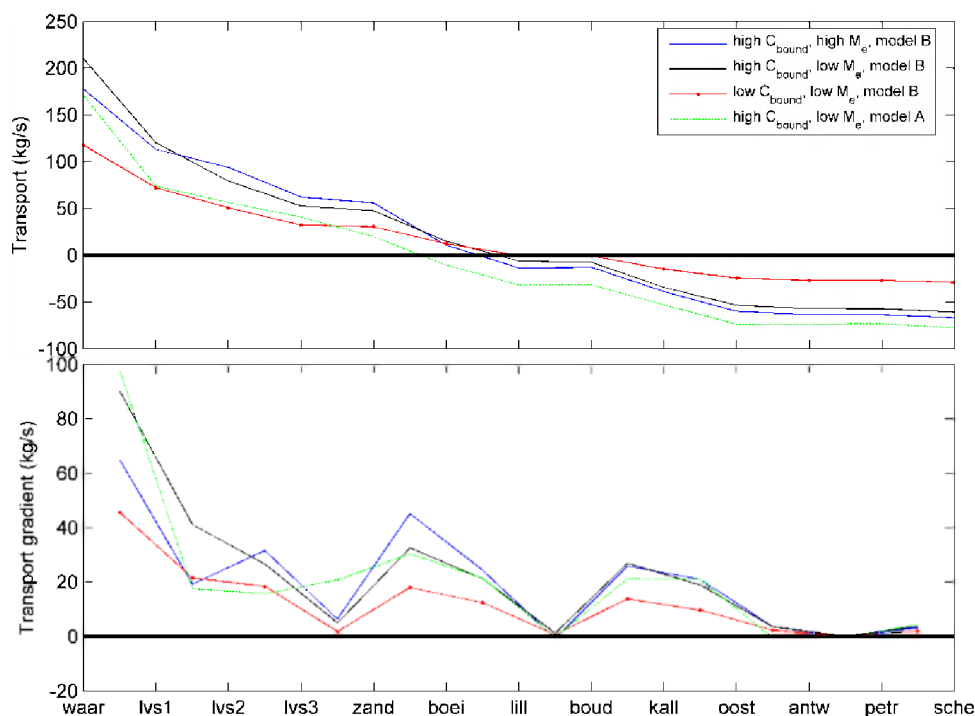
Figure 4.1: Residual sediment transports (upstream-directed transports positive) and longitudinal transport gradients between Waarde (waar) and Schelle (sche) for simulations with several sediment transport settings (see Van Maren and Schramkowski, 2008 for more details). The location lill (Lillo) is closest to the Deurganckdok.

4.2. Sediment source and composition

Sediment transported in suspension, and sediment deposited in the access channels to the locks and to a minor extent in the non-tidal harbour docks, mainly consists of marine and terrestrial mud. The ratio of marine to terrestrial mud increases in the downstream direction, with a particular rapid transition from terrestrial to marine mud near the Deurganckdok.

Wartel et al (1993) have illustrated the percentage of fluvial mud along the estuary : 90% near the Rupel, 80% near Kallo, 70% near Zandvliet decreasing towards 40% near Kruiningen and 0% in the North Sea (Scheur) (Figure 4.4).

These ratios have been confirmed by Wartel and Chen (2000) based on a new survey in 1998, results of which have been described in (Verlaan, 2000) : near Lillo, the marine fraction is around 10% whereas the entrance channels of the Zandvliet-Berendrecht locks (5 km downstream of Lillo), over 40% of the bottom mud is of marine origin The transition between marine and fluvial suspended sediment is, during low to moderate discharge conditions, 20-40 km more upstream of the transition of marine and fluvial bottom sediment. This suggests that deposition mainly occurs during high discharge conditions (Verlaan, 2000).
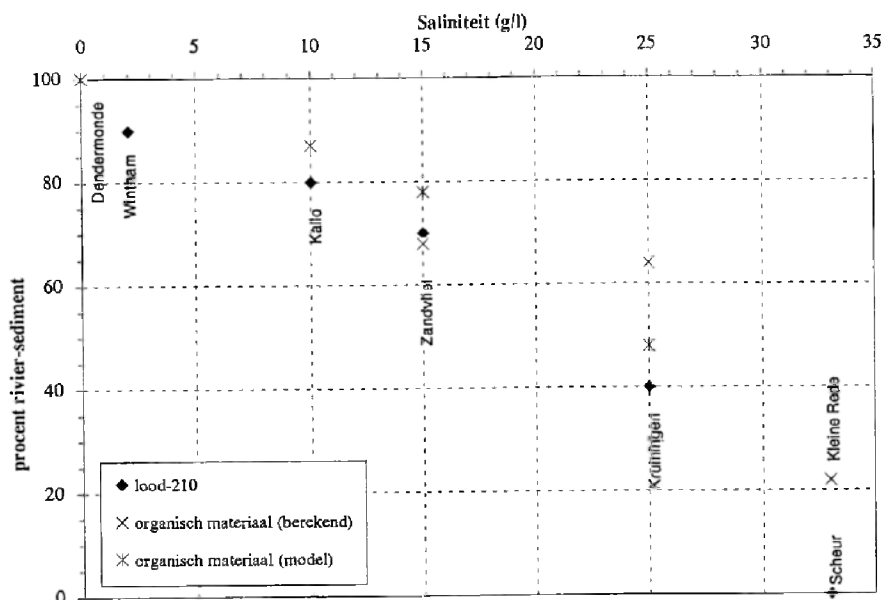
Figure 4.2: Percentage of fluvial mud in the total sediment concentration along the Scheldt (Wartel, 1993)

Bed sediment in the Scheldt is mainly composed of mud in the access channels to the locks, whereas sandy mud, muddy sand, and sand is found in the main channel of the Scheldt (Wartel et al, 2000) and (Wartel and van Eck, 2000), see (Figure 4.3). Sand or hard bottom is generally found in the outer bends, where flow velocities are higher, whereas sandy mud occurs in the inner bends. In-between, the bed is mainly composed of muddy sand. This bed composition suggests that mud is advected upstream and downstream with the tidal currents, and is mainly deposited in the harbour docks. Some sediment is occasionally deposited on the inner bend, where it mixes with sand deposits. Another bottom sediment analysis has been made by McLaren to determine the percentage of sand along the river Scheldt. These data have been processed in view of the sand transport modelling for the tidal dock (Figure 4.4) (IMDC, 1998b)

The terrestrial input of mud has been quantified by IMDC (1993). The total input of terrestrial mud is estimated as 0.66 – 1.16 million ton, most of which originates from the Scheldt and Rupel basins (each contributing approximately the same amount of mud). Most of this sediment enters the basin through natural erosion (67-75%), with domestic and industrial contributions of 12 – 22% and around 10%, respectively. Wartel (1972) describes the terrestrial input between 0.64 and 1 million ton/yr, based on research by Gilles and Lorent (1966). According to Wollast and Marijns, 1981 (cited by Verlaan, 1998), however, the terrestrial input is 0.75 million ton/year, with much larger domestic and industrial contributions (25% and 39%, respectively).

Figure 4.3: Bed sediment composition of the lower Sea Scheldt, from Wartel, Parker and Francken (2000)
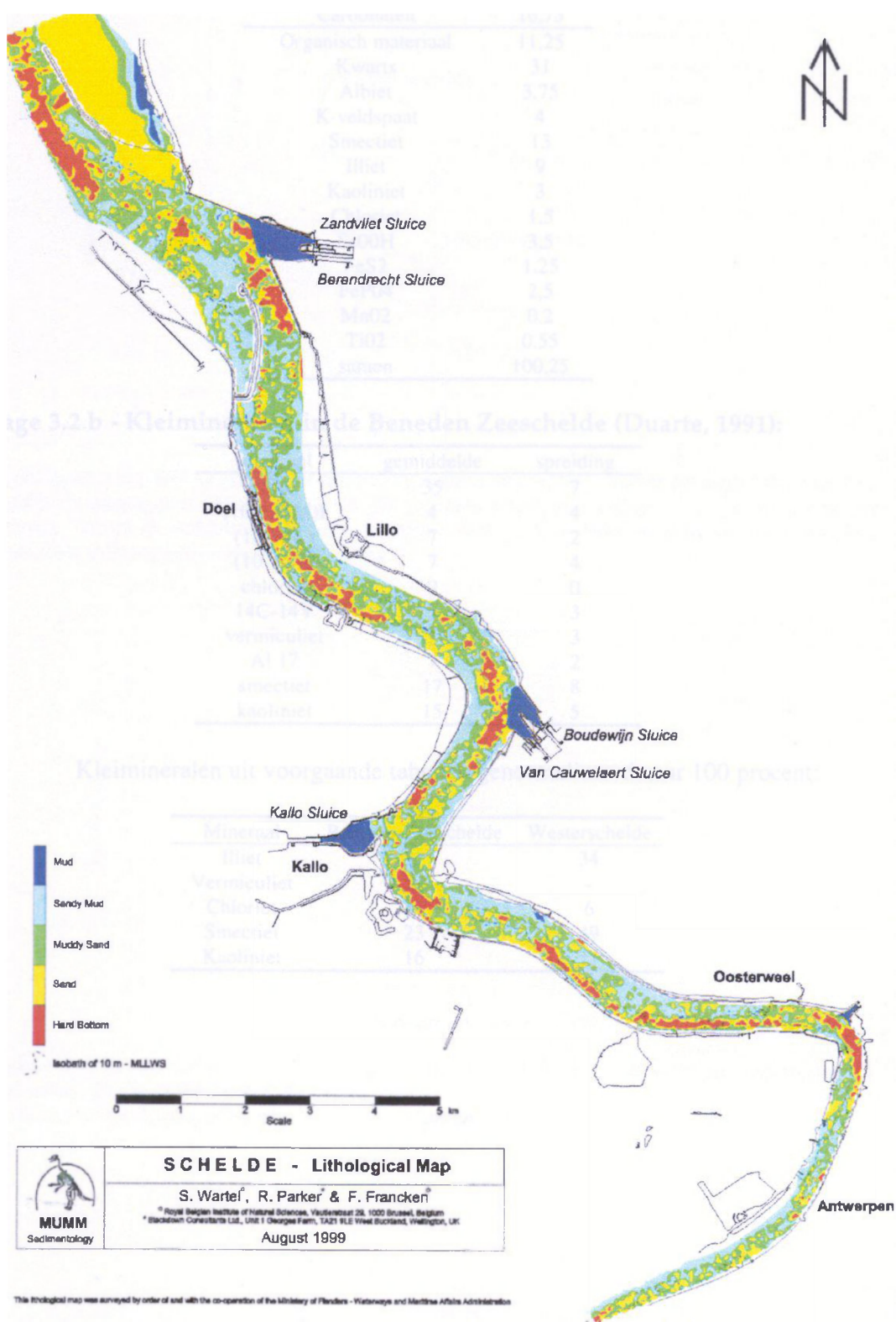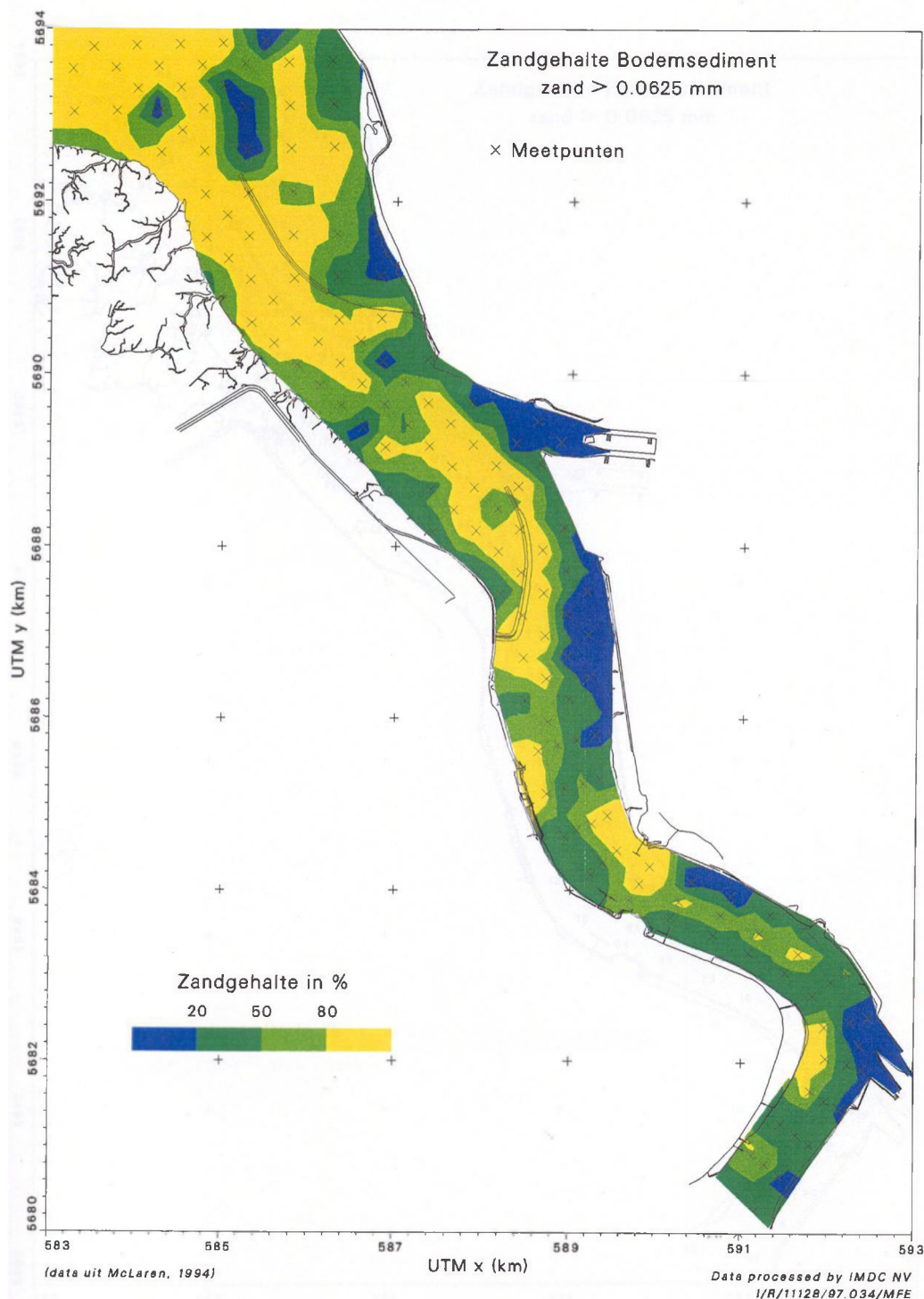
Figure 4.4: percentage of sand in the bottom sediments (IMDC, 1998b)

In recent years mitigation measures have been implemented in flanders to rduce soil erosion in the catchment of the Scheldt basin. Nevertheless no evidence can be found in the sediment transport measurements at the upstream boundaries of the tidal part of the Scheldt basin.

Waterbouwkundig Laboratorium reports the input of fine sediments (1992-2009) on average at around 220.000 ton/year (dry solids) as indicated in Figure 4.5. More details are given in (IMDC, 2011).
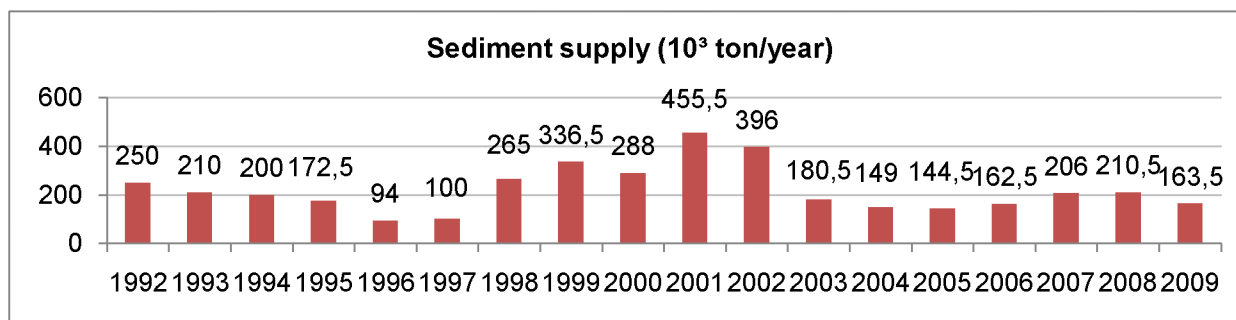
Figure 4.5: Evolution of total yearly terrestrial input of mud toward sthe Beneden-Zeeschelde (in 10³ ton) (data Waterbouwkundig Laboratorium Borgerhout, WL 2011a).

The marine mud in the Scheldt estuary originates from the English Channel and the Flemish Banks. The amount of marine mud entering at the mouth is largely unknown, but estimated to vary between 50.000 and 350.000 ton/yr (Verlaan, 1998).

4.3. Tidal asymmetry

4.3.1. Introduction

Tidal asymmetry in the Western Scheldt, and its consequences for the residual transport of sediment, has received considerable attention. Sediment is transported upstream through asymmetry of the M4 overtides in a partly standing, partly progressive tidal wave. In comparison, tidal asymmetry in the lower Sea Scheldt has received far less attention. As a result, it is not known what the relative contributions of estuarine circulation and tidal asymmetry are for the formation of the Estuarine Turbidity Maximum in the Port of Antwerp. In this chapter we aim to determine the role of tidal asymmetry in the residual transport of sediment in the lower Sea Scheldt.

The general theory of the residual transport of sediment in general, and of fine sediment in particular, by M2-M4 tidal asymmetry is treated in section 4.3.2. The effect of tidal asymmetry on the residual transport in the lower Sea Scheldt is analyzed in section 4.3.3.

4.3.2. General theory: net sediment transport by tidal asymmetry

In most temperate regions, the dominant astronomical tidal constituents are M2 and S2. Their interaction is responsible for the spring-neap tidal cycle. However, because there is no phase coupling between M2 and S2, their interaction does not contribute to a net transport of sediment. The net transport of sediment by tidal currents is mainly related to the interaction between M2 and its overtide M4. M4 is generated by friction of the M2 tidal wave over the bed, and therefore increases with decreasing water depth. The type and direction of tidal asymmetry depends on the phase angle between M2 and M4. The tidal varying water level is defined as

$$H = H_2 \cos\ \omega t - \phi_2\ + H_4 \cos\ 2\omega t - \phi_4$$

where H is the water depth, the subscripts 2 and 4 denote M2 and M4, respectively, t is time, ω is M2 angular frequency, and ϕ the phase. This expression can be rewritten in a timeframe relative to the phase of M2 t', using $\omega t = \omega t' + \phi_2$:

$$H = H_2 \cos\ \omega t'\ + H_4 \cos\ 2\omega t' - (\phi_4 - 2\phi_2)$$
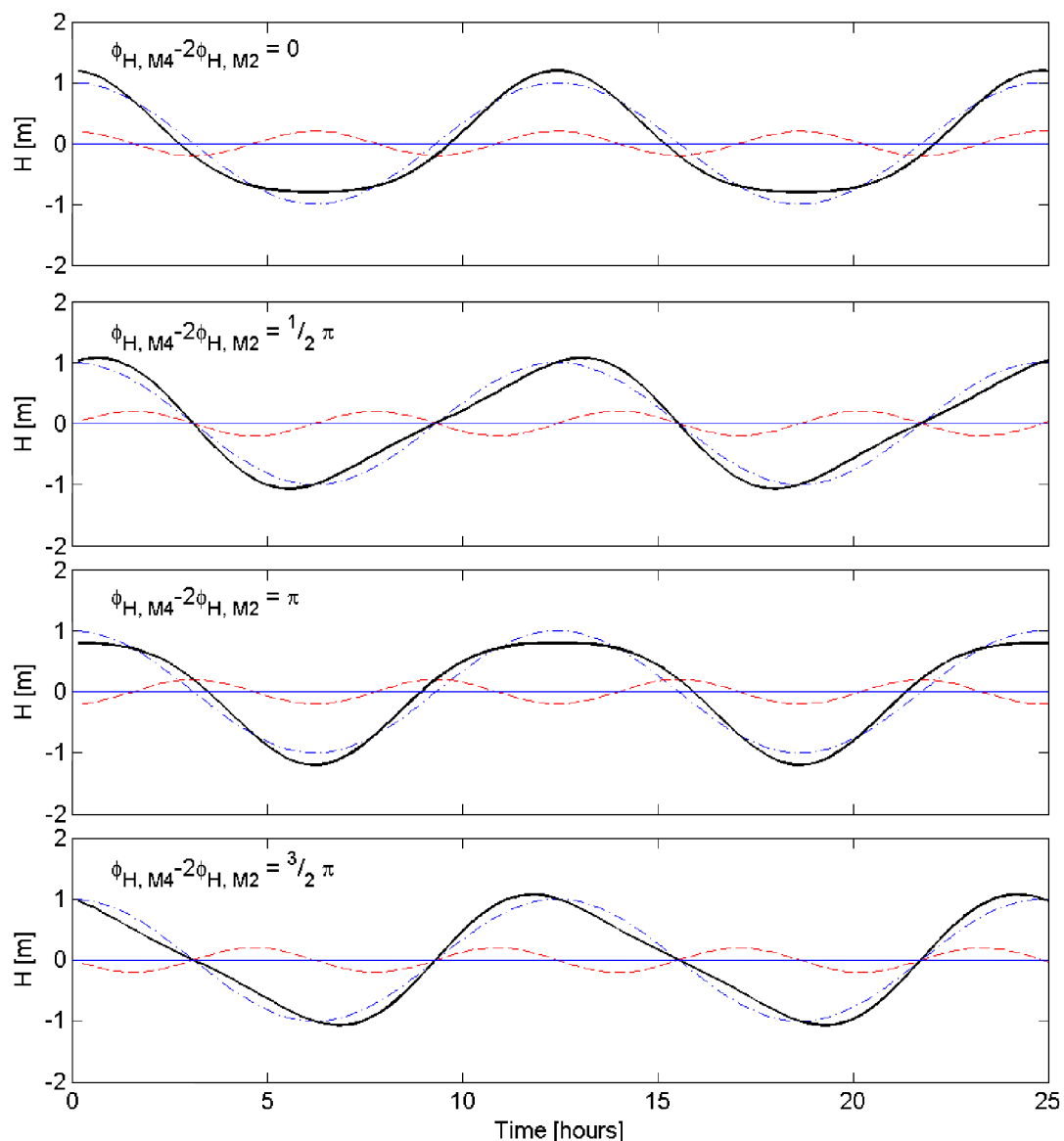
Figure 4.6: Time series of water level h of M2 (blue), M4 (red), and combined (black), $H_{M4} = 0.2H_{M2}$, and a phase lag of 0, 1/2 π, π, and ¾π.

This implies that the phase lag between M2 and M4 should be expressed as $\phi_4 - 2\phi_2$. Using a phase lag of 0, 1/2 π, π, and ¾π, results in 4 distinct tidal water level signals (see Figure 4.7). The first is characterized by a long low water (LW) period and short high water (HW) period; the

duration of rising water and falling water is equal (corresponding to flood and ebb, resp., in a standing tidal wave). The second is characterized by equal HW and LW periods but different ebb and flood periods. The third and fourth are exact opposites of the first two.
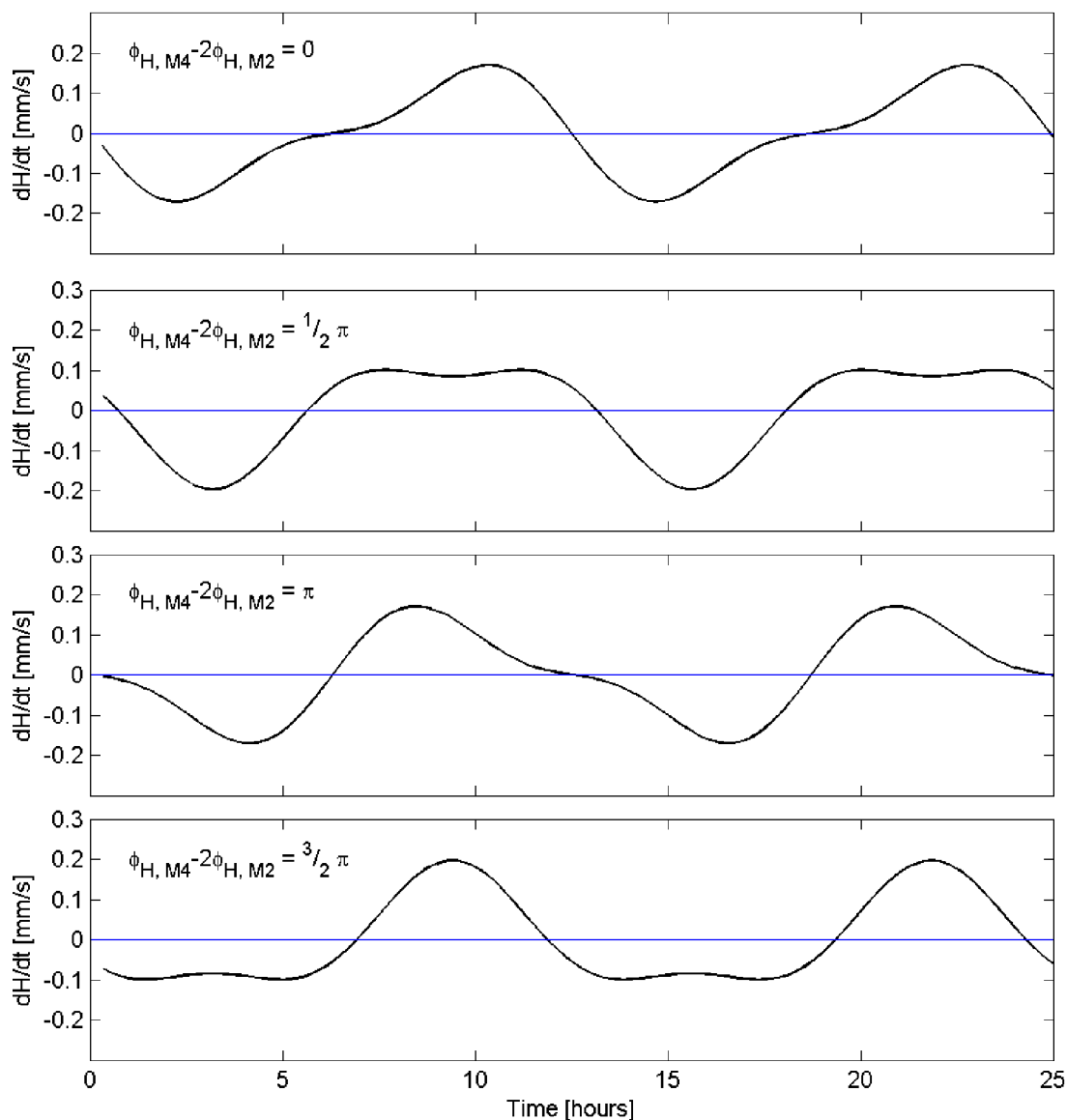
Figure 4.7: Timeseries of water level variation dh/dt of M2 and M4 combined, using $H_{M4} = 0.2H_{M2}$, and a phase lag of the water levels of 0, 1/2 π, π, and ¾π. A positive dh/dt implies flood currents. Note that the phase lags are those of the water levels, and not of dh/dt.

The implication of these water level variations can be assessed by assuming that the currents are driven by the instantaneous water level gradients, which, in turn, are determined by the temporal water level variation *dh/dt*. This shows that a phase lag of 0 or π results in equal flood and ebb

velocities, but different slack tide conditions whereas a phase difference of ½ π and ¾ π produce an asymmetry in the flow velocity. The implications for sediment transport are elaborated below for an asymmetry of the flow velocity and for the slack tide period. Note that we use the phase difference of water levels, and not currents, and assume a more or less standing tidal wave.

4.3.2.1. Maximum flow asymmetry

An asymmetry of maximum flow velocity results in a net transport of sediment because sediment transport scales with u^3 to u^5 (where u is the current velocity), providing sufficient sediment is available to be eroded. For $\phi_4 - 2\phi_2$ = ¼π - ¾π, sediment will be transported in the direction of the ebb current (as long as the shear stress exceeds the critical shear stress for erosion), whereas sediment will be transported in the direction of the flood current for $\phi_4 - 2\phi_2$ = 1¼π - 1¾π. If the amount of (fine) sediment is limited, an asymmetry in maximum flow velocity does not necessarily lead to a residual transport of sediments because all sediment is then already entrained at lower flow velocities. Furthermore, the contribution of the maximum flow asymmetry increases with the critical shear stress for erosion, and therefore it is especially important for sand transport.

4.3.2.2. Slack tide period asymmetry

In the absence of asymmetries in maximum flow velocities, sediment may be transported by an asymmetry in HW and LW slack periods, because sediment transport does not increase linearly with flow velocity. A short HW slack period and a long LW slack period occurs from $\phi_4 - 2\phi_2$ = -¼π to ¼π, and a short LW slack period and a long HW slack period occurs from $\phi_4 - 2\phi_2$ = $^3/_4\pi$ to 1¼π. Sediment transport does not increase linearly with flow velocity because:

1. The sediment concentration increases linearly with the cubed flow velocity (However, in starved bed conditions, which is more common for fine sediment, the sediment concentration is determined by the amount of sediment available rather than the flow velocity).

2. There is a critical velocity threshold for erosion

3. The concentration profile is not vertically uniform, depending on the mixing time and the settling velocity.

As a result, the vertical concentration profile and/or the sediment concentration magnitude during ebb differs from that during flood, while the ebb and flow velocities may be equal. The resulting residual transport of sediment is known as the settling lag effect.

When the flow velocity is insufficient to keep sediments in suspension, particles will settle, but will still be transported by the waning current. In the case of a short HW slack period and a long LW slack period ($\phi_4 - 2\phi_2$ = -¼π to ¼π), sediment is entrained at the beginning of the ebb, and rapidly vertically mixed. During the long waning stage of the ebb, sediments are still in suspension and transported in the ebb direction. At the end of ebb, most sediment has settled from suspension. During the first part of the subsequent flood, the currents are too weak to erode, or to vertically mix sediments. Sediments are eroded/ fully mixed only during the second part of the flood, and begin to settle from suspension at the final stage of the flood. However, before sediment has fully settled from suspension, the flow has already reversed and ebb currents are strong. This has the following implications:

(1) More sediment may be transported during peak ebb currents than during peak flood currents, because the water column is already fully mixed at the beginning of peak ebb currents.

(2)   More sediment will be transported during weak ebb velocities than during weak flood velocities. During the periods of weak ebb currents, sediment is vertically mixed and sediment is transported in the ebb direction (because this period is directly after a period of high flow velocities). During periods of weak flood currents, only a low amount of sediment is transported in suspension (because this period is directly after a period of low flow velocities, and sediment is not vertically mixed).

Of these two effects, the second will probably be more important for residual transport. This depends, however, on vertical mixing times, settling times, and critical shear stress for velocities. The higher the critical flow velocity for resuspension, the stronger effect 2) is. Similarly, the longer the time required for vertical mixing, the stronger effect 2) is. This time may be estimated from the timescale T needed to vertically mix sediment, using $T = H^2 / \varepsilon$, where ε is a mixing coefficient approximated by $\varepsilon = \frac{1}{6} \kappa u_* H$. Here κ equals 0.41 and $u_* = \sqrt{g} \, \overline{u} / C$, where $\overline{u}$ is the depth-averaged velocity, g the gravitational acceleration, and C the Chézy roughness. With a typical water depth of 15 m and a Chézy roughness of 75 m$^{1/2}$/s, the resulting timescales for full vertical mixing of 1.5 to 2.5 hours for depth-averaged velocities of 1 to 0.5 m/s (Figure 4.8, Figure 4.67). This is 20% less using Chézy = 60 m$^{1/2}$/s; around 1.2-2 hours. This indicates that the transport during weak ebb currents (fully mixed initial sediment concentration profile) is higher than during strong flood currents (no vertically mixed sediment concentration profile). It also indicates that the sediment concentration profiles will be fully mixed at the beginning of both high flood flow velocities and high ebb flow velocities, and therefore the effect of the settling lag is probably not very important during periods of maximal flow velocities.
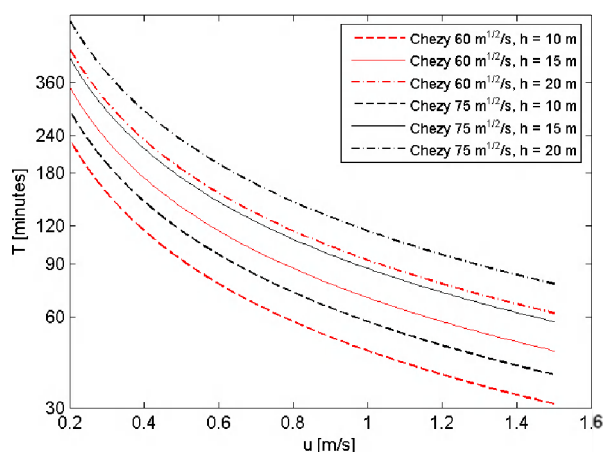
Figure 4.8: Timescale required to vertically mix sediment, for a water depth of 10, 15 and 20 m, and a Chézy roughness value of 60 m$^{1/2}$/s (red) and 75 m$^{1/2}$/s (black).

4.3.2.3. Combinations of maximum flow asymmetry and slack tide asymmetry

When $\phi_4 - 2\phi_2$ is not exactly 0, ½π, π, or 1½π, then a combination of flow asymmetry and slack tide asymmetry will occur. With $\phi_4 - 2\phi_2$ between 1½π and 0, and between ½π and π, the residual transport of sediment resulting from the two types of tidal asymmetry, are in opposite direction. Which of the two mechanisms is dominant is difficult to predict. Generally, the importance of maximum flow asymmetry increases with the critical shear stress for erosion, and is therefore especially important for sand. Slack tide asymmetry is not important when sediment is rapidly mixed and has no critical shear stress for erosion (i.e. very fine sediment in shallow water), or when the settling velocity is very high and sediment responds instantaneously to the flow (such as

sand). The net direction of sediment is therefore difficult to predict when $\phi_4 - 2\phi_2 =$ 1½π - 0, and when $\phi_4 - 2\phi_2 =$ ½π - π.

4.3.3. Tidal asymmetry in the lower Sea Scheldt

4.3.3.1. Methods

The tidal asymmetry in the lower Sea Scheldt is mainly analyzed using the 3D mud model. The model is used rather than observations because (1) flow velocity measurements are mainly positioned outside the main channel of the Scheldt while the interest here is on the flow velocities in the channel, (2) the model provides a vertical profile of flow velocities, and (3) the model provides continuous time series. The water levels and flow velocities are reproduced very accurately by the model, and therefore the use of model results does not have any drawbacks.

The computed flow velocity (time series length of 3 months) is analyzed in the time-domain, by computing the maximum flow velocity profiles during ebb and during flood and by computing the magnitude and the direction of the residual flow velocity (see app. A). The water levels are analyzed in the time domain by computing the ratio of the rising water period T_{fl} and the falling water period T_{eb}, and by computing the time that the water level is above average water level ($T_{h>hm}$) and below average water level ($T_{h<hm}$). Additionally, the water levels and flow velocity profiles are analyzed in the frequency domain using harmonic analysis (see e.g. Pugh, 1987). The vertical tide (water levels) and the horizontal tide (flow velocities) is harmonically analyzed for 17 tidal constituents (the diurnals Q1, O1, P1, and K1, the semi-diurnal constituents N2, M2, L2, S2, and K2, the quarter diurnal constituents (first overtides) 3MS4, MN4, M4, and MS4, and other higher harmonics 2MN6, M6, 2MS6, and M8). The flow velocities are analysed in x- and y direction and subsequently transformed in a major flow direction and minor flow direction with tidal ellipses (Xu, 2000).

4.3.3.2. Water level

The analysis of the water levels reveals that

1) The period of rising water T_{fl} is shorter than the period of falling water T_{eb} ($T_{fl} < T_{eb}$). The T_{fl} / T_{eb} ratio is 0.88 near the land van Saeftinghe (sta5): see appendix C. Location lvs2 is too close to the downstream model boundary, which is a cross-sectional varying combination of water level and discharge, and therefore the water levels are not reliable. The T_{fl} / T_{eb} ratio decrease in the downstream direction, to 0.86 near the Deurganckdok, 0.84 near Kallo, and 0.76 near Schelle. This is consistent with Claessens and Belmans, 1984 (cited by Fettweis et al., 1998), who observed a T_{fl} / T_{eb} ratio decrease of 0.88 at the mouth to 0.75 at Schelle.

2) The period that the water levels are above mean water level ($T_{h>hm}$) is shorter than the period that the water levels are below mean water level ($T_{h<hm}$).

The first ($T_{fl} < T_{eb}$) is consistent with a phase lag $\phi_4 - 2\phi_2$ of 1½π (see Figure 4.7) whereas the second ($T_{h>hm}$ is shorter than $T_{h<hm}$) is typical for a phase lag of 0 (or 2π). Hence, the phase lag should be somewhere between 1½π and 2π. This is consistent with the phase lag $\phi_4 - 2\phi_2$ computed with the harmonic analysis: $\phi_{h,M4} - 2\phi_{h,M2}$ increases in the upstream direction from 360° or 2π (Land van Saeftinghe, see $\phi_{h,M4} - 2\phi_{h,M2}$ in the lower right of (Annex-Figure B-2) and (Annex-Figure B-23) to 320° or approximately 1¾π near Kallo (Annex-Figure B-11). At the upstream model boundary near Schelle the phase lag is 290° or nearly 1½π. (Annex-Figure B-12) The decreasing phase lag in the upstream direction indicates a shift from maximum flow asymmetry near the Dutch-Belgian border, to dominantly slack tide asymmetry further upstream. Also, the phase

difference between the water level and flow velocity of the M2 tide is close to 270°, typical for a standing wave (subtract $\phi_{u,M2}$ from $\phi_{h,M2}$ in the lower right of (Annex-Figure B-21
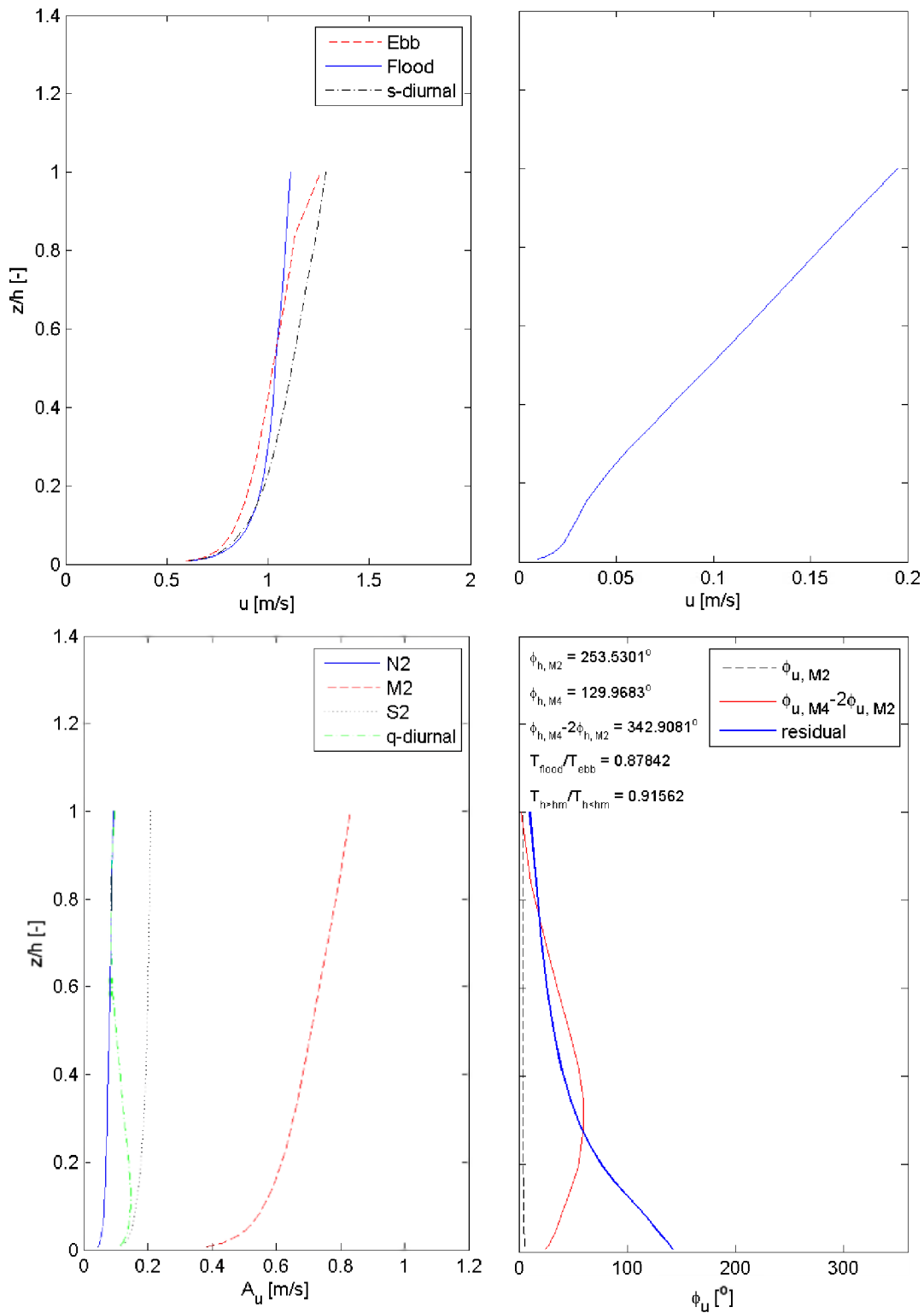
Annex-Figure B-2: Water levels and flow velocity parameters at station sta 5. See page C9 for a description

) to (Annex-Figure B-2). Consequently, the tidal asymmetry schematised in (Figure 4.7) and (Figure 4.7) can be applied to the Scheldt River. This implies that:

1) The flood currents should be higher than the ebb currents ($T_{fl} < T_{eb}$, see (Figure 4.6) and (Figure 4.7). This results in a residual transport of sediment in the flood direction.

2) The flood currents peak at the end of the flood, and the ebb currents at the beginning of the ebb (slack tide asymmetry because $T_{h>hm} < T_{h<hm}$, see (Figure 4.6) and (Figure 4.7). This promotes a residual fine sediment transport in the ebb direction.

4.3.3.3. *Flow velocity*

The   maximum   flow   velocity   profiles   (Annex-Figure   B-21
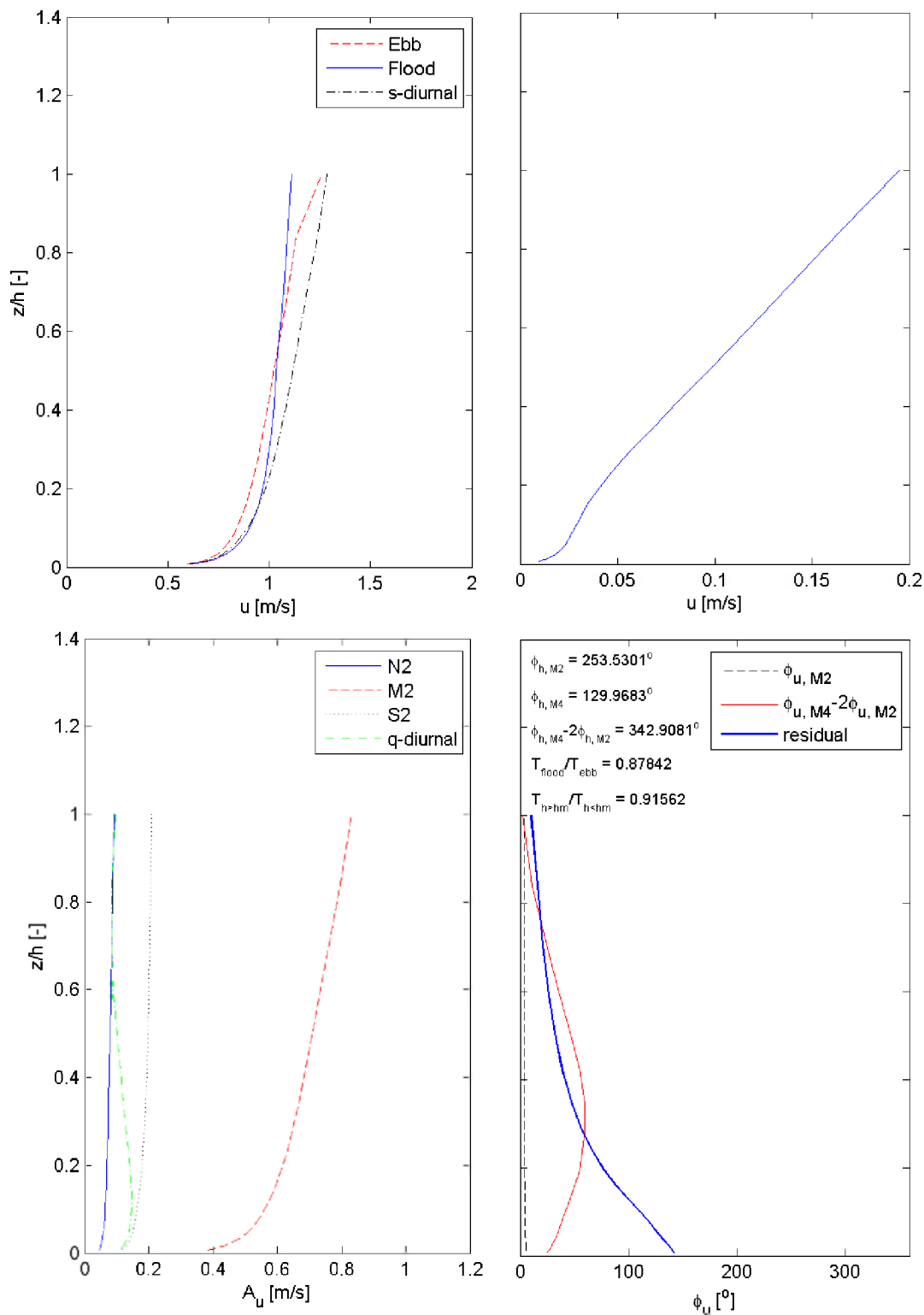
Annex-Figure B-2: Water levels and flow velocity parameters at station sta 5. See page C9 for a description

) to (Annex-Figure B-2) reveal consistent flood dominance throughout the lower Sea Scheldt. Only upstream of the Deurganckdok (near the Leidam and the Land van Saeftinghe) the near-surface flow velocities are highest during the ebb, whereas the near-bottom flows are maximal during the flood. This is caused by residual flow: see the next section. The flow velocity profiles along the K-transect (Ka-Kf) show that the flood dominance is even stronger on the shallow inner bend (Kd-Kf) than the main channel (Ka-Kc). However, this is probably bathymetry-induced and therefore local. A comparison of the maximum ebb- and flood velocity with harmonic flow velocities shows that the flood velocities are approximately equal to the sum of all the semi-diurnal flow velocities whereas the ebb velocities are substantially lower. The difference in maximum ebb velocity and flood velocity is close to the sum of the quarter diurnals (mainly M4), showing that tidal asymmetry is largely responsible for the flow asymmetry. This is therefore consistent with the observed shorter flood period than ebb period in the water levels.
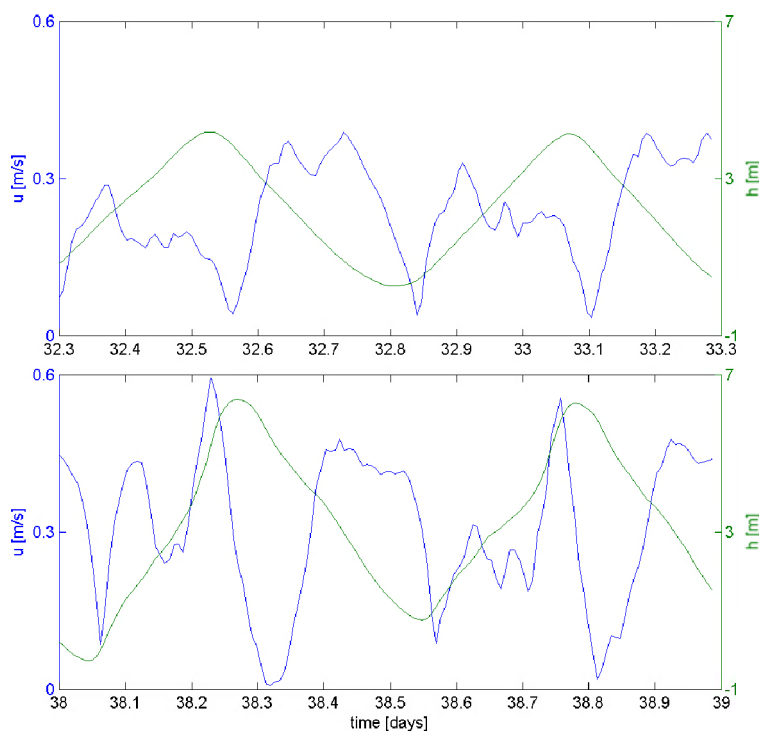
Figure 4.9: Water level (green) and absolute near-bed flow velocity (blue) during neap tide (top) and spring tide (bottom), at station Ka.

Time series of computed flow velocities (Figure 4.9) show that during spring tide, the flood velocities indeed peak at the end of the flood, whereas the ebb currents peak more at the beginning of the ebb. This is consistent with the $T_{h>hm} < T_{h<hm}$. However, during neap tide, the flood current peak occurs at the beginning of the flood while the ebb currents are also stronger than the flood currents. This is probably caused by superposition of flow velocities of the higher harmonics of M2 and S2 combined (3MS4, MS4) which (partly) cancel out during neap tides. This pronounced tidal asymmetry (flood peaks at the end of flood during spring tides and at the beginning of flood during neap tides, and flood-dominant during spring tides and ebb-dominance

during neap tides) is also observed at long-term measurement stations Lillo, Hoboken, Boerenschans, Oosterweel left bank. Buoy 84 and Buoy 97 are always flood-dominant, but the current velocity peak occurs at the end of flood only during spring tide. Station Oosterweel is strongly ebb-dominant. However, measurement stations are not very suitable for analysis of ebb- or flood dominance because they are usually placed out of the main channel, and are therefore influenced by the local bathymetry. Along the K-transect, for instance, the model results show a strong increase of the flood dominance from the main channel (Ka) towards the flats on the inner bend (Kf).

4.3.3.4. Sediment dynamics

From the M2-M4 asymmetry in combination with model results and field observation, it is concluded that there is a flood –dominant maximum flow asymmetry in the downstream part of the lower Sea Scheldt, and a slack-tide period asymmetry with a long slack tide period at LW and a short period at HW at spring tides upstream of Antwerp. A longer LW slack tide period than HW slack tide produces a net residual transport of fine sediment in the ebb direction (see the previous section). Both mechanisms promote a residual transport of sediment in opposite directions, but establishing which mechanism is more important for residual transport is more difficult. Possibly, with only tidal asymmetry as the dominant sediment transport mechanism, sediment convergence (and therefore an ETM) is to be expected in the lower Sea Scheldt.

4.4. Gravitational circulation and residual flow

When a river flows into an estuary, it produces a residual flow velocity. Without any density effects, the vertical residual velocity profile is more or less logarithmic. However, fresh water is less dense than salt water. When an estuary is not permanently fully mixed, a relatively larger part of the fresh water flowing into an estuary is therefore transported downstream in the upper layers. The upper layer is relatively fresh water, separated from more saline near-bottom water by a halocline. In partly mixed estuaries, salt water may be entrained in the less saline surface layer. Continuity then requires that salt water is transported upstream in the bottom layer. This upstream-directed bottom flow is less pronounced in strongly stratified estuaries (because salt water entrainment rates are lower) or in fully mixed estuaries (Dyer, 1994). Vertical gravitational circulation (also known as estuarine circulation) is therefore the deviation of the residual flow velocity profile from a logarithmic flow velocity profile, caused by fresh water flow. If a fresh-water induced gravitational circulation exists, it produces a seaward transport of water and suspended sediment in the upper layer of the flow, and a landward transport of suspended sediment near bottom. This has two important implications:

1) The sediment concentration is higher near bed than near-surface, and therefore a residual flood current near the bed and a residual ebb current near the surface result in a residual transport of sediment in the flood direction.

2) The near-bed flood currents are higher (and last longer) than the near-bed ebb currents. And since the sediment transport scales with a certain power of the flow velocity (usually 3 or 4), this also results in a residual sediment transport in the flood direction.

In the Lower Sea Scheldt, the residual flow velocity peaks at 0.2 m/s (see upper right panel of (Annex-Figure B-21) to (Annex-Figure B-23). The residual flow is always highest near the surface, and directed in the downstream direction. The direction of the residual flow rotates from surface to bottom (see lower right panel). At some locations the direction of the residual flow near bottom is almost normal to surface flow (the K-transect, see (Annex-Figure B-4) to (Annex-Figure B-46). This

is a combination of secondary flow and gravitational circulation. The direction of the residual flow near the bed never is in the upstream direction. Upstream of Liefkenshoek (Kallo and Schelle, see (Annex-Figure B-11) and (Annex-Figure B-12), the direction of the residual flow is uniform, and directed downstream. But, even though the fresh water flow does not produce an upstream directed residual flow, its interaction with the oscillating tidal currents may still produce an upstream-directed transport of sediment. During the flood, the balance of the barotropic pressure gradient of the tidal wave and the density-driven pressure gradient results in reduced near-surface flow velocities and an increased near-bed flow velocity. The result is that the near-bed flood velocities are higher than the near-bed ebb flow velocities, such as illustrated in the top left of (Annex-Figure B-2) and (Annex-Figure B-23). Although the difference in flow velocity may be small, it may substantially contribute to a net transport of sediment because most sediment is transported near the bed. Therefore, although the effect of fresh water flow on the hydrodynamics is low, it may result in an upstream-directed sediment flux in the downstream reaches of the Sea Scheldt. Further upstream, the flow velocity profilies do not seem to be influenced by density differences. Therefore here the residual fresh water discharge will probably result in a downstream-directed transport of sediment.

An Estuarine Turbidity Maximum (ETM) forms when two residual sediment transport fluxes converge. The analysis of the residual flow velocity and tidal asymmetry indicates that the ETM between the Deurganckdok and Antwerp is probably a combination of downstream transport by residual flow (and possibly slack tide asymmetry). Sediment is probably transported upstream by the flood-dominant maximum flow asymmetry and density-driven flow. The exact location of the ETM is then determined by the upstream decrease in tidal flow asymmetry, the upstream increase in slack tide asymmetry, and the seasonally varying strength of the fresh water discharge.

4.5.   Secondary circulation

The centripetal acceleration needed to keep the flow in a circular path increases with the flow velocity whereas the lateral total pressure gradient is constant over depth. Therefore the surface layer (with high flow velocities) is deflected towards the outer bend while the bottom layers are deflected towards the inner bend (e.g. Jansen et al., 1979). A high vertical velocity gradient, caused by stratification, will therefore lead to a stronger secondary circulation. The sediment concentration is generally highest near the bed, and therefore this curvature-induced near-bed flow from the outer bank to the inner bank results in concentration peaks near the inner bank.

However, Winterwerp (2006) showed that secondary flow patterns may also be in the opposite direction. Due to bathymetric effects, the flow velocities during the flood are higher in the inner bend than in the outer bend. Differential advection of salinity then results in higher salinities in the inner bend than on the outer bend, creating a transverse salinity gradient. This transverse salinity gradient creates a secondary circulation with a near-surface flow towards the inner bend and a near-bed flow to the outer bend. Such a reversal of secondary circulation cells could then result in highest sediment concentrations in the outer bend, rather than the inner bend.

Near the Deurganckdok at the K-transect, the left bank is the outer bend and the right bank the inner bend of the Scheldt. During the ebb, the concentration peak is on the inner bank (Kd in Figure 4.10) and the right hand side of Figure 4.11. However, during the flood, the sediment concentration peak is on the opposite bank (Ka in (Figure 4.10) and the left hand side of Figure

4.12. This is most likely caused by a reversed secondary flow. During the ebb, the concentration peak is on the inner bank.

The location of the concentration peaks are opposite of those at the K-transect at Liefkenshoek, several km upstream of the Deurganckdok. Here, the concentration peak during the flood is on the right bank (Figure 4.12) whereas maximum sediment concentrations during the ebb occur on the left bank (Figure 4.11). However, near Liefkenshoek the left bank is the inner bend and the right bank the outer bend (i.e. opposite to those at the K-transect). Therefore the flood sediment concentration peak occurs is in the outer bend and the ebb concentration peak is in the inner bend. Therefore the general pattern of reversed (anti-clockwise) secondary circulation cells during the flood and clockwise circulation cells during the ebb seems to be the same at Liefkenshoek and at the K-transect.
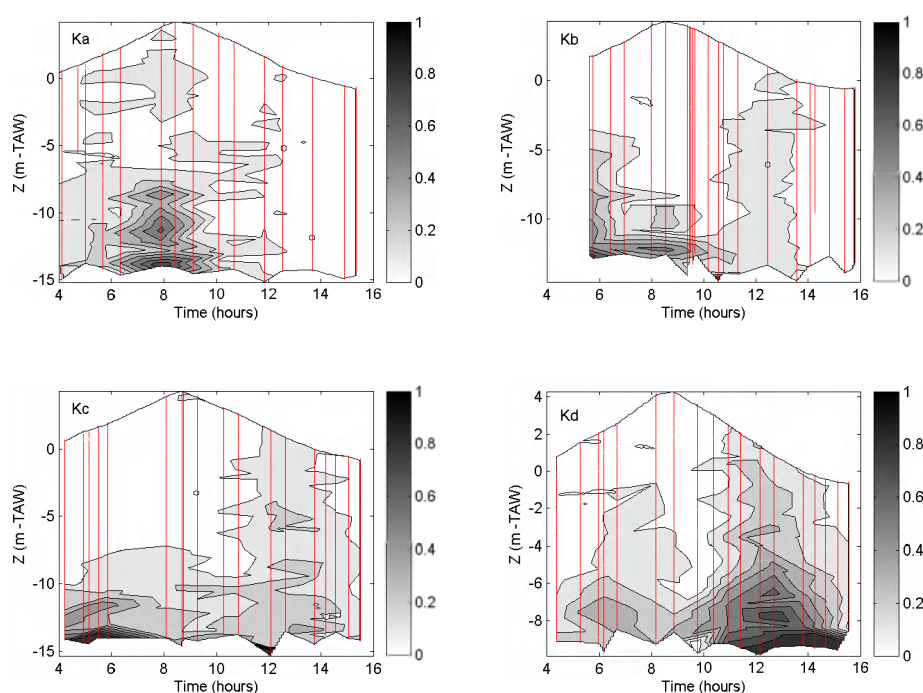
Figure 4.10: Sediment concentration (kgm⁻³) measured with the SiltProfiler at positions a-d of the K-transect locations near the Deurganckdok, on 16 Feb 2005, during the HCBS1 campaign. The vertical lines represent the trajectories of the silt profiler.
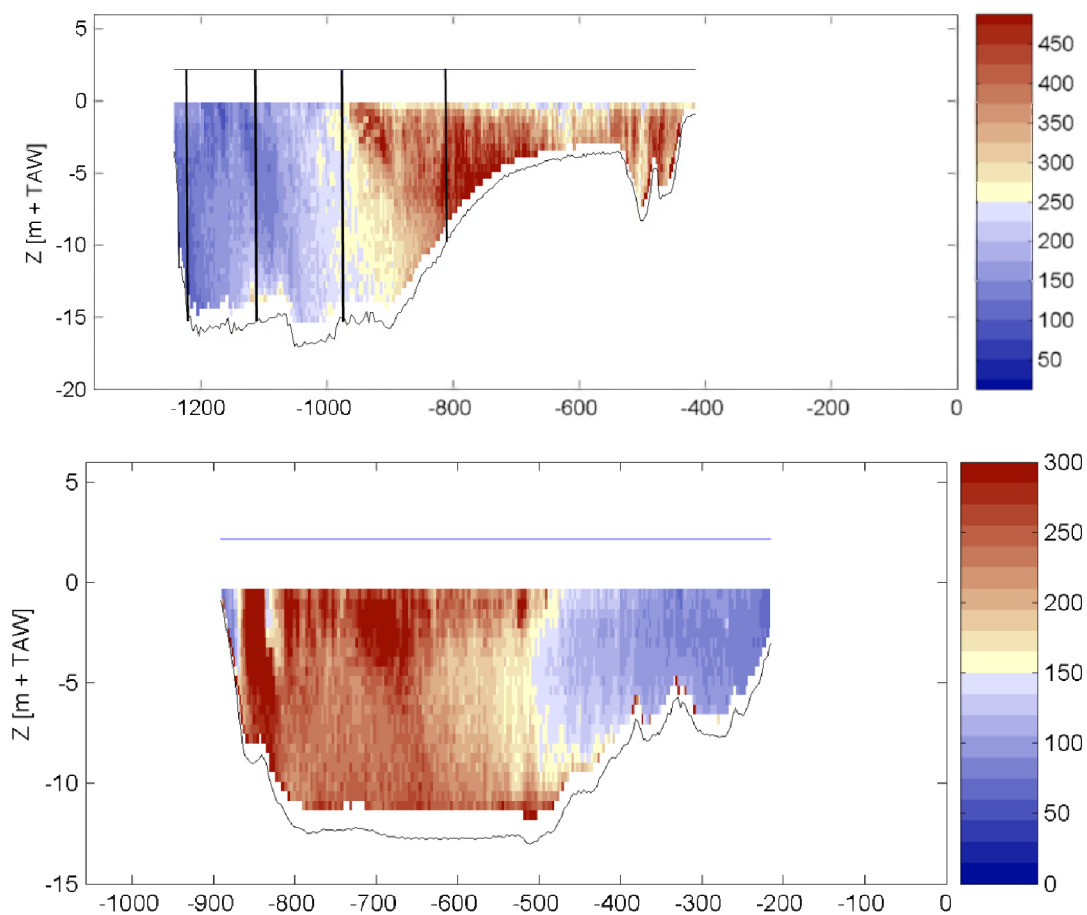
Figure 4.11: Sediment concentration halfway the ebb (22 March 2006, 11:00), with approximate locations of stations Ka to Kd as vertical lines (left to right, respectively) near the K-transect (top)(IMDC, 2206d) and near Liefkenshoek (bottom),(IMDC, 2006e) The X-axis is from the left bank to the right bank.
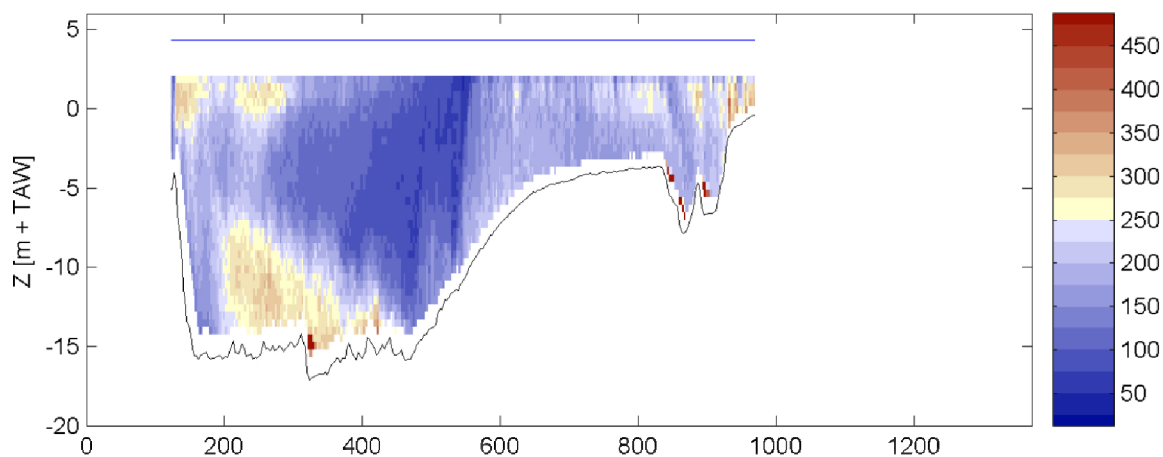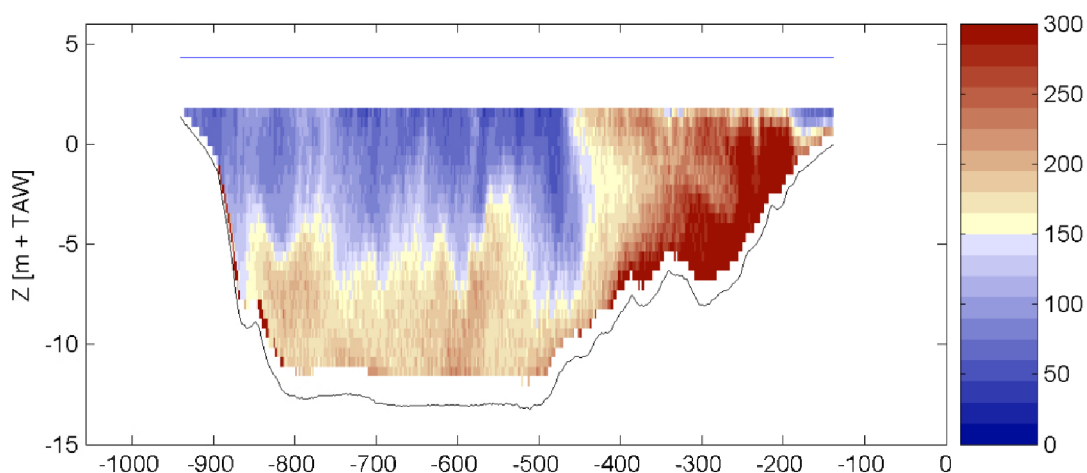
Figure 4.12: Sediment concentration at the end of the flood (22 March 2006, 19:30) near the K-transect (top)(IMDC, 2006d) and near Liefkenshoek (bottom) (IMDC, 2006c), from IMDC report 7.2 and 7.3. The X-axis is from the left bank to the right bank.

4.6.   Wind-induced water level variations

Wind-induced average water level variations (occurring several times per year) are in the order of 1 m (Figure 4.13). During storms from the north to southwest, a large amount of water is transported into the Scheldt estuary. As a results, the water level at the mouth of the Western Scheldt increases approximately 1 m. Travelling further into the Scheldt Estuary, some of the energy in the storm set-up is dissipated (thereby lowering the storm set-up), but the funnel shape of the estuary also concentrates the water mass, thereby increasing the height of the set-up. The February 2005 set-up, resulting in a storm set-up around 1 m near Vlissingen, produced a water level setup of 1.1 m near the Deurganckdok (Figure 4.14). As a net result, the height of the storm setup will probably be around 1 m throughout the estuary.
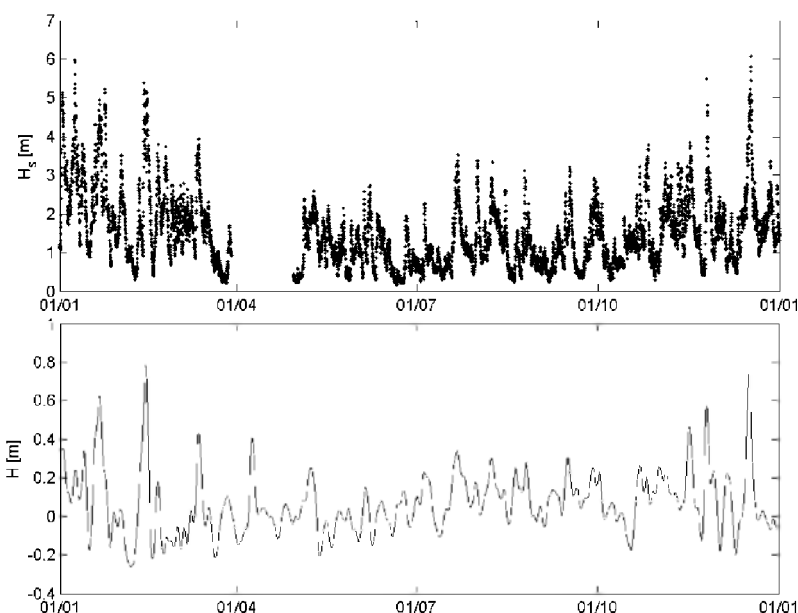
Figure 4.13: Significant wave height (Hₛ) at Eierlandse Gat (North of Texel) and residual water levels at Terneuzen, in 2005
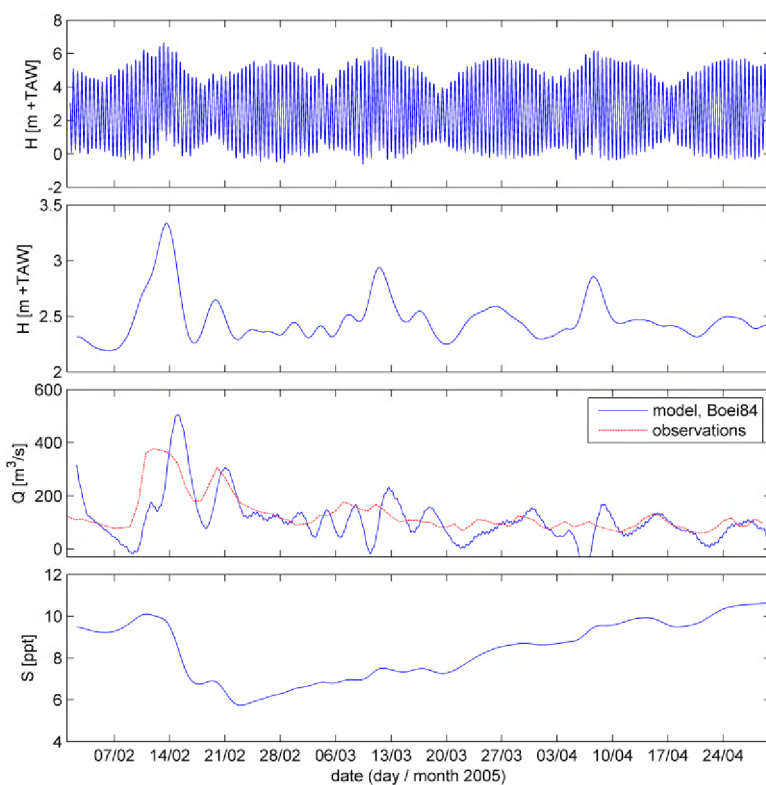
Figure 4.14: Computed water level, low-pass filtered water level, low-pass filtered (and daily) discharge, and low-pass filtered salinity in the Scheldt close to the Deurganckdok, from February through April 2005. From van Maren and Schramkowski, 2008.

The measured sediment concentrations do not significantly increase during the storm set-up (IMDC, 2005k): the sediment concentration at Lillo only varied with the spring-neap tidal cycle. Most of the long-term moorings, however, failed during the period of this storm set-up. The effect of the storm set-up on residual transports is also affected by variations in the flow patterns, which cannot be computed from the long-term moorings because of cross-sectional and vertical variations in flow velocity and sediment concentration. A numerical model which captures all the cross-sectional variations in flow patterns is more suitable for such an analysis. And since the sediment concentrations are not substantially influenced by the storm, the sediment concentrations at the model boundary can be constant.
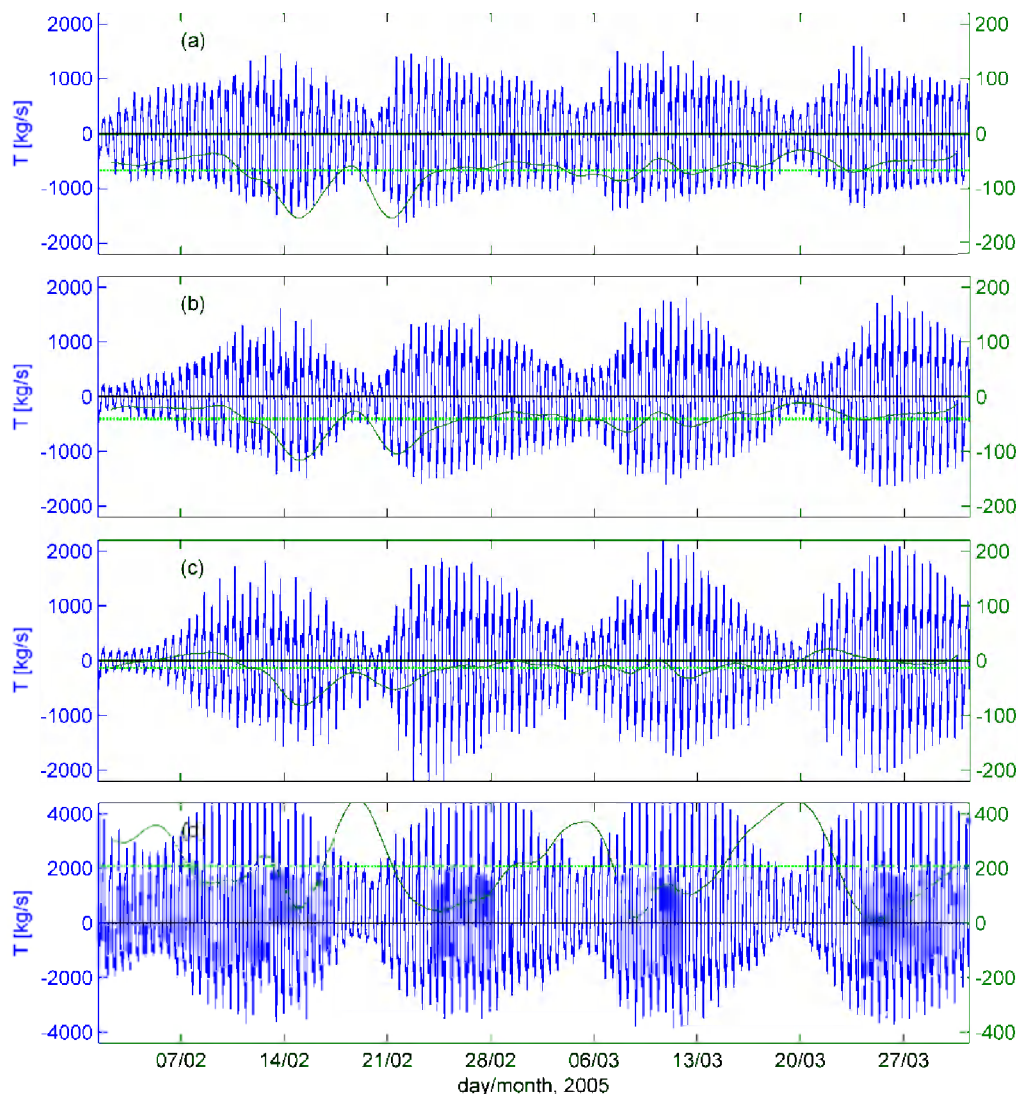
Figure 4.15: Sediment transport T (kg/s, negative values are downstream-directed) near Antwerpen (a), Kallo (b), Deurganckdok (c) and Waarde (d). Blue lines are instantaneous transports (left-hand y-axis), the dark green line is the low-pass filtered sediment transport (right-hand y-axis), and the light green is the average transport (also right-hand y-axis). Note that different scaling of low-pass filtered transports. From van Maren and Schramkowski, 2008.

A storm set-up causes an increase in water levels, net upstream-directed flow velocities, and an increase in salinity up to, or shortly after, the peak of the storm (Figure 4.14). During the waning stage of the storm, the water flows back, resulting in net downstream-directed flow and decreasing salinity. The lowpass filtered discharge (Figure 4.14) is the combined result of the Scheldt River discharge and the low-frequency discharge variations due to meteorological forcing. Model results reported in van Maren and Schramkowski (2008) indicate that surprisingly, the overall effect of a storm is a downstream directed net sediment flux (Figure 4.15). Probably, this is because there is little sediment to erode in the downstream reaches, and therefore increased upstream-directed velocities do not result in a substantial increase in the upstream-directed sediment flux. However, during the subsequent flushing, the higher (downstream-directed) flow velocities are able to resuspend sediment in the more turbid reaches of the Scheldt. The resulting downstream-directed flux peaks at around 1000 kg/s. Hence, according to the model simulations, the net effect of the storm is a downstream flushing of sediment.

The effect of storm-induced water level variation on sedimentation in the Deurganckdok was qualitatively established in van Maren and Schramkowski (2008), using the LTV mud model. These results indicated that the density-driven exchange flows rapidly adapt to a variation in salinity caused by the storm set-up, and that the effect on the total sedimentation is low. The salinity increases during the first phase of the storm set-up, and therefore near-bed inflow into the dock also increases. However, during this phase the sediment concentration is not substantially higher (due to the limited amount of sediment available for erosion downstream of the dock). During the following flushing (when sediment concentrations may be higher because of downward transport of turbid water), the water on the Scheldt is relatively fresh, thereby promoting near-bed outflow.

4.7. Shallow water waves

The effect of shallow water waves on resuspension can only be assessed qualitatively because their effect has not yet been established through measurements or modelling studies.

4.7.1. Wind waves

Wind waves in the lower Sea Scheldt have a short fetch due to the small width ($\approx$ 500 - 1000 m). The longest fetch length is therefore when the wind blows in the direction of the Scheldt River. In that case, the maximum fetch is restricted by the river bends, i.e. several kilometres. The maximum wave height can then be estimated from the wind speed using simple empirical expressions (e.g. Goda, 2003). For average storms (Beaufort 8), the wind speed is 17-20 m/s, resulting in a wave height of 0.3 m and a wave period of 1.5 s (wind perpendicular to the main flow of the river, resulting in a fetch length of 500 m), to a wave height of 0.8 m and a wave period of 3 s (wind parallel to the main flow of the river, resulting in a fetch length of 5000 m). Such waves may substantially contribute to the resuspension of sediment on the tidal flats along the Scheldt River.

Resuspension of sediment on will mainly take place in winter, when storms occasionally occur and the mud flats are not covered by algal mats. This will probably contribute substantially to the amount of sediment in suspension, and at least partly explain the higher turbidity in the Scheldt during winter time. However, the rate of resuspension on the mud flats, and the resulting erosion rates in winter (and sedimentation rates in summer) still needs to be quantified through modelling work or through data analysis.
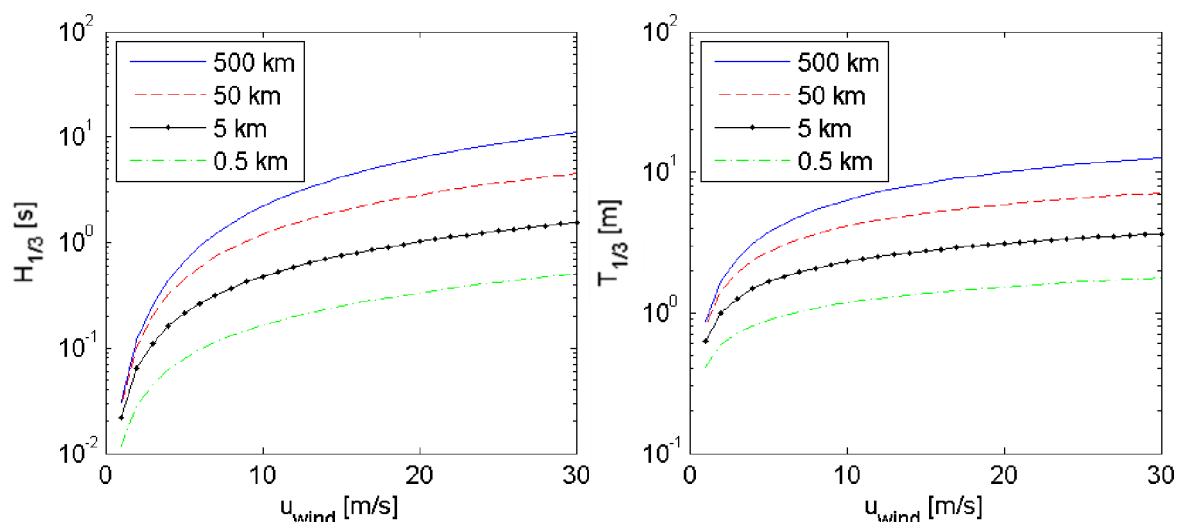
Figure 4.16: Estimate of wave height $H_{1/3}$ and period $T_{1/3}$ as a function of fetch length hand wind velocity u_{wind} measured 10 m above the surface (m/s), based on the Wilson formulas presented in Goda (2003).

4.7.2. Ship traffic

A sensitivity analysis on the potential effect of shipping traffic on suspended sediment concentrations in the Westerns Scheldt and lower Sea Scheldt was made with the LTV mud model by Van Kessel et al. (2007). The effect of shipping traffic was taken into account by increasing the bed shear stress of each grid cell with a value of 0.5 Pa and with a probability of 1%. This resulted in a substantial increase in sediment concentration: near Terneuzen, the long-term average sediment concentration increased with 50%. However, they also concluded that a more detailed and sophisticated analysis of the navigation density in the Scheldt and its influence on bed shear stress is required to draw more definitive conclusions.

4.8. Relocation of dredged material

4.8.1. Maintenance dredging in the Lower Sea Scheldt

4.8.1.1. The navigation channel in the Lower Sea Scheldt

Maintenance dredging works in the Lower Sea Scheldt are executed in the navigation channel as well as in the access channels to the locks. The width of the navigation channel reduces from 300-380m downstream of Deurganckdok to 130-180m further to Wintam, and the depth from 145 dm below LAT to 57 dm below LAT (see Table 4.1).

Table 4.1   Navigation channel dimensions

section	width (m)	depth (dm –LAT)
Downstream Deurganckdok	300-380	-145
Deurganckdok – Kallo lock	250-300	
Kallo - Royerslock	170-220	-77 (Antwerp) -57 (Royerslock)
Royerslock – Wintam lock	130-180	-57

4.8.1.2. Maintenance dredging works in the Lower Sea Scheldt

From 1980 the total volume of maintenance dredging works (in Belgium) was around 2.5 million m³ during the eighties and 2.3 million m³ in the early nineties increasing to 3 to 4 million m³ from 2000 on (Table 4.2). The dredging works are realized with trailing suction hopper dredgers that relocate the dredged material to designated zones.

Table 4.2: Overview of maintenance dredging Works in the Lower Sea Scheldt (1998-2008, info AMT) (Deurganckdok included from 2005 on)

PERIOD	Drempel van Zandvliet	Plaat van Doel	Drempel van Frederik	Drempel van Lillo	Drempel van De Parel	Upstream Kallo	Others	TOTAL
Dredged volume 1998-2008 (MILLION m³/YEAR)								
1998	1,4	0,0	0,6	0,3	0,4	0,0	0,7	3,5
1999	1,3	0,0	0,9	0,4	0,3	0,0	0,7	3,6
2000	1,1	0,0	0,6	0,6	0,3	0,0	0,4	3,0
2001	1,4	0,0	1,0	0,7	0,3	0,0	0,7	4,1
2002	1,5	0,0	0,6	0,6	0,4	0,0	0,5	3,7
2003	1,0	0,0	1,0	0,4	0,3	0,0	0,7	3,4
2004	0,6	0,0	1,2	0,2	0,2	0,0	0,6	2,8
2005	0,9	0,0	0,9	0,7	0,3	0,0	1,0	3,8
2006	0,7	0,0	0,6	0,2	0,4	0,0	1,6	3,5
2007	0,5	0,0	0,5	0,3	0,2	0,0	1,6	3,2
2008	0,8	0,0	1,3	0,2	0,2	0,0	1,2	4,4
Dredged volume: *AVERAGE, MINIMUM AND MAXIMUM OVER THE PERIOD 1998-2008 (MILLION m³/YEAR)*								
Average/ year (1998-2008)	1,0	0,0	0,8	0,4	0,3	0,0	0,8	3,5
minimum (1998-2008)	0,5	0,0	0,5	0,2	0,2	0,0	0,4	2,8
maximum (1998-2008)	1,5	0,0	1,2	0,7	0,4	0,0	1,2	4,4

The most important dredging locations are Drempel van Zandvliet and Drempel van Frederik. *Figure 4.17* clearly indicates that the relative importance of the dredging locations remains reasonably constant for the period 1998-2008. The maintenance dredging activities on Drempel van Krankeloon are more important between 2001 and 2005 and reduce again. In 2005 the dyke between the River Scheldt and Deurganckdok was dredged and maintenance dredging activities took place in the access zone to the dock and in the dock itself.
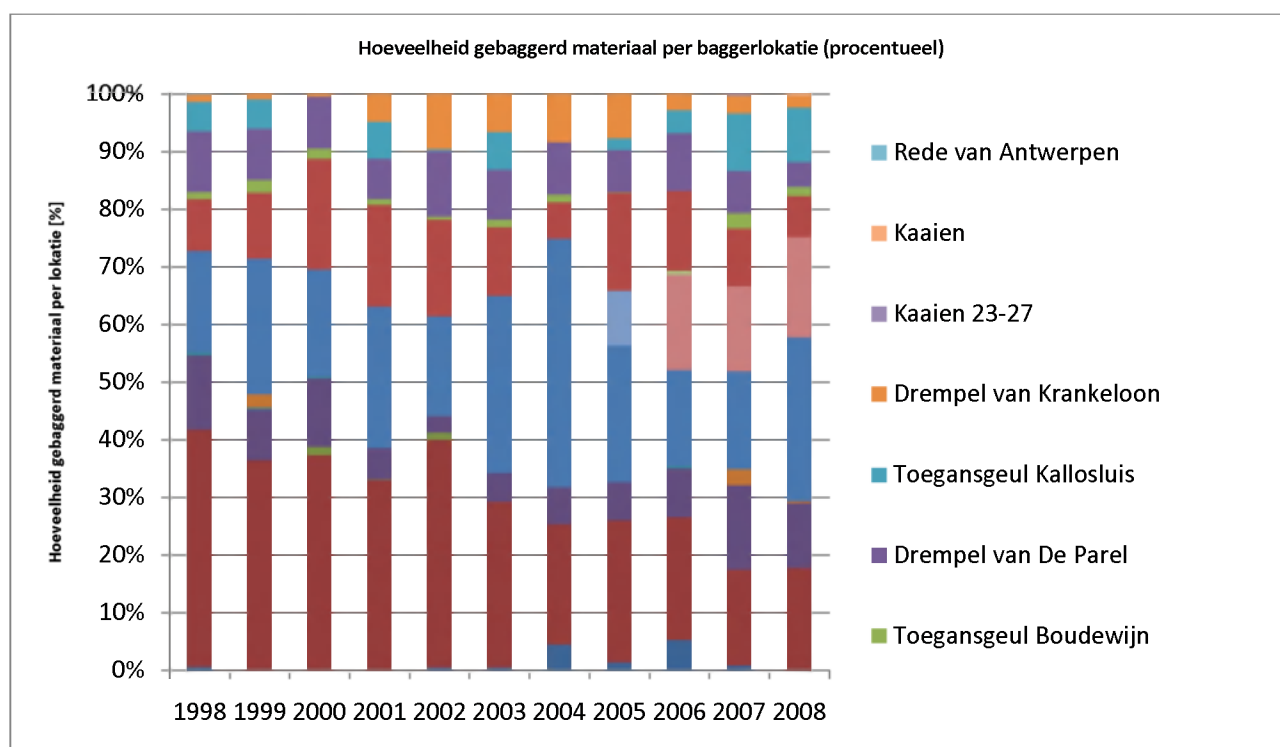
Figure 4.17: Relative importance of dredging locations during the period 1998-2008 (info AMT).

4.8.1.3.   Maintenance dredging in the access channels to the locks

Beside the maintenance dredging Works in the navigation channel along the Lower Sea Scheldt dredging activities take place in the access channels to the locks, in order to maintain the required depth for safe navigation (Table 4.3). This is done with sweepbeam techniques, a mechanical way of transporting mud near the bottom (Claessens and Marain 1988, Sas en Claessens 1988).

Table 4.3 Maintenance depth of locks in the Scheldt River

Lock	Maintenance depth (dm –LAT)
Zandvliet	128
Kallo	107
Boudewijn	97
Van Cauwelaert	91
Royers	57
Wintam	57

The dredged volume in these access channels accounts for around 15-20 % of the total dredged volume, with most important sedimentation in the access channel to Zandvliet- and Berendrecht lock and Kallosluis.

4.8.1.4.   The disposal areas

Table 4.4 gives an overview of the different relocation sites (Figure 4.18).
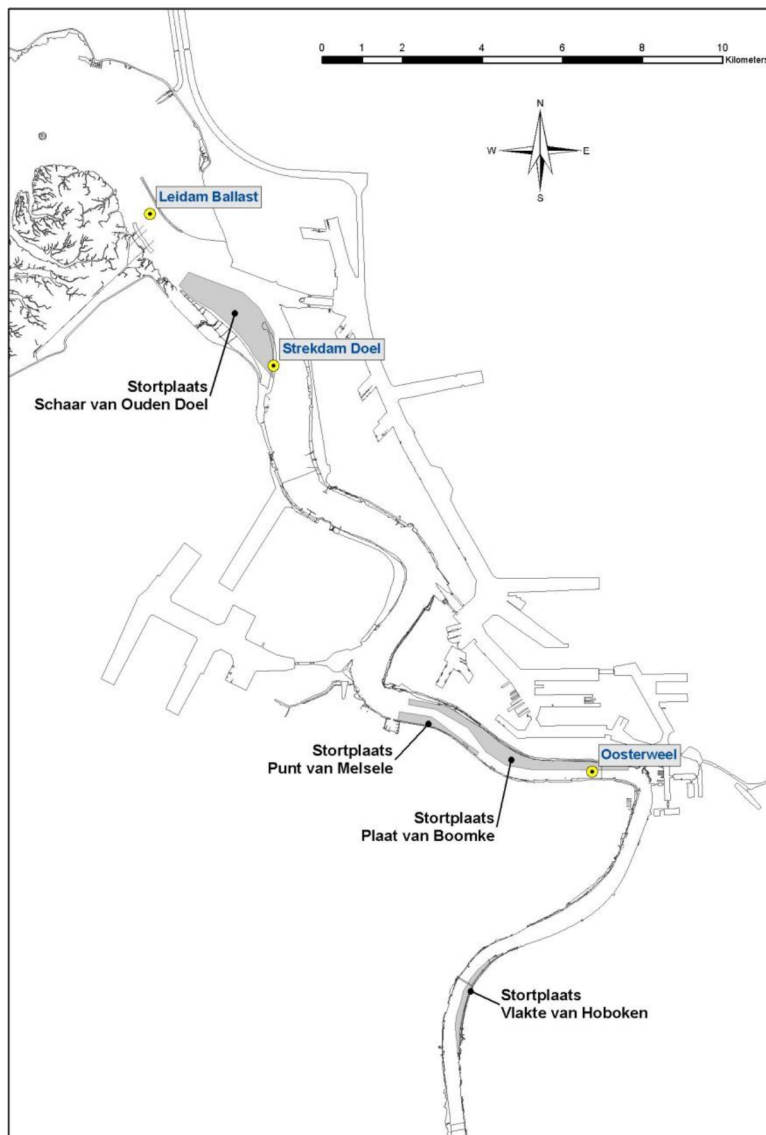
Figure 4.18: Relocation areas: Schaar van Ouden Doel, Plaat van Boomke, Punt van Melsele, Oosterweel, Vlakte van Hoboken

Since 1997-1998 the yearly average volume is around 3.5 million m^3.

Table 4.4: Deposited volumes (million m3) (1998-2008) (info AMT).

YEAR	Schaar van Ouden Doel	Plaat van Boomke	Others	Upstream Kruisschans	TOTAL
YEARLY DUMPED VOLUME (1998-2008) IN MILLION m3/YEAR					
1998	2,6	0,7	0,2	0,0	3,5
1999	2,3	1,2	0,2	0,0	3,6
2000	1,8	1,2	0,0	0,0	3,0
2001	0,6	2,7	0,8	0,0	4,1
2002	0,8	2,9	0,0	0,0	3,7
2003	0,9	2,3	0,2	0,0	3,4
2004	0,3	1,3	1,5	0,0	3,1
2005	1,8	1,8	0,3	0,0	3,8
2006	2,0	1,4	0,0	0,0	3,5
2007	1,1	1,8	0,0	0,0	2,9
2008	2,0	1,9	0,0	0,0	3,9
AVERAGE, MAXIMUM AND MINIMUM 1998-2008 (MILLION m3/YEAR)					
Average/year (1998-2008)	1,4	1,7	0,3	0,0	3,4
2008)	0,3	0,7	0,0	0,0	2,9
maximum (1998-2007)	2,6	2,9	1,5	0,0	4,1

Table 4.5 gives an indication of the monthly variability of the deposited volumes for the area Plaat van Boomke (inclusive of volumes in Punt van Melsele and Oosterweel) (AMT, 2002, 2003, 2004, 2005, 2006b, 2007 en 2008).

Table 4.5: Monthly deposited volumes (1000 m³) Plaat van Boomke (2002-2008)

PERIOD	2002	2003	2004	2005	2006	2007	2008
January	204	316	152	86	94	185	93
February	169	198	101	226	64	257	195
March	390	65	143	228	263	109	89
April	291	127	223	131	111	146	18
May	237	117	0	134	281	262	366
June	296	157	191	288	227	11	61
July	238	101	39	124	45	47	227
August	231	194	0	171	55	293	367
September	132	303	97	93	17	109	83
October	211	456	150	101	217	58	188
November	254	127	184	118	21	249	131
December	212	103	0	61	0	67	89
Total	**2865**	**2265**	**1279**	**1760**	**1396**	**1793**	**1906**
Punt van Melsele	445	596	219	0	0	519	826
Oosterweel			613	851	685	889	814

The dredged sediments can be classified in sandy material and muddy. The sandy material is deposited in the Schaar van Ouden Doel and muddy dredged material is deposited near Plaat van Boomke. From the analysis of the deposited volumes it can be concluded that there is a shift from

sandy towards more muddy dredged sediments. This tendency exists since about 25 years with a maximum between 2000 and 2003 (Figure 4.19).
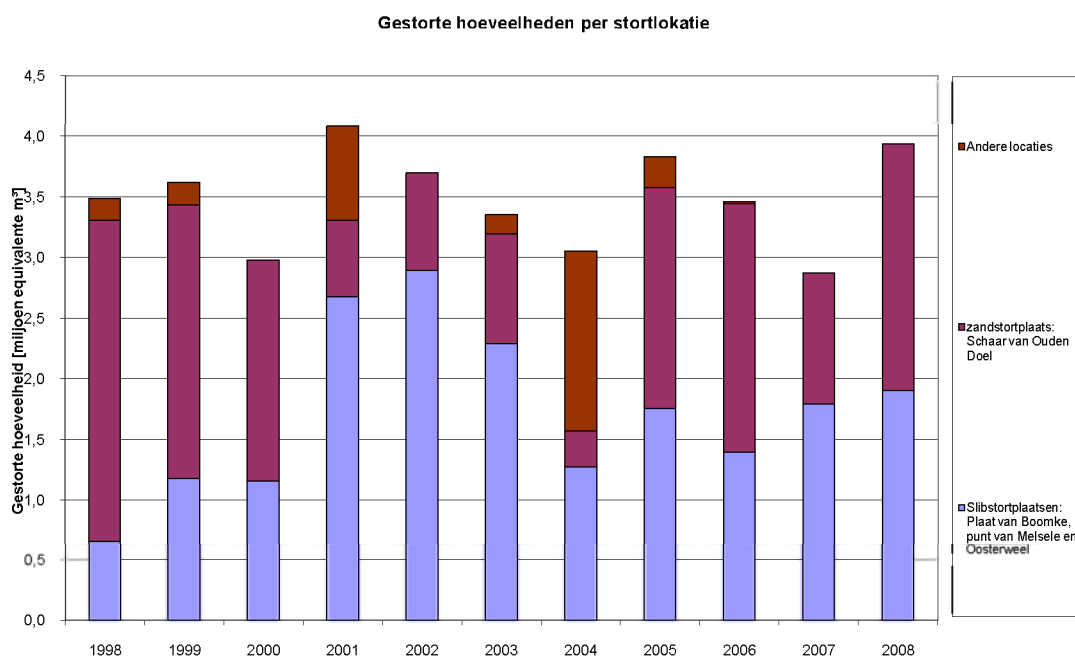
Figure 4.19: Deposited volumes (1998-2008) (info AMT)

The dredged material from the access channels amounts to around 20% of the total volume of dredged material. These sediments are very fine and are always deposited near Plaat van Boomke.

4.8.1.5.   Dredged material from Deurganckdok

Since the opening of Deurganckdok in July 2005 maintenance dredging works take place. Along the quay walls the required depth is maintained with sweep beam techniques, whereas in the central section of the sock hopper dredgers are used to dredge the deposited mud. The sedimentation process in Deurganckdok has been monitored and analysed (IMDC, 2009a). The total deposition is between 2.500.000 TDS (Tonnes dry solids) and 3.000.000 TDS from April 2006 to March 2009.

4.9.   Conclusions

The aim of this chapter was to determine the sediment transport mechanisms in the Lower Sea Scheldt. The main sediment transport mechanisms were concluded to be

1) Upstream-directed sediment transport by tidal maximum flow asymmetry in the lower reaches of the Lower Sea Scheldt, caused by higher flood velocities than ebb velocities.

2) Downstream-directed sediment transport by residual flow upstream of the ETM, approximately upstream of Kallo/Antwerp.

The result is a sediment transport convergence somewhere between Antwerp and the Deurganckdok.

Additional sediment transport mechanisms are:

1) Slack tide asymmetry upstream of Antwerp. The HW slack period is shorter than the LW slack period, resulting in a downstream-directed sediment transport.

2) Secondary flows that generate maximum turbidity on either the left bank or the right bank of the Lower Sea Scheldt. In some cases, the flow direction of this secondary flow corresponds to curvature-induced centripetal acceleration, resulting in near-bottom flows from the outer to the inner bends. However, in some cases this pattern may be reversed due to the longitudinal salinity gradient.

3) The effect of water level setup/setdown, and local wind or ship-generated waves is probably low.

5. MUD CONCENTRATION IN THE LOWER SEA SCHELDT

5.1. The turbidity maximum of the Scheldt

According to literature (Dyer, 1995; Verlaan, 1998) a zone exists in meso- and macrotidal estuaries with higher fine suspended sediment concentrations. To create a persistent turbidity maximum zone the current velocities must be high enough to keep sediments in suspension. The Estuarine Turbidity Maximum (ETM) is usually situated upstream of the saline intrusion boundary, corresponding to salinity values of around 1-5 g/l. for the Lower Sea Scheldt this would imply that at the end of the summer (dry season) when the salinity increases to more than 5 g/l near Oosterweel, the turbidity maximum zone is situated upstream of Oosterweel, whereas during very rainy periods the ETM can move down-estuary near Prosperpolder (e.g. September '98) (Fettweis et al. 1999)..

During the analysis of the long term measurements near Deurganckdok (April 2006-March 2009), it was found that the ETM is situated near Deurganckdok during periods of high runoff (IMDC, 2009a).

These results confirm the findings of Wollast en Marijns (1981) who demonstrated that the ETM is situated nearly 110 km (St. Amands) from the mouth of the estuary during dry periods and around 50 km (between Prosperpolder and Bath) during wet periods.

An illustration of the ETM is given in (*Figure 5.1*).
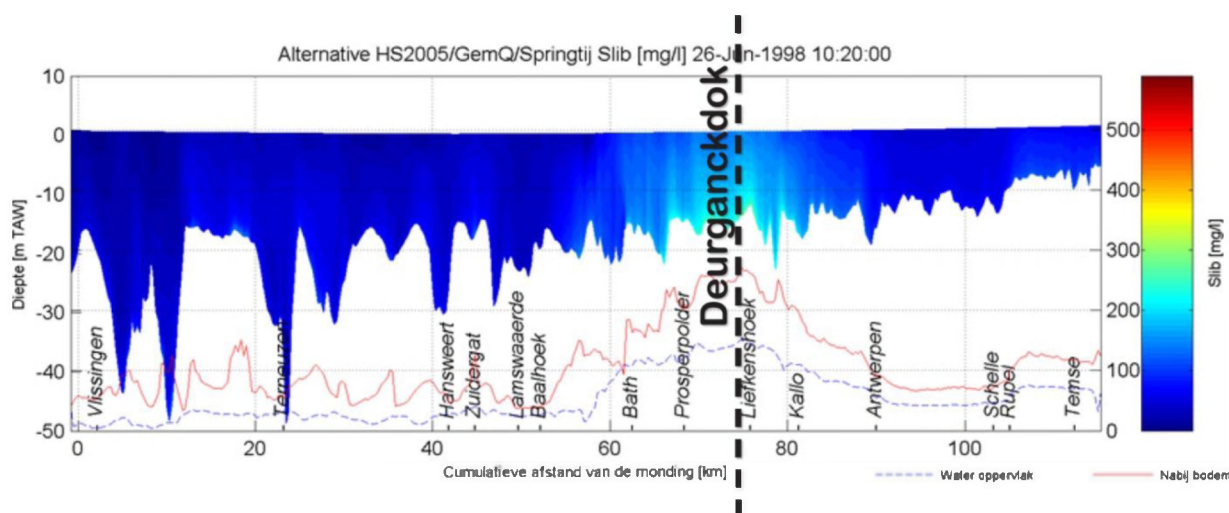
Figure 5.1: ETM during maximum ebb current (springtide and average fresh water input)

The correlation between the fresh water input from the catchment and the suspended sediment concentration has been analyzed near Prosperpolder during the campaigns of September 1992 – December 1993 (Fettweis et al., 1997 and 1998a, 1998b). Also during the measurements (2005-2009) for Deurganckdok this correlation has been found.

The variability of turbidity (and suspended sediment concentration) is illustrated from the observations of suspended matter, executed in the framework of OMES (Figure 5.2) (Van Damme, 2005). Figure 5.2 illustrates the suspended matter in the top part of the water column during the period 2002-2007 (Chen et al., 2008). It is remarkable to see that the zone with high

concentrations has shifted upstream over the years. During the same period the sediment flux has been determined (Figure 5.3) (Maris et al., 2008).
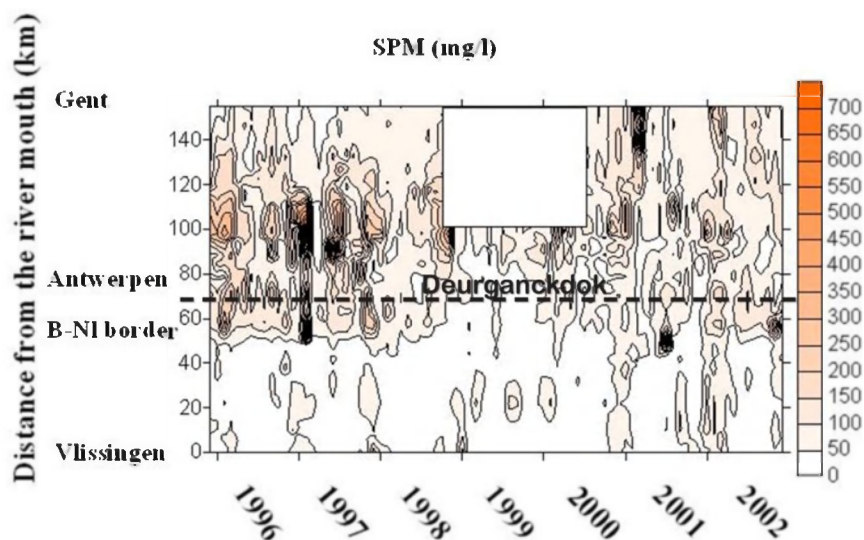
Figure 5.2: Variability of suspended matter along the Scheldt 1996-2002 (Van Damme et al., 2005)
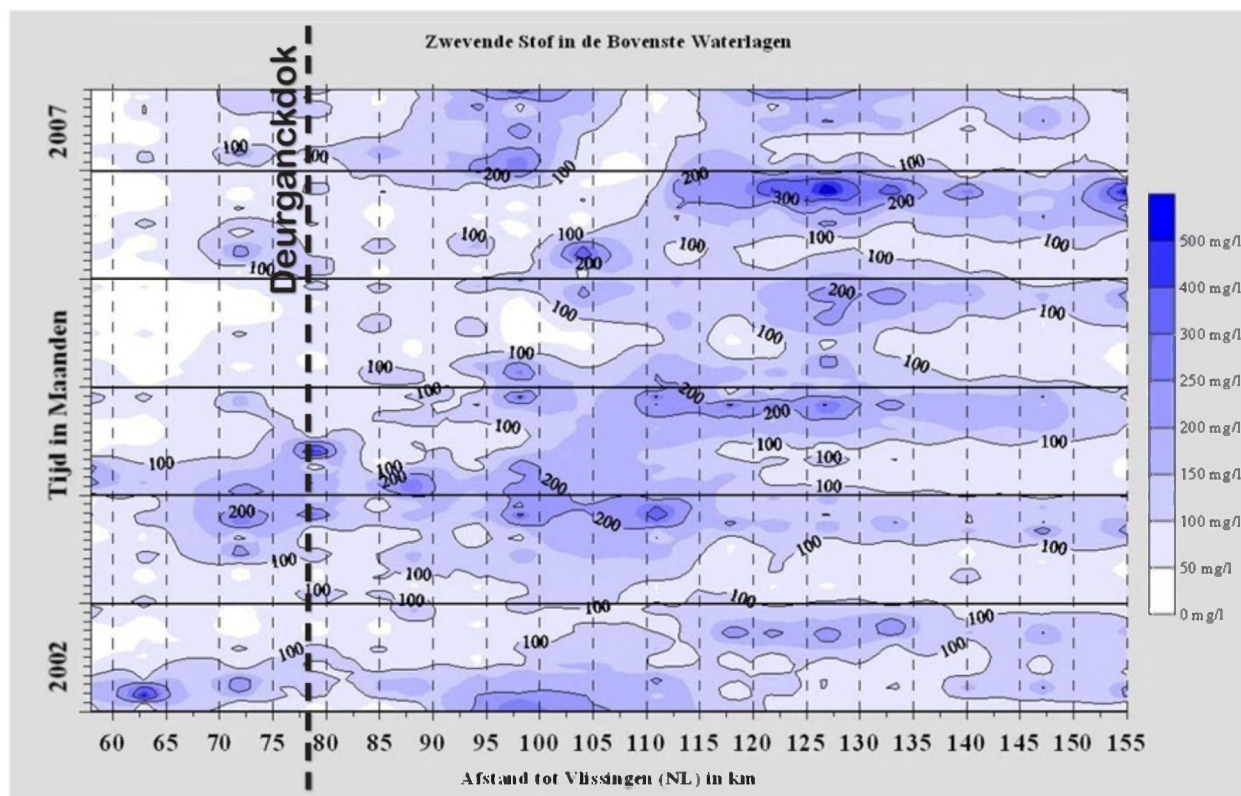
Figure 5.3: Variability of suspended matter along the Scheldt 2002-2007 (Chen et al., 2008)
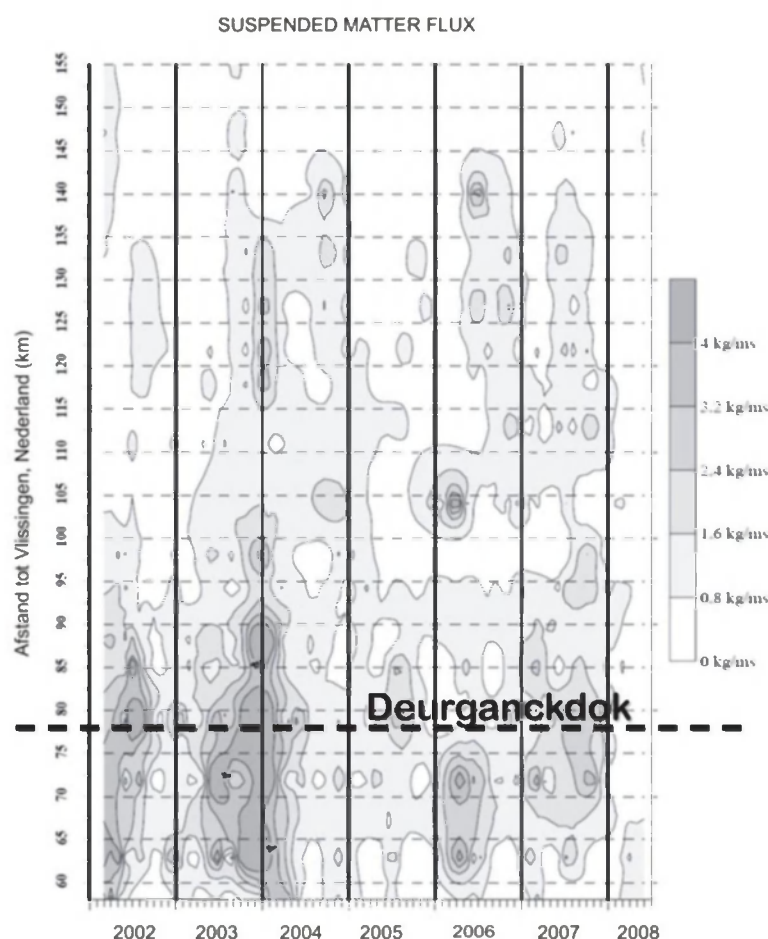
Figure 5.4: Variability of suspended matter along the Scheldt 2002-2008(kg/(m.s) (based on Maris et al., 2008)

5.2. Variability in time of the sediment concentration

The suspended sediment concentration shows a pronounced variation over time. The most important cycles for the suspended sediment concentration are the intra-tidal, the spring-neap, and the seasonal variation. The formation of HCBS depends on the ambient sediment concentration and flow velocity (elaborated in section 7.3), and therefore HCBS may only form during specific parts of these cycles. This section provides an overview of the variation of typical sediment concentrations on the Scheldt throughout the tidal (section 5.2.1), spring-neap (section 5.2.2), and seasonal (section 5.2.3) cycle.

5.2.1. Tidal variation

During the tidal cycle the suspended sediment concentration can vary significantly. This is illustrated with the data from the trough tide measurements (11/03/2008) along a transect just downstream of Deurganckdok (transect K) (IMDC, 2008i). It should be noted that these measurements were made during extreme high water conditions.
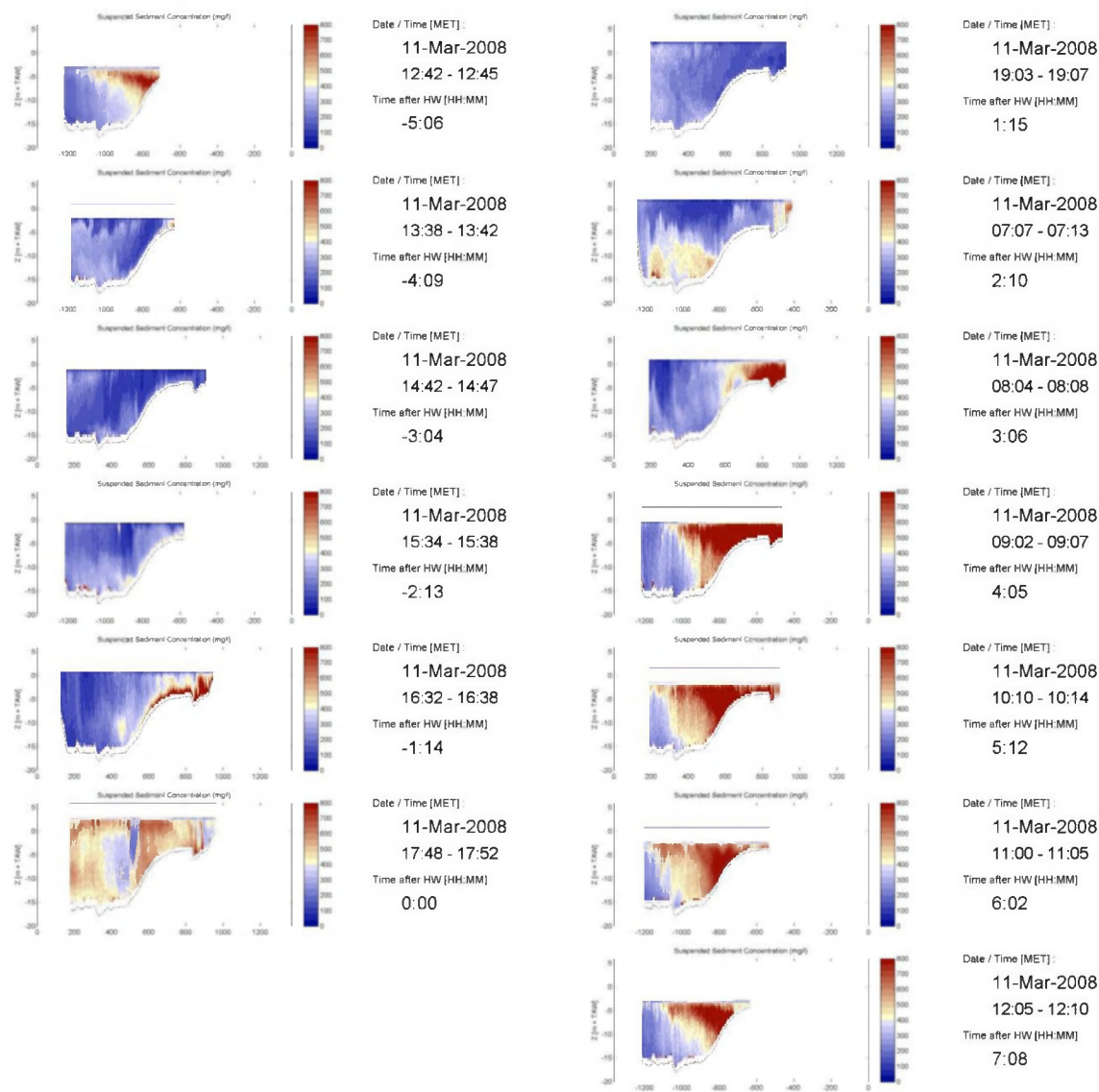
Figure 5.5: Variation of suspended sediment concentration downstream of Deurganckdok – transect K during tidal cycle (IMDC, 2008i).
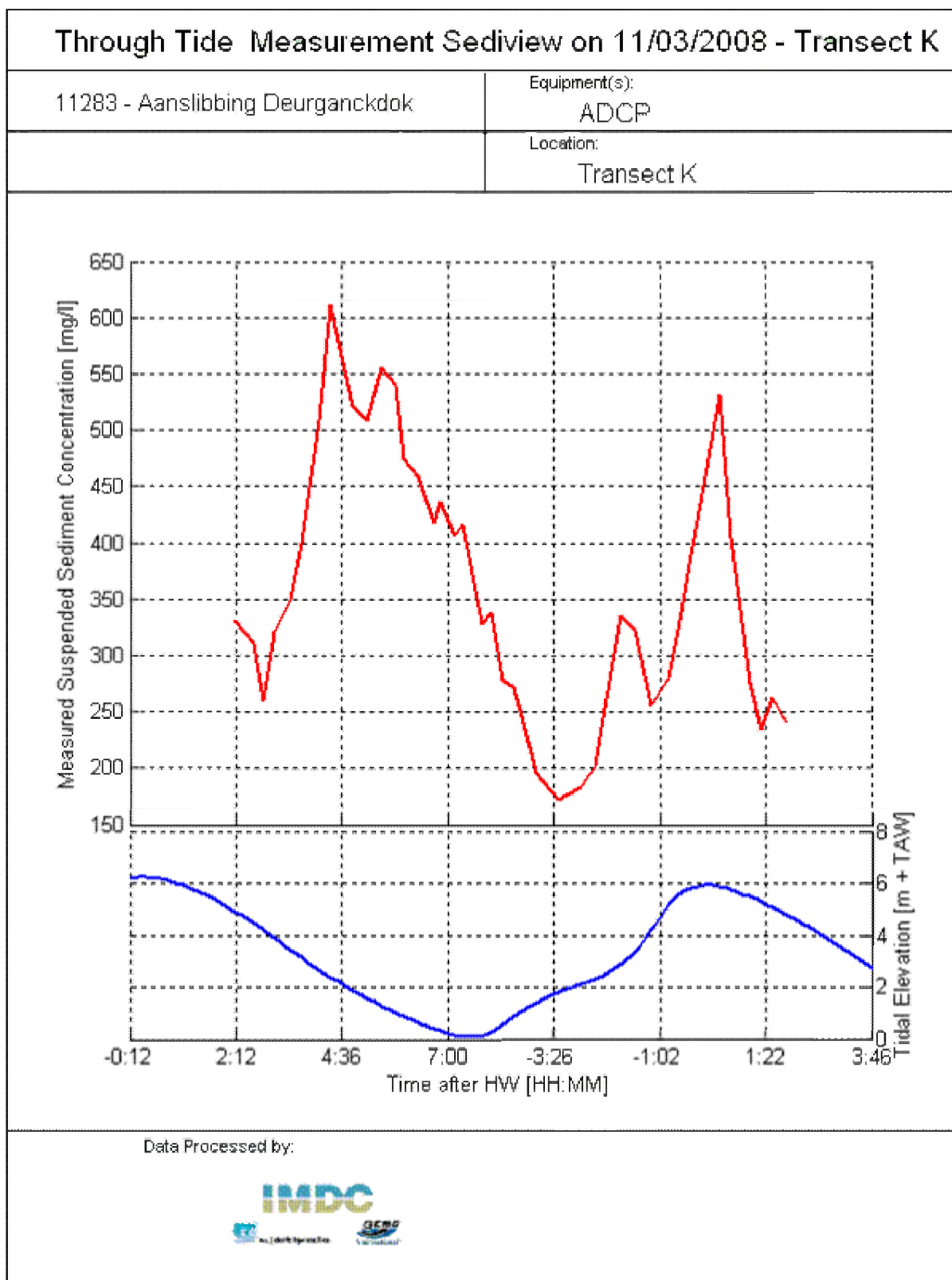
Figure 5.6: Variation of suspended sediment concentration (average of cross section) during tidal cycle (IMDC, 2008i).

During the long term stationary measurements near Buoy 84, buoy 97 and Oosterweel (2005-2008) (IMDC, 2007c), (IMDC, 2008q), the following data were recorded.

Table 5.1: Average ebb phase suspended sediment concentration (mg/l) for an averaged neap, average and spring tide.

| | | 2005 | | | | 2006 | | | | | | | | | | | | 2007 | | |
		sep	okt	nov	dec	jan	feb	mar	apr	may	jun	jul	aug	sep	okt	nov	dec	jan	feb	mar
Buoy 84 (-5.6m TAW)	doodtij	-	114	172	-	149	112	311	200	230	124	106	66	88	89	89	112	134	270	112
	gem tij	-	154	197	-	176	148	399	306	306	164	147	85	95	186	121	113	174	492	208
	springtij	-	178	211	-	211	231	632	509	285	197	128	110	121	252	115	143	271	503	332
Buoy 84 (-8.1m TAW)	doodtij	-	168	255	-	203	233	479	459	467	308	323	109	166	175	190	202	248	454	238
	gem tij	-	221	272	-	240	252	618	663	612	413	346	186	173	355	236	204	285	758	499
	springtij	-	236	295	-	268	335	901	814	596	439	295	220	278	426	223	238	372	855	662
Buoy 97 (-5.3m TAW)	doodtij	-	112	151	186	169	234	462	257	362	178	183	101	140	148	112	199	216	352	346
	gem tij	-	148	187	191	201	204	560	398	437	265	136	119	124	333	156	186	301	601	476
	springtij	-	166	195	209	215	308	697	542	385	303	140	146	201	341	162	199	419	604	512
Buoy 97 (-7.8m TAW)	doodtij	-	186	243	278	234	305	572	413	592	261	255	134	181	222	136	251	399	396	320
	gem tij	-	239	288	289	274	257	668	592	620	389	209	151	160	473	205	236	572	780	461
	springtij	-	273	299	318	297	344	847	871	565	454	236	225	292	508	243	233	727	780	553
Oosterweel (-2.3 TAW)	doodtij	-	-	-	-	93	164	229	143	190	128	78	64	78	135	130	127	155	198	114
	gem tij	-	-	-	-	142	136	258	192	218	190	89	99	105	248	152	138	185	286	193
	springtij	-	-	-	-	149	192	306	208	199	197	113	122	-	246	155	157	228	285	202
Oosterweel (-5.8m TAW)	doodtij	-	-	-	-	181	107	290	184	256	-	94	80	91	118	150	152	159	231	214
	gem tij	-	-	-	-	206	150	345	239	281	229	109	114	119	228	171	153	184	426	284
	springtij	-	-	-	-	225	203	386	262	245	219	119	141	-	316	168	157	287	419	293

| | | 2007 | | | | | | | | | 2008 | | | |
		Apr	May	Jun	Jul	Aug	Sep	Oct	Nov	Dec	Jan	Feb	Mar	Year
Buoy 84 (-8.1 m TAW)	Neap tide	256	176	139	180	239	-	134	216	331	162	-	265	210
	Avg tide	549	201	187	211	281	398	214	333	351	367	-	338	279
	Spring tide	612	289	218	226	342	449	276	524	346	-	-	437	365
Buoy 84 (-5.6 m TAW)	Neap tide	119	100	111	104	176	112	105	164	248	128	258	146	148
	Avg tide	287	122	117	132	216	189	156	256	256	231	324	312	200
	Spring tide	377	182	121	147	287	258	214	416	266	292	-	439	285
Buoy 97 (-7.8 m TAW)	Neap tide	428	365	150	120	325	135	126	234	407	221	436	366	277
	Avg tide	581	413	226	181	371	321	176	442	367	373	510	547	357
	Spring tide	613	620	286	211	560	476	271	883	361	447	544	816	536
Buoy 97 (-5.3 m TAW)	Neap tide	313	242	169	162	285	162	171	229	313	169	379	239	237
	Avg tide	342	256	195	207	319	276	224	286	265	292	456	435	275
	Spring tide	391	312	245	219	360	333	293	278	272	346	484	722	390
Oosterweel (- 5.8 m TAW)	Neap tide	219	-	-	34	271	154	-	-	255	107	473	156	208
	Avg tide	248	-	-	71	225	244	-	-	319	278	460	319	279
	Spring tide	267	-	-	56	286	274	-	-	427	276	579	476	358
Oosterweel (- 2.3 m TAW)	Neap tide	162	160	-	-	136	100	59	137	201	52	318	88	131
	Avg tide	188	159	-	51	162	175	68	471	190	191	343	183	191
	Spring tide	218	167	-	44	211	201	75	730	165	206	402	321	284

Table 5.2: Average flood phase suspended sediment concentration (mg/l) for an averaged neap, average and spring tide.

		2005				2006												2007		
		sep	okt	nov	dec	jan	feb	mar	apr	may	jun	jul	aug	sep	okt	nov	dec	jan	feb	mar
Buoy 84 (-5.6m TAW)	doodtij	-	97	133	-	116	68	140	102	82	59	45	40	44	48	61	72	96	136	80
	gem tij	-	139	171	-	153	114	221	151	158	100	78	56	70	120	91	93	131	297	149
	springtij	-	156	181	-	183	180	348	229	166	126	87	76	78	164	97	115	201	330	228
Buoy 84 (-8.1m TAW)	doodtij	-	161	215	-	184	139	305	293	265	152	137	87	103	119	156	143	205	266	183
	gem tij	-	209	263	-	232	224	444	463	413	268	215	141	136	254	202	167	224	571	372
	springtij	-	231	275	-	278	320	638	662	457	318	220	178	235	332	216	195	316	677	501
Buoy 97 (-5.3m TAW)	doodtij	-	80	105	119	107	85	175	126	147	84	67	47	53	66	66	122	108	115	146
	gem tij	-	102	123	126	123	109	240	151	177	121	70	56	66	128	85	128	175	237	208
	springtij	-	113	133	141	139	181	354	236	160	118	77	70	103	150	89	143	224	243	255
Buoy 97 (-7.8m TAW)	doodtij	-	187	223	254	221	145	338	249	298	141	146	90	117	135	125	227	290	222	218
	gem tij	-	235	264	260	253	192	445	338	342	232	152	103	130	269	177	212	422	549	331
	springtij	-	265	268	298	263	317	666	490	312	248	171	144	228	332	200	211	472	619	411
Oosterweel (-2.3 TAW)	doodtij	-	-	-	-	132	149	242	175	242	159	105	100	107	181	165	138	154	202	95
	gem tij	-	-	-	-	175	149	255	209	260	228	108	136	112	296	186	147	184	279	154
	springtij	-	-	-	-	176	212	303	236	241	255	140	162	-	290	176	138	204	276	153
Oosterweel (-5.8m TAW)	doodtij	-	-	-	-	209	129	286	198	289	-	113	111	112	136	179	170	140	201	159
	gem tij	-	-	-	-	225	165	304	229	309	266	117	143	127	266	200	161	175	357	199
	springtij	-	-	-	-	240	225	359	274	273	285	154	173	-	369	183	167	223	358	198

		2007 Apr	May	Jun	Jul	Aug	Sep	Oct	Nov	Dec	2007 Jan	Feb	Mar	Year
Buoy 84 (-8.1 m TAW)	Neap tide	175	125	97	133	143	-	112	157	270	120	-	227	155
	Avg tide	479	186	164	191	228	331	196	277	294	267	-	329	237
	Spring tide	520	248	193	204	291	373	250	434	312	-	-	363	313
Buoy 84 (-5.6 m TAW)	Neap tide	78	71	-	81	74	68	71	102	170	98	181	93	95
	Avg tide	194	95	89	110	136	128	123	175	196	180	224	190	146
	Spring tide	256	142	94	120	189	183	171	295	214	224	-	273	202
Buoy 97 (-7.8 m TAW)	Neap tide	189	181	148	113	158	106	109	157	267	200	307	240	185
	Avg tide	313	248	181	153	241	242	157	315	282	307	419	350	258
	Spring tide	409	311	268	165	368	331	232	574	319	371	485	569	384
Buoy 97 (-5.3 m TAW)	Neap tide	153	130	113	114	133	104	107	141	125	100	129	74	117
	Avg tide	201	150	122	137	185	179	138	186	135	160	202	144	153
	Spring tide	240	187	158	141	220	201	199	183	152	195	270	347	223
Oosterweel (- 5.8 m TAW)	Neap tide	221	-	-	60	309	206	-	-	190	172	397	129	213
	Avg tide	254	-	-	90	284	317	-	-	190	268	414	206	262
	Spring tide	274	-	-	100	349	362	-	-	136	239	490	357	344
Oosterweel (- 2.3 m TAW)	Neap tide	196	311	-	-	215	170	105	222	228	73	328	103	175
	Avg tide	232	302	-	77	241	268	103	588	159	209	377	156	226
	Spring tide	244	339	-	79	343	301	122	844	143	219	391	298	320

Also the through tide measurements near Zandvliet (IMDC-WLB, 1992a; Fettweis et al., 1994) revealed that mud in suspension has a different behaviour and thus different concentration values during flood and ebb. This is due to differences in velocity pattern and velocity profile during flood and ebb.

In the Lower Sea Scheldt the ratio of the time averaged suspended sediment concentration during ebb and flood depends strongly on the location: downstream near Prosperpolder the ratio ranges between 0.5 and 0.9, whereas near Deurganckdok (buoy 84 and 97) the ebb concentration is 1 to 2 times higher than the flood concentration and finally in the vicinity of Oosterweel the ratio ranges again between 0.7 and 0.95.

5.2.2. Spring-neap variation

The velocity pattern during a neap tide is different from the one during a spring tide. The flow during flood is also qualitatively different for a spring tide and a neap tide. During a spring tide the flood velocities are more asymmetric and they display a distinct double peak. During a neap tide the flood course of the velocity occurs more gradually. This means that along neap tide-spring tide cycle the peak flood velocities relatively increases in a more pronounced way than the peak ebb velocities, hence resulting in a relatively higher erosion of sediment during a spring tide flood than during a neap tide flood. For a number of through tide measurements just downstream of Deurganckdok (transect K) the (average) suspended sediment concentration (over the cross section) is illustrated in (Figure 5.8). (IMDC, 2008i).
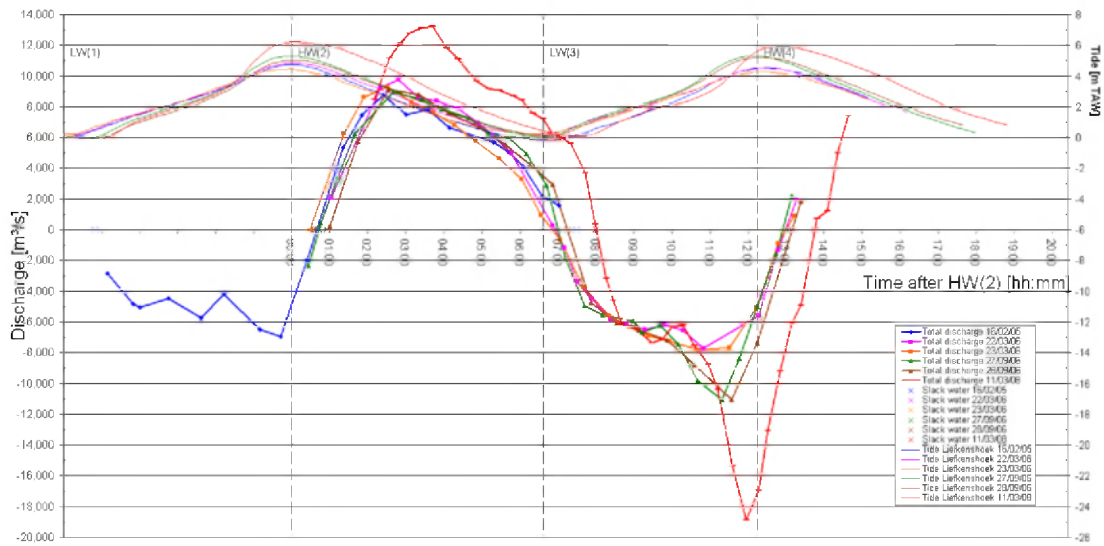
Figure 5.7: Total discharge on 16/02/2005 (Neap tide), 22/03/2006 (Neap tide), 23/09/2006 (Neap tide), 27/09/2006 (Average tide), 28/09/2006 (Average tide) & 11/03/2008 (Spring tide)
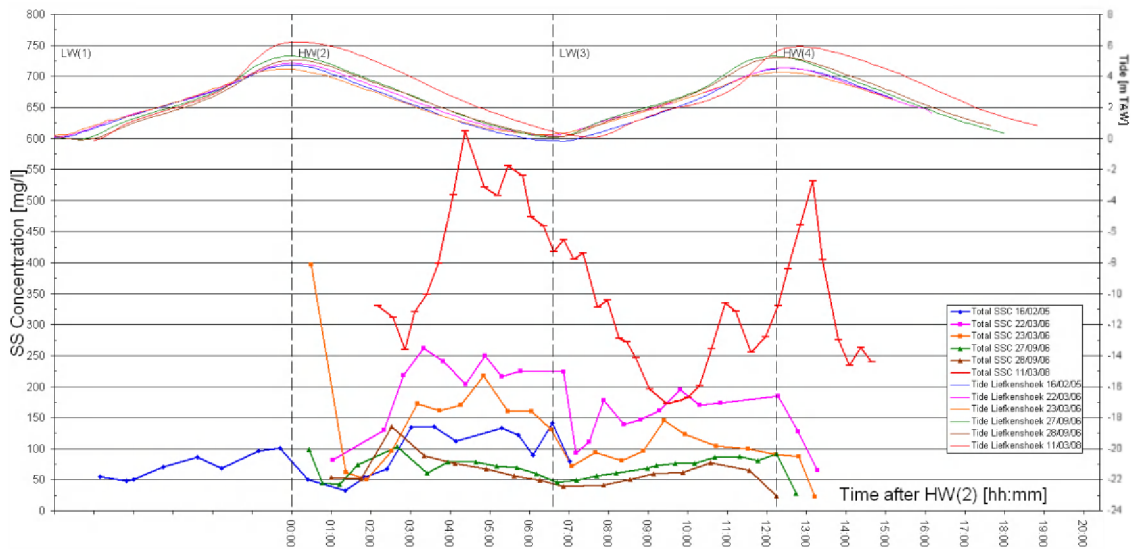
Figure 5.8: SS Concentration 16/02/2005 (Neap tide), 22/03/2006 (Neap tide), 23/09/2006 (Neap tide), 27/09/2006 (Average tide), 28/09/2006 (Average tide) & 11/03/2008 (Spring tide)

Table 5.3: Suspended solids during ebb, flood and measurement campaign on 16/02/2005 (Neap tide), 22/03/2006 (Neap tide), 23/09/2006 (Neap tide), 27/09/2006 (Average tide), 28/09/2006 (Average tide) & 11/03/2008 (Spring tide)

Measurement Day		16/02/'05	22/03/'06	23/03/'06	27/09/'06	28/09/'06	11/03/'08
Tidal coefficient		**0.94**	**0.87**	**0.80**	**1.02**	**0.98**	**1.16**
Ebb	SS Mass [Tonnes]	13 217	27 455	17 301	9 908	10 542	88 476
	SSC [mg/l]	100	202	131	71	78	417
	Tidal Difference [m]	4.95	4.68	4.22	5.26	4.94	6.14
Flood	SS Mass [Tonnes]	-7 386	-19 508	-12 653	-9 843	-8 629	-52 743
	SSC [mg/l]	77	167	105	73	61	297
	Tidal Difference [m]	4.68	4.38	4.06	5.24	5.12	5.85
Net	SS Mass [Tonnes]	5 830	7 947	4 648	64	1 913	35 733
	Duration [HH:MM]	12:40	12:30	12:36	12:14	12:12	12:50

From the stationary measurements (2005-2008) the following conclusions can be drawn:

- In Buoy 84, for instance, the average sediment concentration during a spring tide is 90 to 100% higher than during a neap tide and the increase can mainly be felt during flood (100% and 115%) than during ebb (around 90%).

- In Buoy 97, the increase between neap and spring tide is also larger at flood than at ebb but in a less distinct way (100% and 74% for the lower and upper instrument, 107% and 94% during flood and 93% and 64% for ebb).

The increase in sediment concentration between neap tide and spring is felt in a more pronounced way at the bottom stations during the winter (see also Figure 5.9 andFigure 5.10). In summer, the increase along the cycle is identical for the lower and higher stations.

The neap-spring vaiation of sediment concentration in the Scheldt is also implemented in the siltation model for Deurganckdok as described in secion 4.4 of (IMDC, 2009o).

5.2.3. Seasonal effects

The sediment properties in the Scheldt vary seasonally through:

- An increased sediment resuspension of sediment sored on the mud flats in winter by wind-generated waves in the Scheldt estuary, which is subsequently transported upstream by tidal asymmetry;
- An increased fluvial sediment supply in winter;
- Lower erosion rates in summer due to strengthening of mud deposits by algae
- Higher settling velocities in summer due to increased floc formation

The combination of these processes lead to lower sediment concentrations from June to December, and higher concentrations from December to June (see figures below). This seasonal variation is further complified by shifts in the Estuarine Turbidity Maximum (ETM): a time-variation in SSC on a specific location may therefore reflect an overall increase / decrease in SSC (related

to the seasonal effects described above) but may also be the result of a changing location of the ETM (mainly due to discharge variations, see section 5.1).
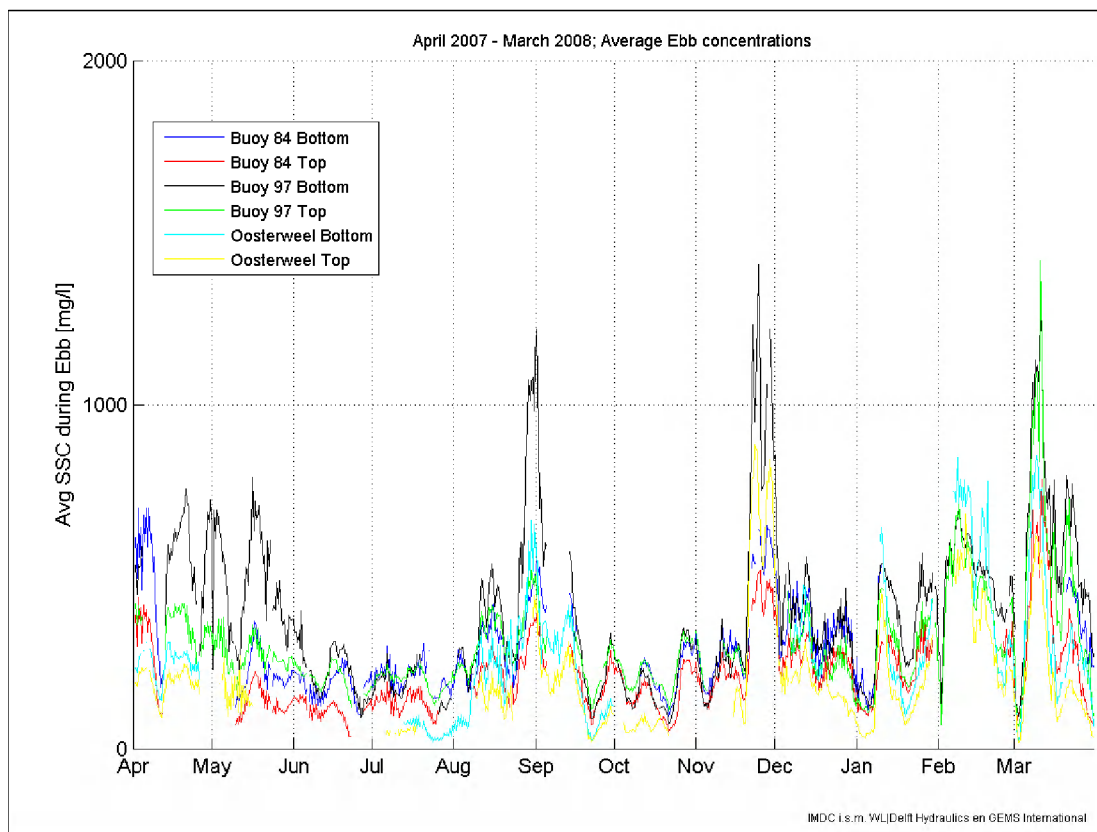
Figure 5.9: Tidally averaged sediment concentrations during Ebb in all measurement stations. April 2007 to March 2008.
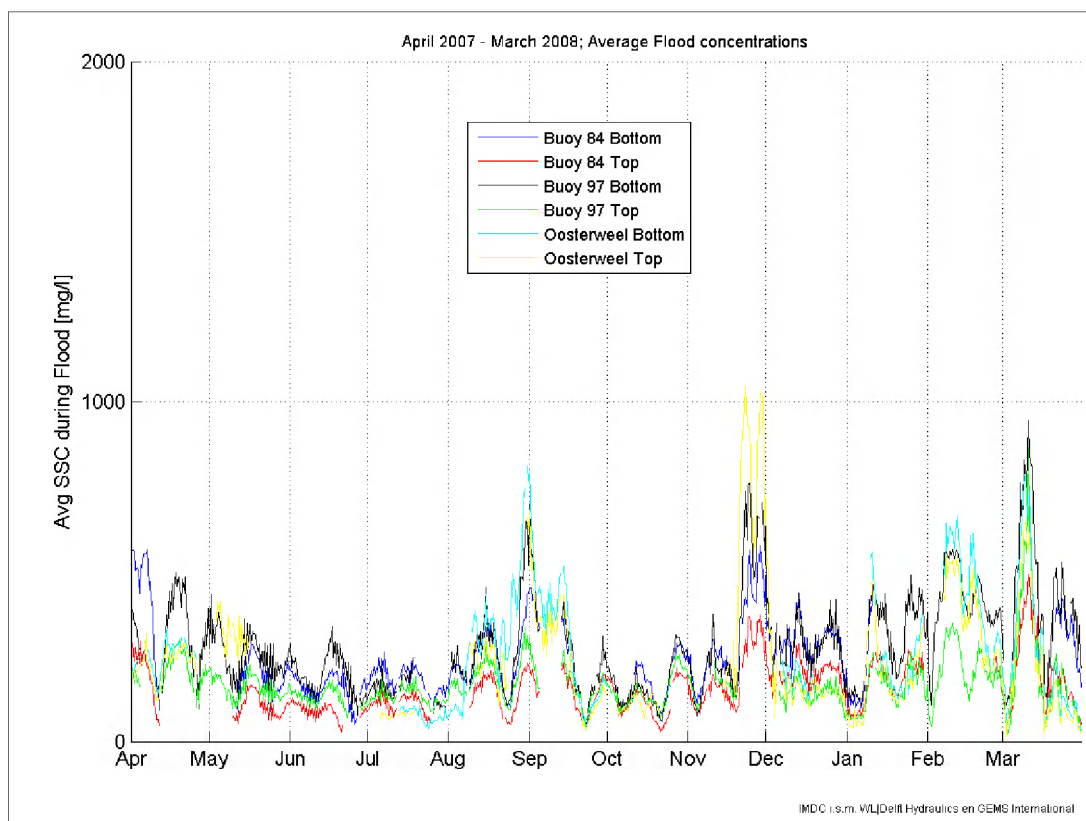
Figure 5.10: Tidally averaged sediment concentrations during Flood in all measurement stations. April 2007 to March 2008.

6. EXCHANGE MECHANISMS

In this chapter the exchange mechanisms for water and sediment are discussed that may occur between an estuary and a tidal dock. First, these mechanisms are discussed from a theoretical point of view. Second, field observations and model simulations for the exchange at Kallo sluice are discussed concisely. Finally, the exchange mechanisms at Deurganckdok are discussed comprehensively, including the effect of seasonal variations and flocculation. Conclusions on the exchange of sediment between the Scheldt and the tidal dock are formulated.

6.1. Processes

Three mechanisms govern the water exchange between the basin and the river (Winterwerp, 2005, see (Figure 6.1):

- Tidal filling and emptying of the basin;

- An eddy in the entrance of the basin;

- A density driven exchange flow resulting from density differences between the estuary and the basin.
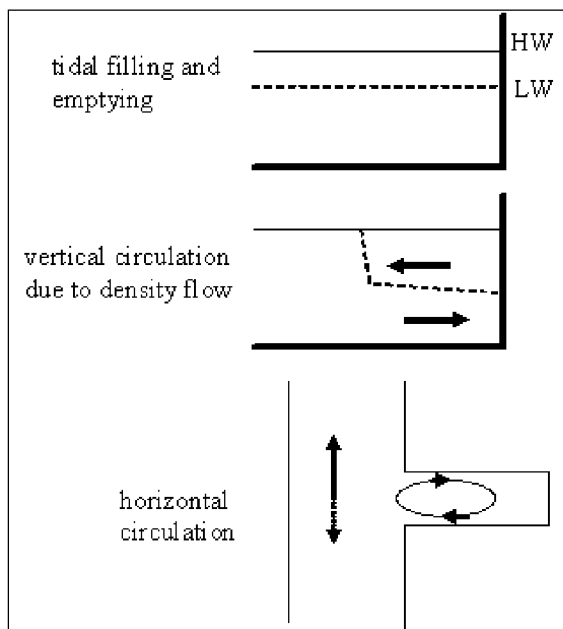
Figure 6.1: Schematised exchange processes between a dock and estuary.

6.1.1. Tidal filling and emptying

The water volume in the basin between HW and LW is imported during rising tide and exported during falling tide via the entrance; these phases have a duration of about half the tidal period.

Therefore the order of magnitude of the flow velocity u_t in the entrance of the basin due to tidal filling and emptying can be estimated as:

$$u_t = \frac{2A_b H}{A_c T}$$

A_b = surface area of the basin

H = difference between HW and LW.

A_c = cross-sectional area of the entrance of the basin,

T = Tidal period, approximately 45,000 sec.

6.1.2. Horizontal entrainment and eddy formation

River flow separates at the upstream corner of the harbour dock, and a turbulent mixing layer forms between harbour dock and the river, which hits the opposite, downstream corner of the dock. The strength of this mixing layer is governed by the geometry of the upstream corner and the stagnation behaviour of the downstream corner (Winterwerp, 2005). In case of steady, uniform river flow, the exchange flow between the dock and the river through a large-scale eddy increases linearly with the river flow velocity. However, in estuarine settings, the mixing layer will be advected into the harbour by tidal filling and by density-driven flow. The depth-averaged horizontal entrainment will therefore be maximal during maximal tidal filling, which is halfway the flood. However, the advection of the eddy by the density-driven current may be more important. Especially the advection of the eddy during near-bed inflow may substantially contribute to net sediment import. Assuming a well-mixed harbour dock, maximum near-bed inflow due to density currents is expected around HW (see the next section). Therefore the import of sediment due to horizontal entrainment (in combination with density-driven flow and tidal filling) is expected to be highest from halfway the flood (maximum effect tidal filling) to HW (maximum effect density-driven flow).

6.1.3. Density-driven exchange flows

The density current between a dock and an estuary is driven by horizontal gradients (between the dock and the estuary) in the vertical density distribution (and therefore the hydrostatic pressure distribution). When the salinity in the estuary is higher than in the dock, the near-bed hydrostatic pressure P ($P = \rho g h$) is highest in the estuary. This results in inflow of saline water into the dock in the lower half of the water column, which is compensated by outflow of less dense surface water. This flow pattern is reversed when the salinity in the dock is higher than in the estuary. When the water masses in the dock and the estuary are fully mixed, near-bed inflow is therefore to be expected from halfway the flood to halfway the ebb, compensated by outflow near-surface. However, the density-driven exchange flows are more complex when the dock is more strongly stratified than the estuary. This situation probably occurs in most estuarine settings because mixing rates in the dock are generally much lower than in the estuary. Near-bed water is then more saline than near the surface, and therefore the residual bottom currents are directed outward whereas residual near-surface currents are directed into the dock.

A theoretical estimate of the propagation velocity of the front of a fresh water plume in a two-layer flow (u_f) is given by Kranenburg (1996):

$$u_f = \left(\varepsilon g \frac{h_1}{h} \frac{(h-h_1)(2h-h_1)}{(1-B_1)h_1 + (1+B_1)h} \right)^{1/2}$$

where h_1 is the thickness of the upper layer, h_2 the thickness of the lower layer, and h the total depth. The relative density ε is given by $(\rho_1-\rho_2)/\rho$, with ρ being the density, and B_1 is a friction coefficient.

6.2. Measurements and simulations Kallosluis

Extensive measurements were carried out at Kallo sluice in 2002, and additional measurements were done during the HCBS1 campaign. The 2002 measurements were used to calibrate the hydrodynamics of the 3D mud model, as described by Wang et al. (2005).

The field data and the model results show that even in the macro-tidal Scheldt, the density-flow-induced vertical circulation is the most important mechanism for exchanging water and sediment between harbour basins and the estuary. The flow velocity due to tidal filling and emptying (about 2 cm/s) is much smaller in magnitude compared to the flow velocity due to the other two mechanisms, which are an order of magnitude higher.

The horizontal circulation generates flow velocities of similar order of magnitude as the density driven vertical circulation, as indicated by the model results, as well as the field measurements. The measured velocities in the eddy are 20 - 30 cm/s (Figure 6.2) and (Figure 6.3). The spatial variation of the horizontal eddy is illustrated in (Figure 6.3). However, horizontal circulation driven by ebb flow appears only to be important during a short time around the LW, just before the LWS.

The vertical density-driven circulation, occurring during the whole flood period, is the most important mechanism for the water exchange between the basin and the estuary (Figure 6.2). The flow through the entrance of the basin is stratified during rising tide, but during falling tide outflow is occurring over the entire water depth. The salinity structure on the other hand shows stratification in the basin almost throughout the whole tidal period. In the river, outside the basin, the salinity shows a well-mixed uniform vertical distribution during most part of the time. Only around the slack waters some stratification occurs. Field observations combined with the modelling results show that this is partly due to the exchange with the basin, because of its stratification and different salinity. This circulation causes inflow in the bottom layer, where the sediment concentration is usually higher. Therefore the density driven vertical circulation is an important mechanism for the sediment import into the basin. Compared with the contribution of tidal filling and the effect of a horizontal eddy, the density-driven flow is probably the most important mechanism for sediment import.

Unfortunately, no sediment concentration measurements are available for the entire tidal cycle. In the 2002 campaigns, backscatter from the ADCP nor OBS sensors on the the CTD were applied. In 2005, point concentration measurements were made during the ebb, whereas ADCP backscatter was recorded at different transects at different phases of the tidal cycle. Hence, a dataset describing the sediment concentration variation near the Kallo sluices is not available.
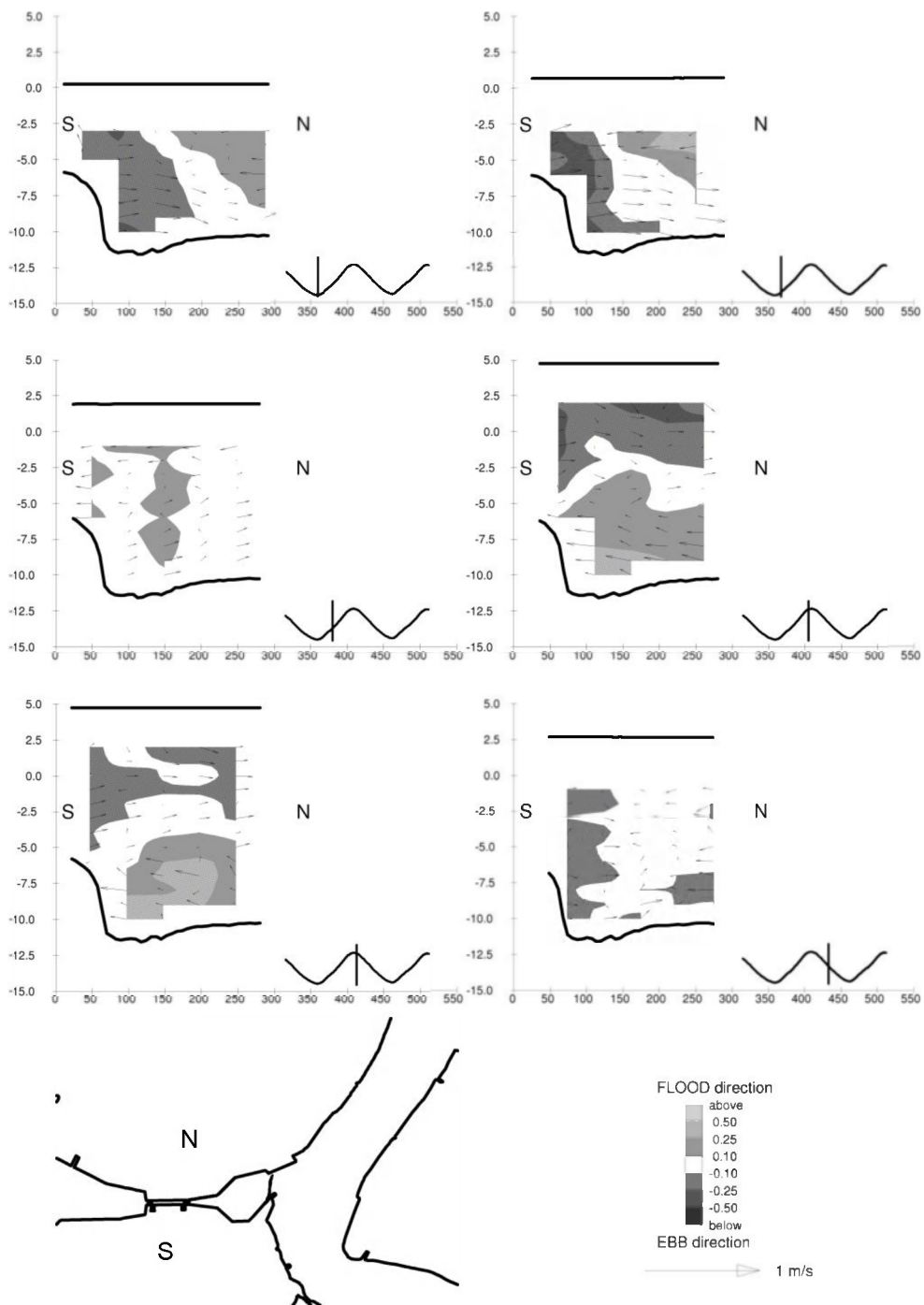
Figure 6.2: Flow velocities in the cross-section at the entrance of the basin (see small map).
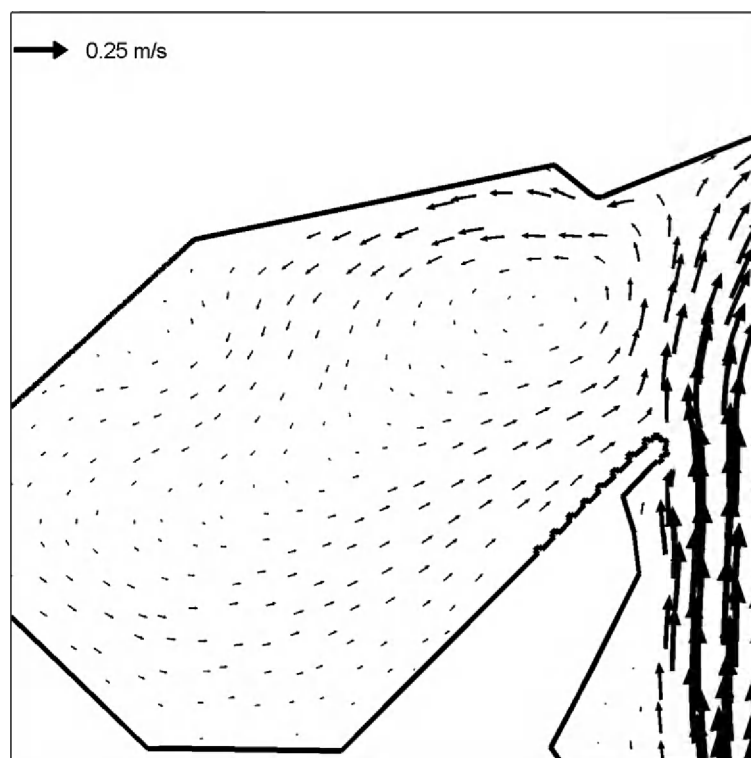
Figure 6.3: Computed depth averaged flow velocity field at 18:00, June 5, 2002, i.e. around LW

6.3. Measurements and simulations Deurganckdok

6.3.1. General circulation and sediment transport patterns

Water and sediment exchange processes between Deurganckdok and the Scheldt are alternating dominated by density-driven flow, horizontal eddies, or a combination of both. Through interpretation of measurements carried out at the entrance of the Deurganckdok, in November 2005, and March and September 2006, in combination with modelling results, we determine the dominant water exchange mechanisms and asses their implications for sediment import into the dock.

1) LW eddy

Horizontal eddies occur around HW slack and around LW slack. The LW slack eddy occurs from around LW until after approximately 1-2 hour after LW, and mainly in the surface layer. The flow on the Scheldt is directed down-estuary, and enters the Deurganckdok at its left bank (See Figure 6.4 and Figure 6.5). The sediment concentration on the left bank of the Scheldt is low, however, while the sediment concentration is high on the right bank of the Scheldt. Therefore the sediment concentration entering the dock through the eddy is around 100 mg/l (March 2006) or less (other surveys). Part of this sediment leaves the dock again at its right bank (see Figure 6.4a), but an additional part flows into the dock. However, since the LW slack eddy is followed by a phase of near-surface inflow and near-bed outflow, sediment that enters the dock through the eddy will be transported out of the dock in the bottom layer see Figure 6.4)a, (Figure 6.7) and (Figure 6.6). This will elaborated in more detail in the next section.
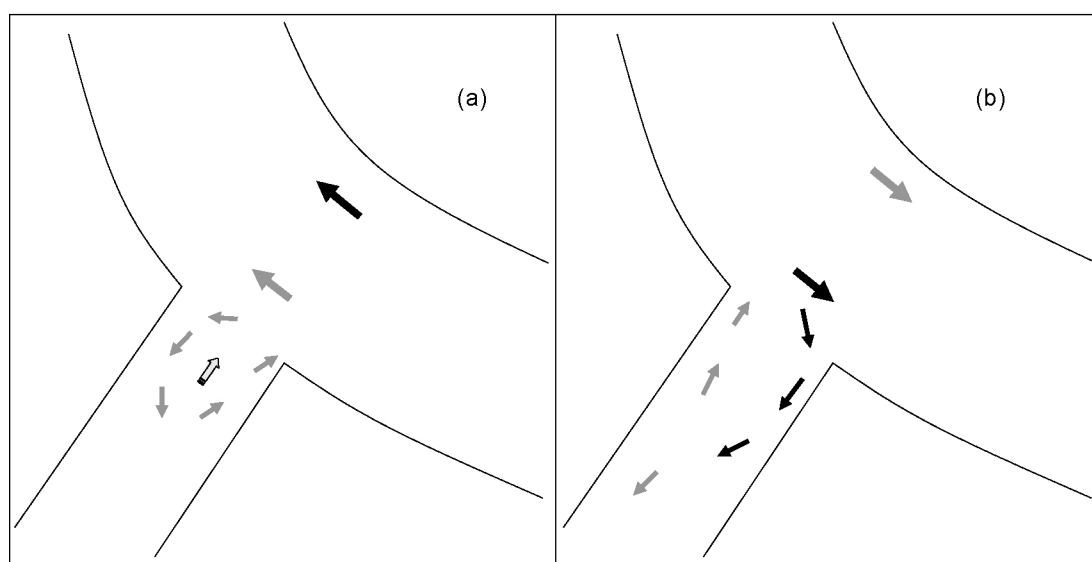
Figure 6.4: Schematized horizontal near-surface circulation around LW slack (a) and near-bottom circulation around HW slack (b). Grey arrows indicate low sediment concentration, black arrows high sediment concentration. The light arrow in (a) represents flow in the bottom layer.
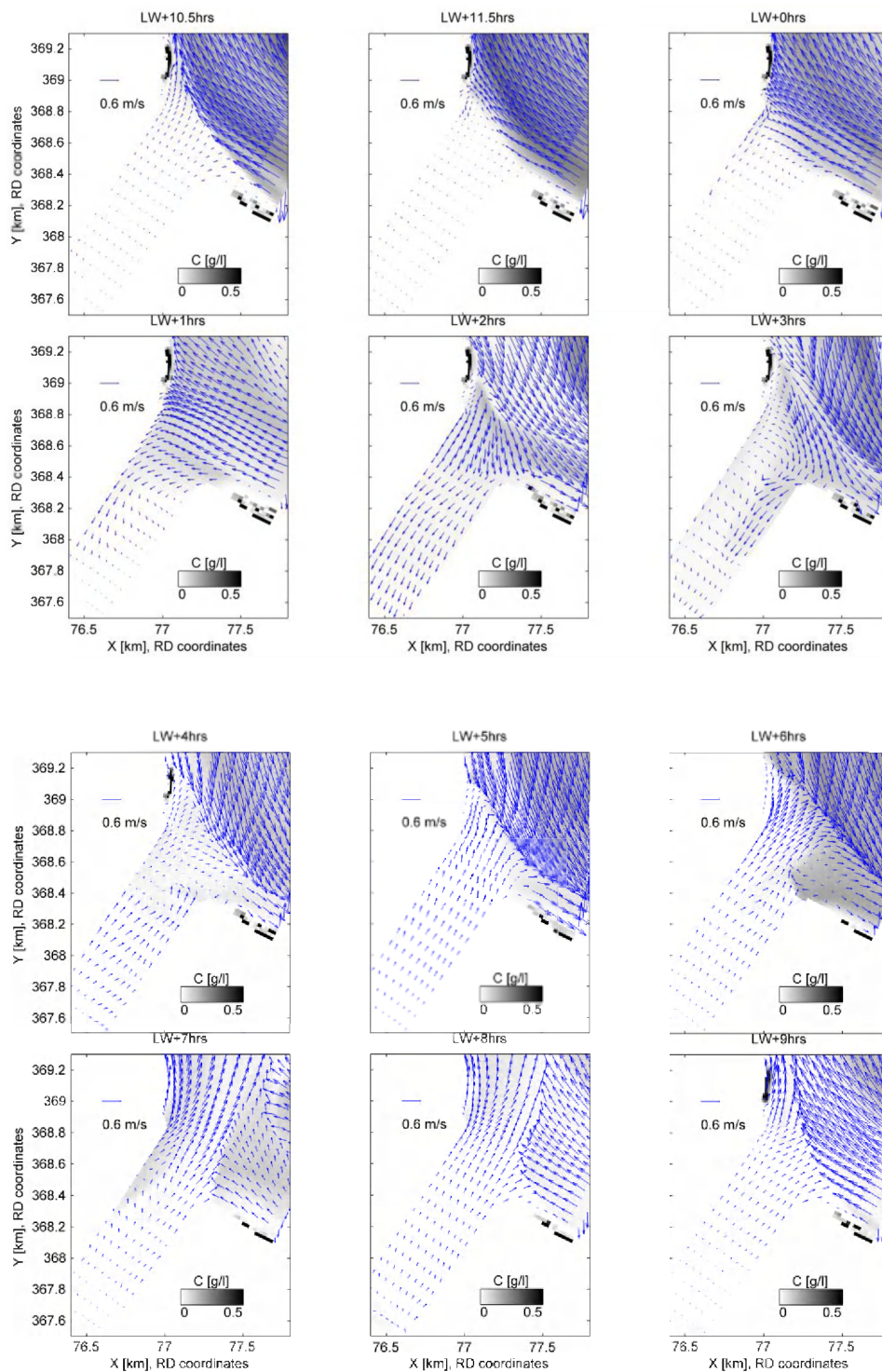
Figure 6.5: Computed hourly near-surface flow velocity pattern (arrows at every 3 grid cells), and sediment concentration (grey shading, in g/l) throughout a tidal cycle, in the entrance of the Deurganckdok.
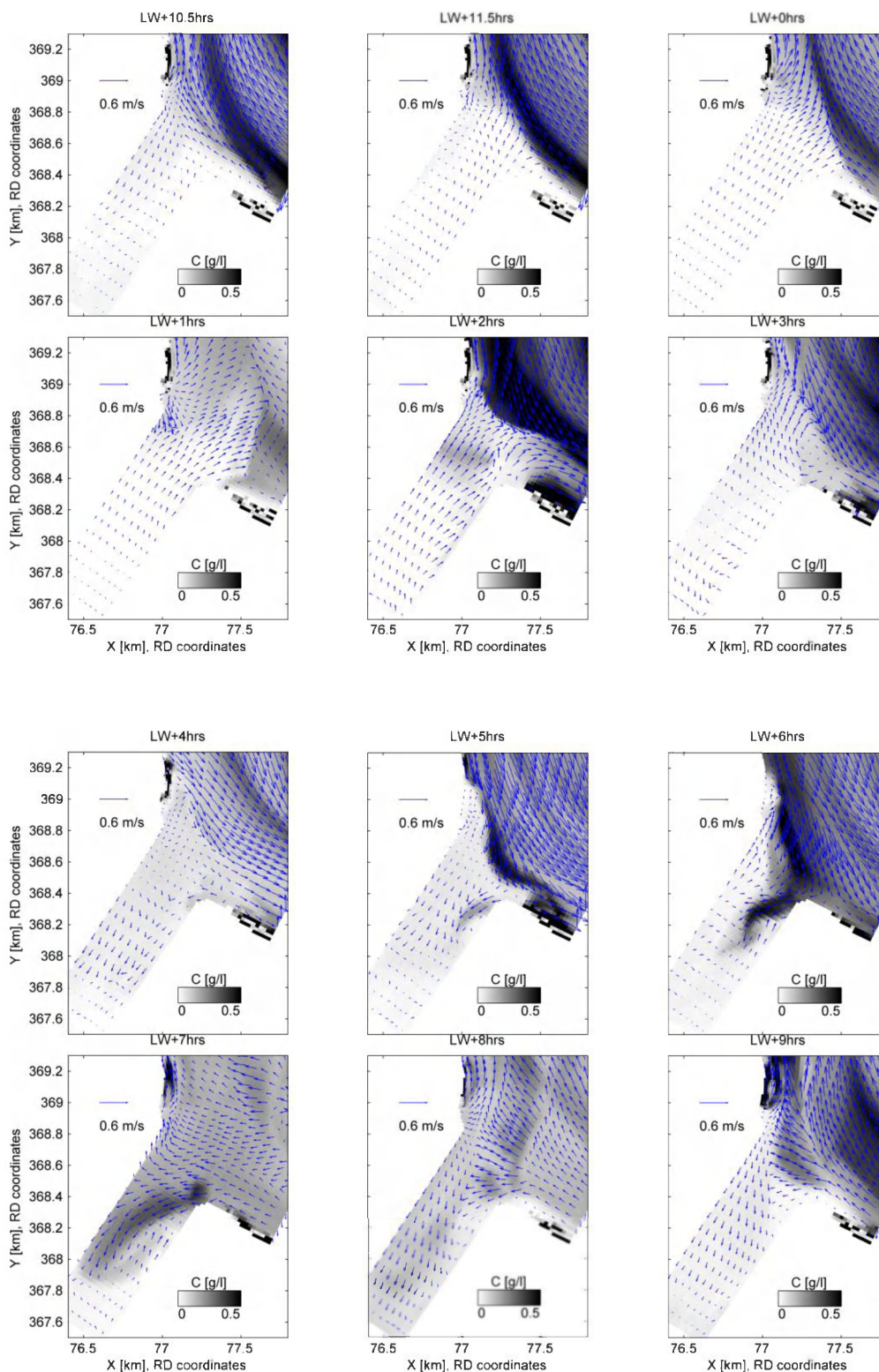
Figure 6.6: Computed hourly near-bottom flow velocity pattern (arrows at every 3 grid cells), and sediment concentration (grey shading, in g/l) throughout a tidal cycle, in the entrance of the Deurganckdok.

2)   Density driven flow with near-surface inflow

A density-driven flow structure with near-surface inflow and outflow near the bed exists from approximately 1 hour after LW until 3 hours after LW. A relatively turbid water mass (concentration up to 150 mg/l in March 2006) enters the dock in the surface layer (Figure 6.7a and Figure 6.8). However, after one hour the sediment concentration in the bottom layer has also increased (Figure 6.7c), because sediment entering in the surface layer settles from suspension in the dock (Figure 6.7b) after which it is transported out of the dock. Two hours after the initial sediment influx in the top layer, the highest turbidity can be observed in the bottom layer (Figure 6.7d and Figure 6.9). This implies that a substantial part of sediment that entered the dock through the surface layer is transported out of the dock again in the bottom layer.
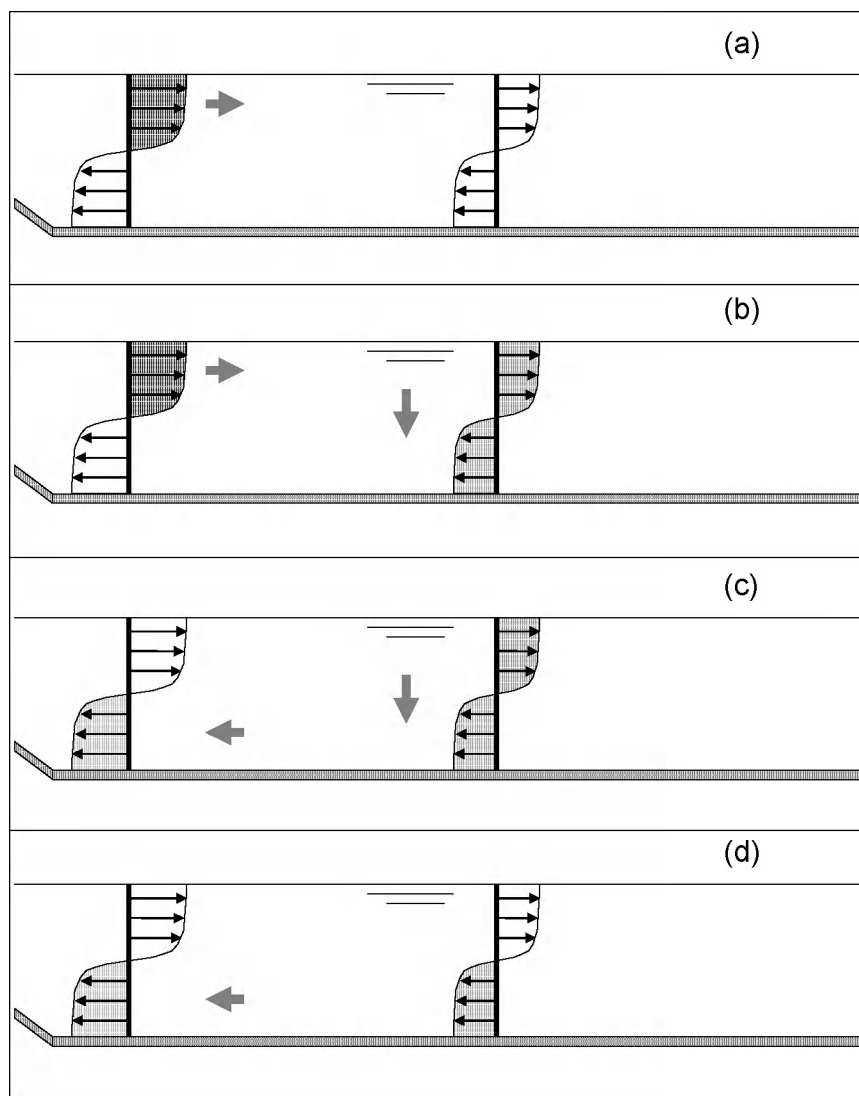
Figure 6.7: Schematization of sediment influx during first half of flood (dock entrance on the left).

Figure 6.8: Current velocity normal to the cross section (top, m/s, outflow positive) and sediment concentration (bottom, mg/l) measured at the dock entrance on 22 March 2006, from 15:07 to 15:11 (1 hour after LW). The cross section is parallel to the Scheldt in the entrance of the Deurganckdok, with the left bank of the Deurganckdok (facing the Scheldt) on the left. From IMDC report DGD 2.3.

The propagation velocity of the surface plume can be computed from the equation of Kranenburg (1996), given in the section above. With typical values of $\rho_1 - \rho_2 = 1.5$ kg/m^3, $h = 15$, $h_1 = 7$ m, $h_2 = 8$ m, B1 varying between 0 (no friction) and 1 (maximal friction), the propagation speed of the surface plume u_f varies between 0.2 and 0.24 m/s. This solution is only slightly influenced by the relative thickness of h_1 and h_2. With a block-shaped exchange (such as in the Deurganckdok), the density-driven flow velocity is approximately equal in to the propagation speed of the density current. This can be verified with salinity measurements at 4 locations between the landward end of the dock and the Scheldt (Figure 6.10). The salinity on the Scheldt is lowest at the end of the ebb period, which is around LW in the lower Sea Scheldt. During this period the salinity on the river is lower than in the dock, resulting in outflow near-bottom and inflow near the water surface. As a result, a patch of water with low salinity propagates into the dock near the surface. The distance between the dock entrance (dgd3) to the station 500 m from the end of the dock (dgd1) is 1000 m, which is traversed by the low salinity plume in 1 hour and 30 minutes. Hence, the propagation velocity is 19 cm/s which compares reasonably with the computed propagation speed.
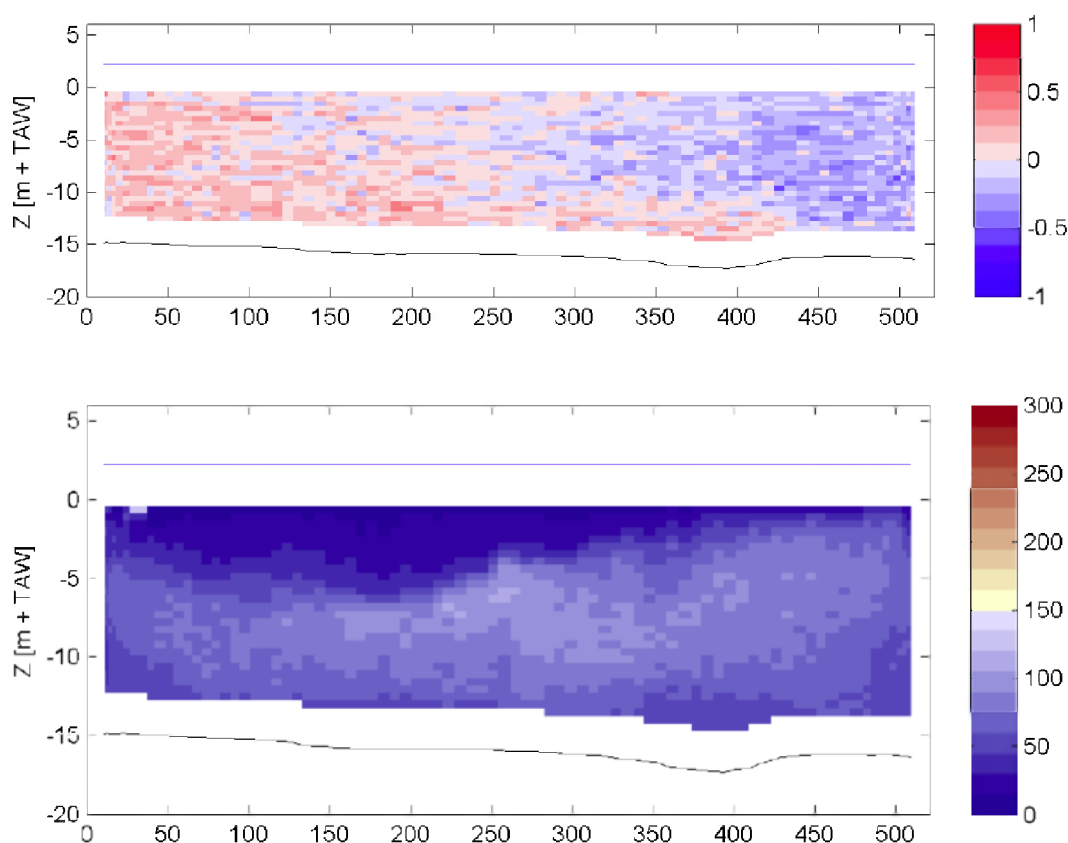
Figure 6.9: Current velocity normal to the cross section (top, m/s, outflow positive) and sediment concentration (bottom, mg/l) measured at the dock entrance on 22 March 2006, from 17:07 to 17:11 (3 hours after LW). The cross section is parallel to the Scheldt in the entrance of the Deurganckdok, with the left bank of the Deurganckdok (facing the Scheldt) on the left. From IMDC report DGD 2.3.

3)   HW eddy

A horizontal eddy enters the dock at its right-hand side at the end of the flood (LW +3 to +7 hours; around HW). Initially, the eddy occurs near the surface (see Figure 6.5), when flood velocities coincide with near-surface inflow. When the magnitude of the density-driven flows decreases, and even more after their direction has reversed, this eddy mainly enters the dock near the bottom (Figure 6.6). In contrast with the LW eddy, the sediment concentration is highest on the left bank of the Scheldt during the HW eddy (*i.e.* close to the Deurganckdok). The sediment concentration at the dock entrance exceeds 300 mg/l, and therefore a substantial amount of sediment flows into the dock. The largest sediment influx is about 2 hrs before HW (Figure 6.11). Part of this sediment flows back into the Scheldt (See Figure 6.4b), but another part flows into the dock. As the HW eddy partly overlaps with a near-bed inflow phase (see next section and Figure 6.12), most of this sediment remains in the dock. Model simulations indicate that most sediment entering the dock is through this large-scale eddy (e.g. van Maren, 2007).
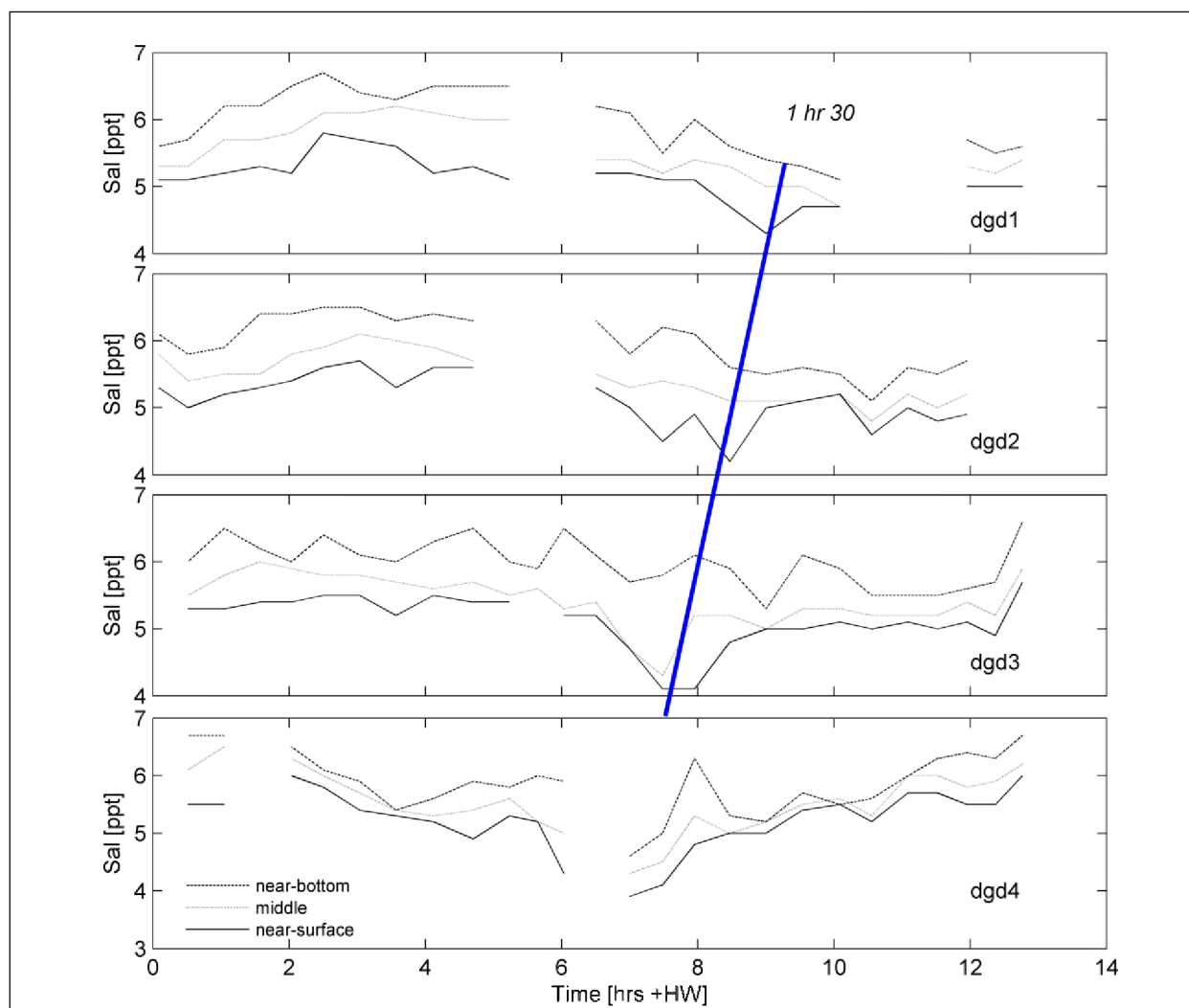
Figure 6.10: Measured salinity near-surface (solid line) halfway the water column (dotted line) and near the bed (dashed line), measured at locations dgd1-dgd4 on 21 March 2006 (from IMDC report 7.1).

4)   Density driven flow with near-bed inflow

Around HW, this horizontal eddy circulation gradually changes into a two-layer density driven flow with near-bed inflow (Figure 6.12 and Figure 6.13). At the period of this transition, the sediment concentration is high, up to 250 mg/l (Figure 6.13). This sediment enters the dock, and is followed by several hours of constant near-bed inflow. Therefore most sediment will settle in the dock. After deposition, the outward-directed flow velocities are too low to resuspend the sediment, and therefore most sediment that enters the dock during this period is trapped in the dock.
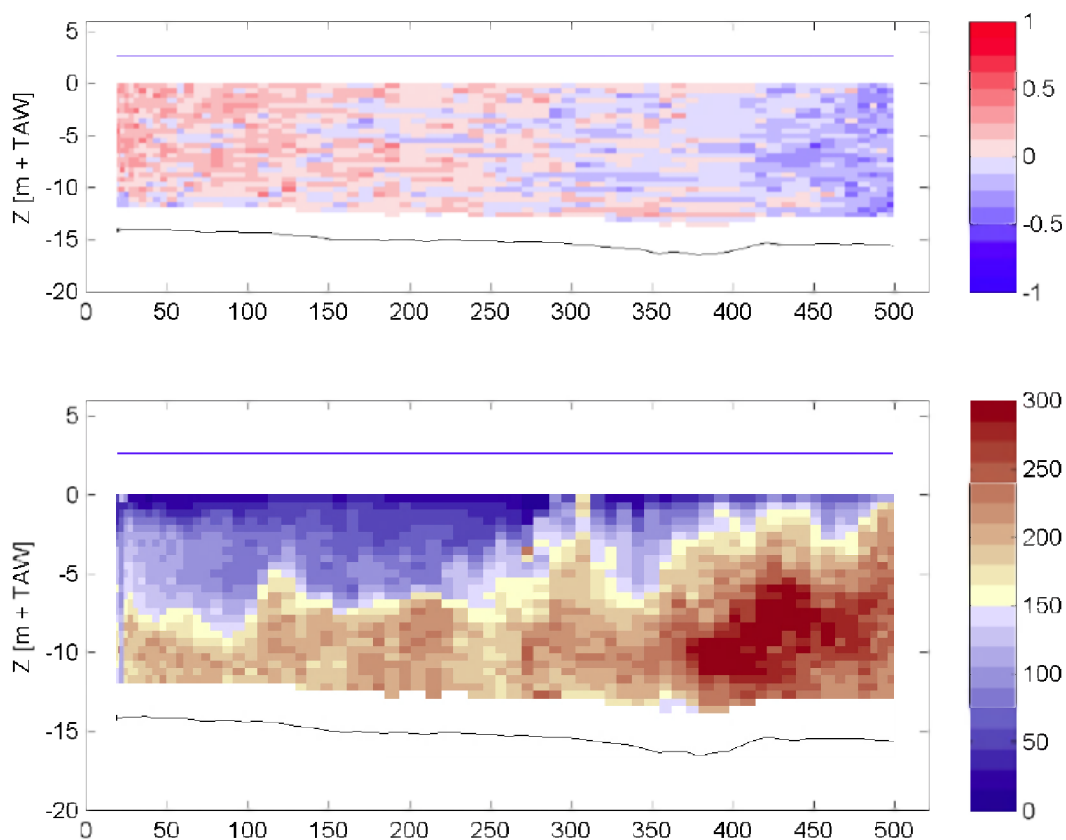
Figure 6.11: Current velocity normal to the cross section (top, m/s, outflow positive) and sediment concentration (bottom, mg/l) measured at the dock entrance on 22 March 2006, from 17:36 to 17:39 (3.5 hours after LW). The cross section is parallel to the Scheldt in the entrance of the Deurganckdok, with the left bank of the Deurganckdok (facing the Scheldt) on the left. From IMDC report DGD 2.3.
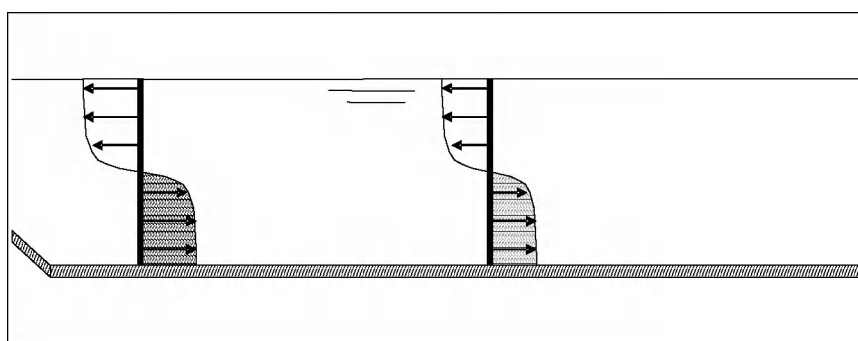
Figure 6.12: Schematization of sediment entering the dock around HW slack and the first half of the ebb (dock entrance on the left.
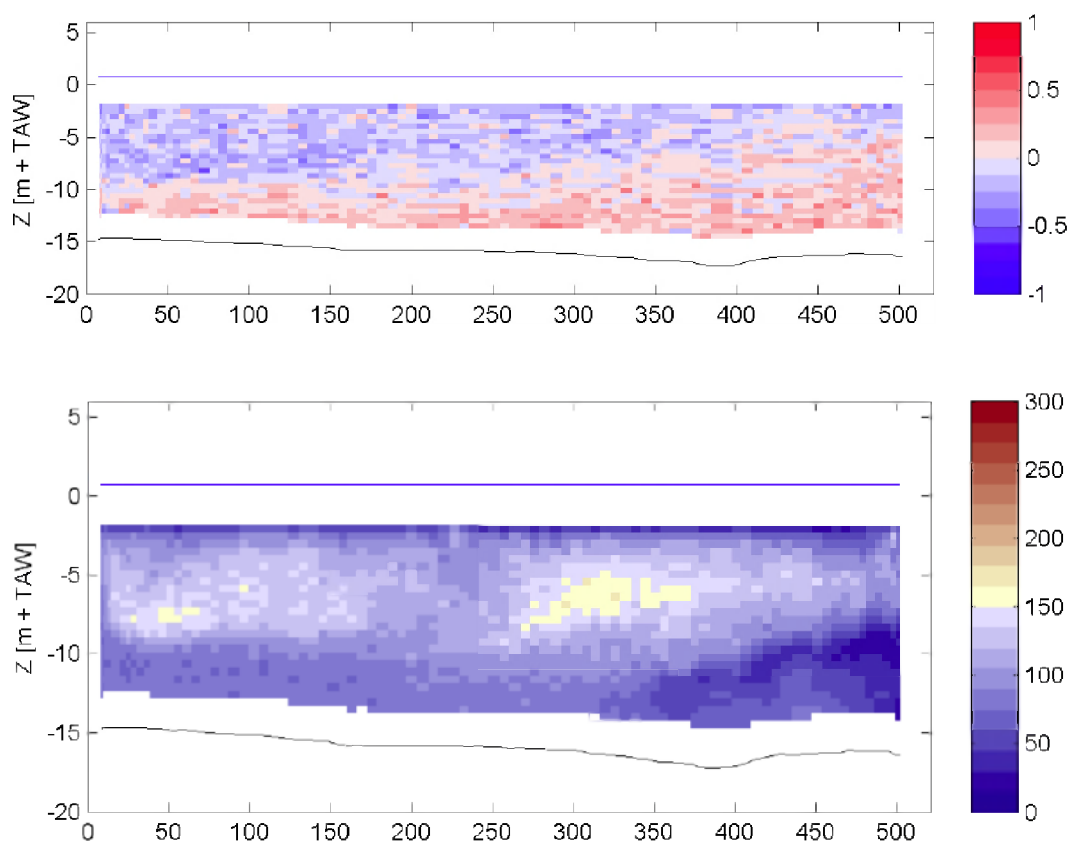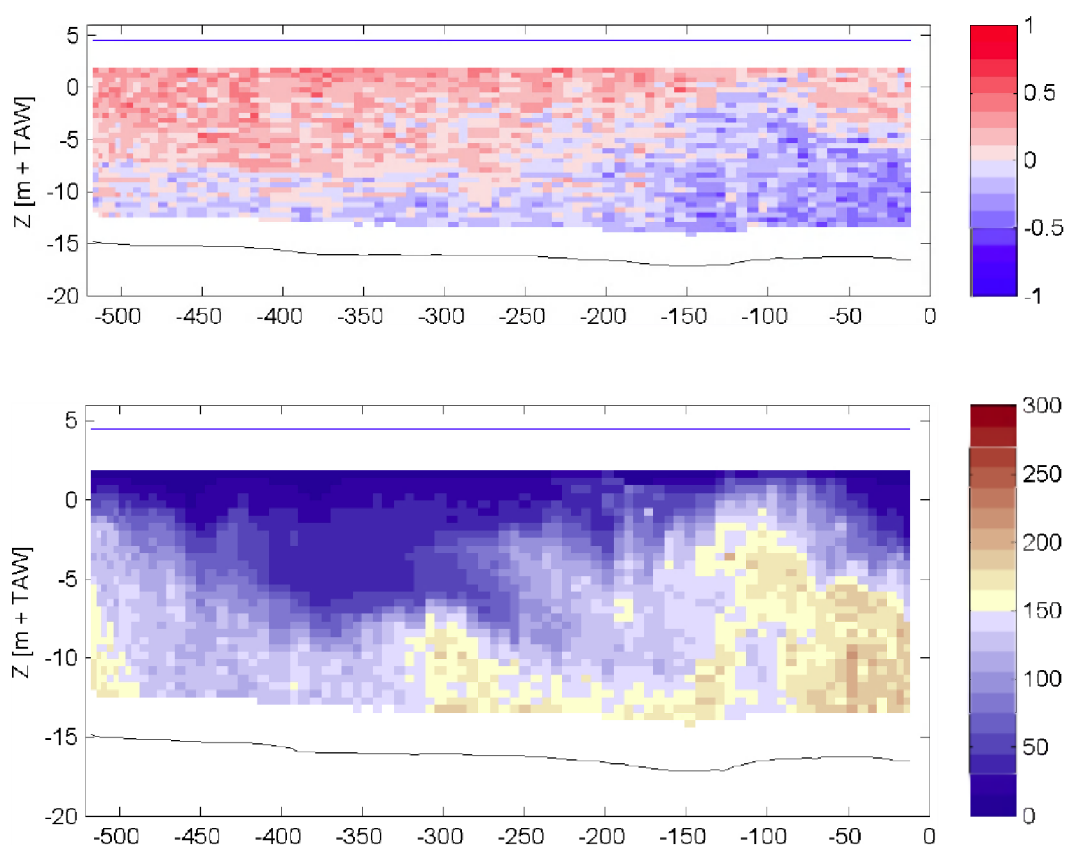
Figure 6.13: Current velocity normal to the cross section (top, m/s, outflow positive) and sediment concentration (bottom, mg/l) measured at the dock entrance on 22 March 2006, from 19:50 to 19:54 (HW). The cross section is parallel to the Scheldt in the entrance of the Deurganckdok, with the left bank of the Deurganckdok (facing the Scheldt) on the left. From IMDC report DGD 2.3.

6.3.2. Seasonal variation of circulation and sediment transport patterns

The seasonal variation of sediment concentration on the Scheldt is analyzed in section 5.2.3, and therefore here we only discuss the seasonal variation of sediment concentration on the Scheldt briefly, and focus on the aspects of sediment concentration relevant for sediment import into the Deurganckdok. Sediment that contributes substantially to sedimentation in the Deurganckdok is sediment transported by water masses during the second half of the flood at the left bank of the Scheldt (Van Maren, 2007). These water masses are measured at locations Ka and Kb, in winter 2005 and 2006, and during the summer/autumn of 2006. These measurements reveal that the peak sediment concentrations in winter are 3-5 times higher than the summer/autumn sediment concentrations (see Figure 6.14). This corresponds with the long-term sediment concentration measurements which show that the March 2006 peak concentrations were about 5 times higher than the September 2006 peak sediment concentration (IMDC report HCBS 5.6). However, the sediment concentrations in March were the highest of 2006, whereas the sediment concentrations in September 2006 were relatively low. On average, peak sediment concentrations in winter are 2-3 times higher than in summer. Consequently, estimates of sediment fluxes into the dock based on of long-term sediment concentration measurements (IMDC report DGD 4.1) also indicate that winter sediment influx is 2-3 times higher than summer influx.
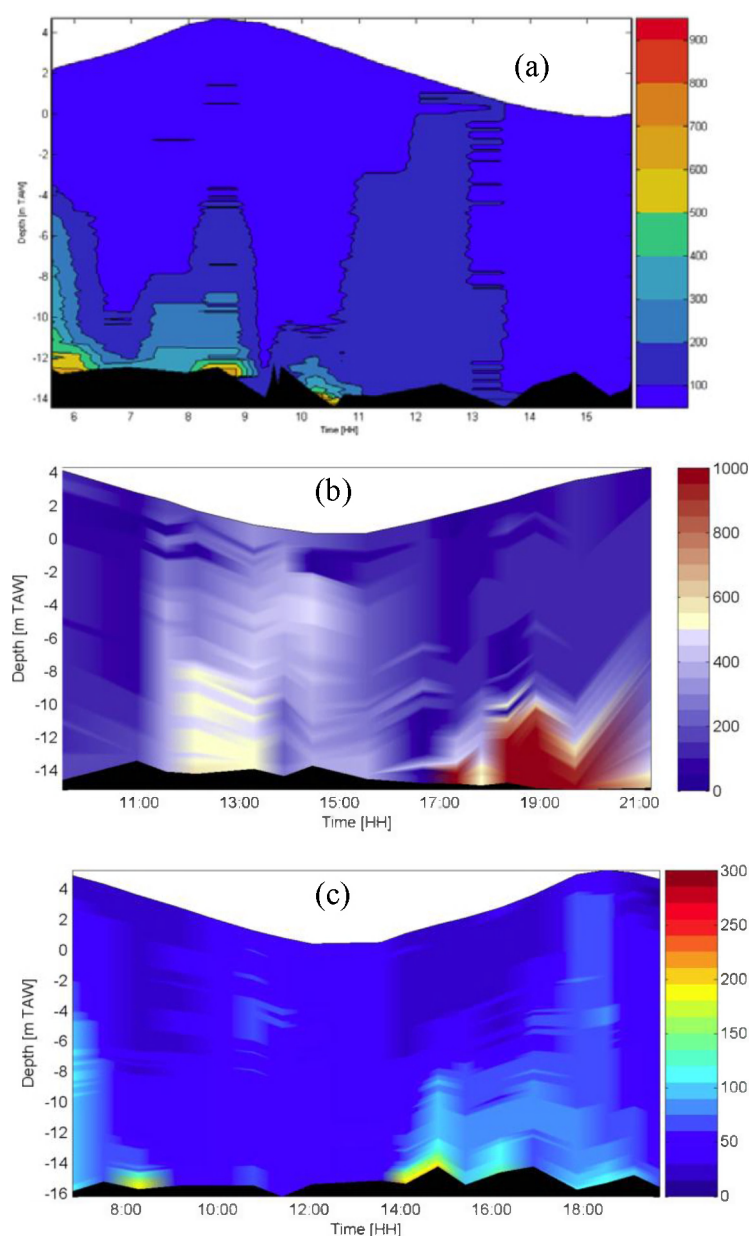
Figure 6.14: Measured sediment concentration at location Kb, using the SiltProfiler (a and c) or OBS (b), on 16 February 2005 (a, from IMDC report 2.5), 23 March 2006 (b, IMDC report 7.5), and on 28 September 2006 (c, from IMDC report 11.3). Note the different scales: the sediment concentration in (a) and (b) ranges from 0 to 1000 mg/l while the sediment concentration in (c) ranges from 0 to 300 mg/l).

The flow pattern at the entrance of the Deurganckdok is remarkably constant through time. Comparing the measured flow velocities on 17 Nov 2005 (IMDC report DGD-flux 1), 22 March 2006 (IMDC report DGD 2.3), and 27 Sep 2006 (IMDC report DGD 2.4) shows that the dominant exchange mechanisms (horizontal eddies, density-driven flow) are very similar in phasing and in magnitude. The flow velocities normal to the cross section at these three dates, one hour after HW (a period during which a relatively large amount of sediment enters the dock), illustrate this (Figure 6.15). The river discharge during all 3 measurement periods was relatively similar, and low. The

discharges were 90, 90, and 30 m³/s for 17 Nov 2005, 22 March 2006, and 27 Sep 2006, respectively. However, numerical model simulations indicate that the water masses in the dock respond rapidly to a changing salinity on the Scheldt (caused by discharge variations), and therefore the density-driven flows between the Scheldt and the dock (which are determined by gradients in density) are not significantly affected by salinity variations (van Maren and Schramkowski, 2008). Only rapid salinity variations (such as during a large flood) substantially change the density-driven flow patterns illustrated by Figure 6.15.
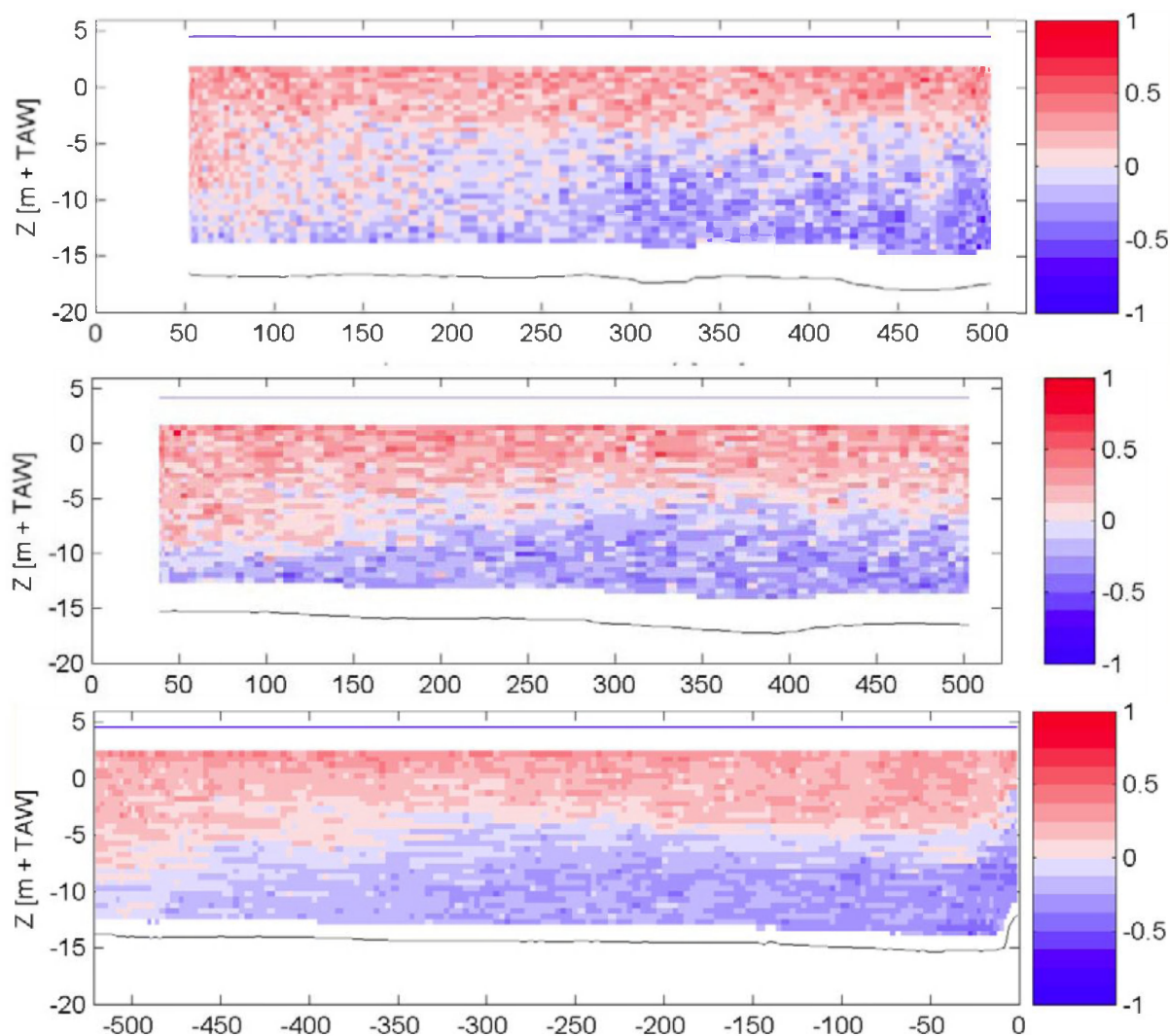
Figure 6.15: Current velocity normal to the cross section measured on 17 Nov 2005 (top), 22 March 2006 (middle), and 27 Sep 2006 (bottom), at the entrance of the Deurganckdok. The cross section is parallel to the Scheldt in the entrance of the Deurganckdok, with the left bank of the Deurganckdok (facing the Scheldt) on the left (note that the scale of the x-axis is defined differently in September 2006). From IMDC report DGD 2.4.
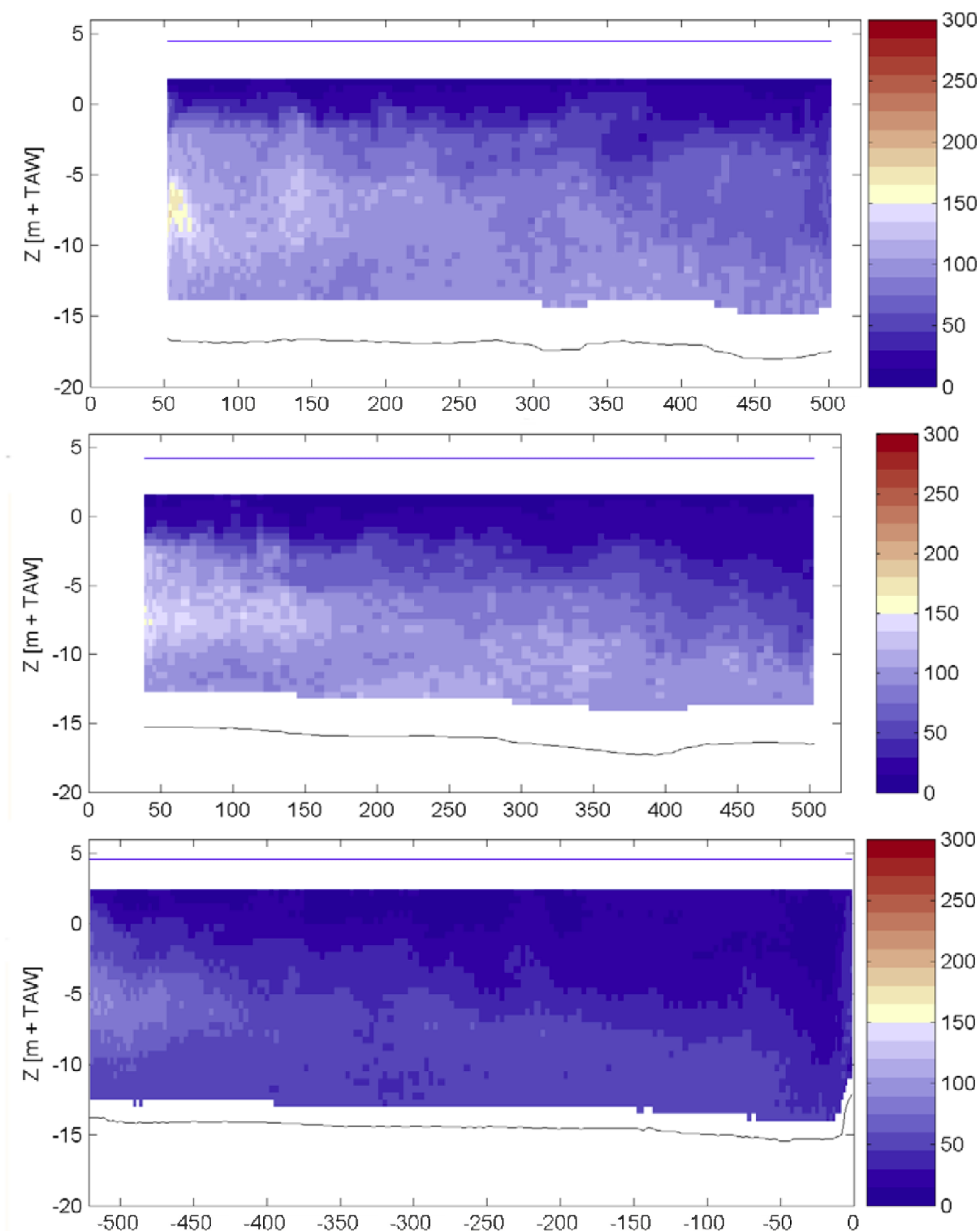
Figure 6.16: Sediment concentrations measured on 17 Nov 2005 (top), 22 March 2006 (middle), and 27 Sep 2006 (bottom), at the entrance of the Deurganckdok. The cross section is parallel to the Scheldt in the entrance of the Deurganckdok, with the left bank of the Deurganckdok (facing the Scheldt) on the left (note that the scale of the x-axis is defined differently in September 2006). From IMDC report DGD 2.4.

The maximum sediment concentration at the entrance of the dock, based on ADCP backscatter, (Figure 6.16) varies from 150-200 mg/l in March 2006 or November 2005 to 100 mg/l in September 2006. Also SiltProfiler measurements obtained at the dock entrance (IMDC reports DGD 2.1 and DGD 2.2) reveal sediment concentrations peaks from 100 mg/l (September 2006) to 300 mg/l (March 2006). More or less simultaneous measurements on the K-transect (March 2006 and September 2006) indicate, however, that the concentrations on the Scheldt are 5 times higher in March than in September 2006. It therefore seems that the seasonal variation of sediment concentration in the dock is less than that in the Scheldt itself (a factor 2-3 and a factor 5, respectively).

It is also noted that the peak sediment concentrations measured at the dock entrance (100 in summer and around 200-300 mg/l in winter) are a factor 2-4 lower than those measured at the K-transect (200 in summer and 600-1000 mg/l in winter). The question is whether this difference is related to the timing of the measurements (where the dock surveys may have been made during a period of low ambient sediment concentrations), or to spatial variations. However, the March 2006 and the September 2006 surveys in the dock were made one day before and one day after the surveys at the K-transect, respectively. Therefore the conditions are not substantially different. Additionally, a large sediment concentration difference between the Scheldt and the dock is also computed with the numerical model. Base on both these arguments, it appears that the peak sediment concentration of water masses entering the dock is 2-4 times lower than the peak sediment concentration on the Scheldt. The reasons for this may be that (1) mainly river water that flows close to the river bank (where the flow velocity, and hence the sediment concentration, is lower) enters the Deurganckdok, and/or (2) a substantial amount of sediment is rapidly deposited.

It is concluded that the sediment concentrations in the Deurganckdok are lower than on the Scheldt. Also the seasonal variation of sediment concentration is less pronounced than on the Scheldt. As a result, the concentration of water masses entering the dock are around 100 mg/l in summer, which is 2 times lower than on the Scheldt, and around 200-300 mg/l in winter, which is approximately 4 times lower than sediment concentrations on the Scheldt.

6.3.3. Flocculation characteristics during HCBS2

The INSSEV flocculation measurements (IMDC report 9) were conducted at three locations on three subsequent days, in September 2006. Measurements near the future CDW revealed three sediment concentration peaks: the first shortly after LW, the second halfway the flood, and the third around HW (Figure 6.17). Within these three peaks, the shear stresses were highest in the LW concentration peak (1.4 N/m^2 versus 1.0 N/m^2 in the other two). The resulting high floc break-up rates produced the lowest floc size and settling velocity. During the second peak, the shear stress was lower and therefore the floc size higher, but due to a dominance of microflocs, the average settling velocity was comparable. The shear stress and sediment concentration were similar in the third concentration peak shortly before HW. However, this peak was followed by a phase with lower concentration and low shear stresses, a large amount of macroflocs and therefore substantially higher settling velocities.
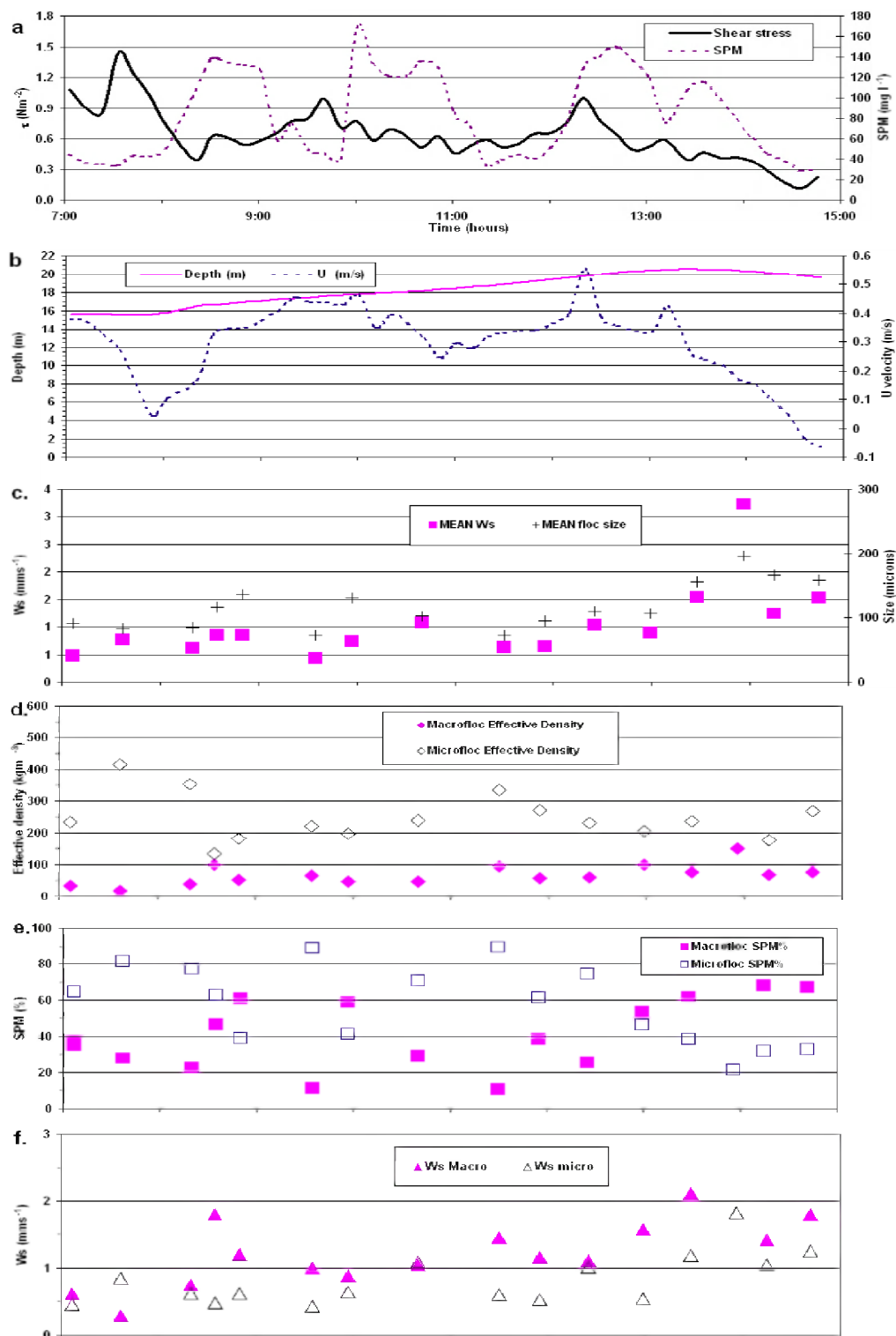
Figure 6.17: Time series of floc properties on 5 September 2006 (location CDW). a) shear stress and SPM, b) water depth, c) mean floc size and settling velocity, d) macrofloc and microfloc effective density, e) macrofloc and microfloc SPM distribution, and f) macrofloc and microfloc settling velocity. From IMDC report 9.
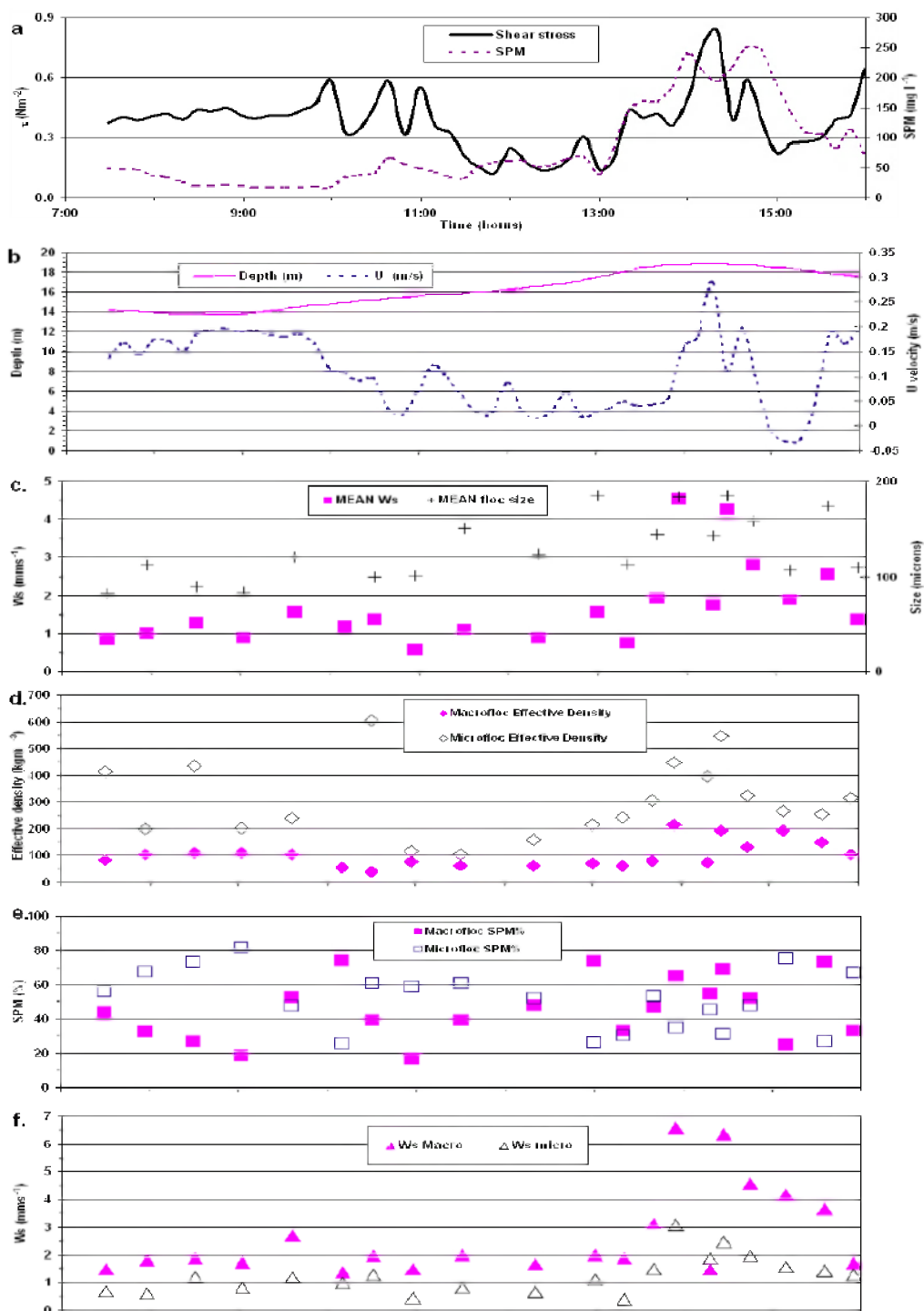
Figure 6.18: Time series of floc properties on 6 September 2006 (location sill). a) shear stress and SPM, b) water depth, c) mean floc size and settling velocity, d) macrofloc and microfloc effective density, e) macrofloc and microfloc SPM distribution, and f) macrofloc and microfloc settling velocity. From IMDC report 9.
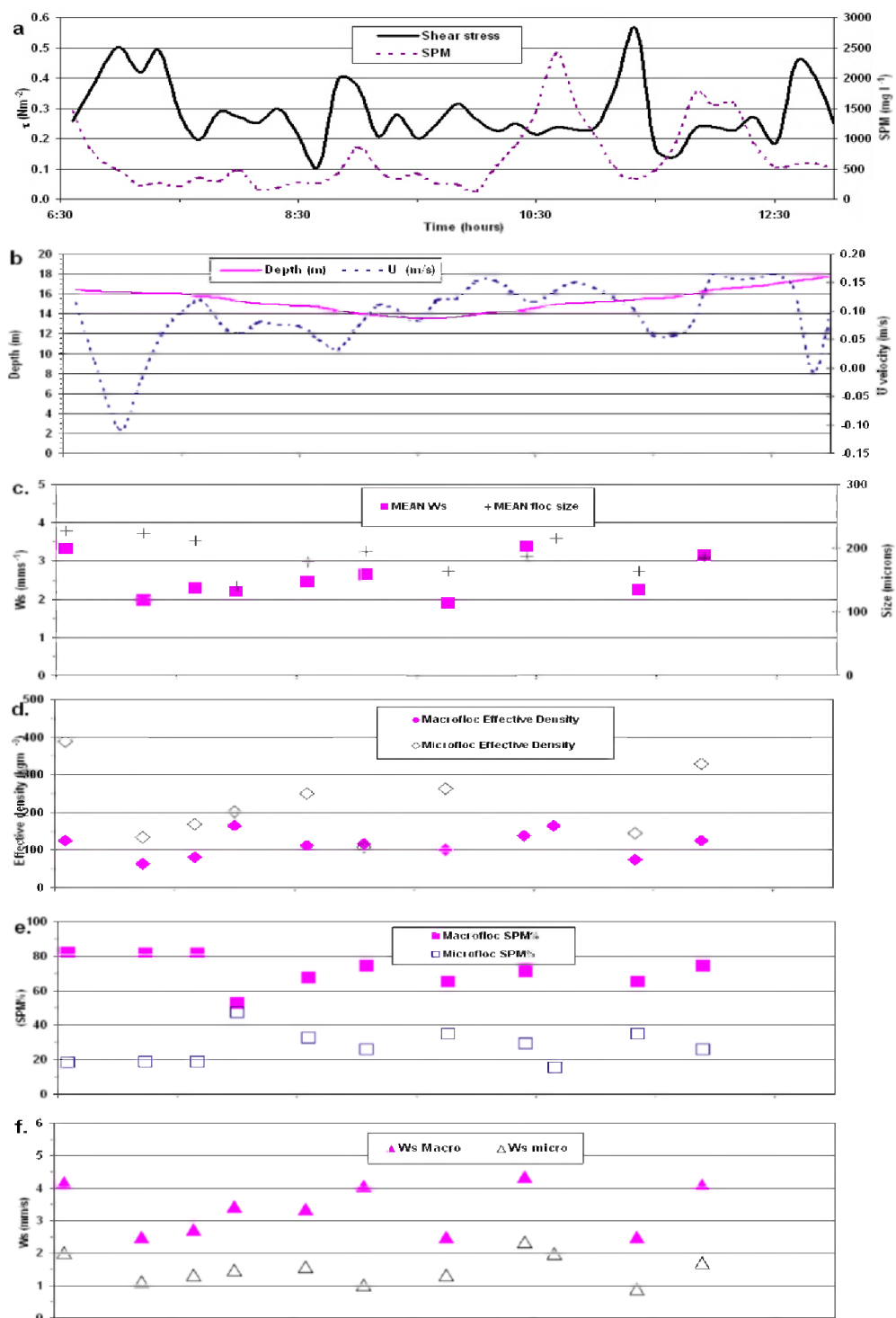
Figure 6.19: Time series of floc properties on 7 September 2006 (location Deurganckdok). a) shear stress and SPM, b) water depth, c) mean floc size and settling velocity, d) macrofloc and microfloc effective density, e) macrofloc and microfloc SPM distribution, and f) macrofloc and microfloc settling velocity. From IMDC report 9.

The shear stresses at the DGD sill on the right bank of the Deurganckdok (facing the Scheldt) on the following day were substantially lower, peaking at 0.8 N/m^2. Only one distinct high sediment concentration peak was observed at the sill. This peak coincides with the third peak of the previous day, and is caused by an eddy deflected into the dock shortly before HW (see previous section). The settling velocity in this peak is high, and dominated by macroflocs (similar to the previous day) However, the concentration near the bed and near the surface is substantially higher than that measured the previous day. Therefore, it seems that this sediment patch is of different origin than that measured at the CDW location. The sediment patch measured on the sill is probably part of the main stream of the Scheldt, whereas sediment observed on the CDW location is probably locally resuspended.

The shear stress on the left bank of the DGD peaks at 0.5 N/m^2. Sediment concentrations are substantially higher than during the other two surveys, ranging from several 100's to over 2,000 mg/l. Macroflocs dominate the floc suspension throughout the tidal cycle, resulting in settling velocities of several mm/s. During a larger part of the ebb, inflow occurs (probably as density-driven near-bed inflow, see the section above) with a sediment concentration around several 100's mg/l. Since the observations on the Scheldt and on the sill showed both a dominance of microflocs, the dominance of macroflocs even during inflow implies that microflocs rapidly evolve into macroflocs. High concentrations (> 1g/l) occur during the first half of the flood, during which the near-bed flow is directed out of the dock. During this time, a highly concentrated bottom current that must have been formed further away in the dock, is transported towards the Scheldt.

Comparing the INSSEV sediment concentration measurements carried out in the dock on 7 September 2006 (IMDC report 9) with sediment concentrations measured on the dock entrance on 26 September, especially the location Xa (IMDC report DGD 2.2) reveals that these surveys may not be very representative for the entire dock. Both locations were relatively close together, with the exception that the INSSEV measurements were done very close to the quay wall and the Xa survey was approximately 100 m from the quay wall. However, the sediment concentration at the INSSEV location was up to 2000 mg/l whereas that at Ka is up to only 100 mg/l. The ambient conditions (IMDC report 5.6) were, however, not substantially different. Although the sediment concentration at the beginning of September was slightly higher than at the end of September, the difference seems insufficient to explain the large variation in measured sediment concentrations. Also, the sediment concentration measured on the sill on the right hand side of the dock (facing the Scheldt) is more consistent with the 26 September survey: the sediment concentration peaks at 200 mg/l during the INSSEV survey, and at 100 mg/l on 26 September (location Zc, which is closest to the INSSEV location). Such a relatively small difference may be attributed to variations in the sediment concentration on the Scheldt. However, the difference of 100 mg/l and 2000 mg/l may not. Therefore the sediment concentration close to the quay walls appears to be substantially higher than further away from the walls. Hence, the INSSEV flocculation observations in the dock may not be entirely representative for the larger part of the dock.

6.3.4. Conclusions

The exchange of water and sediment between the dock and the Scheldt occurs through an eddy around LW and around HW, and as a density current with near-bed inflow (mainly during the ebb) and near-surface inflow (mainly during the flood).

A large amount of sediment enters the dock in the HW eddy, because the sediment concentration on the left bank of the Scheldt is high around this time. The settling velocity of this sediment is high due to dominance of macroflocs. Part of this sediment immediately flows out of the dock again, but the remainder flows further into the dock. This sediment is trapped in the dock, because the HW eddy is followed by a prolonged period of near-bed inflow. An additional amount of sediment enters during a phase of near-bed inflow. The settling velocity of this sediment is lower than that of sediment that entered in the large scale eddy. However, sediment that entered the dock in the inflowing bottom layer is trapped in the dock because there is no mechanism to transport it out of the dock again.

The sediment concentration is much lower in the eddy that enters the dock during low water, as high sediment concentrations occur on the opposite Scheldt bank (the right bank). Also, the low water eddy coincides with near surface inflow and near-bed outflow, and therefore this eddy is most pronounced near the surface, where sediment concentrations are lower. Additionally, because this phase is followed by a period of near-bed outflow, this sediment is (at least partly) transported out of the dock again. Finally, the sediment influx during near-surface inflow is low because sediment settles out from the surface layer into the bottom layer, and is transported out of the dock in the bottom current.

Sediment that flows into the dock is moderately concentrated, with peaks up to several 100's mg/l. The peak sediment concentration is 2-3 times lower than that on the Scheldt. During summer conditions, the concentration of inflowing water is around 100 mg/l, which is about half that on the Scheldt. During winter conditions, the concentration of inflowing water masses are up to 300 mg/l, which is 3-4 times lower than concentrations on the Scheldt.

7. NEAR-BED SEDIMENT CONCENTRATION AND TRANSPORT

This chapter discusses the occurrence of highly concentrated sediment suspensions near the bed, the measurement and modelling of these layers and their significance for siltation rates. First, observations on the near-bed concentration are discussed (section 7.1). This section is followed by a short discussion of model results (section 7.2). Subsequently, the likelihood of occurrence of highly concentrated layers is evaluated from a theoretical analysis (section 7.3). If such layers occur, the question is whether and, if so, how they may be transported. The resulting sediment flux is compared with the sediment flux of the dilute suspension in the upper part of the water column (section 7.4)). After a discussion on flocculation (section 7.5), the occurrence of HCBS layers near Kallo and Deurganckdok is evaluated, including the effect of the sill between the Scheldt estuary and DGD (section 7.6). Finally, the numerical modelling of HCBS layers is discussed (section 7.7).

7.1. Near-bed observations

7.1.1. Frame data and quality

Two large measurement frames, each equipped with 2 EMC current meters, 2 OBS sensors, a pressure sensor, an ALTUS echo sounding device, and an ARGUS sediment concentration array, was deployed during several measurement campaigns in and in the vicinity of the Deurganckdok. The ARGUS consists of 96 backscatter infrared laser sensors, embedded in a stainless steel rod, measure the vertical structure of the suspended sediment concentration. The ALTUS is a high frequency acoustic altimeter that precisely quantifies (with an accuracy of 2 mm) changes of bottom elevation.

The first campaign was the HCBS 1 campaign, during which one frame measured in February 2005 (downstream of the Deurganckdok) and March 2005 (near Buoy 84), reported in IMDC report 2.7 The frame also measured in March 2006, during the HCBS2 campaign, on the location of the envisaged CDW (IMDC report 8.1). During the Deurganckdok campaigns, two frames were deployed simultaneously: one on the location of the envisaged CDW, and one the sill of the Deurganckdok. Simultaneous surveys were done in April-May 2006 (IMDC report DGD 2.6), July-November 2006 (IMDC report DGD 2.7) and February – March 2007 (IMDC report DGD 2.8). Of these campaigns, the measurements from 2006 Deurganckdok campaigns contain the most valuable data, because

- Measurements were carried out simultaneously with two frames (in contrast with the HCBS1 and HCBS2 campaigns)

- Measurements were carried out for a relatively long period (several months at a single location), in contrast with the HCBS1 and HCBS2 campaigns

- Most of the important instruments functioned properly, in contrast with the HCBS1 measurements downstream of the Deurganckdok, and the CDW frame of the 2007 Deurganckdok measurements.

- Most of the ship borne measurements (discussed in the previous chapters) were done in 2006.

Therefore the 2006 simultaneous measurement frames will be analyzed here in more detail.
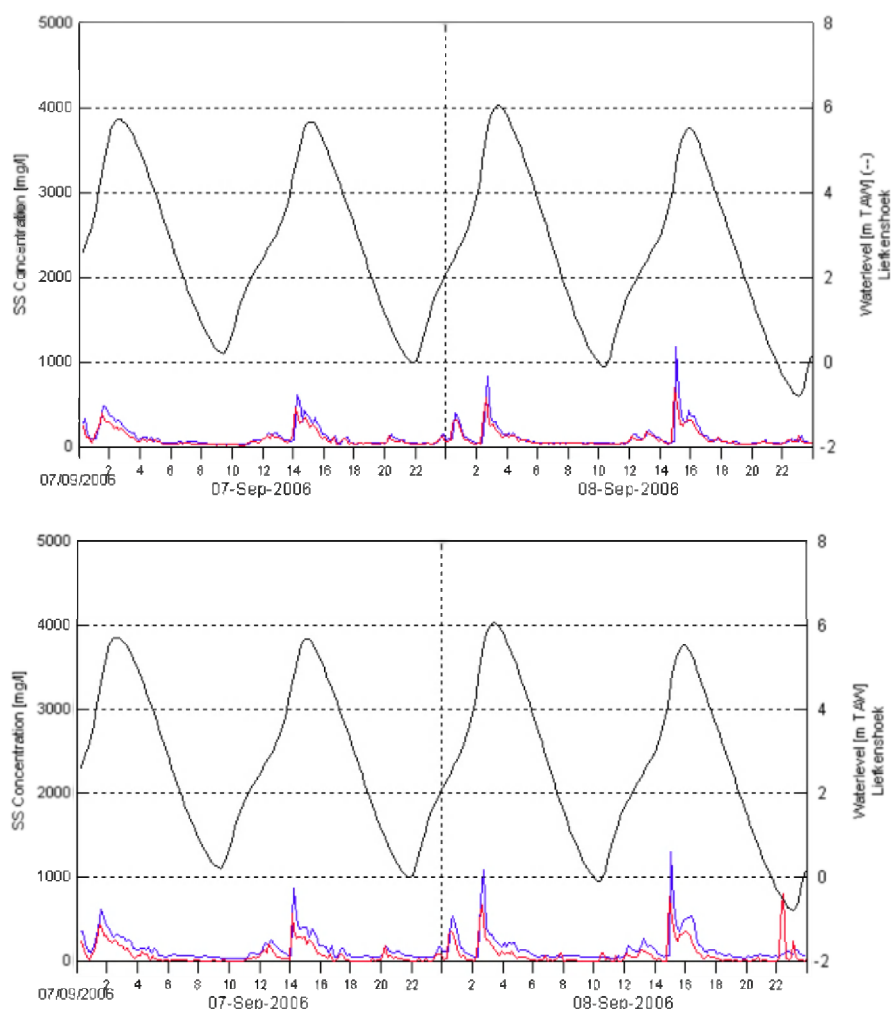
Figure 7.1: Comparison of sediment concentrations measured with the ARGUS sensors (red) to sediment concentrations measured with the RCM9 OBS (1 m above the bed, top, in blue) and concentrations measured with the Valeport (0.1 m above the bed, bottom, in blue), at the sill location, September 2006. From IMDC report DGD 2.7.

The measurements are summarized in Appendix E (Annex-Figure D-21) to (Annex-Figure D-5): ARGUS sediment concentration measurements, depth measured by the ALTUS h_A, flow velocity u, water depth h, and the sediment flux S. S is defined as uC, with u the velocity measured with the upper EMF and C the concentration measured with the ARGUS at 90 cm above the bed. Inspecting the frame data, however, reveals several strange observations. Especially the ARGUS data contains several errors:

- Some sediment concentration measurements are increasing in time. This occurs on the CDW location in August 2006 (Annex-Figure D-2), and on the sill in May 2006 (Annex-Figure D-3), and August and October 2006 (Annex-Figure D-4). This may be caused by the frame sliding sideways into deeper water or mud, by rapid sedimentation, or by bio fouling of the instruments. The measurements with the CDW frame (Annex-Figure D-2) seem to be sliding away in deeper water, because the water depth is steadily increasing. Part of the instruments on the April and May 2006 sill frame measurements are covered in sediment, demonstrated by high and constant near-bed sediment concentrations, and malfunctioning ALTUS and lower

EMF sensors. It is not clear what caused the increase in sediment concentration in August and October 2006. Possibly the instruments are suffering from algae growth (bio fouling).

- During several deployments, the observed concentrations are constant in time, but the vertical distribution is very irregular (September 2006 on the sill, (Annex-Figure D-4). Probably the ARGUS was therefore not working properly.

- During some of the measurements, several ARGUS sensors measure constantly higher sediment concentrations than sensors below or above. This is observed on the CDW location in May 2006 (Annex-Figure D-21) and September 2006 (Annex-Figure D-2), and on the sill in May 2006 (Annex-Figure D-3) and April 2007 (Annex-Figure D-5). Comparing the OBS sensors that were also placed on the frame, with the ARGUS results, however, shows that the ARGUS sensors that do work properly, compare well with the separate OBS measurements (see the example in Figure 7.1).

- Some sediment concentration measurements are too low, such as measured on the sill in March 2007 (Annex-Figure D-5). The sediment concentration remains below 50 mg/l, which is much lower than any of the other measurements.

In addition to the ARGUS, also some of the other instruments yield strange or missing data. The lower EMF did not function well on the CDW location in August and September 2006, and on the sill location in May, August, and October 2006 and March and April 2007. Also the fact that the bottom EMF sensor recorded velocities equal or even higher than the top EMF sensor (April 2006 on the CDW location, August and September 2006 on the sill location) suggest some error. The Altus worked infrequently in August 2006 on the CDW, and in April and May 2006 on the sill.

Therefore the frame measurements have to be interpreted with care, and may not be suitable for a detailed quantitative analysis. The data are useful, however, for a qualitative analysis on erosion and sedimentation processes. This will be done in the following sections.

7.1.2. Tidal variation

A sediment plume enters the Deurganckdok around HW in a large eddy, as detailed in chapters 4 and 6. On the sill of the Deurganckdok, this eddy results in flow velocity peaks with relatively high sediment concentration (Figure 7.2) and (Figure 7.3). Three of these peaks are illustrated as A, B, and C in (Figure 7.2). Phase A is a low flow velocity ($\approx$ 0.25 m/s at 0.9 m above the bed), low sediment concentration (0.5 g/l near-bed) peak. Phase B is a high flow velocity ($\approx$ 0.4 m/s at 0.9 m above the bed), high sediment concentration (>1 g/l near-bed) peak, and phase C is a high flow velocity ($\approx$ 0.4 m/s at 0.9 m above the bed), low sediment concentration peak (0.5 g/l near-bed). Sedimentation occurs during phase B (decreasing h in the second panel of (Figure 7.2), whereas sediment is eroded during phase A and C. This suggests that the flow velocity of 0.25 cm/s is sufficient to erode sediment on the sill. However, when the sediment concentration is sufficiently high (C > 1 g/l) sediment is deposited, even though the flow velocity is higher (u $\approx$ 0.4 m/s). This deposition may be the result of a collapsing sediment concentration profile, and will be analyzed in more detail in section 7.3. However, the response of the sediment bed to flow velocity and sediment concentration is not always as in phases A, B, and C. Approximately 25 hours later, the patterns of erosion and deposition are very similar to the patterns described with phases A, B, and C (also Figure 7.2). During comparable hydrodynamic and sedimentary conditions (i.e. Figure 7.3 and Figure 7.4), there is no pronounced erosion/deposition/erosion sequence as in phases A, B, and C.

It should also be noted that throughout most of the frame measurements, sedimentation prevails rather than erosion (such as in April 2006). Especially in February – April 2007 the sedimentation

rates are up to 15 cm/week (see Appendix E). A detail of this period (given in Figure 7.4) shows that sedimentation is more or less continuous and only compensated by short periods of erosion during flow velocity peaks (u ≈ 0.6 m/s). These flow velocity peaks coincide with sediment concentrations of about 0.5 g/l.

The bed level near the future CDW (the CDW frame) remains more or less constant throughout the deployment period (see Appendix E). Some sedimentation (less than 0.5 cm) occurs during the flood (1-2 hours after LW to 1-2 hours after HW). The same amount is eroded during the following ebb period. The flow velocity during both erosion and deposition is the same (u ≈ 0.35 m/s). Hence, the higher sediment concentration during the flood results in deposition, and not a difference in flow velocity. Also, the period of deposition on the sill and in the DGD is approximately the same. Therefore sediment is not eroded at the future CDW location, and subsequently deposited in the dock, but sedimentation occurs simultaneously over the whole sill-CDW area, during the flood and around HW.
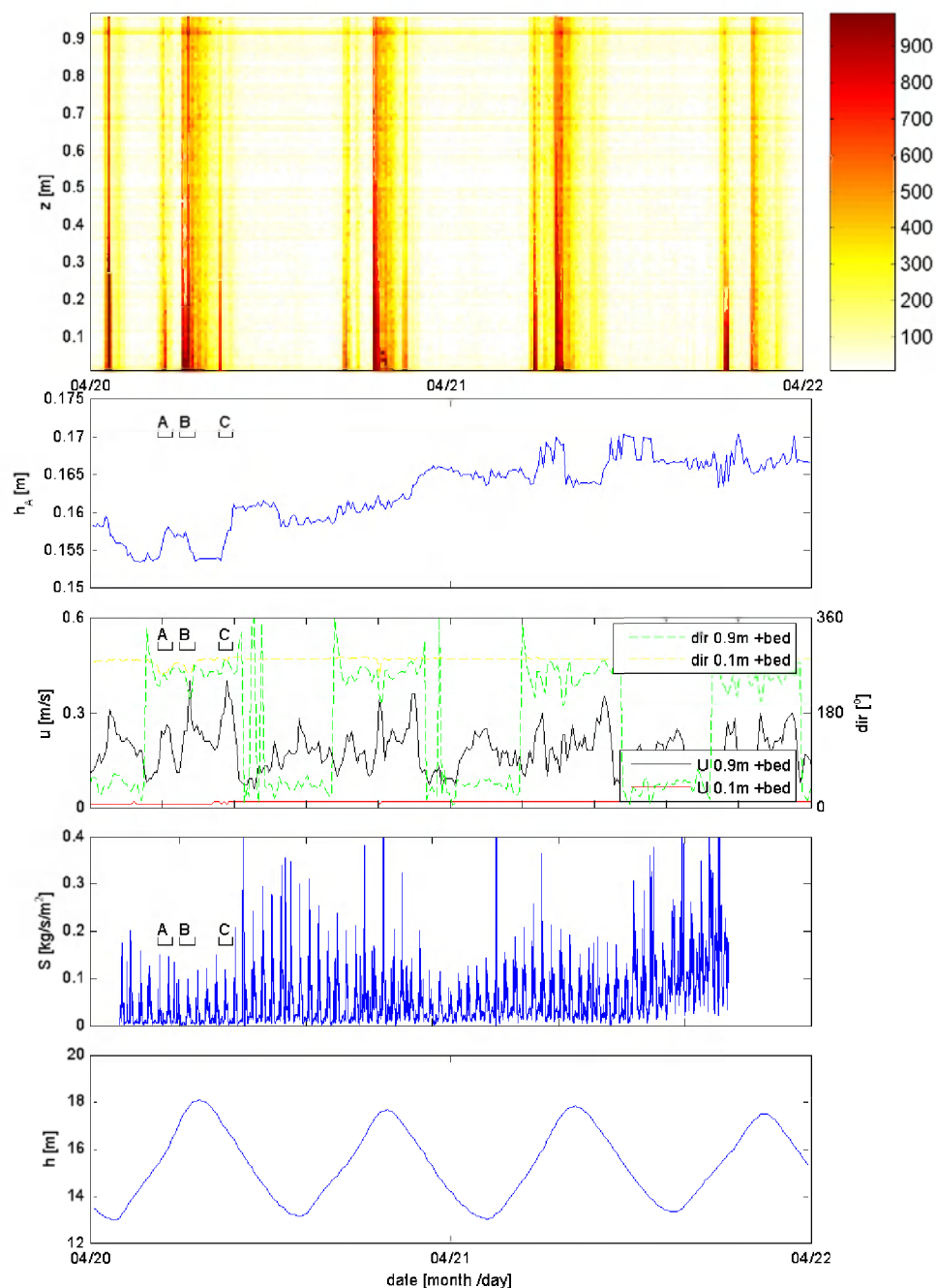
Figure 7.2: From top to bottom: sediment concentration (mg/l), measured with the ARGUS; depth h_A measured with the ALTUS (average of 4 beams, with an increasing h_A being erosion); flow velocity and direction measured with both currents meters (although the bottom meter was not functioning properly); sediment flux S, computed with the upper EMF and ARGUS sensor at 90 cm above the bed, and water depth h, measured at the sill of the Deurganckdok, in April 2006.
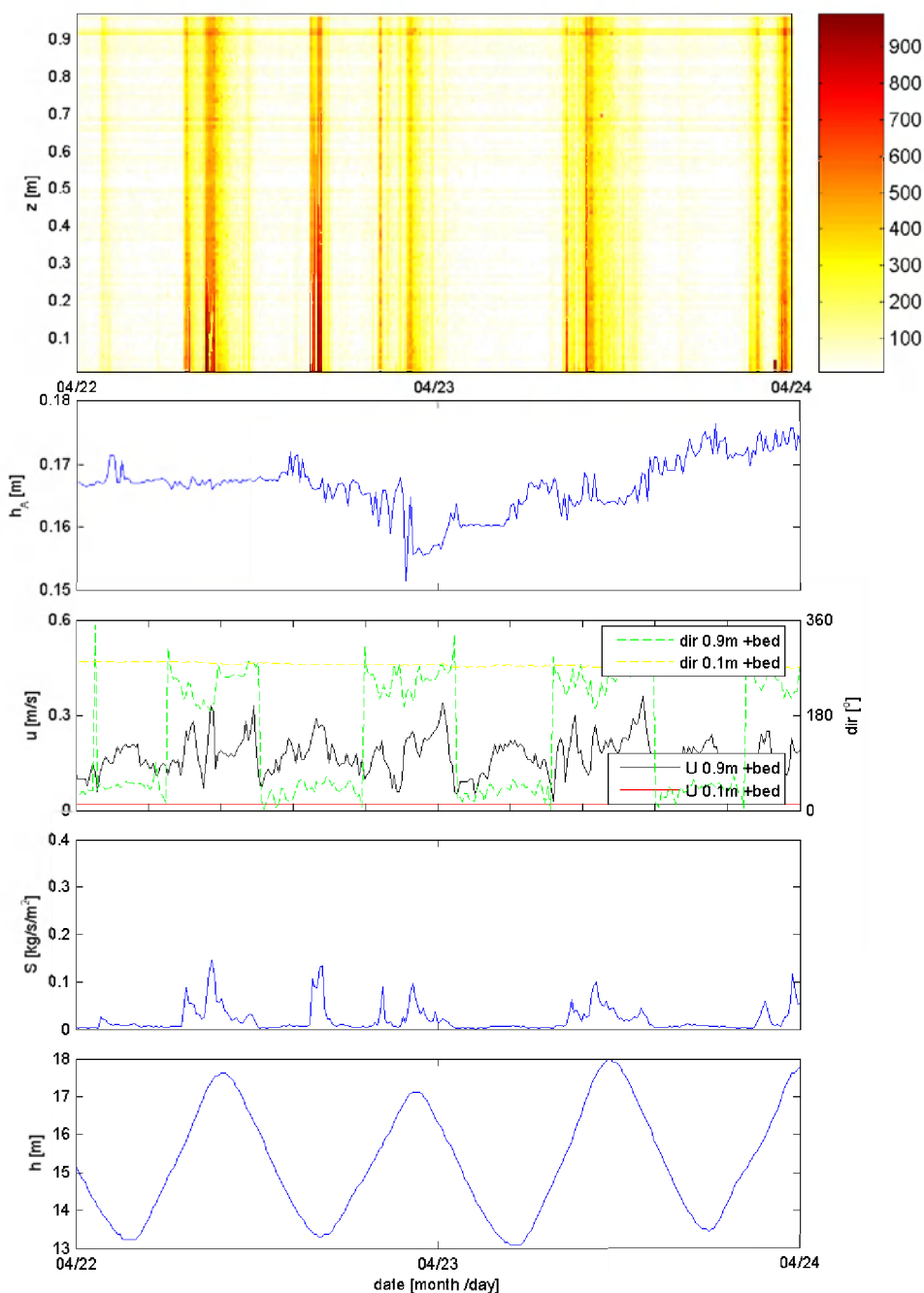
Figure 7.3: From top to bottom: sediment concentration (mg/l), measured with the ARGUS; depth h_A measured with the ALTUS (average of 4 beams, with an increasing h_A being erosion); flow velocity and direction measured with both currents meters (although the bottom meter was not functioning properly); sediment flux S, computed with the upper EMF and ARGUS sensor at 90 cm above the bed, and water depth h, measured at the sill of the Deurganckdok, in April 2006.
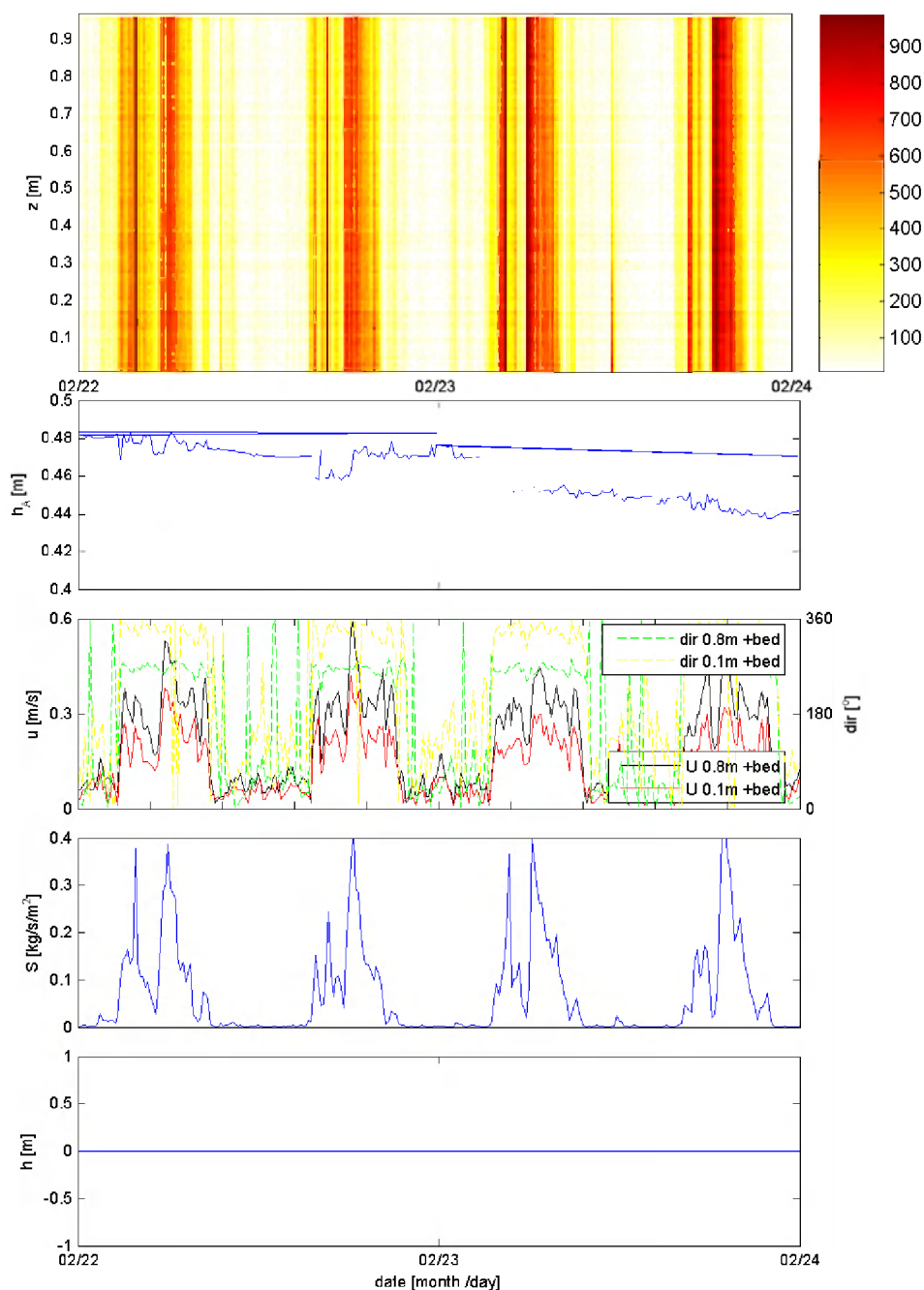
Figure 7.4: From top to bottom: sediment concentration (mg/l), measured with the ARGUS; depth h_A measured with the ALTUS (average of 4 beams, with an increasing h_A being erosion); flow velocity and direction measured with both currents meters (although the bottom meter was not functioning properly); sediment flux S, computed with the upper EMF and ARGUS sensor at 90 cm above the bed, and water depth h (malfunctioning), measured at the sill of the Deurganckdok, in February 2007.
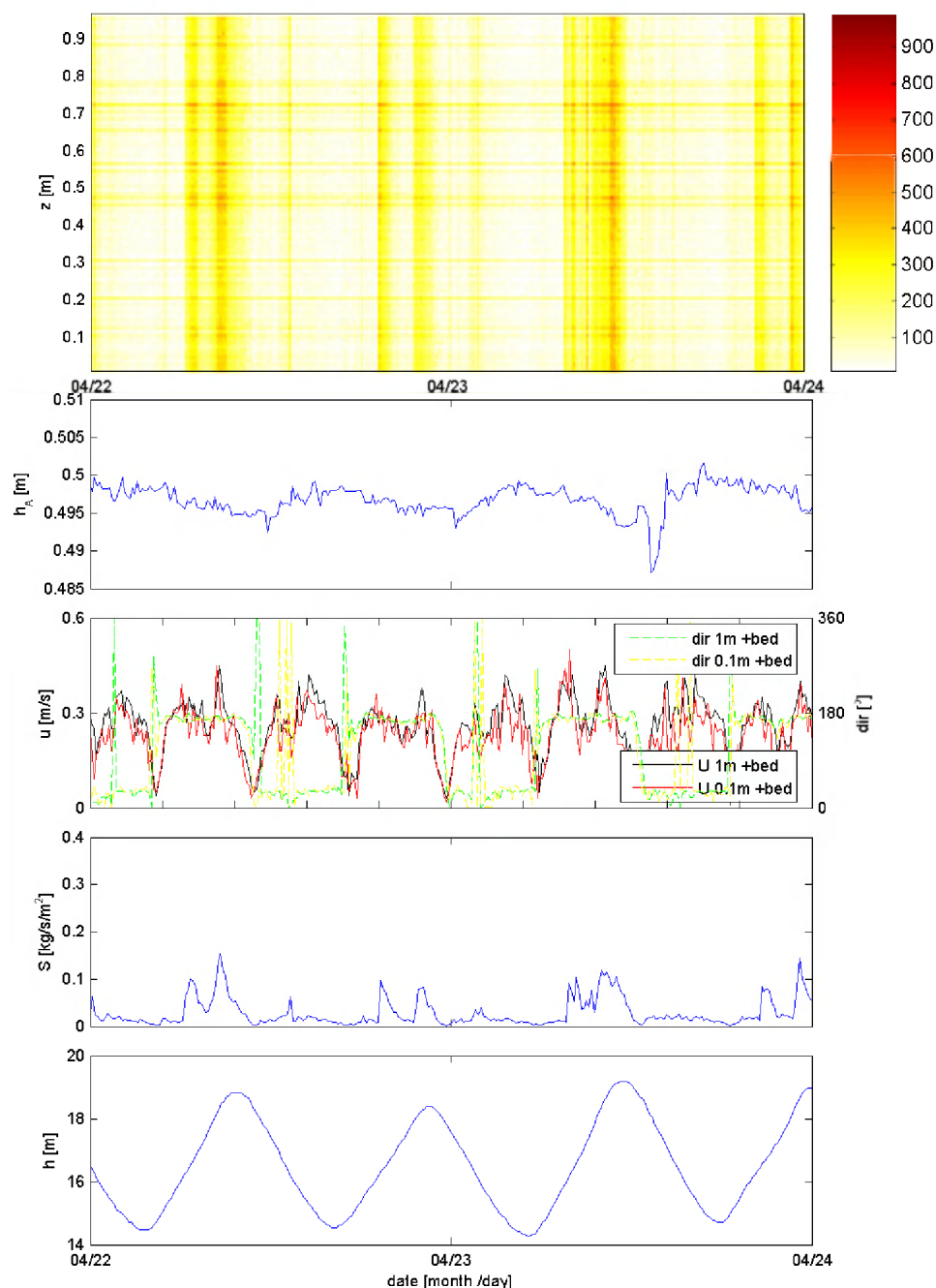
Figure 7.5: From top to bottom: sediment concentration (mg/l), measured with the ARGUS; depth h_A measured with the ALTUS (average of 4 beams, with an increasing h_A being erosion); flow velocity and direction measured with both currents meters (although the bottom meter was not functioning properly); sediment flux S, computed with the upper EMF and ARGUS sensor at 90 cm above the bed, and water depth h, measured at the future CDW location, downstream of the Deurganckdok, in April 2006.

7.1.3. Spring-neap variation

Interpretation of the spring-neap variation in sediment concentration and bed level variation is difficult, as:

- The measurement frames are retrieved and replaced every two weeks. After each new deployment the hydraulic and sedimentary conditions have changed, and the local equilibrium in sediment concentration/ amount of bed sediment may be disrupted, thereby obscuring the spring-neap pattern. Some deployment periods (of two weeks) were characterized by higher or lower sediment concentrations than others. Also, erosion prevailed during one two-week deployment, whereas deposition or a constant bed level prevails during the next.

- There is a trend in some of the observations, possibly due to sliding of the frame into deeper water (i.e. the CDW frame in July-August 2006) or (bio-) fouling (both frames in July-October 2006).

Nevertheless, interpretation of the frame data in appendix E provides the following information:

- There is a clear spring-neap variation in velocity. At the sill, the spring tide maximum flow velocities are approximately two times the maximum neap tide flow velocities. At the CDW location, the spring tide maximum flow velocities are approximately 1.5 times the maximum neap tide flow velocities.

- There is no spring-neap variation in erosion or sedimentation. The sedimentation rate only varies within each two week deployment during the July – October sill deployment, with higher accretion rates at the beginning of the two-week period than at the end. However, the frame is retrieved and replaced at spring tide, and therefore the slow and rapid accretion occurs both during spring tide. Hence, the changing accretion rate probably reflects the achievement of a local equilibrium, rather than a spring-neap variation.

- There is no clear spring-neap variation in sediment concentration. This is surprising since long-term measurements on the Scheldt clearly show a spring-neap variation in sediment concentration. Therefore it seems that the magnitude of possible corruptions of the sediment concentration sensors is comparable to the spring-neap cycle in sediment concentration.

7.1.4. Seasonal variation

Erosion prevailed on the sill during the first weeks of the March-April 2006 deployment, indicated by a gradual increase of h (see Appendix E) of approximately 2 cm/week. The other surveys, on the other hand, show a persistent sedimentation (increasing bed level in the ARGUS survey, May 2006, and decreasing depth recorded with the ALTUS in the July-October 2006 and the March-April 2007 surveys): up to 15 cm/week in April 2007, and about 5 cm/week in April 2006 and September-October 2006. This cannot be explained with physical seasonally-varying processes. The intertidal variation in bed levels, sediment concentration and flow velocity (section 7.1.1) suggest that there is close morphodynamic equilibrium where a high sediment concentration or low flow velocity results in deposition, and conversely a low sediment concentration or high flow velocity results in erosion. And since the sediment concentrations on the Scheldt are approximately two times higher in winter than in summer (based on long-term moorings such as the nearby Boei84 and Boei97), it would be expected that deposition rates are higher in winter than in summer. This does not follow from the frame measurements. However, also the seasonal variation in sediment concentration measured at the frames is less pronounced than that in the long-term measurement stations. Probably, the variance in sediment concentration introduced by different

deployment locations and trends caused by sliding or fouling (see section 7.1.2), exceed the seasonal variation in sediment concentration (similar to the spring-neap variation, see 7.1.2).

7.2. Summary of model results

The behaviour if the 3D mud model (van Maren et al, 2007) has been calibrated extensively against the sediment concentration measurements done on the Scheldt River (the K-transect). It has been validated with deposition rates in the dock. This revealed that although the magnitude of the sediment influx is reasonably reproduced, but the pattern was not. A problem with this validation is, however, that sedimentation in the dock is strongly influenced by maintenance dredging, capital dredging, and shipping. The model predicts high sedimentation rates on the sill, but since the sill is dredged almost every week, the measured deposition rates are low. Nevertheless, the model results have not yet been compared with the sill frame measurements. Therefore an example of 2 days of modelled sediment concentration, bed level variation, flow velocity and water levels, are presented in a similar way to the measurements (Figure 7.6). This can be compared with measurements, such as those in (Figure 7.2).

The model captures some of the essential aspects of the processes on the sill, but also has some deficiencies. The modelled bed level variation is similar to observation in the sense that high flow velocities and low sediment concentrations lead to erosion. The following phase with high sediment concentrations with comparable flow velocities, however, leads to deposition. It therefore seems that the model captures the saturation of the concentration profile, which was concluded to be responsible for the sedimentation on the sill (see the previous section). Also, the modelled sediment concentration is vertically more or less uniform, which is in line with the observations. There are also some shortcomings in the model. The modelled flow velocity is less spiky than the observed flow velocity: the modelled horizontal eddy is more constant in time and space than in reality. Secondly, the sediment concentration is rather low. The sediment concentrations computed with optimal settings (see Van Maren 2007) lead to concentrations on the sill that are more or less typical for summer conditions, but too low for winter conditions. Thirdly, the modelled bed level variation is typically less than 0.5 cm while the measured tidal variation easily exceeds 1 cm. This may reflect the relative low amount of sediment transported in suspension computed by the model.
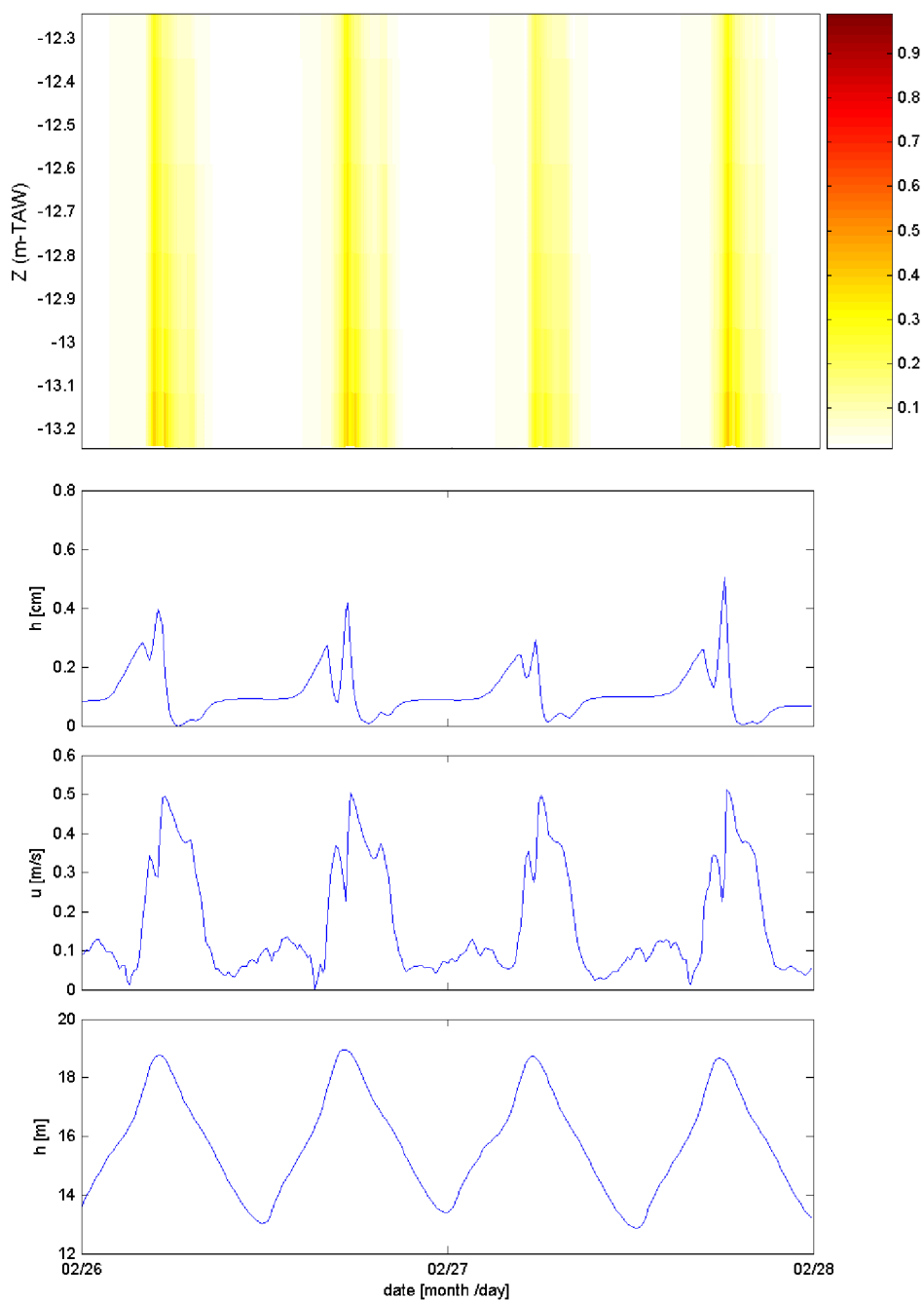
Figure 7.6: From top to bottom: 1. sediment concentration; 2. difference between the maximum and actual bed level (comparable with ARGUS results); 3. velocity at approximately 80 cm above the bed; 4. water level, computed at the location of the Deurganckdok sill frame, using validated model settings (flocculation model B, τ_{cr}=0.06 Pa and M_e=6.7 10^{-2}).

7.3. Formation of HCBS

Under equilibrium conditions, the vertical sediment concentration profile may be described with the Rouse profile:

$$c\left(z\right) = c_a \left(\frac{h-z}{z}\frac{a}{h-a}\right)^{z_*}$$

where h is the water depth, a is a reference level above the bed at which $c = c_a$ and z_* is the Rouse number defined as:

$$z_* = \frac{h w_s}{4\varepsilon_{s,max}} = \frac{w_s}{\kappa u_*}$$

where w_s is the settling velocity and $\varepsilon_{s,max}$ is the maximum eddy diffusivity. The Rouse profile assumes a parabolic eddy diffusivity according to:

$$\varepsilon\left(z\right) = 4\varepsilon_{s,max}\frac{z}{h}\left(\frac{h-z}{h}\right) \quad \text{with } \varepsilon_{s,max} = \tfrac{1}{4}\kappa u_* h$$

The shear stress velocity u_* is derived from the depth-averaged velocity u and the bed friction according to:

$$u_* = \sqrt{\frac{\tau_b}{\rho}} = u\frac{\sqrt{g}}{C} \quad \text{with } C = 18\log\left(\frac{12h}{r}\right)$$

where C is the Chézy coefficient, r is the bottom roughness height, τ_b is bed shear stress and ρ is the water density.

The steepness of the vertical sediment concentration profile depends on the value of the Rouse number z_*. A high settling velocity, a low current velocity and a smooth bed favours a steep vertical profile, whereas a low settling velocity, a high current velocity and a rough bed favours a uniform vertical profile. For $z_* > 3$ bed load transport dominates.

(Figure 7.7) shows Rouse vertical concentration profiles for typical Sea Scheldt conditions. During ebb and flood, the fraction of $w_s < 1$ mm/s is well mixed. During slack water, the profile of the fraction > 1 mm/s becomes steep. (Figure 7.7) illustrates that both well-mixed and stratified conditions may occur in the Sea Scheldt.
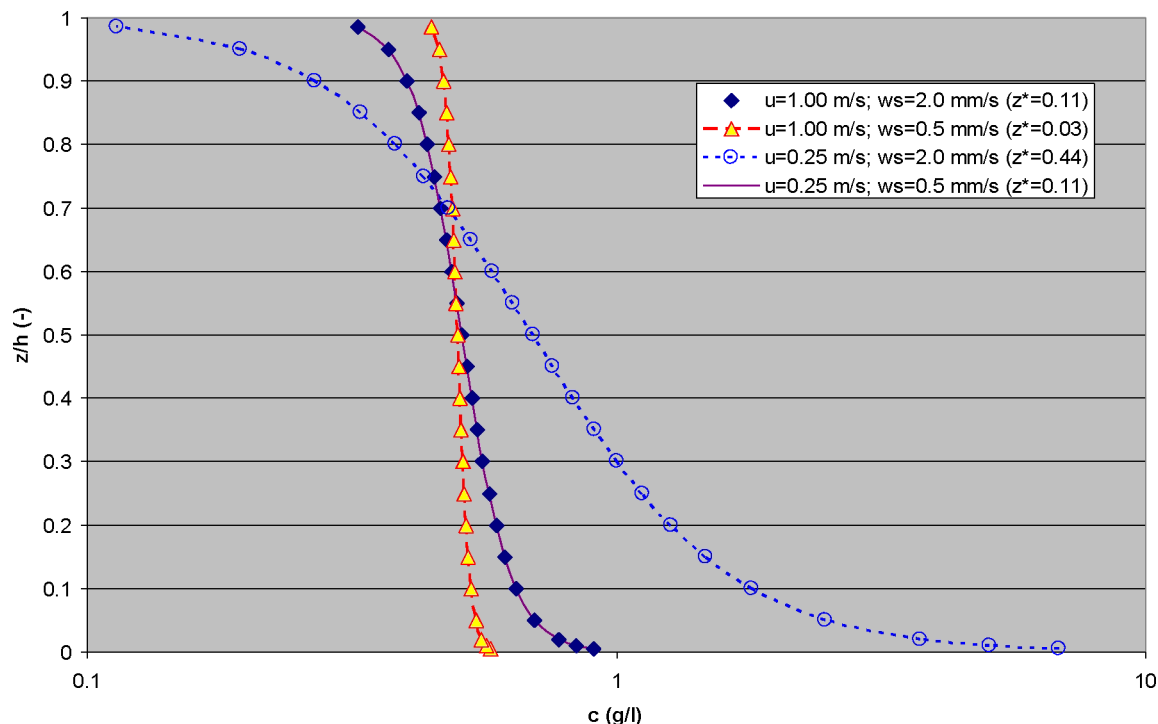
Figure 7.7: Rouse concentration profiles for typical Sea Scheldt conditions (h = 15 m; C = 70 m$^{0.5}$/s; w$_s$= 0.5 and 2 mm/s and u = 0.25 and 1 m/s). Note that the profiles for u = 1 m/s, w$_s$ = 2 mm/s and u = 0.25 m/s, w$_s$ = 0.5 mm/s are identical, as their Rouse numbers z$_*$ are equal. Note logarithmic scale on x-axis and relative depth (z/h) on y-axis. C$_{avg}$ = 0.5 g/l.

The Rouse profile is based on a number of assumptions which may be violated in the Sea Scheldt. The most important ones are discussed here:

1. Uniform sediment fraction

2. Equilibrium (i.e. no time derivative)

3. Parabolic eddy diffusivity profile

Because of the first assumption, the modelled near-surface and near-bed concentration may deviate from the observed ones. At slack water, the finest fraction may not settle, which –if not presented in the Rouse profile– results in an underestimation of the surface concentration. At ebb and flood tide, the coarsest fraction may still settle, which – if not presented in the Rouse profile– results in an underestimation of the near-bed concentration. By taking into account multiple sediment fractions (*i.e.* by taking the sum of the profiles of several uniform fractions), a more accurate description of observed concentration profiles may be obtained.

The second assumption (*i.e.* equilibrium) forms an important limitation for tidal flows, as the equilibrium profile during slack water may never be attained because of the short duration of the slack. A typical time scale to reach equilibrium is the required sediment settling time: $t_{eq} = h/w_s$. For h = 15 m and w_s = 0.5 mm/s, t_{eq} = 8.3h. For h = 15 m and w_s = 2 mm/s, t_{eq} = 2.1h. This demonstrates that except for the coarsest fraction (w_s > 0.5 mm/s), the duration of slack water is too short to reach a new equilibrium profile. However, sediment near the bed may still settle.

The third assumption (*i.e.* a parabolic diffusivity profile) may be violated because of three effects:

1. temperature-induced density gradients

2. salinity-induced density gradients

3. sediment induced density gradients

4. Acceleration or deceleration

5. Waves

Density gradients of sufficient strength tend to dampen turbulent mixing. A criterion for turbulence damping is the flux Richardson number:

$$Ri_f = -\frac{\rho_s - \rho_w}{\rho_s}\frac{g\overline{w'c'}}{\rho\overline{u'w'}\partial u/\partial z}$$

where the prime is the fluctuating part of the horizontal velocity u, the vertical velocity w and the sediment concentration c. Assuming local equilibrium between settling and mixing, and that the turbulent fluxes are generated by the mean velocity gradient (the Boussinesq assumption), the flux Richardson number can be rewritten into:

$$Ri_f = -\frac{\rho_s - \rho_w}{\rho_s}\frac{gw_sc}{\rho v_T(\partial u/\partial z)^2}$$

where v_T is the viscosity.

For Ri > 0.2, turbulence is damped and the stratification remains stable.

For each °C temperature increase, the water density decreases with about 0.2 kg/m^3. For each ppt salinity increase, the water density increases with about 0.8 kg/m^3. For each kg/m^3 sediment concentration increase, the bulk density of the suspension increases with about 0.6 kg/m^3.

The observed salinity difference in the Sea Scheldt between the surface and the bed is typically 0.5 ppt. Few observations show a gradient larger than 1 ppt. The observed temperature difference is less than 0.5 °C (neglecting a thin layer near the surface in which a larger temperature difference is sometimes observed). This leads to the conclusion that in the Sea Scheldt, salinity-induced density gradients are much more important than temperature-induced density gradients. The salinity difference between surface and bottom typically results in a density difference of 0.4 kg/m^3 and a density gradient of 0.03 kg/m^3/m. Sediment-induced density gradients start to dominate the overall density gradients for near-bed sediment concentrations over 1 kg/m^3 (the surface concentration typically remains below 0.2 kg/m^3, resulting in a sediment-induced density difference of 0.5 kg/m^3 and a density gradient of 0.03 kg/ m^3/m).

A first-order approximation of the velocity gradient is the ratio of depth-averaged velocity and water depth. With the examples of u = 1 m/s and 0.25 m/s and a water depth of 15 m, du/dz is 0.067 1/s and 0.017 1/s, respectively. With typical values for the settling velocity and the sediment concentration (w_s =1 10^{-3} to 1 10^{-4} m/s and c around 100 mg/l), and assuming a parabolic velocity profile, the water column will be stable at u = 1 m/s but unstable at u = 0.25 m/s.

Turbulence damping may therefore occur during slack water and HCBS formation may initiate. HCBS layers are an effective trapping mechanism for sediment: sediment may enter from the water column above by settling, but can not be re-mixed upwards because of the density gradient acting as a 'lid'. As this mechanism further increases the density gradient and reduces mixing, a bifurcation may occur leading to a stable HCBS layer. According to Winterwerp (1999), the

expression for the vertical concentration profile c_s (z) at which saturation occurs for steady-state conditions is:

$$c_s\ z\ = \frac{0.15\rho}{\Delta g\kappa}\frac{u_*^3}{hw_s}\left(\frac{h}{z}-1\right)$$

where u_* is the shear velocity, h water depth, w_s the local settling velocity and κ the von Kármán constant. Herein the effect of salinity and temperature-induced density gradients is still neglected; they will result in a lower saturation concentration. Integrating this equation over depth yields (Winterwerp, 1999):

$$C_s = K_s\frac{\rho}{\Delta g}\frac{u_*^3}{hw_s}$$

Table 7.1 shows the depth-averaged saturation concentration C_s for our example of u = 1 and 0.25 m/s and w_s = 0.5 and 2 mm/s. For slack water, the saturation concentration lies well below typically observed depth-averaged concentration levels. This relation is visualized in more detail in Figure 7.8. Depending on the settling velocity, the flow becomes saturated at concentrations typically low for the Scheldt (0.1 g/l) at velocities less than 0.15 to 0.3 m/s (for small to large settling velocities, respectively). For typically high sediment concentrations (0.5 g/l) the critical velocity is 0.05 to 0.1 m/s higher. This implies that fluid mud can only form on the Scheldt at slack tide, but throughout the tide in the locks (with typical maximum flow velocities around 0.3 m/s).

Table 7.1: Depth-averaged saturation concentration C_s for h = 15 m; C = 70 $m^{0.5}$/s; K_s = 1.325, and w_s= 0.5 and 2 mm/s and u = 0.25 and 1 m/s.

w_s / u	0.25 m/s	1 m/s
0.5 mm/s	0.04 kg/m^3	2.76 kg/m^3
2 mm/s	0.01 kg/m^3	0.69 kg/m^3
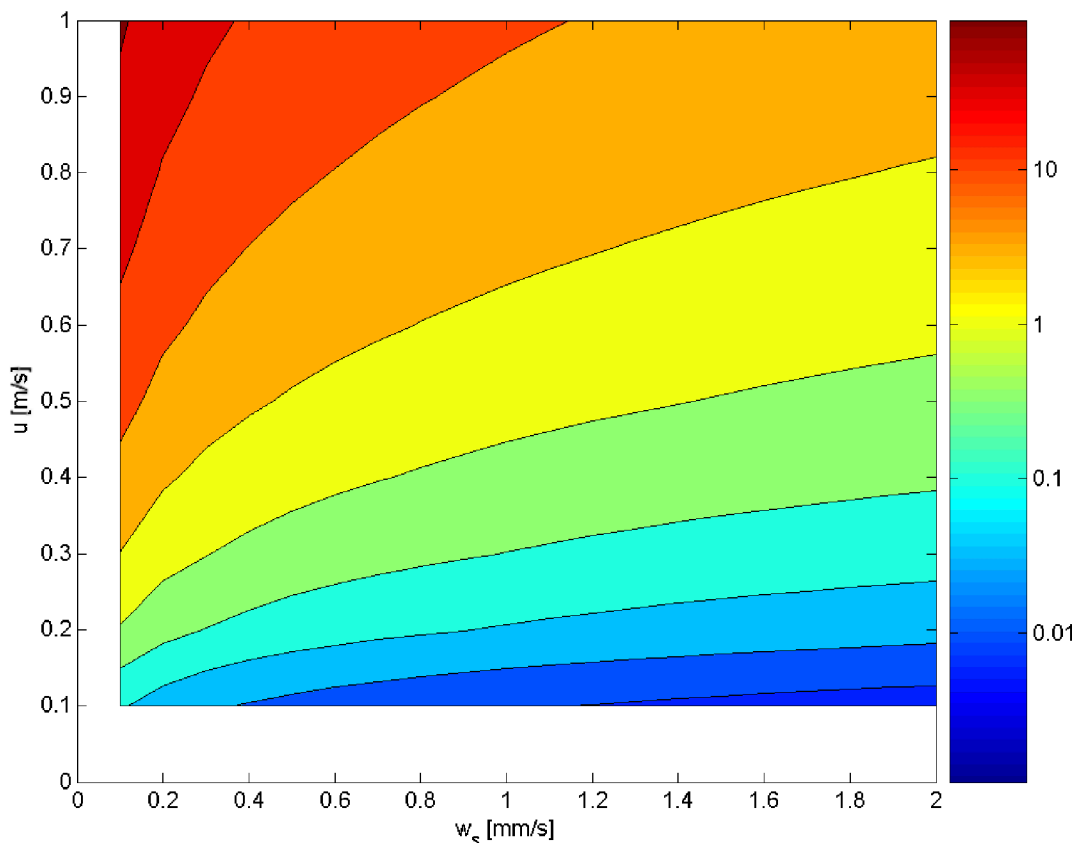
Figure 7.8 Saturation concentration C_s (in kg/m³) as a function of settling velocity and depth-averaged flow velocity, using h = 15 m; C = 70 m$^{0.5}$/s; K_s = 1.325,

Although the analysis above demonstrates that a HCBS layer will start to form during slack tide, the main question is whether the HCBS layer remains intact after the tidal current has increased in strength again or re-mixing occurs with the overlying water column. To address this question, a 1DV numerical model is applied, as an analytical evaluation is not straightforward (Winterwerp, 1999).

The 1DV model is applied in two modes, both stationary and tidal. The stationary results are compared with the analytical results discussed above. Subsequently, the tidal mode is applied to evaluate the criteria for re-mixing after slack water.

(Figure 7.9) shows a comparison between results obtained with the 1DV model in stationary mode and Rouse equilibrium profiles. For the cases u = 1 m/s and w_s = 0.5 and 2 mm/s, 1DV and Rouse profiles are similar, but not identical. This may be explained by differences in mixing: in the 1DV model, a k-ε turbulence closure model is used, whereas the Rouse profile is based on a parabolic eddy viscosity profile. For the cases u = 0.25 m/s and w_s = 0.5 and 2 mm/s, the 1DV model computes a collapse of the concentration profile because of sediment-induced turbulence damping. This is in agreement with Table 7.1, which indicates that for u = 0.25 m/s, the sediment concentration for which saturation occurs (0.04 and 0.01 g/l for w_s = 0.5 and 2 mm/s, respectively) lies well below the applied initial concentration (0.5 g/l). Based on the saturation criterion, a

concentration collapse at a velocity just under 0.9 m/s for w_s = 2 mm/s. Indeed, the 1DV model computes such a collapse for a velocity between 0.8 and 0.9 m/s.
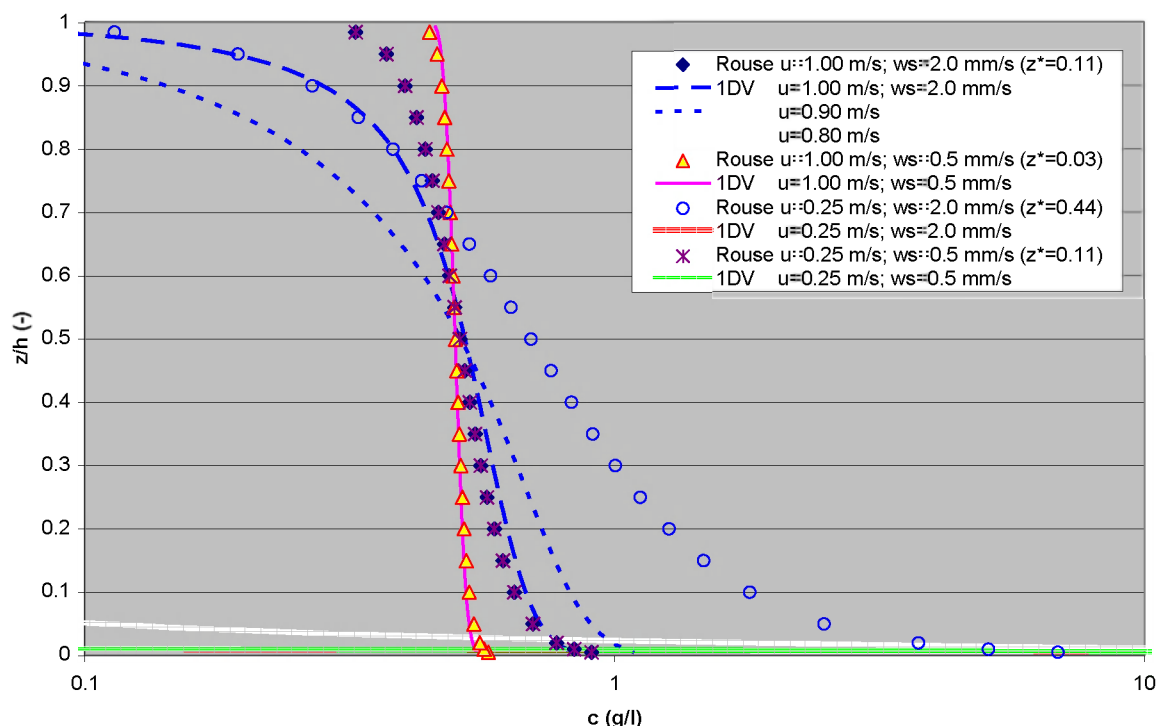
Figure 7.9: Comparison of stationary 1DV results with Rouse profiles for equal conditions (h = 15 m; C = 70 $m^{0.5}$/s; w_s= 0.5 and 2 mm/s and u = 0.25 and 1 m/s). C_{avg} = 0.5 g/l.

The next step is to apply the 1DV model to tidal conditions. An idealised sinusoidal tide with a period of 12.5h has been applied with several velocity amplitudes (in the range 0.25 – 2 m/s). As initial condition, a depth-averaged concentration of 0.1 g/l has been applied.

From the tidal simulations it is concluded that the tidal velocity at which an irreversible sediment concentration collapse occurs is somewhat reduced compared to the steady case. For w_s = 0.5 mm/s, the profile collapses for a tidal velocity amplitude between 0.5 and 0.4 m/s, whereas for the steady case the collapse occurs between 0.4 and 0.3 m/s (Figure 7.10). For w_s = 2 mm/s, the profile collapses for a tidal velocity amplitude between 0.7 and 0.6 m/s, whereas for the steady case the collapse occurs between 0.6 and 0.5 m/s (see Figure 7.11).

At higher tidal amplitudes, the concentration profile still partly collapses during slack water due to particle settling, but the sediment is remixed through the water column during ebb or flood. This is illustrated in (Figure 7.12).
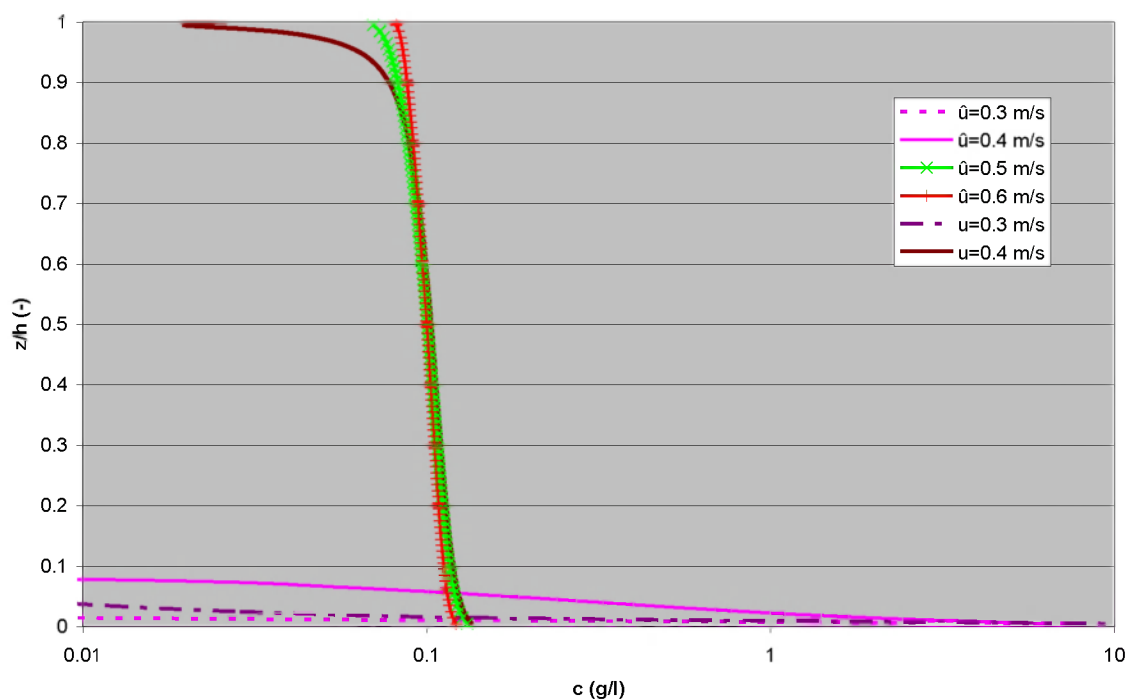
Figure 7.10: Sediment concentration profiles (in g/l) at maximum tidal velocity computed with 1DV model for different tidal velocity amplitudes (û = 0.3, 0.4, 0.5 and 0.6 m/s) and two steady current magnitudes (u = 0.3 and 0.4 m/s). w_s = 0.5 mm/s, C_{avg} = 0.1 g/l.

Figure 7.11: Sediment concentration profiles (in g/l) at maximum tidal velocity computed with 1DV model for different tidal velocity amplitudes (û = 0.5, 0.6, 0.7 and 1.0 m/s) and two steady current magnitudes (u = 0.5 and 0.6 m/s). w_s = 2.0 mm/s, C_{avg} = 0.1 g/l.

Figure 7.12: Vertical sediment concentration profiles during maximal flood velocity (MFV) and slack water for non-saturated conditions, compu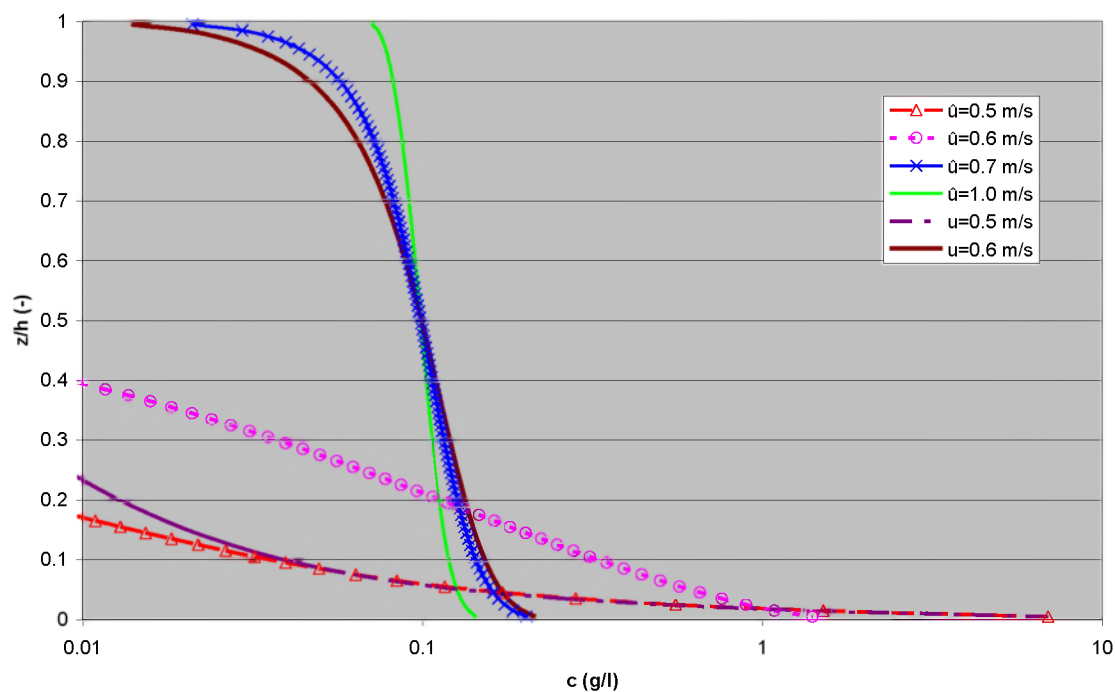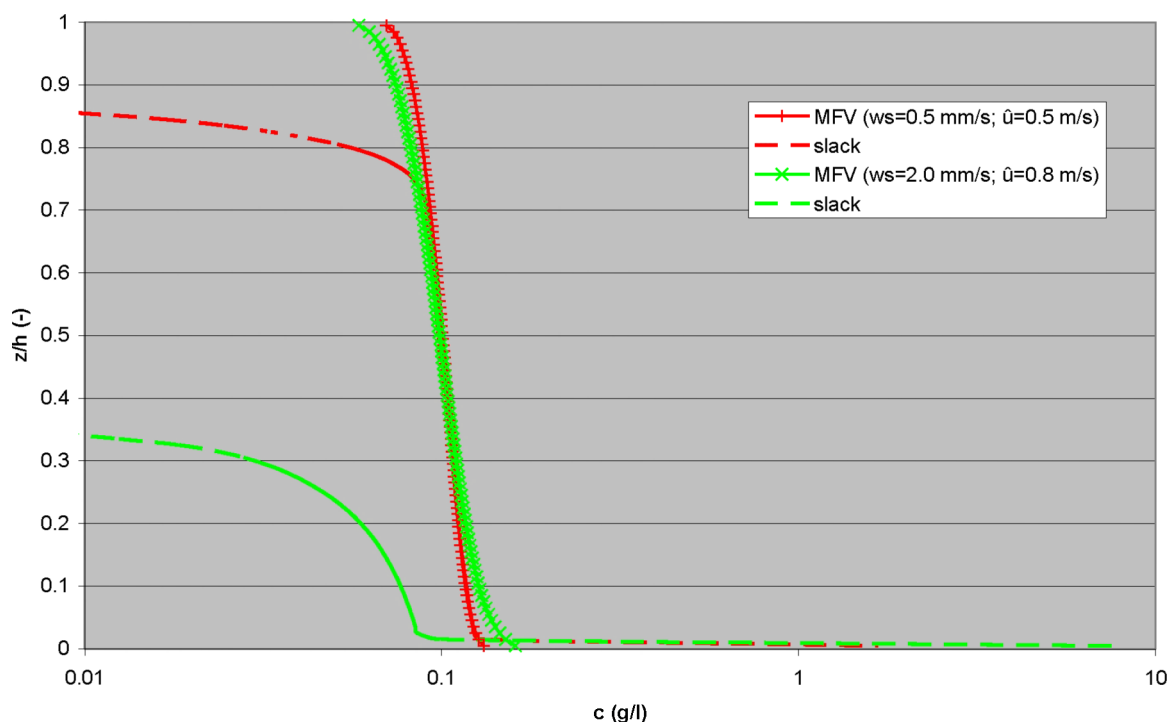ted with 1DV model (w_s = 2 mm/s: $\hat{u}_{tide}$ = 0.8 m/s; w_s = 0.5 mm/s: $\hat{u}_{tide}$ = 0.5 m/s). C_{avg} = 0.1 g/l.

These simulations show that HCBS layers may be formed and remain in the Sea Scheldt in areas with sufficiently low maximum tidal velocities (roughly below 0.5 m/s, but this depends on the sediment properties and supply). HCBS layers may act as an effective sediment trap if the residence time of the water above the HCBS exceeds the particle settling time.

By definition, 1DV simulations assume spatial uniformity. In reality, the interaction of bathymetry, current patterns and the spatial distribution of suspended sediment will result in specific areas where HCBS formation is likely and other areas where the generation of such layers is impossible due to strong tidal mixing. It is noted that in areas where HCBS formation is impossible, they may still be observed due to advection. Through advection of HCBS layers, the local sediment availability may strongly increase, thus triggering saturation, even though tidal currents are relatively strong.

Additionally, the 1DV simulations are done for unidirectional flow velocity, where a deviation from a logarithmic velocity profile is only related to sediment-induced density effects. However, in the Deurganckdok, a two-layer flow system exists for a substantial part of the tidal cycle. Here, HCBS may form during period of near-bed inflow of turbid water and outflow of (clearer) surface water. Hence, turbulence is not only generated at the bed, but also at the density interface between the surface layer and the bottom layer. Also, the effective depth decreases due to 2-layer flow, which increases the saturation concentration, and therefore HCBS formation.

7.4. Transport of HCBS

In this section two questions are addressed: first, to establish the conditions for which near-bed transport becomes the dominant contribution to total transport and second, to investigate the conditions for which HCBS layers may or may not be transported.

The sediment flux is the product of the velocity and sediment concentration profile. The latter has been discussed to some extent in the previous section. (Figure 7.13) shows the vertical distribution of the sediment flux for different Rouse numbers. The Rouse number z* is defined as

$$z* = \frac{w_s}{\kappa u_*}$$

where w_s is the settling velocity of the sediment, u_* is the bed shear velocity and κ the von Kármán constant (0.41). For z* < 0.1, the flux is nearly uniformly distributed over the water column, but for z* > 1, near-bed transport dominates the total transport. This is also true in case of a saturated sediment concentration profile (at z* = 0.11 for the applied conditions). When the flow is saturated, turbulent mixing is damped by the sediment-induced vertical density gradient to such a degree that sediment can no longer be held in suspension. The result is a collapse of the sediment concentration profile. (Figure 7.14) shows that over 50% of the cumulative sediment flux occurs in the lower 10% of the water column for z* > 1 and also in case of saturated conditions. In these conditions, focus should be on the measurement and analysis of the near-bed current and sediment distribution patterns near the bed, as these will contribute most to sediment transport and siltation such as near DGD.
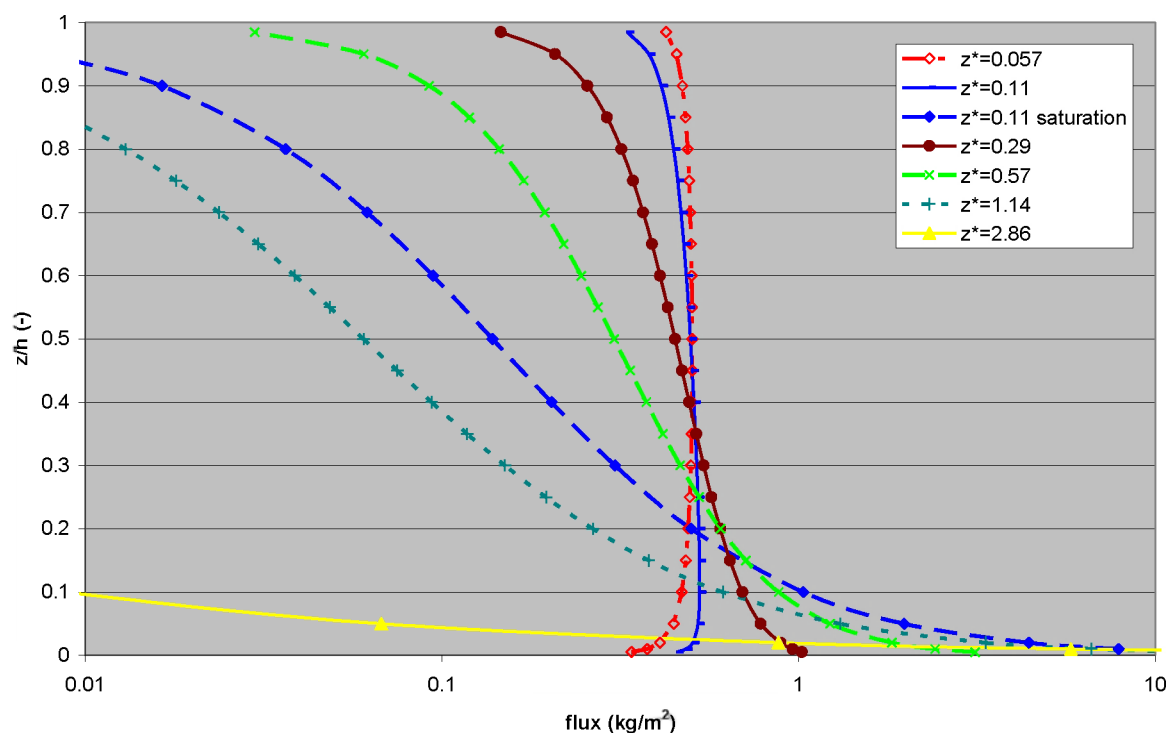
Figure 7.13: Vertical distribution of sediment flux using a logarithmic velocity profile and a Rouse equilibrium profile for different Rouse numbers. C_{avg} = 0.5 g/l; h = 15 m; u_{avg} = 0.95 m/s; C = 70 $m^{0.5}$/s. At w_s = 2 mm/s (z* = 0.11) saturation occurs (also shown).
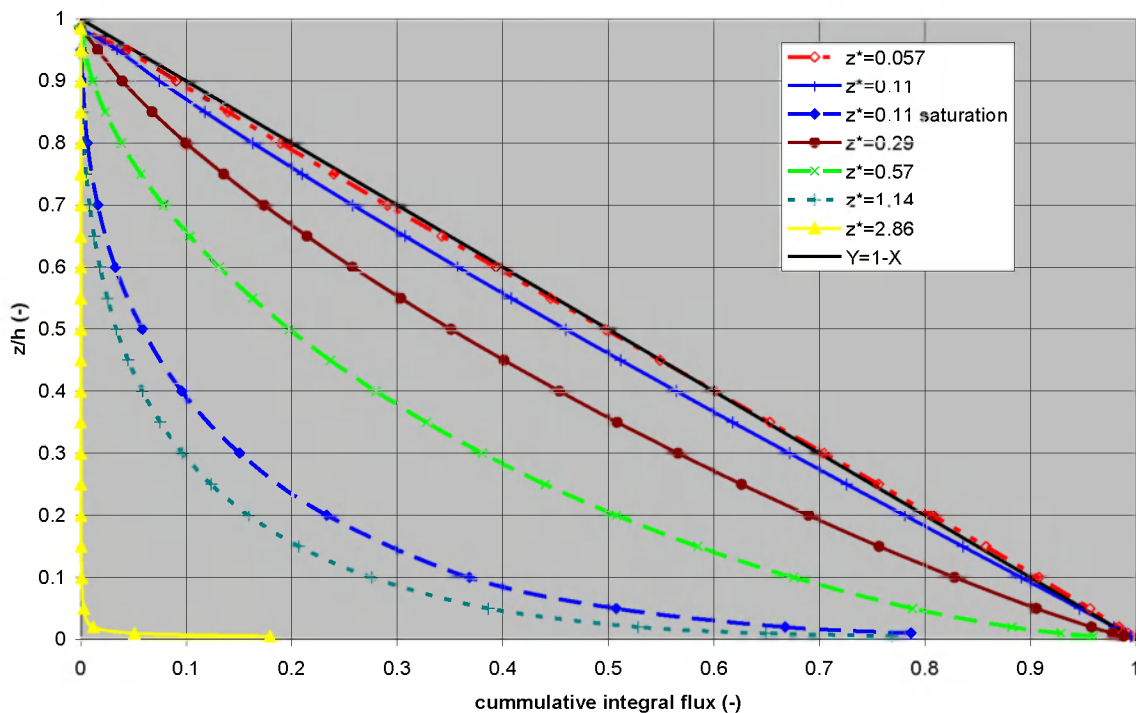
Figure 7.14: Cumulative integral flux using a logarithmic velocity profile and a Rouse equilibrium profile for different Rouse numbers. C_{avg} = 0.5 g/l; h = 15 m; u_{avg} = 0.95 m/s; C = 70 $m^{0.5}$/s. At w_s = 2 mm/s (z^* = 0.11) saturation occurs (also shown). See also Figure 7.13.
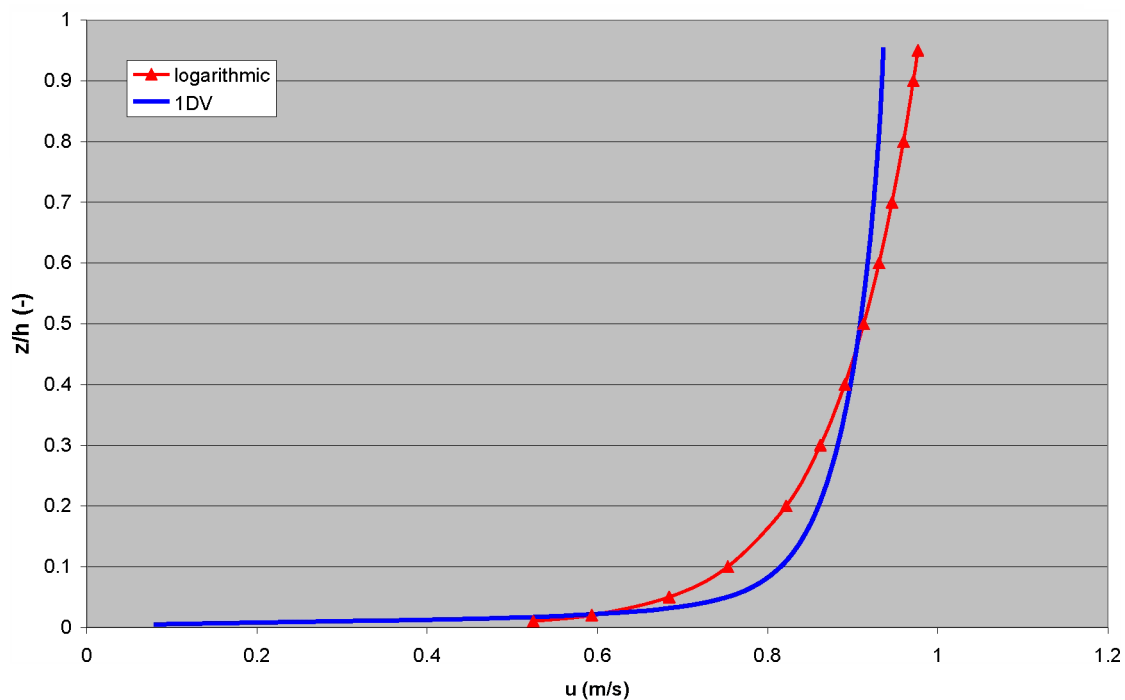

Figure 7.15: Velocity profile for u_{avg} = 0.9 m/s for logarithmic profile with C = 70 $m^{0.5}$/s and from 1DV model at saturation; h = 15 m.

Because of sediment-induced density gradients that influence the turbulence structure of the water column, the velocity gradient is modified. This is illustrated in (Figure 7.15), in which the velocity profile in the case of saturation is steeper than the logarithmic profile. Because of turbulence damping, the apparent bottom roughness decreases.

For the typical depth (15 m), tidal velocity (1 m/s) and particle settling velocity (2 mm/s) near DGD, conditions for which near-bed sediment transport is dominant may occur during slack water and in case of the presence of a HCBS layer. For other conditions fine sediment transport in the whole water column should be considered.

The next question to address is how HCBS layers may be transported from their location of generation to other locations. Transport is either caused by interfacial shear, gravity or pressure gradients.

- **Interfacial shear** is generated the interface roughness and the velocity difference between the two layers considered: $\tau_i = f_i \, \rho \, (u_1 - u_2)^2$. τ_i has the same order of the bed shear stress. Shear stress generated by gravity amounts to $\tau_g = \Delta\rho g h \sin\alpha$, with $\Delta\rho$ the density difference between HCBS layer and water, h the HCBS layer thickness and α the bed slope. A horizontal pressure gradient dp/dx generates a shear shear stress $\tau_p = h \, (dp/dx)$. Depending on the ambient conditions, one or more mechanisms may contribute to the transport of HCBS.

- Transport will only occur if the shear exceeds the yield strength of the HCBS layer. The yield strength of mud depends on its bulk density. For mud from the Sea Scheldt the following empirical relationship is derived from yield strength measurement: $\tau_y = a \, (\Delta\rho)^b$, with $a = 4.5 \, 10^{-12}$ Pa and $b = 5.7$ (Figure 2.4) (de Wit, 1995). The resulting yield strength is then used to determine the stability of the fluid mud or HCBS layer (Figure 7.17). Typically, thicker and denser layers are more likely to be transported by gravity force, whereas thinner, less dense layers are more likely to be driven by interfacial shear. For example a HCBS layer with $\Delta\rho = 1$ kg/m^3 and thickness 0.1 m on a bed with slope 0.01 experiences a gravitational shear stress of only 0.01 Pa, which less than a typical interfacial shear stress of 0.1 to 1 Pa. Such relatively thin and low-concentrated layers are therefore predominantly driven by interfacial shear. However, a fluid mud layer $\Delta\rho = 100$ kg/m^3 and thickness 1 m on a bed with slope 0.01 experiences a gravitational shear stress of 10 Pa, well above the typical interfacial shear stress. The dynamics of such relatively thick and high-concentrated layers are therefore often decoupled from the overlying water body.
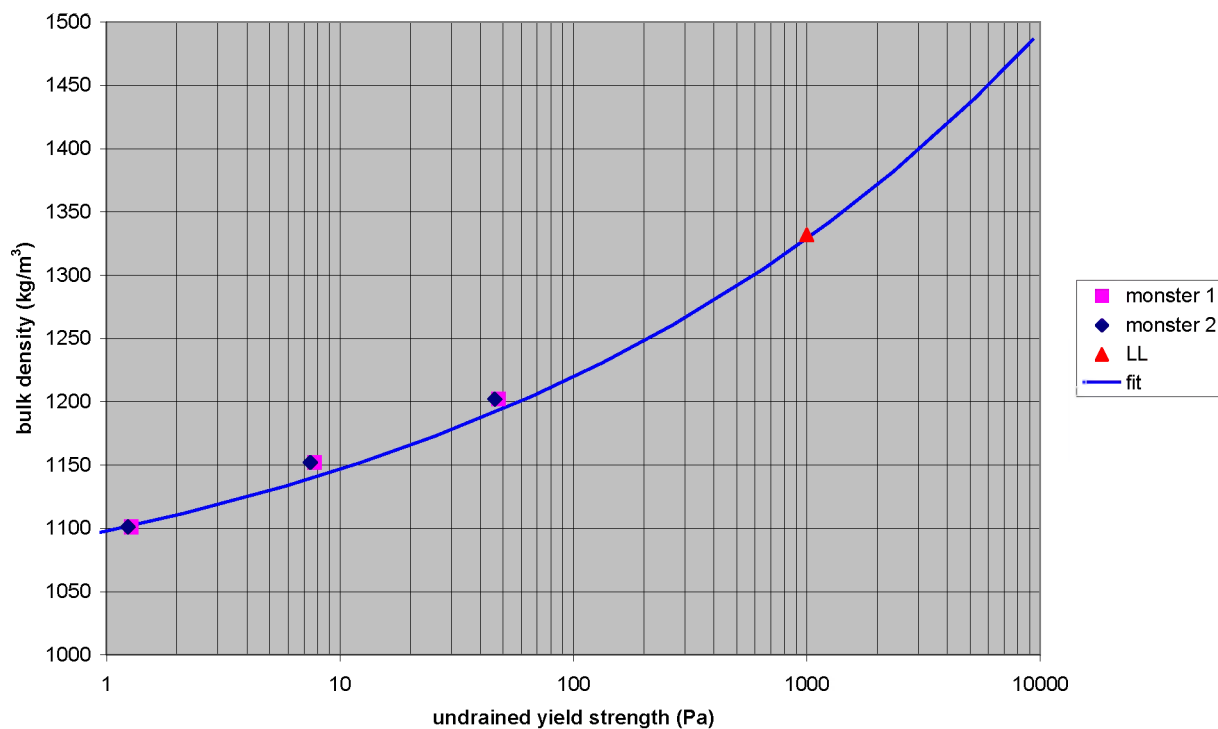
Figure 7.16: Relationship between bulk density and undrained yield strength for Sea Scheldt mud.
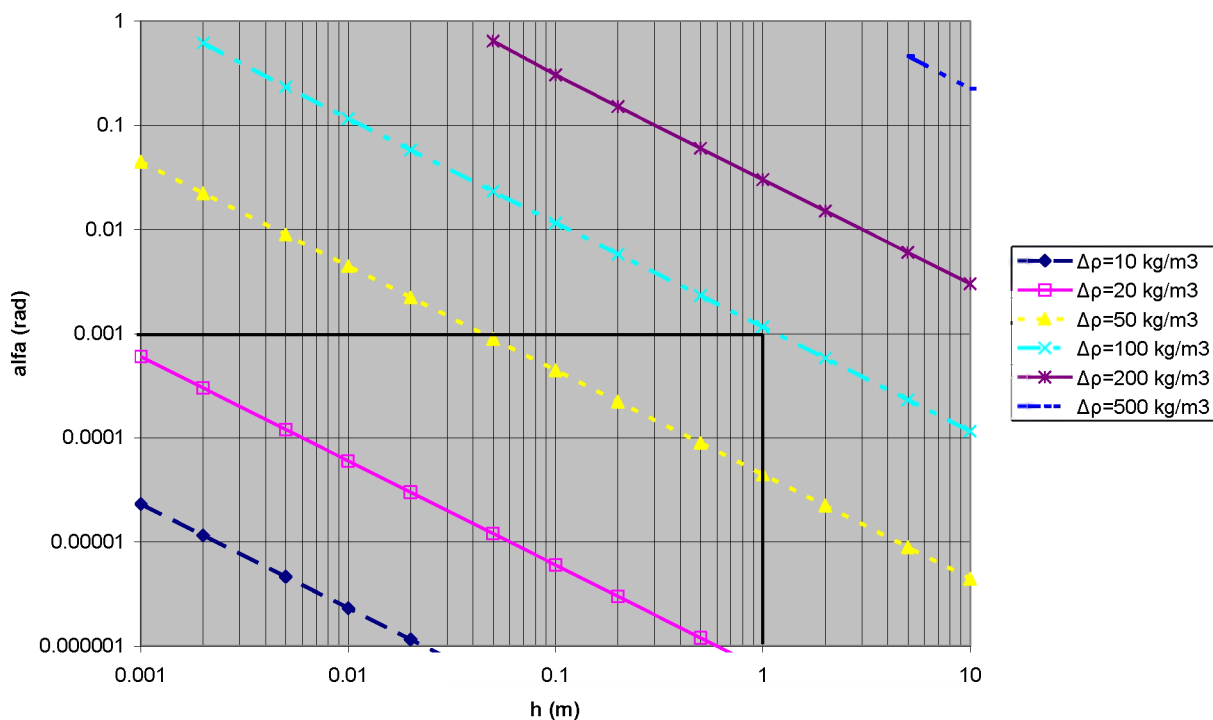

Figure 7.17: Stability criterion of mud layer with thickness h and excess density Δρ on a bed slope α. A mud layer with thickness 1 m and excess density 100 kg/m^3 has a critical bed slope of 0.001 rad.

7.5.   Flocculation and settling

In dynamic environments, such as estuaries and coastal waters, the settling velocity of cohesive sediment may vary largely in time and space by flocculation effects: see *e.g.* Van Leussen (1994), Winterwerp (2002), Winterwerp *et al.* (2006a). Flocculation is governed by (1) Brownian motions causing the particles to collide to form aggregates, (2) differential settling (particles with a large settling velocity will overtake particles with a low settling velocity, and collisions between these particles may result in aggregation and (3) shear effects (particles carried by eddies collide and form flocs whereas turbulent shear may disrupt the flocs again, causing floc break-up. In estuarine and coastal environments, the effects of Brownian motion and differential settling are probably negligible. Therefore the size of flocs is mainly governed by the degree of turbulence and the amount of particles in suspension.

With increasing turbulence, the collision frequency increases, thereby accelerating the time that flocs are formed. However, the equilibrium floc size D_e itself is not determined by the collision frequency. Rather, D_e is regulated by floc break-up due to turbulent shear and the amount of primary particles in suspension. The equilibrium floc size scales approximately linearly with the sediment concentration C, and inversely with the root of the turbulent shear (approximated with the dissipation parameter G), as (Winterwerp, 2002):

$$D_e = D_p + \frac{k_a C}{k_b G}$$

Where D_p is the size of the primary particle and k_a and k_b are empirical coefficients. As a result, the equilibrium floc size is maximal at low shear and high sediment concentration. However, since the timescales for floc formation become very large at low shear rates, the equilibrium flow size is not reached in most estuarine environments. Therefore the actual floc size is low at both very high and very low shear rates, with a maximal floc size in-between.

The settling velocity of flocs increases with the floc size, but decreases with the sediment concentration due to hindered settling effects. All these effects have been incorporated in a heuristic flocculation model that computes the effective settling velocity from turbulent shear (or relative kinetic energy) and sediment concentration, and has been calibrated against Scheldt data (Winterwerp et al., 2006a), see (Figure 7.18).
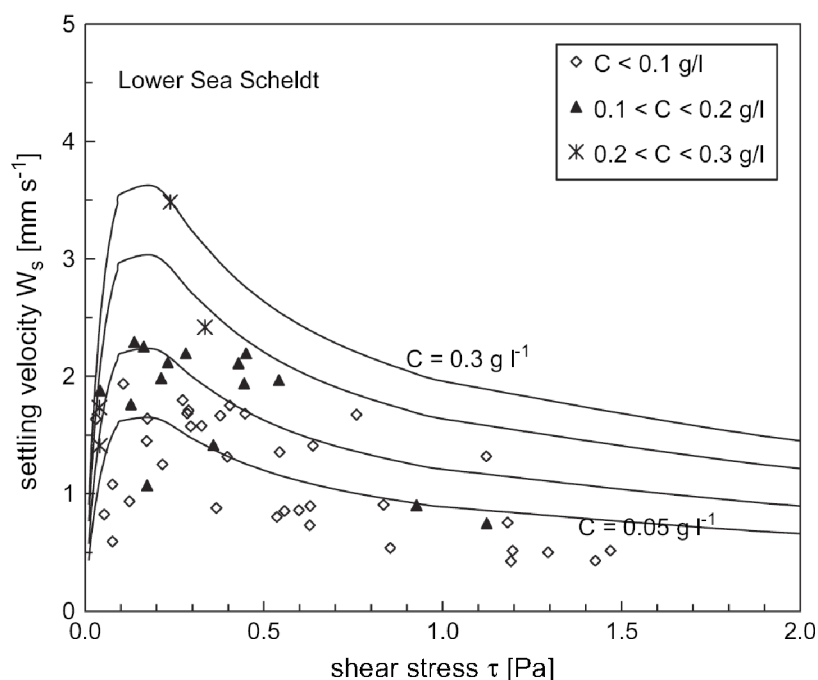
Figure 7.18: Sediment settling velocity in relation to the shear stress and the sediment concentration, calibrated with INNSEV measurements collected near the Deurganckdok in 2005 (Winterwerp et al. (2006a)).

This dependence of settling velocity on turbulence further complicates the picture of saturation presented in section 7.3, in which a constant settling velocity is applied. Therefore influence of flocculation on saturation is first estimated from the INNSEV measurements (Figure 6.17) to (Figure 6.19). On the Scheldt, the near-bed (0.65 m above the bed) shear stress is between 0.4 Pa (slack tide) to 1.5 Pa (peak currents). On the sill, the near-bed shear stress varies from 0.2 (slack tide) to 0.8 Pa (maximum flow). During the inflow of the turbid eddy, around HW, the shear stress is between 0.5 and 0.8 Pa. In the dock itself, the near bed shear stresses vary from 0.2 to 0.5 Pa. Hence, the shear stress in the dock is within the range of maximal settling velocities, whereas the shear stress in the Scheldt is much higher than the optimal shear stress for flocculation. On the Scheldt, high settling velocities can only be expected around slack tide. On the sill, the shear stress is within the range of maximal settling velocities throughout most of the tidal cycle, but higher during the inflow period of the turbulent eddy. Still, because of the high sediment concentrations during the inflow period of the eddy, the sediment settling velocities are maximal.

The flow velocity in the turbid eddy decreases as it propagates into Deurganckdok. At the moment that it flows over the sill, the shear stress is higher than the shear stress at which the settling velocity is maximal. This has two important implications. First, the saturation concentration decreases in time (and with the distance into the dock) as the eddy flows into the dock. With sufficiently high sediment concentrations in the inflowing eddy, at a certain time (and location in the dock) saturation is expected. A second effect of the decreasing flow velocities in the eddy is that the shear stress also decreases in time and with the distance into the dock. Since the shear stress on the sill is higher than the optimal sediment settling velocity shear stress (around 0.2 Pa), the sediment settling velocity can be expected to increase in time (and with the distance into the dock). Therefore the capacity concentration decreases not only due to decreasing flow velocities, but also due to increasing settling velocities.

7.6. HCBS occurrence near Kallo and Deurganckdok

In order to evaluate the occurrence of HCBS near Kallo or Deurganckdok, and to assess its contribution to sedimentation rates, it is necessary to establish how the occurrence and the effects of HCBS can be recognized from the field observations. The highly concentrated layer can be driven by the flow dynamics of the upper layer along the density interface, and may therefore be mobile. Velocities up to 0.75 m/s have been measured in HCBS layers in the Loire estuary (Bruens, 2003). Turbulence is generated near the bed, and dissipated at the lutocline. Therefore the HCBS layer itself is usually turbulent, sometimes more turbulent than the dilute suspension above. An additional distinct feature of HCBS is that either the upper water layer may entrain the HCBS layer, resulting in a lowering of the concentration in the HCBS layer while the lutocline height remains constant, or that HCBS layer may entrain the overlying water layer, leading to a lowering of the concentration while the lutocline rises (Bruens, 2003). Which of both effects occurs depends on the level of turbulence in both layers.

7.6.1. Sediment concentration

The sediment concentration measured with the SiltProfiler near Kallo and Deurganckdok never exceeds 1.5 g/l. Near the Deurganckdok, the sediment concentration reaches 1 g/l near the bed only, shortly after maximum flow velocities, and during winter. Near Kallo, only detailed concentration measurements have been made in winter. Sediment concentration profiles measured during periods of peak sediment concentrations (Figure 7.19) and (Figure 7.20) demonstrate that the sediment concentration peaks in the bottom meters, and that a substantial vertical sediment concentration gradient of several 100's mg/l/m exists. Such a concentration gradient produces a density gradient of up to 0.2 $kg/m^3/m$. This is insufficient to substantially dampen turbulent mixing at high flow velocities (over 1 m/s depth-averaged currents): a qualitative analysis of measured flow velocities reveals no appreciable modification from a standard logarithmic velocity profile. Some reduction of turbulent exchange is to be expected during the sediment settling following the period with high sediment concentrations *i.e.* during the slack tide following the peak flow velocities.

The question is whether the observed near-bed high concentration layers may have their own dynamics, or are predominantly dragged along by the overlying water. The concentration at which turbulence is damped by the sediment density effects increases with the flow velocity u (approximately with u^3). At the concentrations typically observed in the Scheldt, turbulence is sufficiently damped to develop a lutocline at flow velocities around 0.5 m/s (see section 7.3). The depth-averaged concentration required to damp turbulent mixing at peak flow velocities (1-1.5 m/s) is probably several g/l, which is much higher than the observed sediment concentration of around 1 g/l near the bed only (and 0.1-0.3 depth-averaged). In the docks, the flow velocities are sufficiently low that the concentration profile collapses. However, these environments are so low energetic, that the high concentration layer immediately begins to deposit and consolidate, and therefore only consolidating muds (which may be mobile initially) are formed. This can be further analysed with density measurements in the docks.

It is therefore concluded that although some features of HCBS are found in the measurements, it is a transient rather than a persistent state. At the Scheldt, the peak velocities are too high for a HCBS layer to survive throughout the tide. In Deurganckdok HCBS will disappear because of settling. So only temporarily and locally (at locations with intermediate dynamics), HCBS layers may occur.
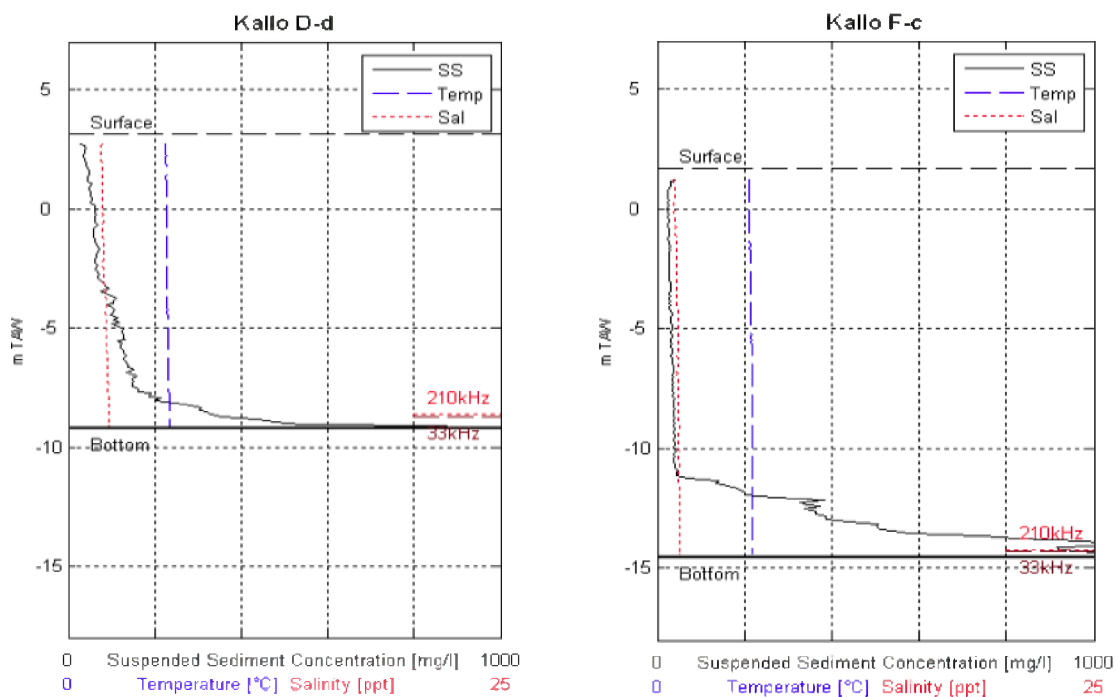
Figure 7.19: Sediment concentration, salinity, and temperature profiles near Kallo measured during peak sediment concentrations with the SiltProfiler. Left: Kallo Dd (right bank, upstream of Kallo) on 18/02/2005, 12h 42, 2 hrs after HW and right: Kallo Fc (right bank, downstream of Kallo) on 18/02/2005, 6:49, 4 hors before HW.

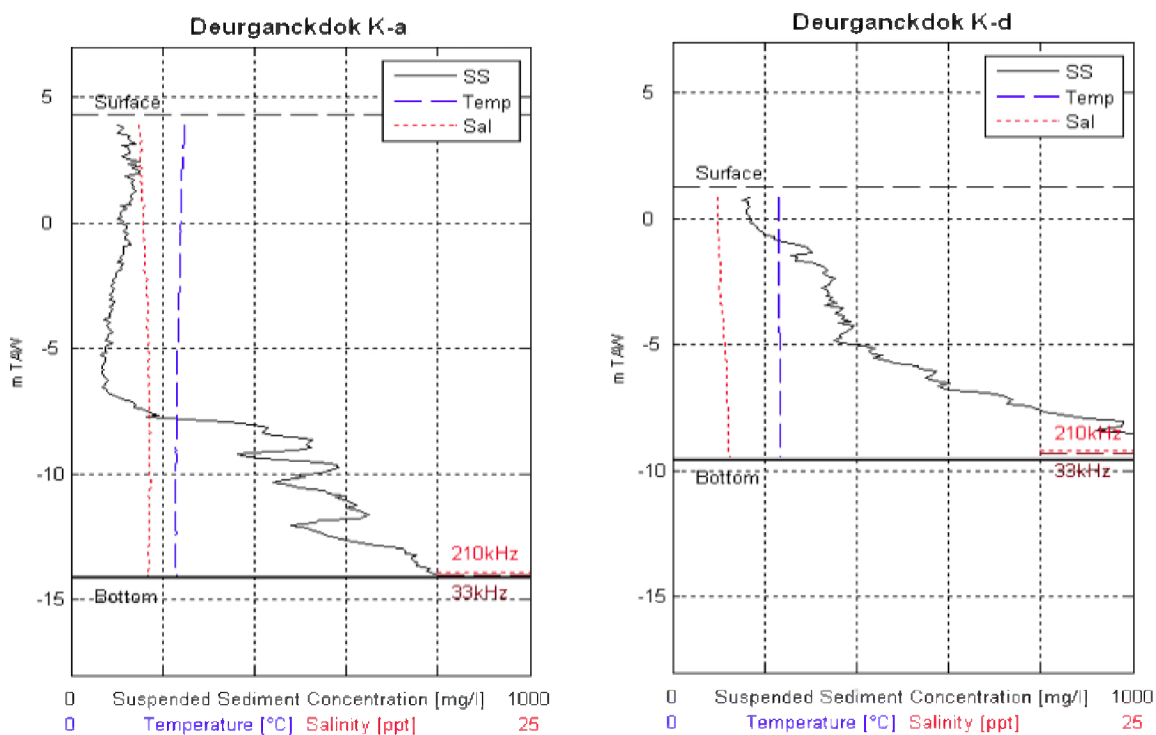*Figure 7.20: Sediment concentration, salinity, and temperature profiles near Deurganckdok measured with the SiltProfiler during peak sediment concentrations. Deurganckdok Ka (left bank), 16/02/2005, 7 hr*

52, 1 hour before HW (left) and Deurganckdok Kd (right bank), 16/02/2005, 12 hr 42, 4 hours after HW.

7.6.2. Density of sediment deposits

Measurements with the NaviTracker only reveal fluid mud layers in the basins (both Kallo and Deurganckdok), and not at the Scheldt itself. The measurements in the Deurganckdok are much more detailed than in Kallo, and therefore these are discussed in greater detail.

The mud is better consolidated at the entrance of the dock, than at the far end of the dock (Figure 7.21). In November and December 2005 the deposition rates in the landward end of the dock (1200 -1600 m) was close to 1 meter per month in response to an extension of the dock that was excavated in November 2005. In the other parts of the dock the average deposition rate was around 0.2 meter per month. The required time for consolidation increases quadratically with the thickness of the deposit, and therefore the consolidation time at the end of the dock is 25 times higher than at the beginning of the dock. Surprisingly, however, is that in 2006 the head of the dock was also less consolidated than the entrance, even though no capital dredging had taken place in 2006. Possibly, this spatial gradient reflects a different type of sediment or floc, where only the smallest sediment particles/flocs are able to be transported to the head of the dock.
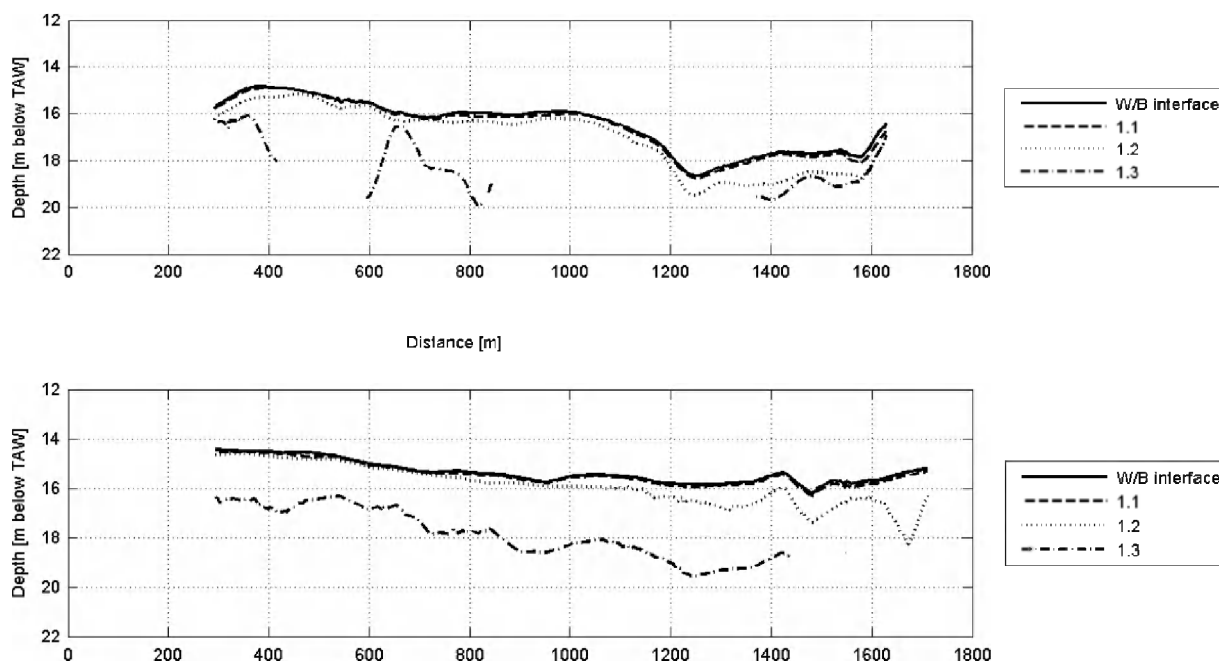
Figure 7.21: Lines of equal density measured in the longitudinal direction of the centre of the Deurganckdok, measured with the NaviTracker on 13 December 2005 top, (from IMDC report DGD 1.6) and on 20 September 2006 (from IMDC report DGD 1.5). The distance on the X-axis is from the Scheldt into the dock. The section between 1200 and 1600 m was recently excavated in November-December 2005.

7.6.3. Effect of the sill

It is noteworthy that the near-bed sediment concentrations observed with the SiltProfiler on the Scheldt River (Figure 7.19) seems to be higher than the sediment concentration observed on the sill with the ARGUS sensors on the sill frame. This may be caused by the fact that the sill is about 2 m higher than the bed of the River Scheldt. Hence, the turbid near-bottom layer that forms shortly after the peak currents is blocked by the sill and cannot be transported into the dock. Possibly

more important, it also implies that the highly concentrated lower layers in the dock are not transported out of the dock. Hence, the Deurganckdok is an effective sediment trap.

The main purpose of the sill is to prevent HCBS layers that could form on the Scheldt, to propagate into the dock. The observations suggest that fluid mud layers are absent or short-lived, and if existent relatively thin. If such layers do indeed not exist, the sill may be counterproductive by blocking fluid mud layers from propagating out of the dock into the Scheldt, while simultaneously not substantially blocking sediment import. Especially with the deepening of the Scheldt, where the depth of the Deurganckdok is comparable with the depth of the Scheldt, removing the sill may lead to reduced siltation rates in the dock. On the other hand, even though HCBS layers may not exist, the salinity-driven density currents generate near-bed flows into the dock during a period with large near-bed sediment concentrations (High Water). This sediment flux may be reduced with a sill. Due to these two opposing effects, the net effect of the sill on siltation rates is difficult to predict.

7.6.4. Comparison with other systems

In the above sections we conclude that HCBS layers are not persistent in the Scheldt, as the flow velocity in the Scheldt is so high that much higher sediment concentrations are required for HCBS to remain stable at peak velocity. A sufficient amount of sediment is available for the formation of HCBS in the docks, where the flow velocity is much lower. Here, however, the flow velocity is so low that sediment deposits and starts to consolidate almost instantly: HCBS cannot be maintained at such low turbulence levels. Also the bed level gradients (observed, but even more when correcting for dredged sediment masses) are probably too steep for HCBS to play an important role in suspended sediment transport into the dock.

The minor role of HCBS in the transport of sediment in the Scheldt River is further illustrated by the examples presented in section 2.3. In these examples, highly concentrated near-bed suspensions have typical concentrations of several g/l to tens of g/l. This is an order of magnitude higher than the concentrations observed in the Scheldt.

7.7. Numerical modelling of HCBS in the Lower Sea Scheldt

In order to detail the procedures for modelling of HCBS in the Scheldt, we have to discriminate between several zones where substantially different profiles play a role. These zones are the main channel of the Scheldt estuary, the harbour docks, and the sill in-between the dock and the river.

The main channel of the Scheldt estuary is characterized by high current velocities and sediment concentrations up to 1 g/l. The highest near-bed sediment concentration occurs shortly after HW. Part of the sediment is temporarily deposited, forming a thin layer. Due to its small thickness the layer consolidates fast, and therefore consolidation time does play a minor role. With the subsequent increasing tidal currents, this sediment is eroded again, and mixed over the water column. This type of erosion/sedimentation behaviour can be well simulated with a numerical model in which the Partheniades-Krone formulations for erosion E and deposition D are implemented. These read:

$$D = w_s C$$

$$E = M\ \tau_b - \tau_{cr}\ /\tau_b \text{ for } \tau_b > \tau_{cr}$$

Here τ_b is the bed shear stress, τ_{cr} is the critical shear stress for erosion, and M is an erosion parameter. However, in most numerical models, τ_b is computed with a roughness parameterization which governs the large-scale hydrodynamics. This includes form roughness (ripples, dunes) which does not affect the erosion of mud particles. For erosion of mud, the skin friction (roughness caused by the small-scale particles) is more important. And therefore the skin friction caused by sand beds (relatively rough) is substantially different from the skin friction over mud beds (hydraulically smooth). In an area with spatially varying mud deposits and sand areas, the erosion and deposition should preferably computed using a skin friction formulation. Therefore the Soulsby and Clarke (2005) skin friction formulations have been implemented in the 3D mud model of the Lower Sea Scheldt.

The Deurganckdok is a low energy environment where sediment settles from suspension, and consolidates. The dock is a very effective sediment trap, and sediment that enters the dock near the bed (either within density currents, or as an eddy) will not escape through natural processes (until the dock has filled up with fine sediments until the high water line). In order to compute the formation of a consolidating sediment mass in a numerical model, two processes have to be adapted / implemented. First, the Partheniades-Krone deposition term has to be switched off, because otherwise all sediment near the bed will be added to the bed at a rate determined by $w_s C$.

Secondly, formulations have to be implemented which compute the increase of sediment concentration at the bed (hindered settling, consolidation), but also the re-entrainment of the consolidating mud. All these processes have been implemented in the 3D mud special version of Delft3D, but is has not yet been properly calibrated and validated. If only the deposition term D is switched off, and hindered settling is implemented (such as in the standard Delft3D), the sediment concentration would remain too high, and sediment would be entrained by the near bed currents. When the near-bed flow is directed out of the dock, sediment would then be transported out of the dock. A second alternative is to apply the deposition term D. Sediment that settles to the bed of the dock would then immediately deposit, and will not be eroded again because the flow velocities are too low. This modelling procedure will accurately compute the net sediment deposition (because the dock is an effective sediment trap). However, the spatial deposition pattern is also influenced by mobile fluid muds, which tend to flatten the bathymetry. Although the analysis of the bottom profiles indicated that substantial bed level gradients (1:50) exist, computing the bed level only resulting from settling from suspension will probably lead to steeper bed topography gradients.

The sill, in-between the Deurganckdok and the River Scheldt, is the area where turbid Scheldt water rapidly decelerates. Probably, the result of the decreasing flow velocity, in combination with the increasing sediment settling velocity, results in a collapse of the concentration profile. Even using the Partheniades-Krone deposition term, the increase of the sediment concentration near the bed will exceed the deposition rate, and therefore highly concentrated bottom layers will be formed. The main process required to model this saturation, is a coupling between the sediment concentration, the fluid density, and a turbulence model. This is part of standard Delft3D. This saturation and high deposition rates are probably reasonably simulated with the 3D mud model, because the deposition rates on the sill are very high (see Van Maren, 2007 and Van Maren et al., 2007). Also the temporal pattern of erosion and accretion modelled on the location of the sill frame (Figure 7.6) are in line with the observations. Furthermore, the suspension flowing over the sill into the dock rapidly decreases its flow velocity. As a result of the decreasing shear stresses, the floc size, and therefore settling velocity increases. Reproducing this process requires the use of a flocculation model (such as Winterwerp, 2006a), which has therefore been implemented in the 3D mud model.

8. SUMMARY AND CONCLUSIONS

The HCBS measurement campaigns and the numerical modelling studies have greatly improved the understanding of the sediment dynamics in the Scheldt. The mud dynamics are governed by a mud patch with a limited amount of sediment that is advected up and down the (dominantly sandy) main channel of the lower Sea Scheldt. During slack tide, sediment is deposited on the bed, where it consolidates quickly due to the low thickness of the deposit. The sediment is re-entrained during the accelerating tidal currents. Fluvial sediment supplied from upstream is transported downstream by the residual discharge, by slack tide asymmetry. The tidal currents in the upstream part of the lower Sea Scheldt are characterized by a slow start of the flood, maximum flood velocities at the end of flood, a short HW slack period, maximum ebb velocities, and then a long period of waning ebb currents. Due to settling lag effects, this produces a net transport of fine sediment in the ebb direction. Simultaneously, sediment is transported upstream from the downstream part of the lower Sea Scheldt due to flood-dominant maximum flow asymmetry. The flood period is short, with relatively high flow velocities, while the ebb period is long, with relatively low flow velocities. In the case of an unlimited supply of sediment, sediment transport is proportional to the 3rd to 4th power of the flow velocity. Therefore this maximum flow asymmetry produces a transport in the flood direction. It should be realized, however, that if the amount of sediment supply is limited, maximum flow asymmetry will not drive a net transport of sediment. However, since the sediment concentrations in the Scheldt show a distinct clear spring-neap tidal variation in sediment concentration, the Scheldt River is not fully supply limited. Therefore maximum flow asymmetry will result in a residual transport of sediment. The upstream and downstream-directed sediment transport paths converge somewhere between Deurganckdok and Antwerp, forming the turbidity maximum. Sediment is transported into the docks, were it accumulates. This sediment can only be returned to the systems when dredged and relocated in the main stream of the Scheldt.

The measurements during the HCBS and Deurganckdok campaigns reveal that the sediment concentrations rarely exceed 1 g/l. This is insufficient to substantially influence the flow velocity at maximal current velocities, and to form thick, consolidating mud deposits at slack tide. As a result, these highly concentrated layers are not stable, are entrained by the accelerating tidal flow, and therefore do not propagate into the docks as sediment-density driven near-bottom currents. This is substantiated by the observed horizontal bed level variations, of which the gradient seems too steep for HCBS currents to play an important role in the sediment influx. However, sediment will be partly redistributed by mobile muds, although the bed level gradients are probably also too steep for mobile muds to play an important role in the redistribution of sediment. This is because the sediment accumulation rate is sufficiently low for sediment to consolidate relatively rapid.

Therefore most sediment enters the dock as a suspension with concentrations of 10's to 100's mg/l, in a combination of density currents, tidal filling, and horizontal eddies. Most sediment enters the dock in an eddy that enters the dock at HW. Most of this sediment remains in the dock, because it is accompanied and followed by a phase of near-bed inflow. Sediment that enters during phases of near-surface inflow may be (partly) transported out of the dock again in the outward-directed near-bottom currents. It seems likely that the deposition of sediment from suspensions that enter the Deurganckdok near the bed is rapid, because the suspensions become saturated when they flow into the dock. When the velocity is either high or low, and the sediment concentration of the inflowing water is low, sediment is eroded from the sill of the Deurganckdok. However, even with high velocities, sediment is deposited on the sill when the concentrations are high (several 100's mg/l). The flow velocity of this suspension decreases as it enters the dock, leading to a decreasing capacity concentration. At a certain point turbulent mixing is so much

reduced that it cannot overcome the sediment-induced vertical density gradient, and the concentration profile collapses. This is further increased by flocculation effects: the conditions for flocculation improve along with the deceleration of the inflowing currents, leading to larger flocs and a larger settling velocity. This further lowers the saturation concentration, and therefore contributes to rapid settling from suspension.

9. REFERENCES

Arcadis-Technum and IMDC (2007), Basisrapport Slibdynamiek, Milieueffectrapport Verruiming vaargeul Beneden-Zeeschelde en Westerschelde.

Bruens (2003). Entraining mud suspensions. PhD thesis, Delft University.

Chen, M.S., Wartel, S., and Temmerman, S. Seasonal variation of floc charachteristics on tidal flats, the Scheldt estuary. Hydrobiologia 540, p. 181-195.

Claessens, J., and Belmans, H., 1984. Overview of the tidal observations in the Scheldt basin during the decennium 1971-1980, Tijdschrift de openbare werken van Begie, No 3 (in Dutch).

De Wit, P. J., 1995. Liquefaction of cohesive sediments caused by waves. PhD thesis, Delft University, 197 p.

De Nijs, M. A. J., Johan C. Winterwerp and Julie D. Pietrzak (2009). On Harbour siltation in the fresh-salt water mixing region. Continental Shelf Research, Volume 29, Issue 1, pp175-193.

Dyer, K. R., (1994). Estuarine sediment transport and deposition. In Pye, K., Sediment transport and depositional processes. Blackwell Scientific Publications, Oxford, pp. 193-218.

Dyer (1997). Estuaries, a Physical Introduction. Wiley, Chichester, 195 p.

Fettweis M. and M. Sas (1994). De complexe stroming in de toegangsgeul van de Zandvliet- en Berendrechtsluis: Inzicht via metingen en modellering. Water, Nr. 77, 109-116.

Fettweis M., M. Sas and L. Meyvis (1994). Analyse van stroom- en sedimentmetingen ter hoogte van de Drempel van Zandvliet (Schelde). Water, Nr. 76, 88-99.

Fettweis M., M. Sas, J. Monbaliu & E. Taverniers (1997). Langdurige meting van slibconcentratie, saliniteit en temperatuur te Prosperpolder (Beneden-Zeeschelde). Water, Nr. 92, 15-26.

Fettweis M., M. Sas & J. Monbaliu (1998a). Seasonal, neap-spring and tidal variation of cohesive sediment concentration in the Scheldt estuary, Belgium. Estuarine, Coastal and Shelf Science, 47, 21-36.

Fettweiss M, Sas M, Smitz H & Thibaut W (1999a): Mud deposition in the new tidal dock (Deurganckdock), harbour of Antwerp, 12th International Harbour Congress, Antwerp.

Fettweis, M., T. Ysebaert, M. Sas & Meire P. (1999b). Sedimentologische en biologische processen en de erosiegevoeligheid van cohesieve sedimenten op enkele slikken in de Beneden-Zeeschelde. te verschijnen in Water.

Goda, Y. (2003). Revisiting Wilson's Formulas for Simplified Wind-Wave Prediction. J. Waterway, Ports, Coastal and ocean Engineering 129 (2), p. 93-95.

Groen, P. (1967). On the residual transport of suspended matter by an alternating tidal current. Netherlands Journal of Sea Research 3-4, 564-574.

IMDC, 1993. Gedrag van particulair materiaal in het Schelde estuarium. Final report for BMM.

IMDC 1998a Containerdock West, Hydrodynamic- sedimentological study, final report, (I/RA/11128/98.029/MFE).

IMDC (1998b) Containerdok West, Hydraulisch-sedimentologisch onderzoek. Deelrapport 6 Onderzoek Drempel van Frederik, (I/RA/11128/97.034/MFE)

IMDC (2002a) Studie Densiteitsstroming in het kader van LTV Schelde, Factual data report I/RA/11216/02.029/CMA Verslag van de ADCP metingen te Merelbeke

IMDC (2002b) Studie Densiteitsstroming in het kader van LTV Schelde, Factual data report I/RA/11216/02.037/CMA Verslag van de stroom-en saliniteitsmeting te Waarde op 05/06/2002

IMDC (2002c) Studie Densiteitsstroming in het kader van LTV Schelde, Factual data report I/RA/11216/02.038/CMA Verslag van de stroom-en saliniteitsmeting te Waarde op 12/06/2002

IMDC (2002d) Studie Densiteitsstroming in het kader van LTV Schelde, Factual data report I/RA/11216/02.039/CMA Verslag van de stroom- en saliniteitsmeting te Oosterweel op 05/06/2002

IMDC (2002e) Studie Densiteitsstroming in het kader van LTV Schelde, Factual data report I/RA/11216/02.040/CMA Verslag van de stroom- en saliniteitsmeting te Oosterweel op 12/06/2002

IMDC (2002f) Studie Densiteitsstroming in het kader van LTV Schelde, Factual data report I/RA/11216/02.041/CMA Verslag van de stroom- en saliniteitsmetingen in de omgeving van het toekomstige Deurganckdok op 05/06/2002

IMDC (2002g) Studie Densiteitsstroming in het kader van LTV Schelde, Factual data report I/RA/11216/02.042/CMA Verslag van de stroom- en saliniteitsmetingen in de omgeving van het toekomstige Deurganckdok op 12/06/2002

IMDC (2002h) Studie Densiteitsstroming in het kader van LTV Schelde, Factual data report I/RA/11216/02.043/CMA Verslag van de stroom- en saliniteitsmetingen in de omgeving van de Kallosluis op 05/06/2002

IMDC (2002i) Studie Densiteitsstroming in het kader van LTV Schelde, Factual data report I/RA/11216/02.044/CMA Verslag van de stroom- en saliniteitsmetingen in de omgeving van de Kallosluis op 12/06/2002

IMDC (2002j) Studie Densiteitsstroming in het kader van LTV Schelde, Factual data report I/RA/11216/02.046/FDK Verslag van de langdurige stroom- en saliniteitsmetingen langs de Beneden Zeeschelde

IMDC (2002k) Studie Densiteitsstroming in het kader van LTV Schelde, Factual data report I/RA/11216/02.047/FDK Verslag van de langdurige stroom- en saliniteitsmetingen ter hoogte van de Kallosluis.

IMDC (2002l) Studie Densiteitsstroming in het kader van LTV Schelde, Factual data report I/RA/11216/02.045/CMA

IMDC (2005a). Uitbreiding studie densiteitsstromingen in de Beneden Zeeschelde in het kader van LTV Meetcampagne naar hooggeconcentreerde slibsuspensies Deelrapport 1: Test survey 17/02/2005, I/RA/11265/05.008/MSA, in opdracht van AWZ.

IMDC (2005b). Uitbreiding studie densiteitsstromingen in de Beneden Zeeschelde in het kader van LTV Meetcampagne naar hooggeconcentreerde slibsuspensies Deelrapport 2.1: Deurganckdok 17/02/2005, I/RA/11265/05.009/MSA, in opdracht van AWZ.

IMDC (2005c). Uitbreiding studie densiteitsstromingen in de Beneden Zeeschelde in het kader van LTV Meetcampagne naar hooggeconcentreerde slibsuspensies Deelrapport 2.2: Zandvliet 17/02/2005, I/RA/11265/05.010/MSA, in opdracht van AWZ.

IMDC (2005d). Uitbreiding studie densiteitsstromingen in de Beneden Zeeschelde in het kader van LTV Meetcampagne naar hooggeconcentreerde slibsuspensies Deelrapport 2.3: Liefkenshoek 17/02/2005, I/RA/11265/05.0011/MSA, in opdracht van AWZ.

IMDC (2005e). Uitbreiding studie densiteitsstromingen in de Beneden Zeeschelde in het kader van LTV Meetcampagne naar hooggeconcentreerde slibsuspensies Deelrapport 2.4: Schelle 17/02/2005, I/RA/11265/05.0012/MSA, in opdracht van AWZ.

IMDC (2005f). Uitbreiding studie densiteitsstromingen in de Beneden Zeeschelde in het kader van LTV Meetcampagne naar hooggeconcentreerde slibsuspensies Deelrapport 2.5: Deurganckdok 16/02/2005, I/RA/11265/05.013/MSA, in opdracht van AWZ.

IMDC (2005g). Uitbreiding studie densiteitsstromingen in de Beneden Zeeschelde in het kader van LTV Meetcampagne naar hooggeconcentreerde slibsuspensies Deelrapport 2.6: Kallosluis 18/02/2005, I/RA/11265/05.014/MSA, in opdracht van AWZ.

IMDC (2005h). Uitbreiding studie densiteitsstromingen in de Beneden Zeeschelde in het kader van LTV Meetcampagne naar hooggeconcentreerde slibsuspensies Deelrapport 2.7: Near bed continious monitoring: february 2005, I/RA/11265/05.015/MSA, in opdracht van AWZ.

IMDC (2005i). Uitbreiding studie densiteitsstromingen in de Beneden Zeeschelde in het kader van LTV Meetcampagne naar hooggeconcentreerde slibsuspensies Deelrapport 3: Settling velocity INSSEV february 2005, I/RA/11265/05.016/MSA, in opdracht van AWZ.

IMDC (2005j). Uitbreiding studie densiteitsstromingen in de Beneden Zeeschelde in het kader van LTV Meetcampagne naar hooggeconcentreerde slibsuspensies Deelrapport 4: Cohesive sediment properties february 2005, I/RA/11265/05.017/MSA, in opdracht van AWZ.

IMDC (2005k). Uitbreiding studie densiteitsstromingen in de Beneden Zeeschelde in het kader van LTV Meetcampagne naar hooggeconcentreerde slibsuspensies Deelrapport 5.1: Overview of ambient conditions in the river Scheldt January-June 2005, I/RA/11265/05.018/MSA, in opdracht van AWZ.

IMDC (2005l). Uitbreiding studie densiteitsstromingen in de Beneden Zeeschelde in het kader van LTV Meetcampagne naar hooggeconcentreerde slibsuspensies Deelrapport 5.2: Overview of ambient conditions in the river Scheldt July-December 2005, I/RA/11265/05.019/MSA, in opdracht van AWZ.

IMDC (2006a). Uitbreiding studie densiteitsstromingen in de Beneden Zeeschelde in het kader van LTV Meetcampagne naar hooggeconcentreerde slibsuspensies Deelrapport 5.3 Overview of ambient conditions in the river Scheldt – January-June 2006 (I/RA/11291/06.088/MSA), in opdracht van AWZ.

IMDC (2006b). Uitbreiding studie densiteitsstromingen in de Beneden Zeeschelde in het kader van LTV Meetcampagne naar hooggeconcentreerde slibsuspensies Deelrapport 6.1 Winter Calibration (I/RA/11291/06.092/MSA), in opdracht van AWZ.

IMDC (2006c). Uitbreiding studie densiteitsstromingen in de Beneden Zeeschelde in het kader van LTV Meetcampagne naar hooggeconcentreerde slibsuspensies Deelrapport 7.1 21/3 Scheldewacht – Deurganckdok – Salinity Distribution (I/RA/11291/06.094/MSA), in opdracht van AWZ.

IMDC (2006d). Uitbreiding studie densiteitsstromingen in de Beneden Zeeschelde in het kader van LTV Meetcampagne naar hooggeconcentreerde slibsuspensies Deelrapport 7.2 22/3 Parel 2 – Deurganckdok (I/RA/11291/06.095/MSA), in opdracht van AWZ.

IMDC (2006e). Uitbreiding studie densiteitsstromingen in de Beneden Zeeschelde in het kader van LTV Meetcampagne naar hooggeconcentreerde slibsuspensies Deelrapport 7.3 22/3 Laure Marie – Liefkenshoek (I/RA/11291/06.096/MSA), in opdracht van AWZ.

IMDC (2006f). Uitbreiding studie densiteitsstromingen in de Beneden Zeeschelde in het kader van LTV Meetcampagne naar hooggeconcentreerde slibsuspensies Deelrapport 7.4 23/3 Parel 2 – Schelle (I/RA/11291/06.097/MSA), in opdracht van AWZ.

IMDC (2006g). Uitbreiding studie densiteitsstromingen in de Beneden Zeeschelde in het kader van LTV Meetcampagne naar hooggeconcentreerde slibsuspensies Deelrapport 7.5 23/3 Laure Marie – Deurganckdok (I/RA/11291/06.098/MSA), in opdracht van AWZ.

IMDC (2006h). Uitbreiding studie densiteitsstromingen in de Beneden Zeeschelde in het kader van LTV Meetcampagne naar hooggeconcentreerde slibsuspensies Deelrapport 7.6 23/3 Veremans Waarde (I/RA/11291/06.099/MSA), in opdracht van AWZ.

IMDC (2006i). Uitbreiding studie densiteitsstromingen in de Beneden Zeeschelde in het kader van LTV Meetcampagne naar hooggeconcentreerde slibsuspensies Deelrapport 8.1 Near bed continuous monitoring winter 2006 (I/RA/11291/06.100/MSA), in opdracht van AWZ.

IMDC (2006j). Uitbreiding studie densiteitsstromingen in de Beneden Zeeschelde in het kader van LTV Meetcampagne naar hooggeconcentreerde slibsuspensies Deelrapport 9 Settling Velocity - INSSEV summer 2006 (I/RA/11291/06.102/MSA), in opdracht van AWZ.

IMDC(2006k)   Mer   Verruiming   Westerschelde,   Nota   Bovenafvoer Scheldebekken,I/NO/11282/06.104/FPE.

IMDC (2006l) Langdurige metingen Deurganckdok: Opvolging en analyse aanslibbing. Deelrapport 1.6 Sediment balance Bathymetry: 2005 – 3/2006 (I/RA/11283/06.118/MSA)

IMDC (2006m) Langdurige metingen Deurganckdok: Opvolging en analyse aanslibbing. Deelrapport 2.1 Through tide measurement SiltProfiler 21/03/2006 Laure Marie (I/RA/11283/06.087/WGO)

IMDC (2006n) Langdurige metingen Deurganckdok: Opvolging en analyse aanslibbing. Deelrapport 2.3 Through tide measurement Sediview spring tide 22/03/2006 Veremans (I/RA/11283/06.110/BDC)

IMDC (2006o) Langdurige metingen Deurganckdok: Opvolging en analyse aanslibbing. Deelrapport 2.4 Through tide measurement Sediview spring tide 27/09/2006 Parel 2 (I/RA/11283/06.119/MSA)

IMDC (2006p) Langdurige metingen Deurganckdok: Opvolging en analyse aanslibbing. Deelrapport 2.6 Saltinity-Silt distribution & Frame Measurements Deurganckdok 13/3/2006 – 31/05/2006 (I/RA/11283/06.121/MSA)

IMDC (2006q) Studie van de stromingsvelden en sedimentuitwisseling aan de ingang van Deurganckdok, Current and Sediment Flux Measurements 17 November 2005 (I/RA/15030/06.021/BDC)

IMDC (2006r) Studie van de stromingsvelden en sedimentuitwisseling aan de ingang van Deurganckdok, Current Measurements 28 November 2005 (I/RA/15030/06.023/BDC)

IMDC (2006s) Studie van de stromingsvelden en sedimentuitwisseling aan de ingang van Deurganckdok, Aditional processing of ADCP and Salinity data 17/11/2005 and 28/11/2005 (I/RA/15030/06.040/BDC)

IMDC (2007a). Uitbreiding studie densiteitsstromingen in de Beneden Zeeschelde in het kader van LTV Meetcampagne naar hooggeconcentreerde slibsuspensies Deelrapport 5.4 Overview of ambient conditions in the river Scheldt – July-December 2006 (I/RA/11291/06.089/MSA), in opdracht van AWZ.

IMDC (2007b). Uitbreiding studie densiteitsstromingen in de Beneden Zeeschelde in het kader van LTV Meetcampagne naar hooggeconcentreerde slibsuspensies Deelrapport 5.5 Overview of ambient conditions in the river Scheldt : RCM-9 buoy 84 & 97 (1/1/2007   -31/3/2007) (I/RA/11291/06.090/MSA), in opdracht van AWZ.

IMDC (2007c). Uitbreiding studie densiteitsstromingen in de Beneden Zeeschelde in het kader van LTV Meetcampagne naar hooggeconcentreerde slibsuspensies Deelrapport 5.6 Analysis of ambient conditions during 2006 (I/RA/11291/06.091/MSA), in opdracht van AWZ.

IMDC (2007d). Uitbreiding studie densiteitsstromingen in de Beneden Zeeschelde in het kader van LTV Meetcampagne naar hooggeconcentreerde slibsuspensies Deelrapport 6.2 Summer Calibration and Final Report (I/RA/11291/06.093/MSA), in opdracht van AWZ.

IMDC (2007e). Uitbreiding studie densiteitsstromingen in de Beneden Zeeschelde in het kader van LTV Meetcampagne naar hooggeconcentreerde slibsuspensies Deelrapport 10 Cohesive sediment properties summer 2006 (I/RA/11291/06.103/MSA), in opdracht van AWZ.

IMDC (2007f). Uitbreiding studie densiteitsstromingen in de Beneden Zeeschelde in het kader van LTV Meetcampagne naar hooggeconcentreerde slibsuspensies Deelrapport 11.1 Through tide Measurement Sediview & SiltProfiler 27/9 Stream - Liefkenshoek (I/RA/11291/06.104/MSA), in opdracht van AWZ.

IMDC (2007g). Uitbreiding studie densiteitsstromingen in de Beneden Zeeschelde in het kader van LTV Meetcampagne naar hooggeconcentreerde slibsuspensies Deelrapport 11.2 Through tide Measurement Sediview 27/9 Veremans - Raai K (I/RA/11291/06.105/MSA), in opdracht van AWZ.

IMDC (2007h). Uitbreiding studie densiteitsstromingen in de Beneden Zeeschelde in het kader van LTV Meetcampagne naar hooggeconcentreerde slibsuspensies Deelrapport 11.3 Through tide Measurement Sediview & SiltProfiler 28/9 Stream - Raai K (I/RA/11291/06.106/MSA), in opdracht van AWZ.

IMDC (2007i). Uitbreiding studie densiteitsstromingen in de Beneden Zeeschelde in het kader van LTV Meetcampagne naar hooggeconcentreerde slibsuspensies Deelrapport 11.4 Through tide Measurement Sediview 28/9 Veremans - Waarde(I/RA/11291/06.107/MSA), in opdracht van AWZ.

IMDC (2007j). Uitbreiding studie densiteitsstromingen in de Beneden Zeeschelde in het kader van LTV Meetcampagne naar hooggeconcentreerde slibsuspensies Deelrapport 11.5 Through tide Measurement Sediview 28/9 Parel 2 - Schelle (I/RA/11291/06.108/MSA), in opdracht van AWZ.

IMDC (2007k). Uitbreiding studie densiteitsstromingen in de Beneden Zeeschelde in het kader van LTV Meetcampagne naar hooggeconcentreerde slibsuspensies Deelrapport 11.6 Through tide Measurement Salinity Distribution 26/9 Scheldewacht – Deurganckdok in opdracht van AWZ.

IMDC (2007l). Uitbreiding studie densiteitsstromingen in de Beneden Zeeschelde in het kader van LTV Meetcampagne naar hooggeconcentreerde slibsuspensies Deelrapport 12 Report concerning the presence of HCBS layers in the Scheldt river (I/RA/11291/06.109/MSA), in opdracht van AWZ.

IMDC(2007m) Langdurige metingen Deurganckdok: Opvolging en analyse aanslibbing. Deelrapport 1.1 Sediment Balance: Three monthly report 1/4/2006 – 30/06/2006 (I/RA/11283/06.113/MSA)

IMDC (2007n) Langdurige metingen Deurganckdok: Opvolging en analyse aanslibbing. Deelrapport 1.2 Sediment Balance: Three monthly report 1/7/2006 – 30/09/2006 (I/RA/11283/06.114/MSA)

IMDC (2007o) Langdurige metingen Deurganckdok: Opvolging en analyse aanslibbing. Deelrapport 1.3 Sediment Balance: Three monthly report 1/10/2006 – 31/12/2006 (I/RA/11283/06.115/MSA)

IMDC (2007p) Langdurige metingen Deurganckdok: Opvolging en analyse aanslibbing. Deelrapport 1.4 Sediment Balance: Three monthly report 1/1/2007 – 31/03/2007 (I/RA/11283/06.116/MSA)

IMDC (2007q) Langdurige metingen Deurganckdok: Opvolging en analyse aanslibbing. Deelrapport 1.5 Annual Sediment Balance (I/RA/11283/06.117/MSA)

IMDC (2007r) Langdurige metingen Deurganckdok: Opvolging en analyse aanslibbing. Deelrapport 2.2 Through tide measurement SiltProfiler 26/09/2006 Stream (I/RA/11283/06.068/MSA)

IMDC (2007s) Langdurige metingen Deurganckdok: Opvolging en analyse aanslibbing. Deelrapport 2.5 Through tide measurement Sediview average tide 24/07/2010 (I/RA/11283/06.120/MSA)

IMDC (2007t) Langdurige metingen Deurganckdok: Opvolging en analyse aanslibbing. Deelrapport 2.7 Salinity-Silt distribution & Frame Measurements Deurganckdok 15/07/2006 – 31/10/2006 (I/RA/11283/06.122/MSA)

IMDC (2007u) Langdurige metingen Deurganckdok: Opvolging en analyse aanslibbing. Deelrapport 2.8 Salinity-Silt distribution & Frame Measurements Deurganckdok 15/01/2007 – 15/03/2007 (I/RA/11283/06.123/MSA)

IMDC (2007v) Langdurige metingen Deurganckdok: Opvolging en analyse aanslibbing. Deelrapport 3.1 Boundary conditions: Three monthly report 1/1/2007 – 31/03/2007 (I/RA/11283/06.127/MSA)

IMDC (2007w) Langdurige metingen Deurganckdok: Opvolging en analyse aanslibbing Deelrapport 1.10: Sediment Balance: Three monthly report 1/4/2007 – 30/06/2007 (I/RA/11283/07.081/MSA)

IMDC (2007x) Langdurige metingen Deurganckdok: Opvolging en analyse aanslibbing. Deelrapport 1.11: Sediment Balance: Three monthly report 1/7/2007 – 30/09/2007 (I/RA/11283/07.082/MSA)

IMDC (2007y) Langdurige metingen Deurganckdok: Opvolging en analyse aanslibbing. Deelrapport 2.16: Salt-Silt distribution Deurganckdok summer (21/6/2007 – 30/07/2007) (I/RA/11283/07.092/MSA)

IMDC (2007z) Langdurige metingen Deurganckdok: Opvolging en analyse aanslibbing. Deelrapport 3.10: Boundary conditions: Three monthly report 1/04/2007 – 30/06/2007 (I/RA/11283/07.097/MSA)

IMDC (2007aa) Langdurige metingen Deurganckdok: Opvolging en analyse aanslibbing. Deelrapport 3.11: Boundary conditions: Two monthly report 1/07/2007 – 30/09/2007 (I/RA/11283/07.098/MSA)

IMDC (2007w) Langdurige metingen Deurganckdok: Opvolging en analyse aanslibbing. Deelrapport 3.2 Boundary condtions: Annual report (I/RA/11283/06.128/MSA)

IMDC (2008a) Langdurige metingen Deurganckdok: Opvolging en analyse aanslibbing. Deelrapport 4.1: Analysis of siltation Processes and Factors (I/RA/11283/06.129/MSA)

IMDC (2008b) Langdurige metingen Deurganckdok: Opvolging en analyse aanslibbing. Deelrapport 1.12: Sediment Balance: Four monthly report 1/9/2007 – 31/12/2007 (I/RA/11283/07.083/MSA)

IMDC (2008c) Langdurige metingen Deurganckdok: Opvolging en analyse aanslibbing. Deelrapport 1.13: Sediment Balance: Four monthly report 1/01/2007 – 31/03/2007 (I/RA/11283/07.084/MSA)

IMDC (2008d) Langdurige metingen Deurganckdok: Opvolging en analyse aanslibbing. Deelrapport 1.14: Annual Sediment Balance. (I/RA/11283/07.085/MSA)

IMDC (2008e) Langdurige metingen Deurganckdok: Opvolging en analyse aanslibbing. Deelrapport 2.09: Calibration stationary equipment autumn (I/RA/11283/07.095/MSA)

IMDC (2008f) Langdurige metingen Deurganckdok: Opvolging en analyse aanslibbing. Deelrapport 2.10: Through tide measurement SiltProfiler 23 October 2007 (I/RA/11283/07.086/MSA)

IMDC (2008g) Langdurige metingen Deurganckdok: Opvolging en analyse aanslibbing. Deelrapport 2.11: Through tide measurement Salinity Profiling winter 12 March 2008 (I/RA/11283/07.087/MSA)

IMDC (2008h) Langdurige metingen Deurganckdok: Opvolging en analyse aanslibbing. Deelrapport 2.12: Through tide measurement Sediview winter 11 March 2008 – Transect I (I/RA/11283/07.088/MSA)

IMDC (2008i) Langdurige metingen Deurganckdok: Opvolging en analyse aanslibbing. Deelrapport 2.13: Through tide measurement Sediview winter 11 March 2008 – Transect K (I/RA/11283/07.089/MSA)

IMDC (2008j) Langdurige metingen Deurganckdok: Opvolging en analyse aanslibbing. Deelrapport 2.14: Through tide measurement Sediview winter 11 March 2008 – Transect DGD (I/RA/11283/07.090/MSA)

IMDC (2008k) Langdurige metingen Deurganckdok: Opvolging en analyse aanslibbing. Deelrapport 2.15: Through tide measurement SiltProfiler winter 12 March 2008 (I/RA/11283/07.091/MSA)

IMDC (2008l) Langdurige metingen Deurganckdok: Opvolging en analyse aanslibbing. Deelrapport 2.17: Salt-Silt distribution & Frame Measurements Deurganckdok autumn (17/9/2007-10/12/2007) (I/RA/11283/07.093/MSA)

IMDC (2008m) Langdurige metingen Deurganckdok: Opvolging en analyse aanslibbing. Deelrapport 2.18: Salt-Silt distribution & Frame Measurements Deurganckdok winter (18/02/2007-31/03/2008) (I/RA/11283/07.094/MSA)

IMDC (2008n) Langdurige metingen Deurganckdok: Opvolging en analyse aanslibbing. Deelrapport 2.19: Calibration stationary & mobile equipment winter (I/RA/11283/07.096/MSA)

IMDC (2008o) Langdurige metingen Deurganckdok: Opvolging en analyse aanslibbing. Deelrapport 3.12: Boundary conditions: Three monthly report 1/9/2007 – 31/12/2007 (I/RA/11283/07.099/MSA)

IMDC (2008p) Langdurige metingen Deurganckdok: Opvolging en analyse aanslibbing. Deelrapport 3.13: Boundary conditions: Three monthly report 1/1/2008 – 31/3/2007 (I/RA/11283/07.100/MSA)

IMDC (2008q) Langdurige metingen Deurganckdok: Opvolging en analyse aanslibbing. Deelrapport 3.14: Boundary conditions: Annual report (I/RA/11283/07.101/MSA)

IMDC (2008r) Langdurige metingen Deurganckdok: Opvolging en analyse aanslibbing. Deelrapport 4.10: Analysis of siltation Processes and Factors (I/RA/11283/07.102/MSA)

IMDC (2008s) Langdurige metingen Deurganckdok: Opvolging en analyse aanslibbing Deelrapport 1.20: Sediment Balance: Three monthly report 1/4/2008 – 30/06/2008 (I/RA/11283/08.076/MSA)

IMDC (2008t) Langdurige metingen Deurganckdok: Opvolging en analyse aanslibbing. Deelrapport 2.20: Through tide measurement Sediview during average tide Spring 2008 – 19 June 2008 (I/RA/11283/08.081/MSA)

IMDC (2008u) Langdurige metingen Deurganckdok: Opvolging en analyse aanslibbing. Deelrapport 2.21: Through tide measurement Sediview during average tide Spring 2008 – 26 June 2008 (I/RA/11283/08.082/MSA)

IMDC (2008v) Langdurige metingen Deurganckdok: Opvolging en analyse aanslibbing Deelrapport 1.21: Sediment Balance: Three monthly report 1/7/2008 – 30/09/2008 (I/RA/11283/08.077/MSA)

IMDC (2008w) Langdurige metingen Deurganckdok: Opvolging en analyse aanslibbing. Deelrapport 2.22: Through tide measurement Sediview during neap tide Summer 2008 – 24 September 2008 (I/RA/11283/08.083/MSA)

IMDC (2008x) Langdurige metingen Deurganckdok: Opvolging en analyse aanslibbing. Deelrapport 2.28: Through tide measurement ADCP eddy Summer 2008 – 1 October 2008 (I/RA/11283/08.089/MSA)

IMDC (2008y) Langdurige metingen Deurganckdok: Opvolging en analyse aanslibbing. Deelrapport 2.32: Salt-Silt distribution Deurganckdok: six monthly report 1/4/2008 – 30/9/2008 (I/RA/11283/08.093/MSA)

IMDC (2008z) Langdurige metingen Deurganckdok: Opvolging en analyse aanslibbing. Deelrapport 3.20: Boundary conditions: Six monthly report 1/4/2008 – 30/09/2008 (I/RA/11283/08.096/MSA)

IMDC (2009a) Langdurige metingen Deurganckdok: Opvolging en analyse aanslibbing. Deelrapport 2.23: Through tide measurement Sediview during spring tide Summer 2008 – 30 September 2008 (I/RA/11283/08.084/MSA)

IMDC (2009b) Langdurige metingen Deurganckdok: Opvolging en analyse aanslibbing. Deelrapport 2.29: Through tide measurement SiltProfiler summer 2008 – 29 September 2008 (I/RA/11283/07.090/MSA)

IMDC (2009c) Langdurige metingen Deurganckdok: Opvolging en analyse aanslibbing. Deelrapport 2.34: Calibration stationary & mobile equipment autumn 2008 (I/RA/11283/08.095/MSA)

IMDC (2009d) Langdurige metingen Deurganckdok: Opvolging en analyse aanslibbing Deelrapport 1.22: Sediment Balance: Three monthly report 1/10/2008 – 31/12/2008 (I/RA/11283/08.078/MSA)

IMDC (2009e) Langdurige metingen Deurganckdok: Opvolging en analyse aanslibbing. Deelrapport 2.24: Through tide measurement Sediview during neap tide Autumn 2008 (I/RA/11283/08.085/MSA)

IMDC (2009f) Langdurige metingen Deurganckdok: Opvolging en analyse aanslibbing. Deelrapport 2.25: Through tide measurement Sediview during spring tide Autumn 2008 (I/RA/11283/08.086/MSA)

IMDC (2009g) Langdurige metingen Deurganckdok: Opvolging en analyse aanslibbing Deelrapport 1.23: Sediment Balance: Three monthly report 1/01/2009 – 31/03/2009 (I/RA/11283/08.079/MSA)

IMDC (2009h) Langdurige metingen Deurganckdok: Opvolging en analyse aanslibbing Deelrapport 1.24: Annual Sediment Balance (I/RA/11283/08.080/MSA)

IMDC (2009i) Langdurige metingen Deurganckdok: Opvolging en analyse aanslibbing. Deelrapport 2.26: Through tide measurement Sediview during neap tide Winter 2009 (I/RA/11283/08.087/MSA)

IMDC (2009j) Langdurige metingen Deurganckdok: Opvolging en analyse aanslibbing. Deelrapport 2.30: Through tide measurement SiltProfiler winter 2009 (I/RA/11283/08.091/MSA)

IMDC (2009k) Langdurige metingen Deurganckdok: Opvolging en analyse aanslibbing. Deelrapport 2.31: Through tide measurement Salinity Profiling winter 2009 (I/RA/11283/08.092/MSA)

IMDC (2009l) Langdurige metingen Deurganckdok: Opvolging en analyse aanslibbing. Deelrapport 2.33: Salt-Silt distribution Deurganckdok: six monthly report 1/10/2008 – 31/3/2009 (I/RA/11283/08.094/MSA)

IMDC (2009m) Langdurige metingen Deurganckdok: Opvolging en analyse aanslibbing. Deelrapport 3.21: Boundary conditions: Six monthly report 1/10/2008 – 31/03/2009 (I/RA/11283/08.097/MSA)

IMDC (2009n) Langdurige metingen Deurganckdok: Opvolging en analyse aanslibbing. Deelrapport 2.27: Through tide measurement Sediview during spring tide Winter 2009 (I/RA/11283/08.088/MSA)

IMDC (2009o) Langdurige metingen Deurganckdok: Opvolging en analyse aanslibbing. Deelrapport 4.20: Analysis of siltation Processes and Factors (I/RA/11283/08.098/MSA)

IMDC (2011) : Verdieping en aanleg bodembescherming ter hoogte van de Noordzeeterminal te Antwerpen, Hydraulisch, sedimentologisch en morfologisch onderzoek (I/RA/11349/09.117/RDS)

IMDC-IN (1998) Containerdok West, Hydraulisch-sedimentologisch onderzoek Deelrapport 3: In situ metingen van de erosiegevoeligheid van slib in de Beneden-Zeeschelde I/RA/11128/98.005/WFE

IMDC-WLH 1995 Containerdock West, Feasibility study, Final report (I/RA/11103/95.027/MFE).

Jansen, P.P., van Bendegom, L., van den Berg, J., de Vries, M., Zanen, A., 1979. Principles of River Engineering, the non-tidal alluvial river. Pitman, London.

LeHir, P. (1997) Fluid and sediment integrated modelling application tor the fluid mud flows in estuaries. In Cohesive Sediments. 4th Nearshore and Estuarine Cohesive Sediment Transport Conference, INTERCOH 1994.

Peters, J.J., (1972). Transports de sediments dans l'estuaire de l'Escaut, laboratoire de recherché Hydrauliques, Anvers.

Postma, H. (1967). Sediment transport and sedimentation in the marine environment. Estuaries 83, pp. 158-179.

Pugh, D. T. (1987). Tides, Surges and mean sea level. Chichester, John Wiley and Sons Ltd.

Sas, M. and Claessens, J. (1988). The impact of flow pattern and sediment transport on maintenance dredging in the Kallo Acces channel. 9th international KVIV congress

Soulsby, R. L. and Clarke, S. (2005). Bed shear stresses under combined waves and currents on smooth and rough beds. Report TR137, HR Wallingford.

Temmerman, S., Bouma, T.J., Govers, G., Wang, Z.B., De Vries, M., Herman, P. (2005) Impact of vegetation on flow routing and sedimentation patterns : Three-dimensional modeling for a tidal marsh. Journal of Geoph. Research, vol 110, F04019.

Uncles, R.J., J.A. Stephens, and D.J. Law (2006). Turbidity maximum in the macrotidal, highly turbid Humber Estuary, UK: Flocs, fluid mud, stationary suspensions and tidal bores. Estuarine, Coastal and Shelf Science 67 (2006) 30-52

Van Damme, S., Struyf, E., Maris, T., Ysebaert, T., Dehairs, F., Tackx, M., Heip, C., Meire, P. (2005), spatial and temporal patters of water quality along the estuarine salinity gradient of the Scheldt estuary (Belgium and The Netherlands) : results of an integrated monitoring approach, Hydrobiologica 540, pp 29-45.

Van Kessel T & Cornellisse JM 2003 Physical Scale Model Zeschelde. Delft Hydraulics, Report Z2516, December 2003.

Van Kessel, T., Vanlede, J., Kuijper, K., and de Kok, J. Further development and first application of a mud transport model for the Scheldt estuary. Report Z4375.

Van Leussen (1994). Estuarine macroflocs and their role in fine-grained sediment transport. PhD thesis, Utrecht University.

Van Maren, D. S., 2007. 3D slibtransport model Zeeschelde, scenario 1-3: Geometrie van de CDW en het Deurganckdok. Z3824.70, rapport IVa-c, 145 p.

Van Maren, D.S., Winterwerp, J.C., and Uittenboogaard, R. (2007) 3D slibtransport model Zeeschelde, report II: Claibration, validation and sensitivity analysis of the 3D mud model.

Van Maren and Schramkowski, 2008. 3D slibtransport model Zeeschelde: seasonal effects.

Verlaan, P.A.J., 1998. Mixing of marine and fluvial particles in the Scheldt estuary. PhD thesis, Delft University, 202 p.

Verlaan, P.A.J., 2000. Marine vs. fluvial bottom mud in the Scheldt Estuary. Est., Coast. and Shelf Science 50, p. 627-638.

Wang, Z. B., Van der Kaaij, T., and Sas, M., 2005. Three-dimensional modelling of hydrodynamics and mud transport in the Beneden Zeeschelde Estuary - Hydrodynamic modelling. Report Z3824.20, Delft Hydraulics.

Wartel, S. (1972), Sedimentologisch onderzoek van de opbouw van het Schelde-estuarium, doctoraatsonderzoek KU Leuven.

Wartel, S., Keppens, E., Nielsen, P., Dehairs, F., Van den Winkel, P. and Cornand, L. (1993), Bepaling van de verhouding Marien en Fluviatiel slib in de Beneden-Zeeschelde.

Wartel,S., Chen,M.,(2000) Bepaling van de verhouding marien – fluviatiel slib in de Beneden-Zeeschelde in het voorjaar van 1998.

Wartel, S.; Francken, F., (1995). Sediment transport and sediment processes in the Scheldt between Zandvliet and Gent [Sedimenttransport en sedimentatieprocessen in de Schelde tussen Zandvliet en Gent]. Algemene Milieu Impaktstudie Sigmaplan (AMIS), AMIS DS6.1-1. KBIN: Brussel, Belgium.

Wartel, S.; Francken, F., (1997a). Sediment transport and sediment processes in the Scheldt between Zandvliet and Gent [Sedimenttransport en sedimentatieprocessen in de Schelde tussen

Zandvliet en Gent]. Algemene Milieu Impaktstudie Sigmaplan (AMIS), AMIS DS6.1-4/1. KBIN: Brussel, Belgium.

Wartel, S.; Francken, F., (1997b). Sediment transport and sediment processes in the Scheldt between Zandvliet and Gent [Sedimenttransport en sedimentatieprocessen in de Schelde tussen Zandvliet en Gent]. Algemene Milieu Impaktstudie Sigmaplan (AMIS), AMIS DS6.1-4/2. KBIN: Brussel, Belgium.

Wartel, S.; Francken, F. et al., (1998). Sediment transport and sediment processes in the Scheldt between Zandvliet and Gent [Sedimenttransport en sedimentatieprocessen in de Schelde tussen Zandvliet en Gent]. Algemene Milieu Impaktstudie Sigmaplan (AMIS), AMIS DS6.1-6. KBIN: Brussel, Belgium.

Wartel, S.; Francken, F., (1998a). Sediment transport and sediment processes in the Scheldt between Zandvliet and Gent: Belgica-measuring campaign 2 [Sedimenttransport en sedimentatieprocessen in de Schelde tussen Zandvliet en Gent: Belgica-meetcampagnes 2]. Algemene Milieu Impaktstudie Sigmaplan (AMIS), AMIS DS6.1-7-vol. II/2. KBIN: Brussel, Belgium.

Wartel, S.; Francken, F., (1998b). Sediment transport and sediment processes in the Scheldt between Zandvliet and Gent: Belgica-measuring campaign 3 [Sedimenttransport en sedimentatieprocessen in de Schelde tussen Zandvliet en Gent: Belgica-meetcampagnes 3]. Algemene Milieu Impaktstudie Sigmaplan (AMIS), AMIS DS6.1-7-vol. II/3. KBIN: Brussel, Belgium.

Wartel, S.; Francken, F., (1998c). Sediment transport and sediment processes in the Scheldt between Zandvliet and Gent: Belgica-measuring campaign 4 [Sedimenttransport en sedimentatieprocessen in de Schelde tussen Zandvliet en Gent: Belgica-meetcampagnes 4]. Algemene Milieu Impaktstudie Sigmaplan (AMIS), AMIS DS6.1-7-vol. II/4. KBIN: Brussel, Belgium.

Wartel, S.; Francken, F., (1998d). Sediment transport and sediment processes in the Scheldt between Zandvliet and Gent: Belgica-measuring campaign 5 [Sedimenttransport en sedimentatieprocessen in de Schelde tussen Zandvliet en Gent: Belgica-meetcampagnes 5]. Algemene Milieu Impaktstudie Sigmaplan (AMIS), AMIS DS6.1-7-vol. II/5. KBIN: Brussel, Belgium.

Wartel, S.; Francken, F., (1998e). Sediment transport and sediment processes in the Scheldt between Zandvliet and Gent: Belgica-measuring campaign 6 [Sedimenttransport en sedimentatieprocessen in de Schelde tussen Zandvliet en Gent: Belgica-meetcampagnes 6]. Algemene Milieu Impaktstudie Sigmaplan (AMIS), AMIS DS6.1-7-vol. II/6. KBIN: Brussel, Belgium.

Wartel, S.; Francken, F., (1998f). Sediment transport and sediment processes in the Scheldt between Zandvliet and Gent: sediment processes on the salt marshes [Sedimenttransport en sedimentatieprocessen in de Schelde tussen Zandvliet en Gent: sedimentatieprocessen op het schor]. Algemene Milieu Impaktstudie Sigmaplan (AMIS), AMIS DS6.1-7-vol. IV. KBIN: Brussel, Belgium.

Wartel, S.; Francken, F., (1998g). Sediment transport and sediment processes in the Scheldt between Zandvliet and Gent: suspended material in the Scheldt [Sedimenttransport en sedimentatieprocessen in de Schelde tussen Zandvliet en Gent: suspensiemateriaal in de Schelde]. Algemene Milieu Impaktstudie Sigmaplan (AMIS), AMIS DS6.1-7-vol. III. KBIN: Brussel, Belgium.

Wartel,S., Parker,R., Francken,F., (2000) Bepaling van de sedimenttypes en opstelling van een lithologische kaart van de Beneden-Zeeschelde, rapport IN

Wartel, S., G.T.M. van Eck (2000). Mud budget of the Scheldt estuary. Koninklijk Belgisch Instituut voor Natuurwetenschappen, Brussel / Rijksinstituut voor Kust en Zee, Middelburg.

Winterwerp, J.C. (1999). On the dynamics of high-concentrated mud suspensions. PhD-thesis Delft University of Technology, Delft, The Netherlands.

Winterwerp (2001). Stratification of mud suspensions by buoyancy and flocculation effects. JGR 106 (10), p. 22559-22574.

Winterwerp (2002). On the flocculation and settling velocity of estuarine mud. Continental Shelf Research 22, p. 1339-1360.

Winterwerp and van Kessel (2003). Sediment transport by sediment-induced density currents. Ocean Dynamics 53 (3), 186-197.

Winterwerp, J.C., A.W. Bruens, N. Gratiot, C. Kranenburg, M. Mory and E.A. Toorman (2002). Dynamics of Concentrated Benthic suspension layers. Proceedings in Marine Science, Volume 5, 2002, Pages 41-55.

Winterwerp, J.C., 2005, Reducing harbor siltation. I: methodology, J. of Waterway, Port, Coastal and Ocean Eng., ASCE, DOI: 10.1061 (ASCE)073-9.

Winterwerp, J. C., A.J. Manning, C. Martens, T. de Mulder, J. Vanlede (2006a) A heuristic formula for turbulence-induced flocculation of cohesive sediment. Estuarine, coastal and shelf Science 68, p 195-207.

Winterwerp, J. C., Wang, Z. B., van der Kaaij, T., Verelst, K., Bijlsma, A., Meersschaut, Y. and Sas, M., 2006b. Flow Velocity profiles in the Lower Sea Scheldt. Ocean Dynamics 56, p 284 - 294.

WL (Waterbouwkundig Laboratorium) (2011a). Sediment input vanuit de bovenlopen. Schriftelijke mededeling Marc Wouters (02-02-2011)

WL Delft-IMDC 2002, Analysis of density currents in the Lower Ses Scheldt, Reports I/RA/11216/02.037-02.047.

WLH 1997 Waaslandhaven Containerdock West, Hydraulic-sedimentologic research, MOD 504/3, Waterbouwkundig Laboratorium.

Wollast, R., and Marijns, A. (1981). Evaluation des contributions de differentes sources de matieres en suspension a l'envasement de l'Escaut. Report no the Mnistry of Public Health and Environment, 152 p.

Xu, Z. (2000). Ellipse parameter conversion and vertical profiles for tidal currents. Bedford Institute of Oceanography, Dartmouth, Nova Scotia, Canada, 20 p.

APPENDIX A.

OVERVIEW OF MEASUREMENTS

A.1 Overview of the measurement locations for the HCBS 1 measurement campaign (February 2005 – December 2005)

Through tide measurements					
Location	Easting (UTM ED 50)		Northing (UTM ED 50)		Period
Kallo – Test (transect B)	Left Bank	Right Bank	Left Bank	Right Bank	02/02/2005
	590901	591298	5678979	5679614	
Kallo – Test (transect C)	Left Bank	Right Bank	Left Bank	Right Bank	02/02/2005
	590394	591389	5679678	5679874	
Kallo – Test (transect D)	Left Bank	Right Bank	Left Bank	Right Bank	02/02/2005
	590542	590815	5680157	5680157	
Kallo – Test (transect E)	Left Bank	Right Bank	Left Bank	Right Bank	02/02/2005
	590390	590423	5680214	5680456	
Kallo – Test (transect F)	Left Bank	Right Bank	Left Bank	Right Bank	02/02/2005
	590999	591155	5680913	5680820	
Kallo – Test (transect G)	Left Bank	Right Bank	Left Bank	Right Bank	02/02/2005
	591506	592214	5681824	5681310	
Deurganckdok – Test (transect I)	Left Bank	Right Bank	Left Bank	Right Bank	03/02/2005
	590400	590556	5683474	5683860	
Deurganckdok – Test (transect J)	Left Bank	Right Bank	Left Bank	Right Bank	03/02/2005
	589117	589395	5684243	5684489	
Deurganckdok – Test (transect K)	Left Bank	Right Bank	Left Bank	Right Bank	03/02/2005
	588641	589014	5684987	5685122	
Deurganckdok – Test (transect L)	Left Bank	Right Bank	Left Bank	Right Bank	03/02/2005
	588350	588977	5686088	5686088	
Deurganckdok – Test (transect M)	Left Bank	Right Bank	Left Bank	Right Bank	03/02/2005
	588191	589627	5687088	5687088	
Deurganckdok (transect K)	Left Bank	Right Bank	Left Bank	Right Bank	16/02/2005
	588484	589775	5684924	5685384	
Deurganckdok	Left Bank	Right Bank	Left Bank	Right Bank	16/02/2005

(transect L)	588216	589639	5686088	589639	
Deurganckdok (transect K)	*Left Bank*	*Right Bank*	*Left Bank*	*Right Bank*	17/02/2005
	588484	589775	5684924	5685383	
Zandvliet (transect Z)	*Left Bank*	*Right Bank*	*Left Bank*	*Right Bank*	17/02/2005
	586726	587757	5688355	5689950	
Liefkenshoek (transect I)	*Left Bank*	*Right Bank*	*Left Bank*	*Right Bank*	17/02/2005
	590318	590771	5683302	5684257	
Schelle (transect S)	*Left Bank*	*Right Bank*	*Left Bank*	*Right Bank*	17/02/2005 & 19/02/2005
	592645	592953	5665794	5665682	
Kallo (transect D)	*Left Bank*	*Right Bank*	*Left Bank*	*Right Bank*	18/02/2005
	590435	591408	5680153	5680172	
Kallo (transect E)	*Left Bank*	*Right Bank*	*Left Bank*	*Right Bank*	18/02/2005
	590386	590428	5680184	5680494	
Kallo (transect F)	*Left Bank*	*Right Bank*	*Left Bank*	*Right Bank*	18/02/2005
	590946	591596	5680947	5680542	

Near bed continuous monitoring

Location	*Easting (UTM ED 50)*	*Northing (UTM ED 50)*	*Period*
Kallo	590767	5680652	03/02/2005 – 11/02/2005
Deurganckdok downstream	588653	5684906	17/02/2005 – 03/03/2005
Buoy 84	589050	5686088	12/03/2005 – 25/03/2005
Deurganckdok upstream	589100	5684230	24/05/2005 – 08/06/2005

Settling velocity – INSSEV

Location	*Easting (UTM ED 50)*	*Northing (UTM ED 50)*	*Period*
Deurganckdok	5885578	5684793	17/02/2005 & 18/02/2005
Kallo	590683	5680551	19/02/2005
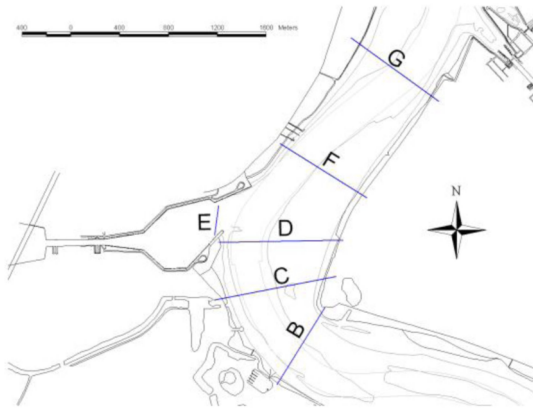
Through tide measurements - Kallo 02/02/2005 (test)
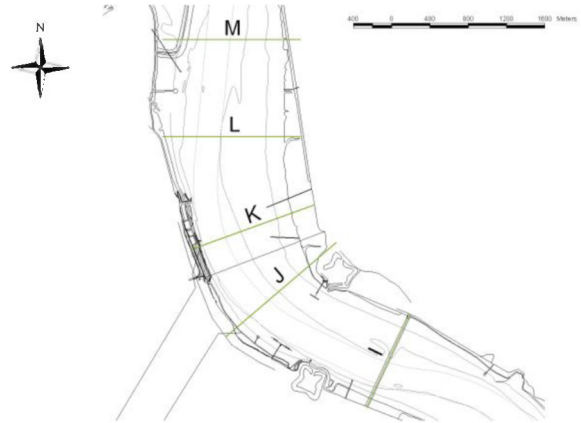
Through tide measurements – Deurganckdok 03/02/2005 (test)
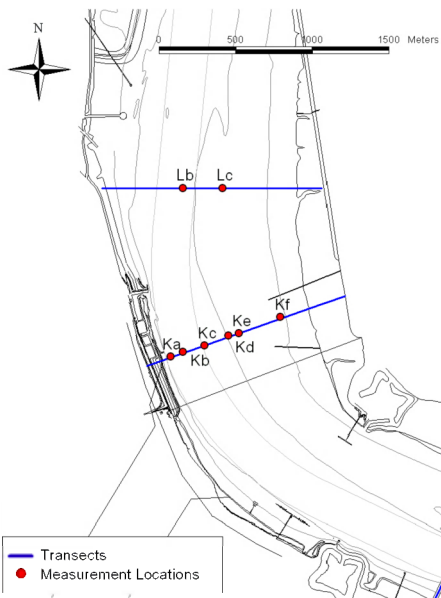
Through tide measurements - Deurganckdok 16/02/2005
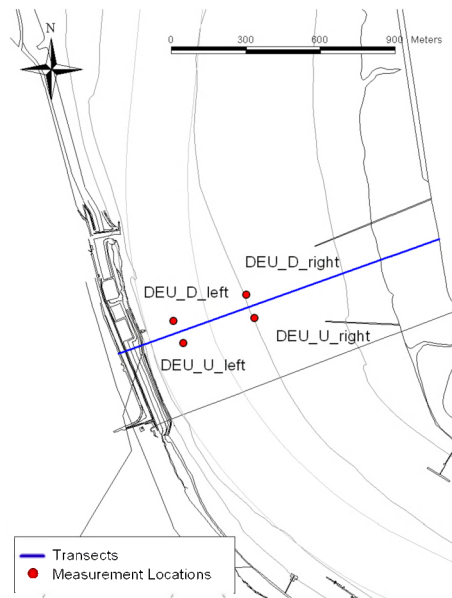
Through tide measurements - Deurganckdok 17/02/2005
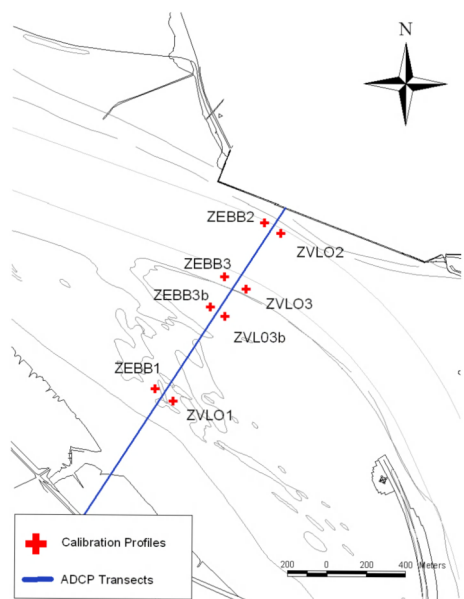
Through tide measurements – Zandvliet 17/02/2005
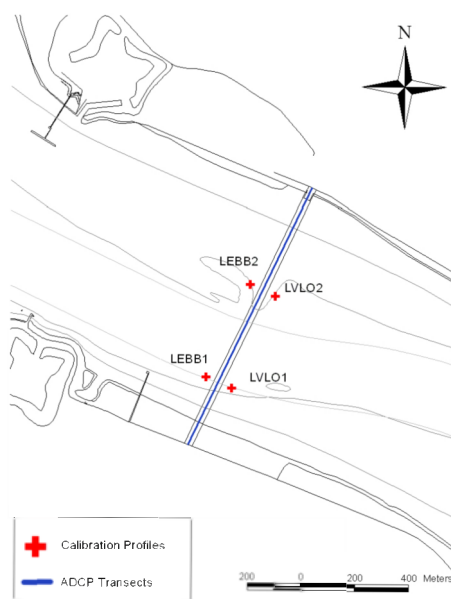
Through tide measurements - Liefkenshoek 17/02/2005
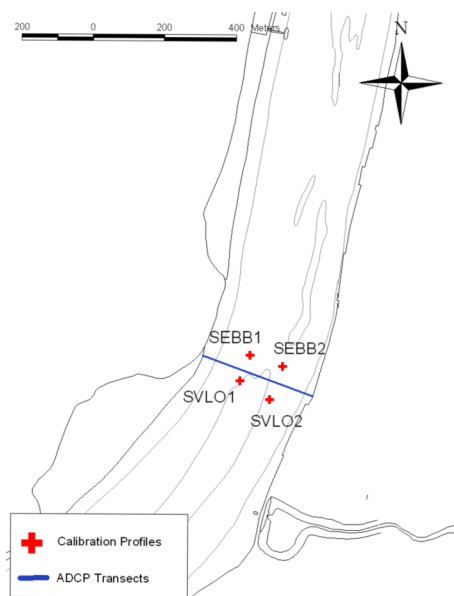
Through tide measurements - Schelle 17/20/2005
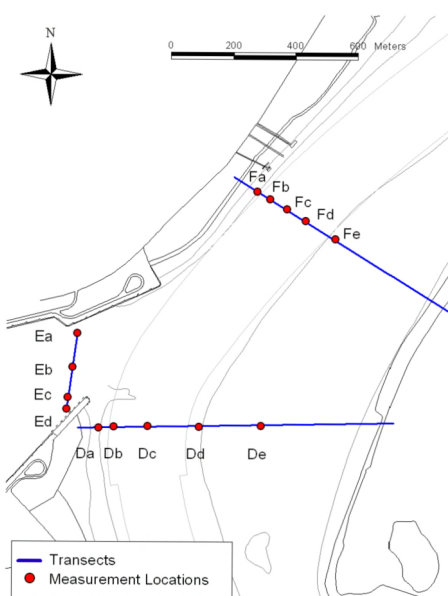
Through tide measurements - Kallo 18/02/2005
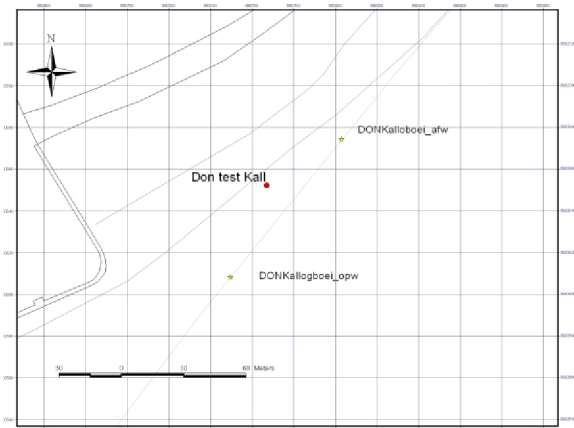
Near bed continuous monitoring - Kallo (test)
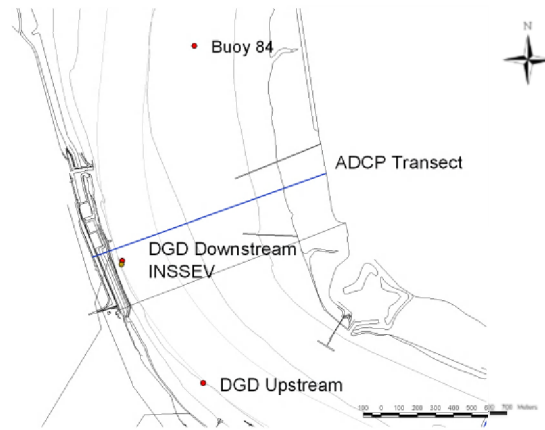
*Near bed continuous monitoring - vicinity
Deurganckdok*
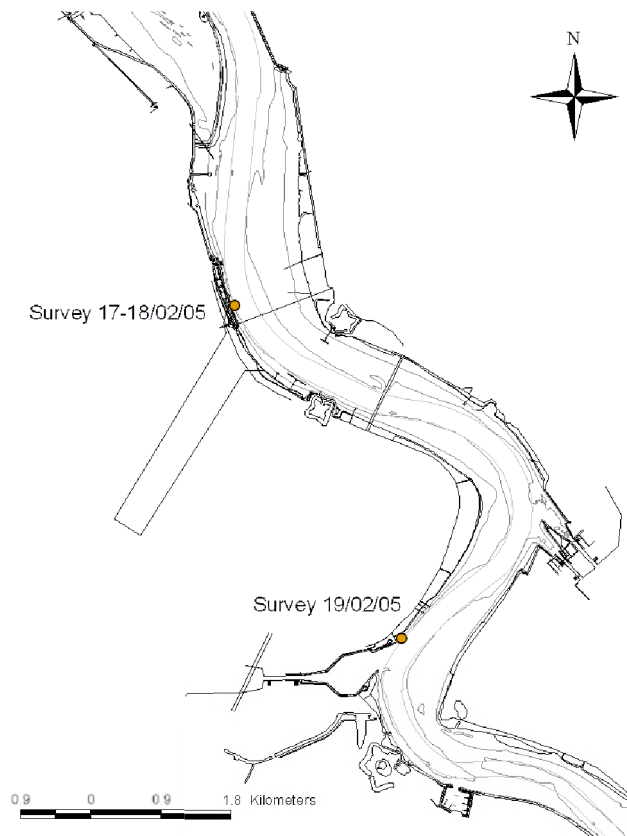
Settling velocity (INSSEV) - Deurganckdok and Kallo

A.2 Overview of the measurement locations for the HCBS 2 measurement campaign (January 2006- December 2006)
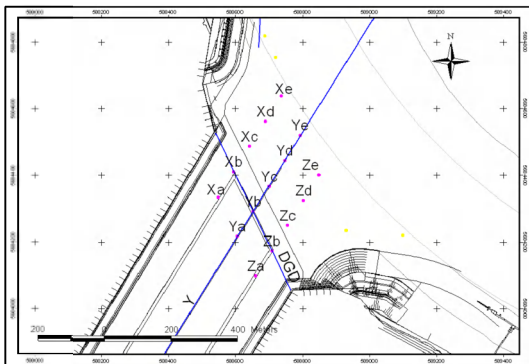
Through tide measurements - Deurganckdok
21/03/2006 & 26/09/2006 (SiltProfiler)
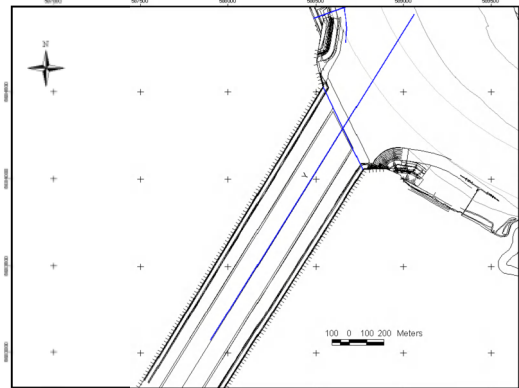
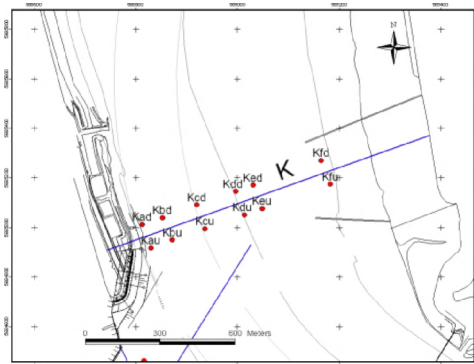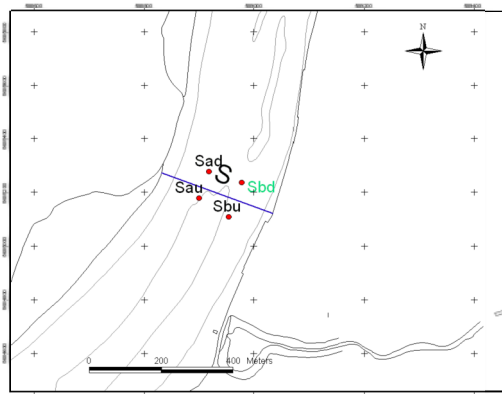*Through tide measurements – Deurganckdok*
21/03/2006 & 26/09/2006 (salinity)
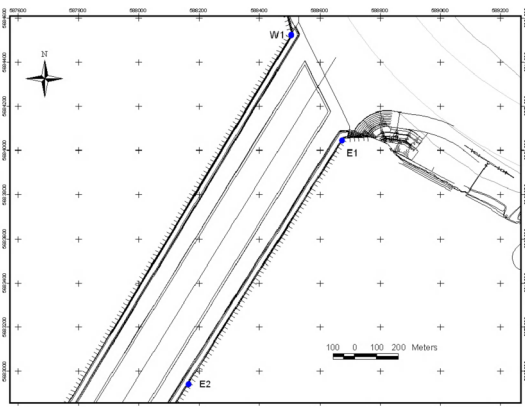
*Long term salinity measurements Deurganckdok*
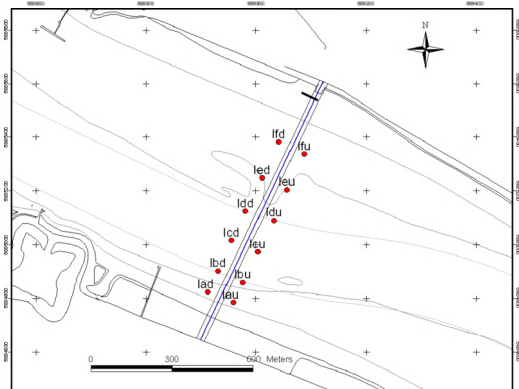
Through tide measurements - Liefkenshoek
22/03/2006 & 27/09/2006 (ADCP+SiltProfiler)
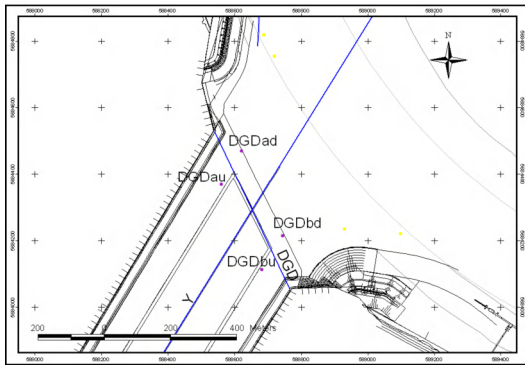
*Through tide measurements - Deurganckdok*
22/03/2006 & 27/09/2006 (ADCP)
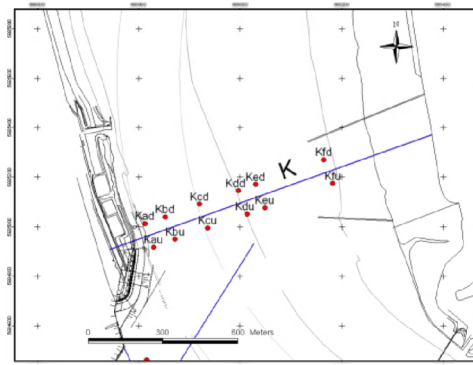
Through tide measurements - Deurganckdok
22/03/2006 & 27/09/2006 (ADCP)
*23/03/2006 & 28/09/2006*
(ADCP+SiltProfiler)
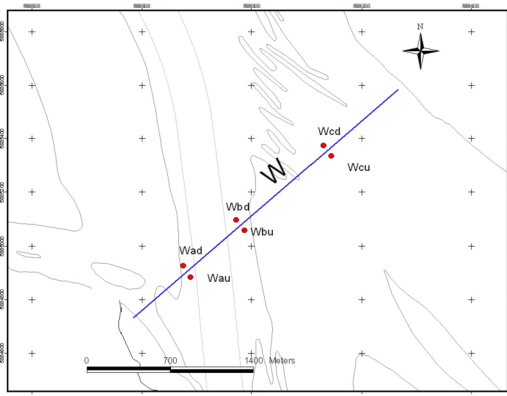
*Through tide measurements - Waarde 23/3/2006 &
28/09/2006 (ADCP)*
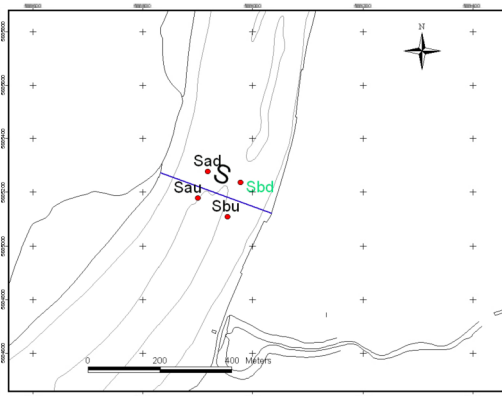
*Through tide measurements - Schelle 23/03/2006 &
28/09/2006 (ADCP)*
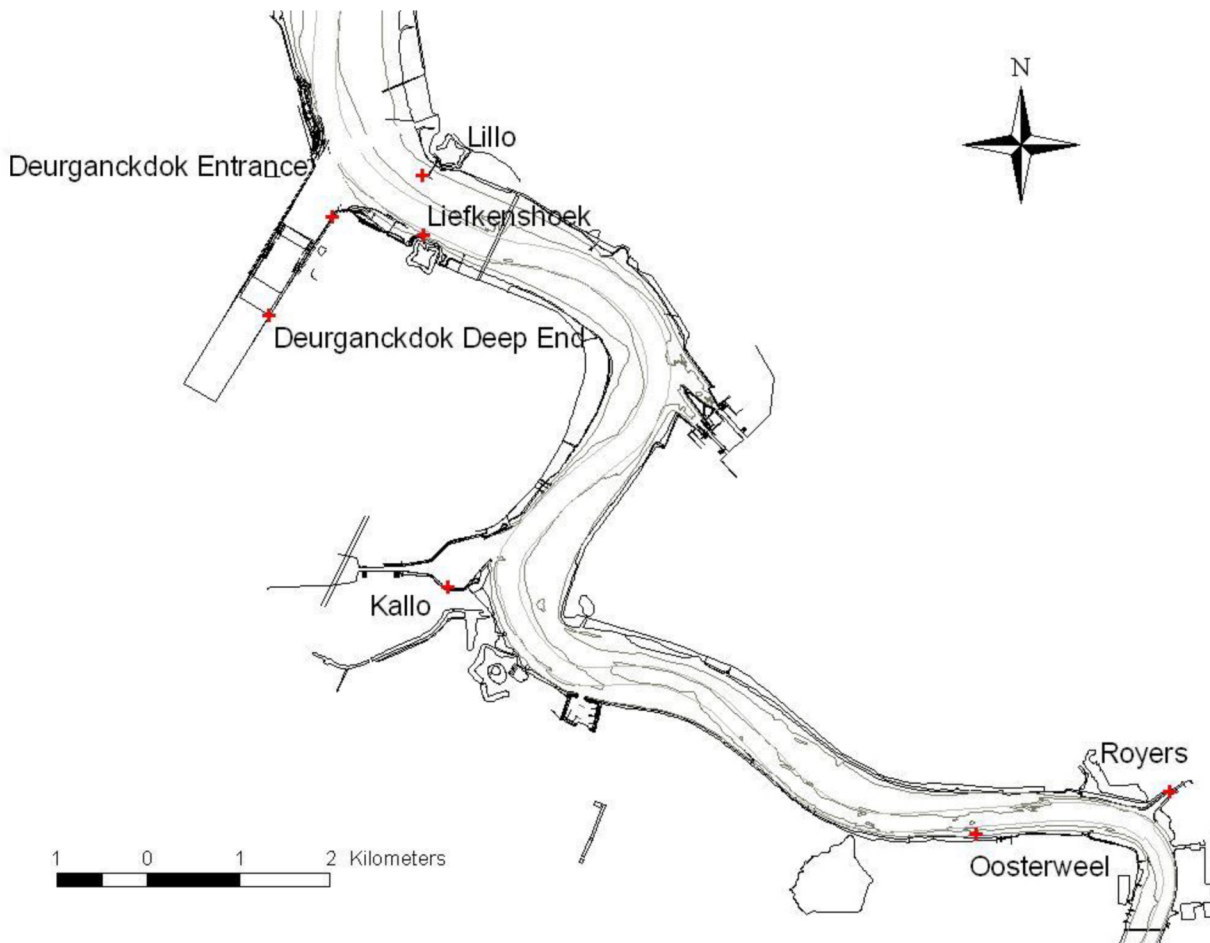
*Calibration measurements – 15/03/2006, 14/04/2006, 23/06/2006 & 18/09/2006*

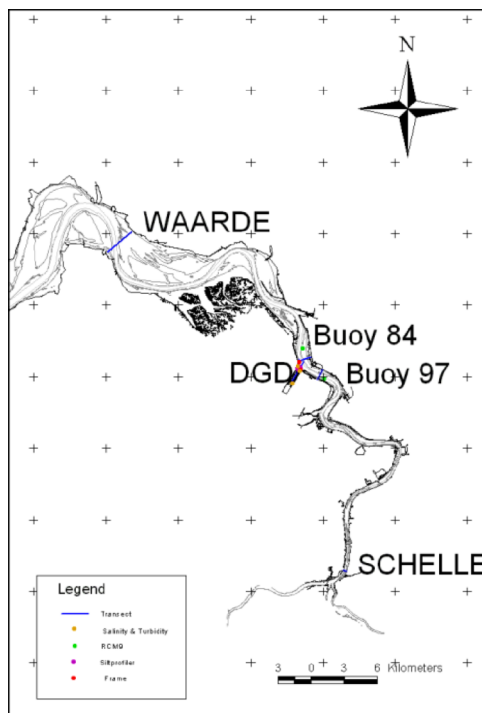Measurement locations and periods for the HCBS2 measurements (01/01/2006 – 31/12/2006)

Through tide measurements: Transects					
Location	*Easting (UTM ED 50)*		*Northing (UTM ED 50)*		*Period*
Deurganckdok (in dock)	*Left Bank*	*Right Bank*	*Left Bank*	*Right Bank*	21/03/2006 & 26/09/2006
(transect Y)	*589059*	591298	*5684948*	*5683077*	
Liefkenshoek	*Left Bank*	*Right Bank*	*Left Bank*	*Right Bank*	22/03/2006 & 27/09/2006
(transect I)	590318	590771	5684257	5683302	
Deurganckdok (downstream)	*Left Bank*	*Right Bank*	*Left Bank*	*Right Bank*	22 & 23/03/2006 & 27 & 28/09/2006
(transect K)	588484	589775	5684924	5685384	
Deurganckdok (in dock)	*Left Bank*	*Right Bank*	*Left Bank*	*Right Bank*	22/03/2006 & 27/09/2006
(transect DGD)	588765	588541	5684056	5684527	
Schelle	*Left Bank*	*Right Bank*	*Left Bank*	*Right Bank*	23/03/2006 & 28/09/2006
(transect S)	592645	592953	5665794	5665682	
Waarde	*Left Bank*	*Right Bank*	*Left Bank*	*Right Bank*	23/03/2006 & 28/09/2006
(transect W)	573541	571318	5696848	5694933	

Through tide measurements: Siltprofiler gauging points

Location	Easting (UTM ED 50)	Northing (UTM ED 50)	Period
Location 1: Xa	588549	5684335	21/03/2006 & 26/09/2006
Location 2: Xb	588596	5684411	
Location 3: Xc	588643	5684486	
Location 4: Xd	588690	5684562	
Location 5: Xe	588737	5684638	
Location 6: Ya	588606	5684217	
Location 7: Yb	588653	5684293	
Location 8: Yc	588700	5684368	
Location 9: Yd	588747	5684444	
Location 10: Ye	588793	5684520	
Location 11: Za	588662	5684099	
Location 12: Zb	588709	5684174	
Location 13: Zc	588756	5684250	
Location 14: Zd	588803	5684326	
Location 15: Ze	588850	5684402	

Near bed continuous monitoring

Location	Easting (UTM ED 50)	Northing (UTM ED 50)	Period
Deurganckdok CDW	588653	5684906	14/03/2006 – 05/04/2006
Deurganckdok CDW	588685	5684880	19/04/2006 – 23/05/2006
Deurganckdok Sill	588805	5684170	19/04/2006 – 23/05/2006
Deurganckdok CDW	588685	5684880	18/07/2006 – 11/10/2006
Deurganckdok Sill	588805	5684170	19/07/2006 – 11/10/2006

Salinty Silt measurements Deurganckdok			
Location	*Easting (UTM ED 50)*	*Northing (UTM ED 50)*	*Period*
P&O 1	588074	5682942	17/03/2006 – 28/04/2006
P&O 2	588767	5684045	17/03/2006 – 28/04/2006
PSA	588536	5684523	17/03/2006 – 28/04/2006
P&O 1	588074	5682942	20/07/2006 – 12/10/2006
P&O 2	588767	5684045	20/07/2006 – 12/10/2006
PSA	588536	5684523	20/07/2006 – 12/10/2006
Settling velocity – INSSEV			
Location	*Easting (UTM ED 50)*	*Northing (UTM ED 50)*	*Period*
Deurganckdok CDW	588717	5684898	05/09/2006
Deurganckdok SILL	588800	5684250	06/09/2006
Deurganckdok Western quay wall	588452	5684355	07/09/2006

*Through tide measurements - Deurganckdok
21/03/2006 & 26/09/2006 (Siltprofiler)*
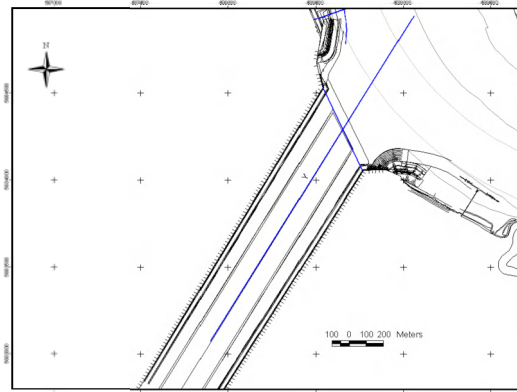
*Through tide measurements – Deurganckdok
21/03/2006 & 26/09/2006 (salinity)*
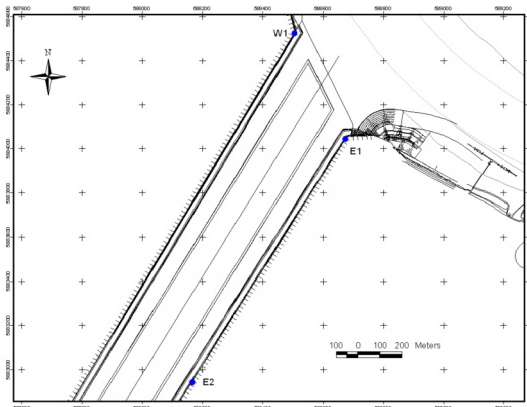
*Long term salinity measurements Deurganckdok
17/03/2006 – 28/04/2006
20/07/2006 – 12/10/2006*
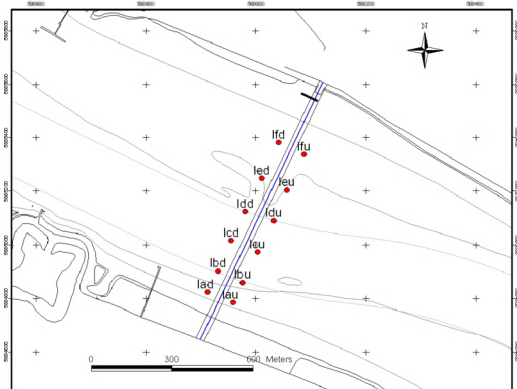
*Through tide measurements - Liefkenshoek
22/03/2006 & 27/09/2006
(ADCP+SiltProfiler)*
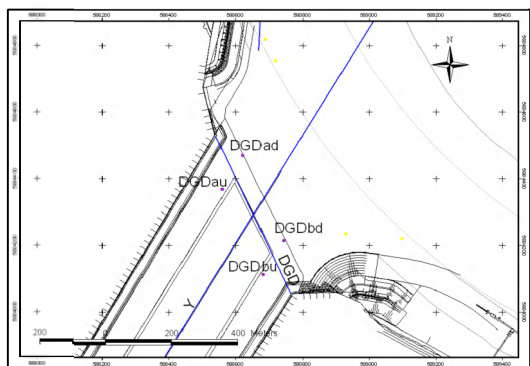
*Through tide measurements - Deurganckdok
22/03/2006 & 27/09/2006 (ADCP)*

*Through tide measurements - Deurganckdok
22/03/2006 & 27/09/2006 (ADCP);
23/03/2006 & 28/09/2006
(ADCP+SiltProfiler)*
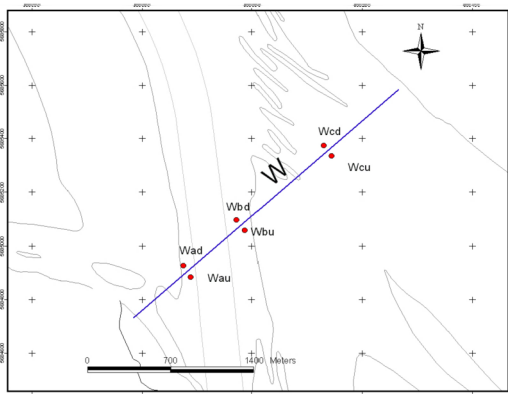
*Through tide measurements - Waarde 23/03/2006 &
28/09/2006 (ADCP)*

*Through tide measurements - Schelle 23/03/2006
& 28/09/2006 (ADCP)*
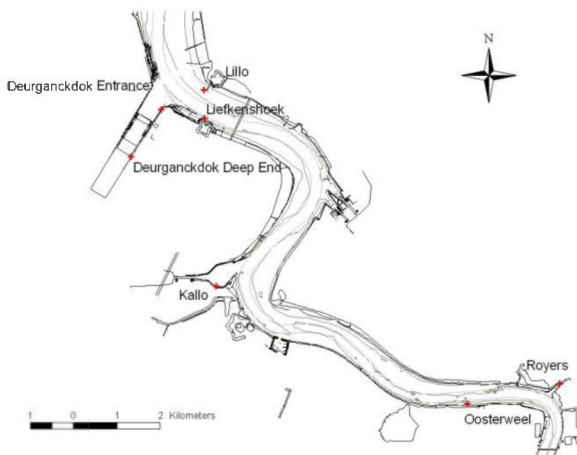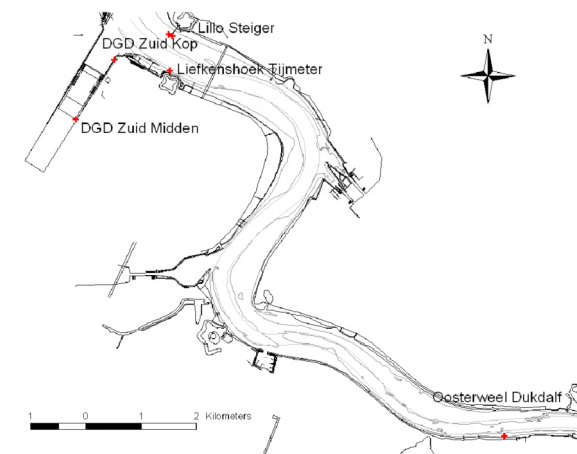
*Calibration measurements - 15/03/2006 &
14/04/2006*

*Calibration measurements – 23/06/2006 &
18/09/2006*
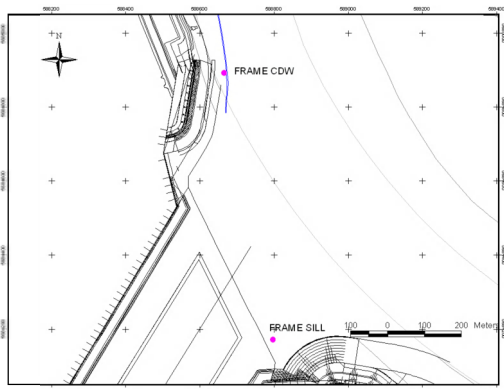
Near bed continuous monitoring
14/03/2006 – 23/05/2006
18/07/2006 – 11/10/2006
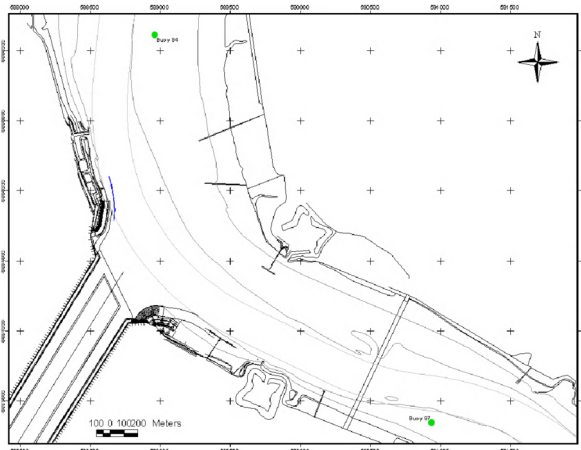
Long term measurements
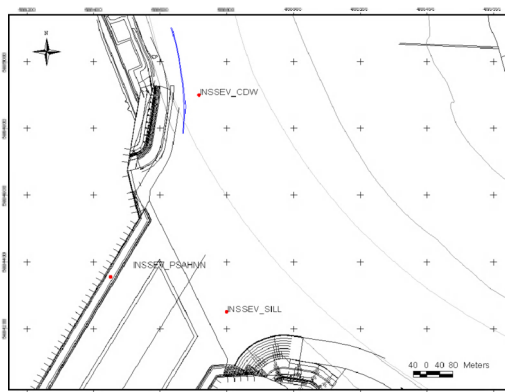
Settling velocity (INSSEV)
05/09/2006 – 07/09/2006

The HCBS2 measurement locations in the
Beneden Zeeschelde (01/01/2006 –
31/12/2006)

A.3 Overview of the measurement locations for the DGD measurement campaign (March 2006 – March 2009)

Through tide measurements: Siltprofiler gauging points

Location	Easting (UTM ED 50)	Northing (UTM ED 50)	Period
Location 1: Xa	588549	5684335	21/03/2006, 26/09/2006, 23/10/2007, 12/03/2008 29/09/2008 13/03/2008
Location 2: Xb	588596	5684411	
Location 3: Xc	588643	5684486	
Location 4: Xd	588690	5684562	
Location 5: Xe	588737	5684638	
Location 6: Ya	588606	5684217	
Location 7: Yb	588653	5684293	
Location 8: Yc	588700	5684368	
Location 9: Yd	588747	5684444	
Location 10: Ye	588793	5684520	
Location 11: Za	588662	5684099	
Location 12: Zb	588709	5684174	
Location 13: Zc	588756	5684250	
Location 14: Zd	588803	5684326	
Location 15: Ze	588850	5684402	

Through tide measurements: Transects

Location	Easting (UTM ED 50)		Northing (UTM ED 50)		Period
Deurganckdok (in dock) (transect Y)	Left Bank	Right Bank	Left Bank	Right Bank	21/03/2006, 26/09/2006 & 12/03/2008
	589059	591298	5684948	5683077	
Liefkenshoek (transect I)	Left Bank	Right Bank	Left Bank	Right Bank	22/03/2006, 27/09/2006 & 11/03/2008
	590318	590771	5684257	5683302	
Deurganckdok (downstream) (transect K)	Left Bank	Right Bank	Left Bank	Right Bank	22 - 23/03/2006, 27 - 28/09/2006 & 11/03/2008
	588484	589775	5684924	5685384	
Deurganckdok (entrance) (transect DGD)	Left Bank	Right Bank	Left Bank	Right Bank	22/03/2006, 27/09/2006, 24/10/2007, 11/03/2008, 19-26/06/2008 24-30/09/2008 2-10/12/2008 6-12/03/2009
	588765	588541	5684056	5684527	
Schelle (transect S)	Left Bank	Right Bank	Left Bank	Right Bank	23/03/2006 & 28/09/2006
	592645	592953	5665794	5665682	
Waarde (transect W)	Left Bank	Right Bank	Left Bank	Right Bank	23/03/2006 & 28/09/2006
	573541	571318	5696848	5694933	
Deurganckdok (in dock) (Transect X, transect Y, transect Z)	North Side	North Side	South Side	South Side	01/10/2008
	588737 588793 588850	5684638 5684520 5684402	588408 588465 588521	5684107 5683989 5683871	

Near bed continuous monitoring

Location	Easting (UTM ED 50)	Northing (UTM ED 50)	Period
Deurganckdok CDW	588653	5684906	14/03/2006 – 05/04/2006
Deurganckdok CDW	588685	5684880	19/04/2006 – 23/05/2006
Deurganckdok Sill	588805	5684170	19/04/2006 – 23/05/2006
Deurganckdok CDW	588685	5684880	18/07/2006 – 11/10/2006
Deurganckdok Sill	588805	5684170	19/07/2006 – 11/10/2006
Deurganckdok CDW	588685	5684880	15/03/2007 – 12/04/2007
Deurganckdok Sill	588805	5684170	09/02/2007 – 18/04/2007
Deurganckdok CDW	588685	5684880	26/09/2007 – 05/12/2007
Deurganckdok Sill	588805	5684170	10/10/2007 – 28/11/2007
Deurganckdok CDW	588685	5684880	20/02/2008 – 02/04/2008
Deurganckdok Sill	588805	5684170	27/02/2008 – 09/04/2008

Salinity Silt measurements Deurganckdok

Location	Easting (UTM ED 50)	Northing (UTM ED 50)	Period
P&O 1	588074	5682942	17/03/2006 – 28/04/2006
P&O 2	588767	5684045	17/03/2006 – 28/04/2006
PSA	588536	5684523	17/03/2006 – 28/04/2006
P&O 1	588074	5682942	20/07/2006 – 12/10/2006
P&O 2	588767	5684045	20/07/2006 – 12/10/2006
PSA	588536	5684523	20/07/2006 – 12/10/2006
P&O 1	588074	5682942	12/02/2007 – 27/03/2007
P&O 2	588767	5684045	12/02/2007 – 27/03/2007
PSA	588536	5684523	12/02/2007 – 27/03/2007
P&O 1	588074	5682942	20/06/2007 – 31/07/2007
P&O 2	588767	5684045	20/06/2007 – 31/07/2007
PSA	588536	5684523	20/06/2007 – 31/07/2007
P&O 1	588074	5682942	17/09/2007 – 10/12/2007
P&O 2	588767	5684045	17/09/2007 – 10/12/2007
PSA	588536	5684523	17/09/2007 – 10/12/2007
N entrance (PSA HNN)	588536	5684523	20/02/2008 – 28/04/2008

S entrance (DB Ports)	588767	5684045	20/02/2008 – 28/04/2008
S middle (DB Ports)	588074	5682942	20/02/2008 – 28/04/2008
S back (DB Ports)	587760	5682449	20/02/2008 – 28/04/2008
N entrance (PSA HNN)	588536	5684523	14/05/2008 – 26/09/2008
S entrance (DB Ports)	588767	5684045	14/05/2008 – 26/09/2008
S middle (DB Ports)	588074	5682942	14/05/2008 – 26/09/2008
S back (DB Ports)	587760	5682449	14/05/2008 – 26/09/2008
N entrance (PSA HNN)	588536	5684523	28/04/2008 – 31/03/2009
S entrance (DB Ports)	588767	5684045	28/04/2008 – 31/03/2009
S middle (DB Ports)	588074	5682942	28/04/2008 – 31/03/2009
S back (DB Ports)	587760	5682449	28/04/2008 – 31/03/2009
N entrance (PSA HNN)	588536	5684523	28/04/2008 – 31/03/2009
S entrance (DB Ports)	588767	5684045	28/04/2008 – 31/03/2009
S middle (DB Ports)	588074	5682942	28/04/2008 – 31/03/2009
S back (DB Ports)	587760	5682449	28/04/2008 – 31/03/2009

Settling velocity – INSSEV			
Location	**Easting (UTM ED 50)**	**Northing (UTM ED 50)**	**Period**
Deurganckdok CDW	588717	5684898	05/09/2006
Deurganckdok SILL	588800	5684250	06/09/2006
Deurganckdok Western quay wall	588452	5684355	07/09/2006

Density profile campaigns
5th September 2007
16th October 2007
16th November 2007
5th December
24th January 2008
22nd February 2008
1st May 2008
5th June 2008
11th August 2008
26th August 2008
11th September 2008
20th October 2008
6th November 2008
30th January 2009
12th March 2009
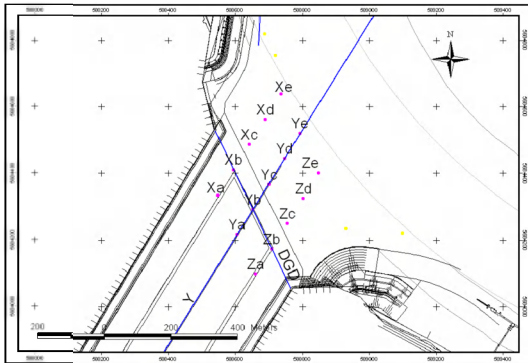
Through tide SiltProfiler measurements – Entrance Deurganckdok
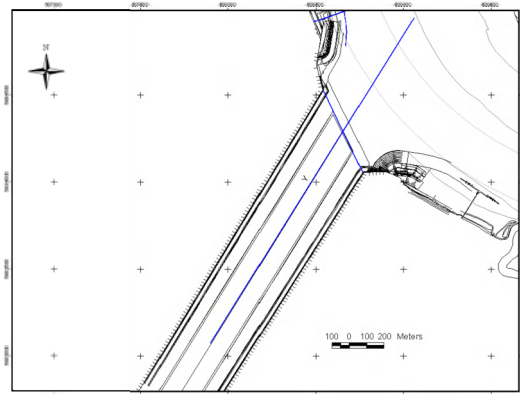
Through tide Salinity measurements – Deurganckdok (transect Y)
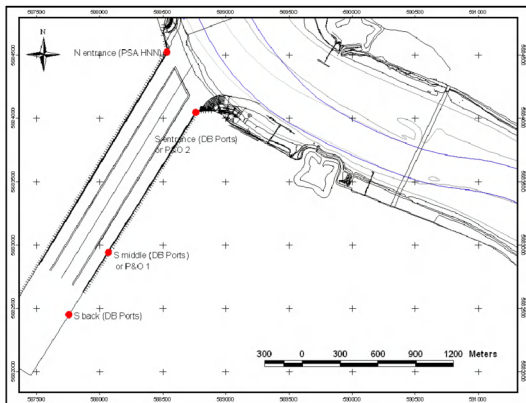
Long term salinity measurements Deurganckdok
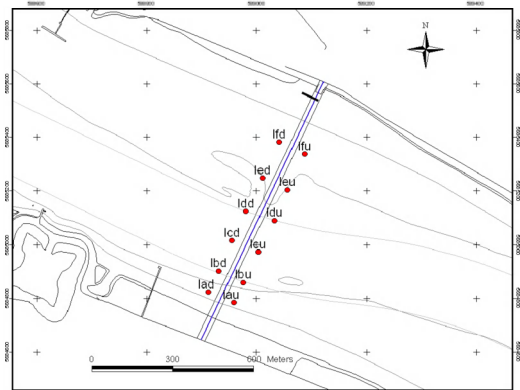
Through tide ADCP & SiltProfiler measurements – Upstream Deurganckdok (transect I)
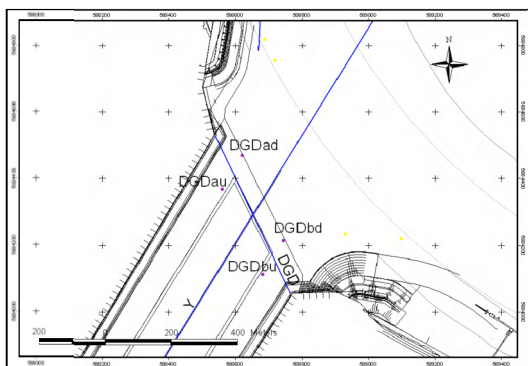
Through tide ADCP measurements – Entrance Deurganckdok (transect DGD)
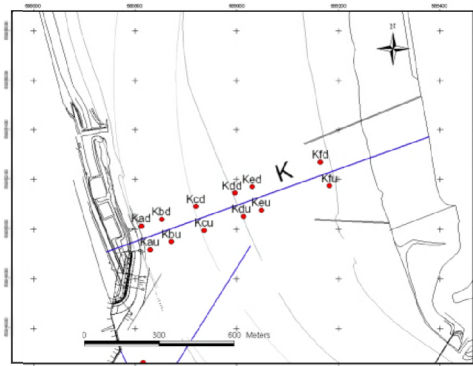
Through tide ADCP & SiltProfiler measurements – Downstream Deurganckdok (Transect K)
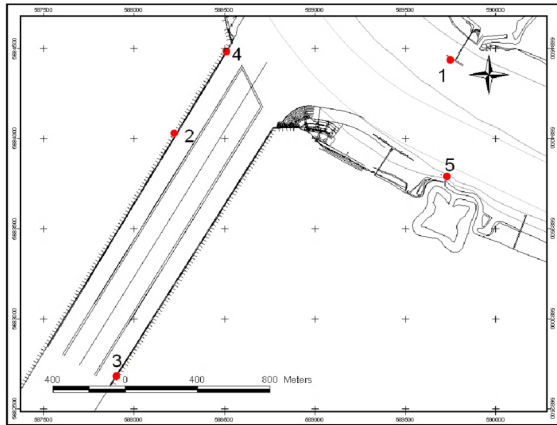
Calibration measurements – 10/09/2008
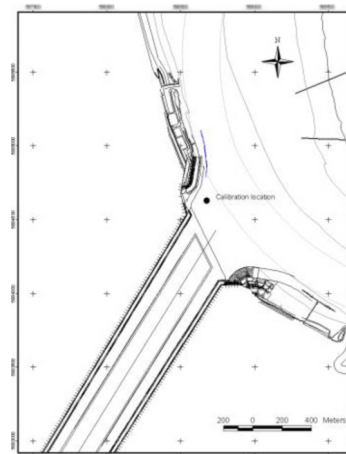
*Calibration measurements –
04/02/2008 & 05/02/2008*
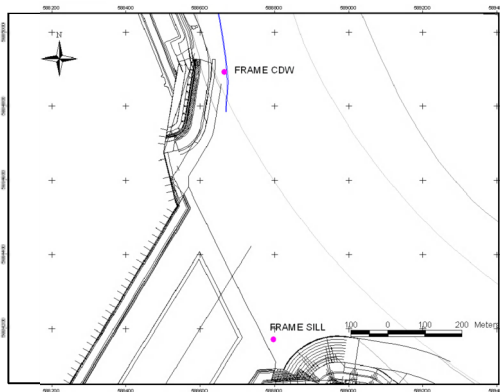
Near bed continuous monitoring
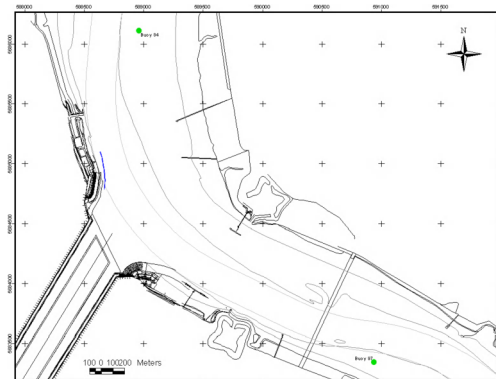
Long term measurements in the Lower Sea Scheldt

APPENDIX B.   HYDRAULIC PARAMETERS

Residual flow velocities, maximum flow velocities, and harmonic analysis of flow velocity profiles and water levels. Top left: maximum flow velocity in ebb and in flood direction, and the flow velocity of the combined semi-diurnal components. Top right: residual flow magnitude (see lower right for direction of residual flow). Lower left: flow velocity profile of N2, M2, S2, and the sum of the quarter diurnals (3MS4, MN4, M4 and MS4). Lower right: direction of the M2 and M4 component of the flow velocity and the residual flow velocity, and properties of water level (text): the pahse of M2 ($\phi_{h,M2}$) and M4 ($\phi_{h,M4}$), the phase lag between M2 and M4 ($\phi_{h,M4} - 2\phi_{h,M2}$), the ratio of the flood period and the ebb period (T_{flood}/T_{ebb}), and the ratio of the high water period and the low water period ($T_{h>hm}/ T_{h<hm}$), where $T_{h>hm}$ ($T_{h<hm}$) is defined as the period that the water levels are higher (lower) than the long-term average water levels .
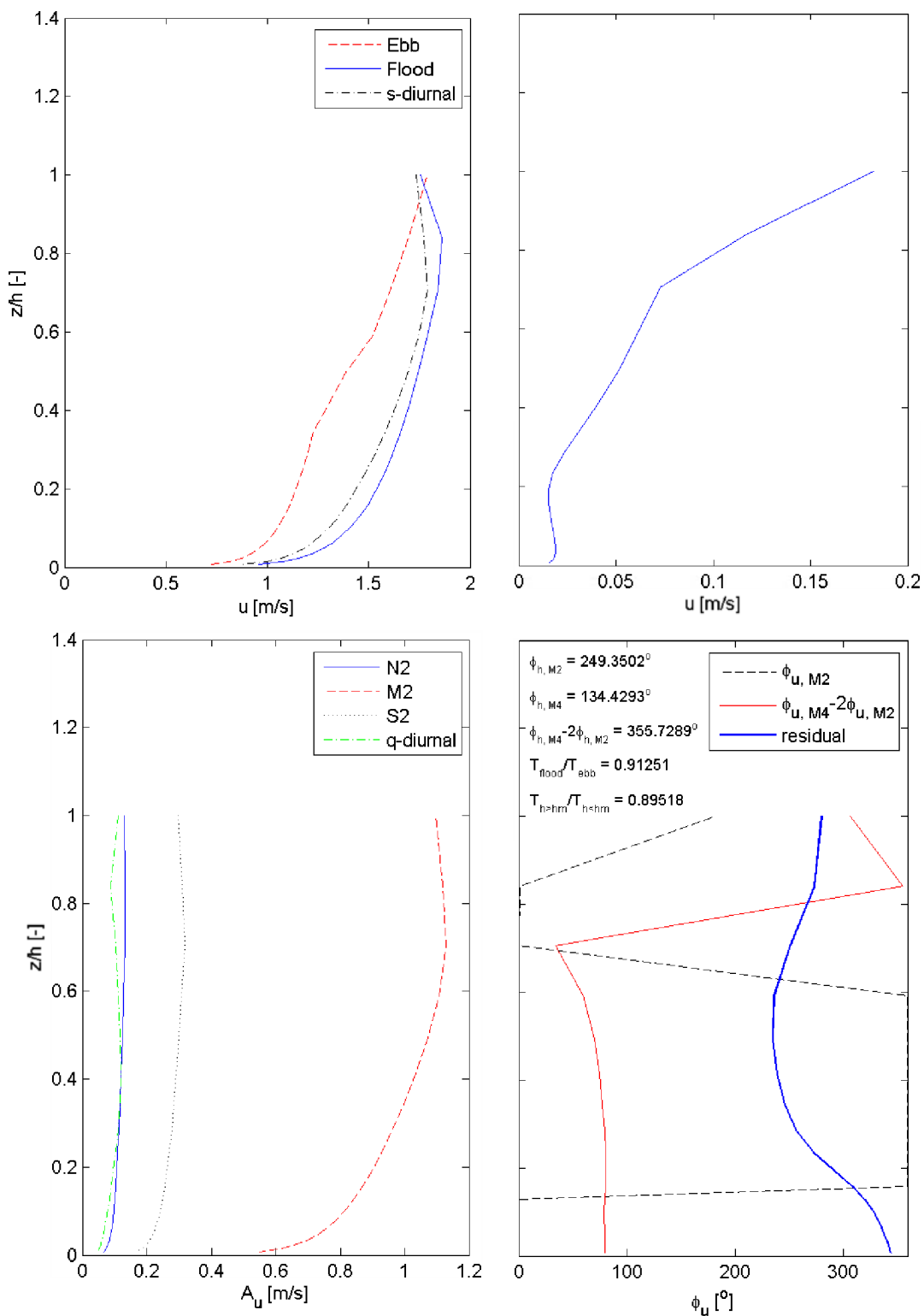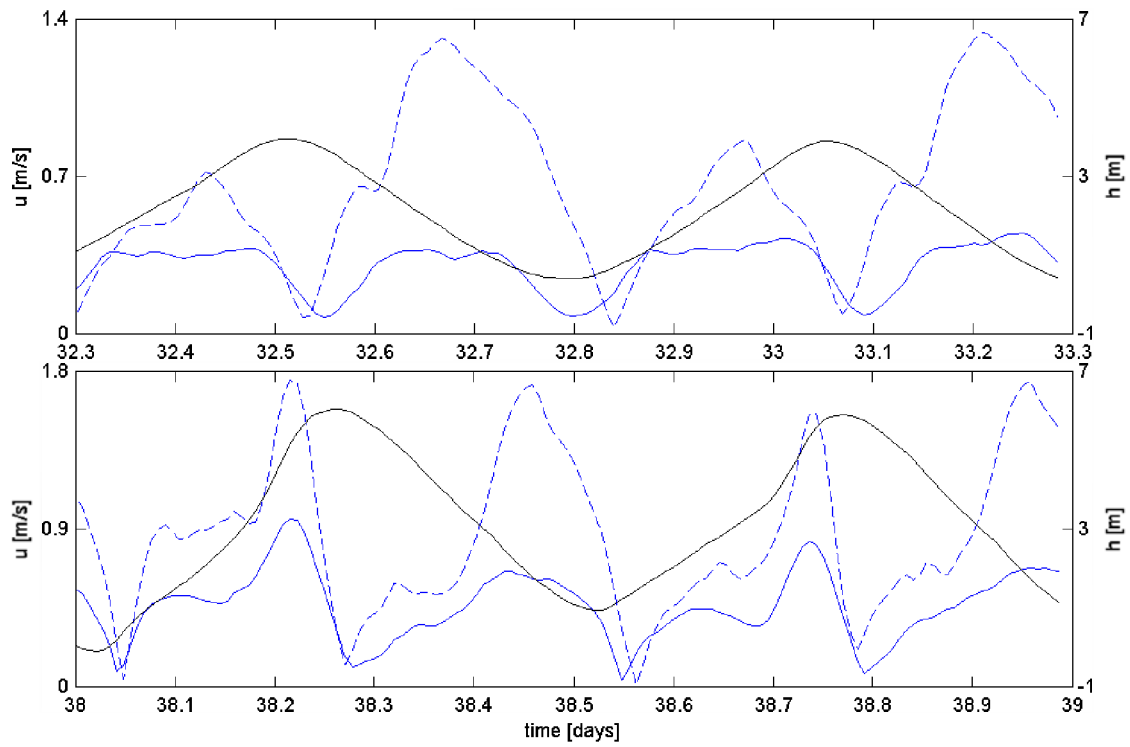
Annex-Figure B-1: Water levels and flow velocity parameters at station lvs2. See page C9 for a description
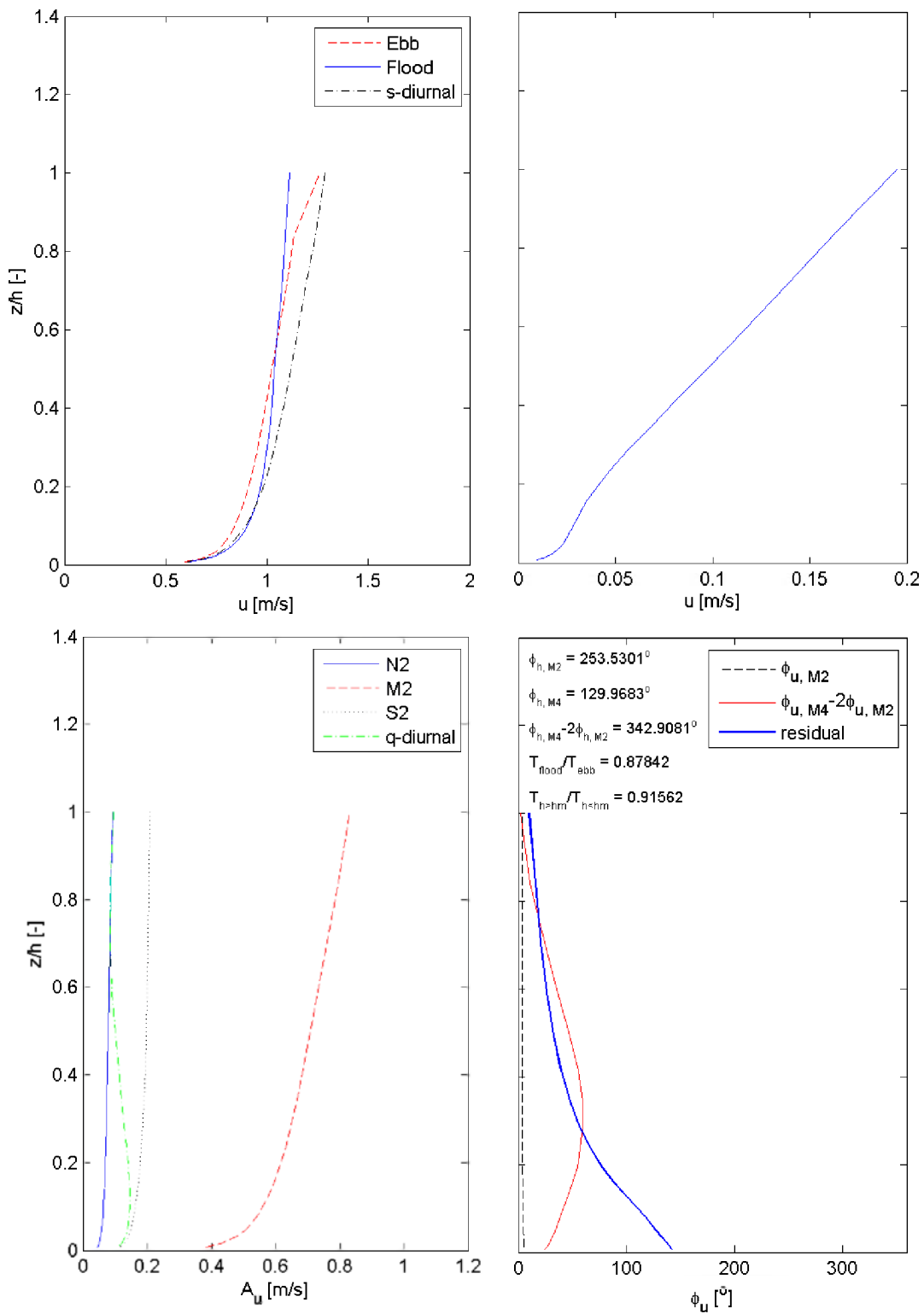
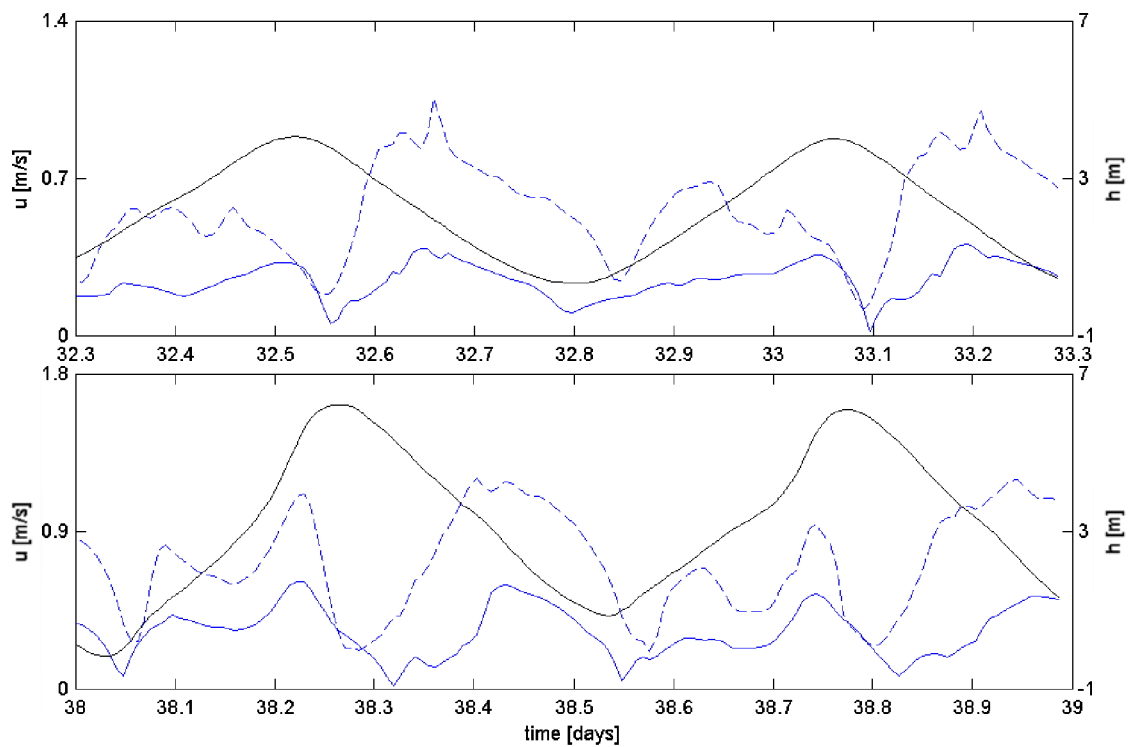*Annex-Figure B-2: Water levels and flow velocity parameters at station sta 5. See page C9 for a description*
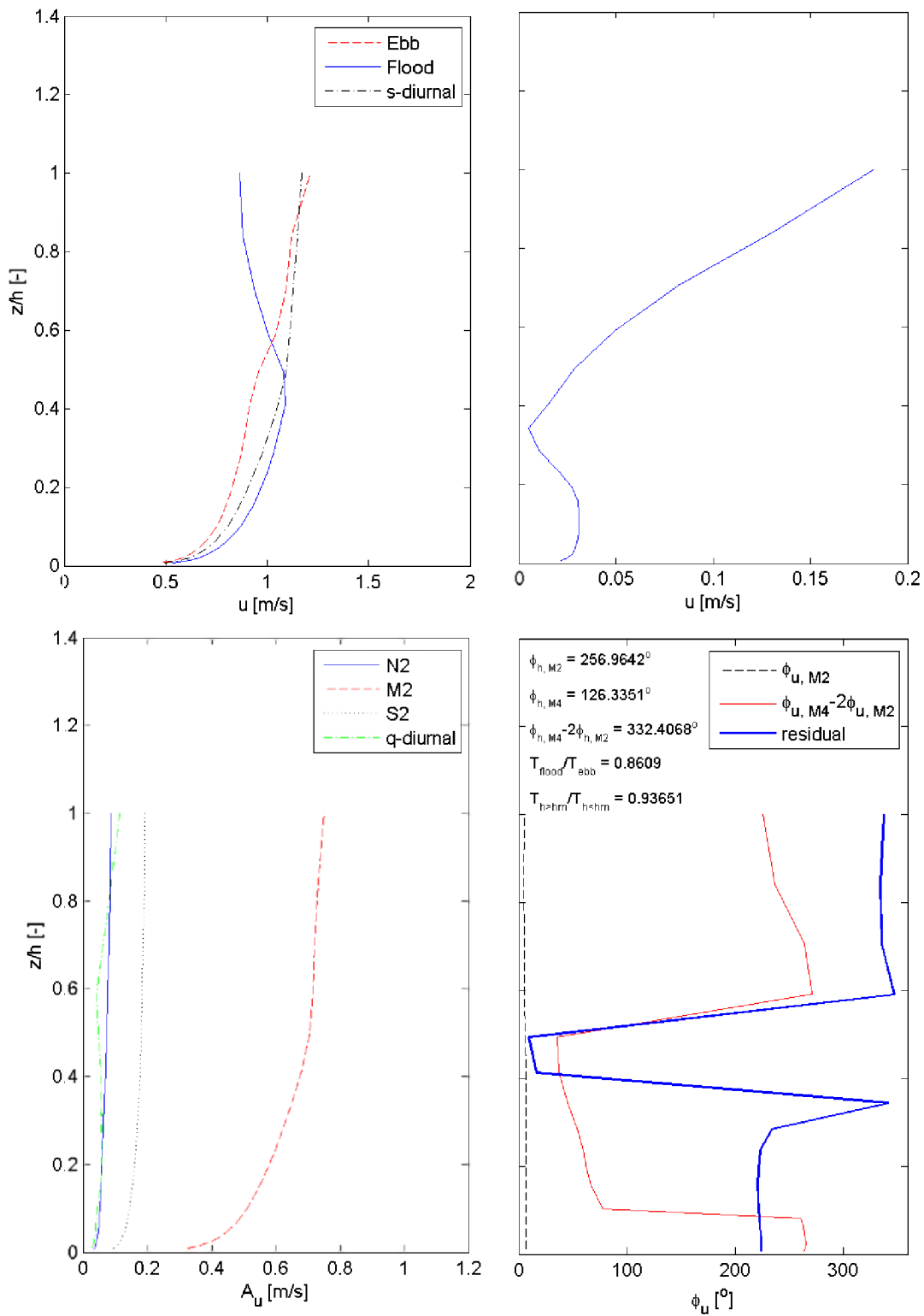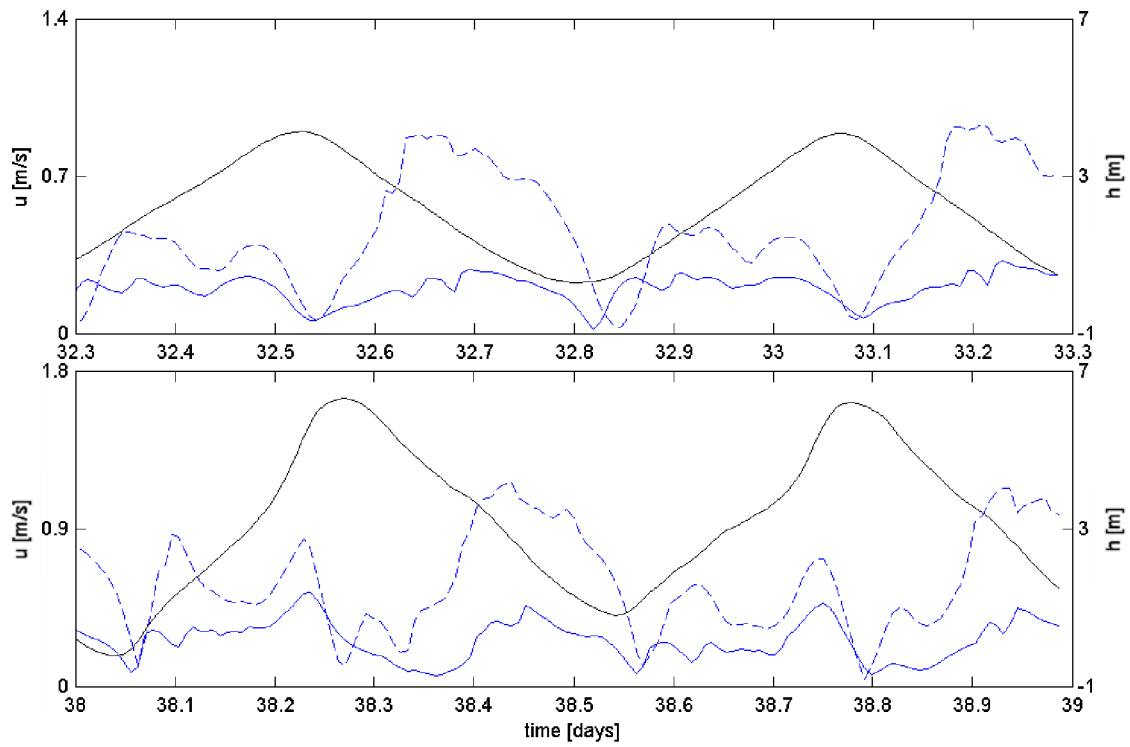
Annex-Figure B-3: Water levels and flow velocity parameters at station Leidam. See page C9 for a description
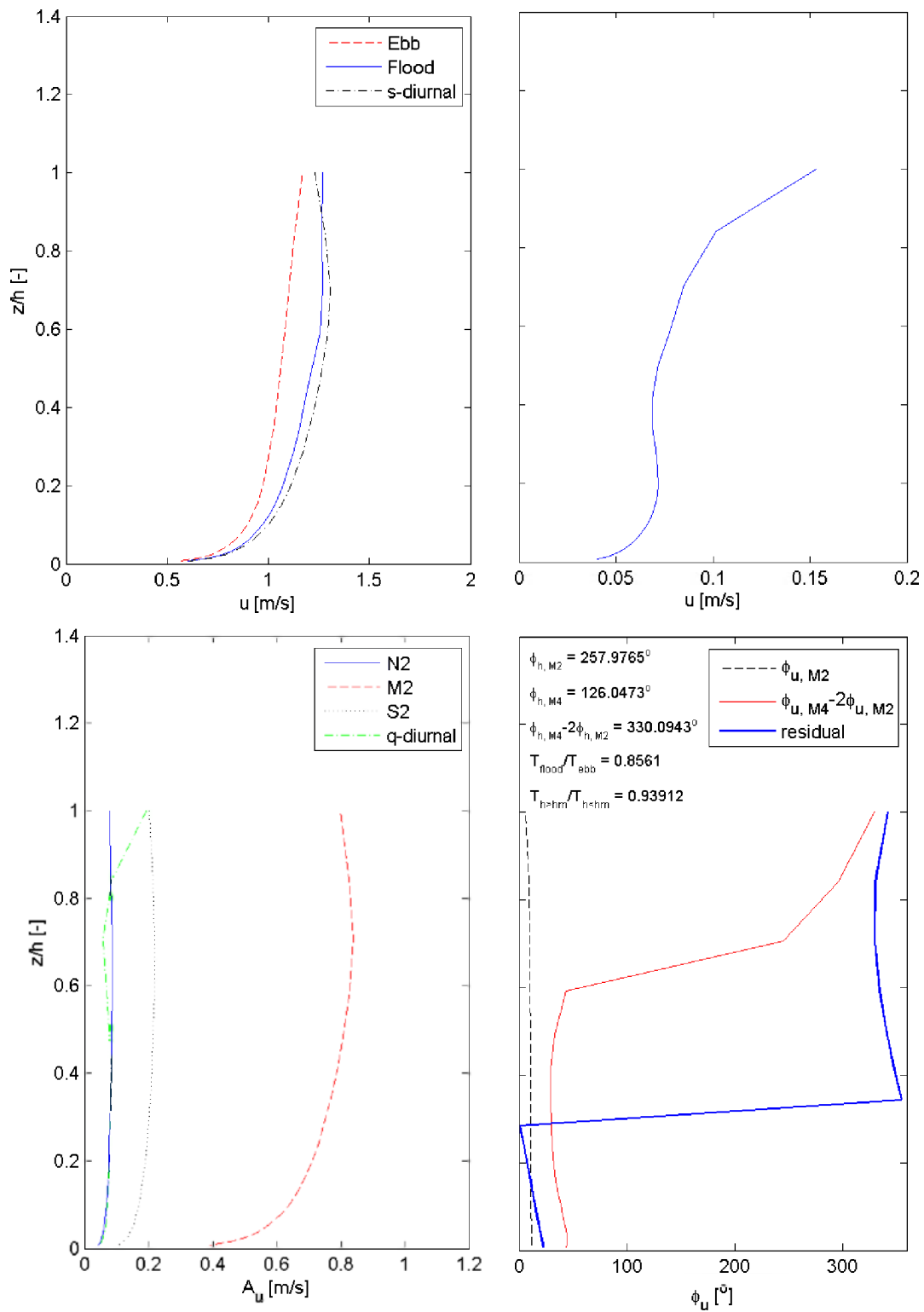
Annex-Figure B-4: Water levels and flow velocity parameters at station Ka. See page C9 for a description
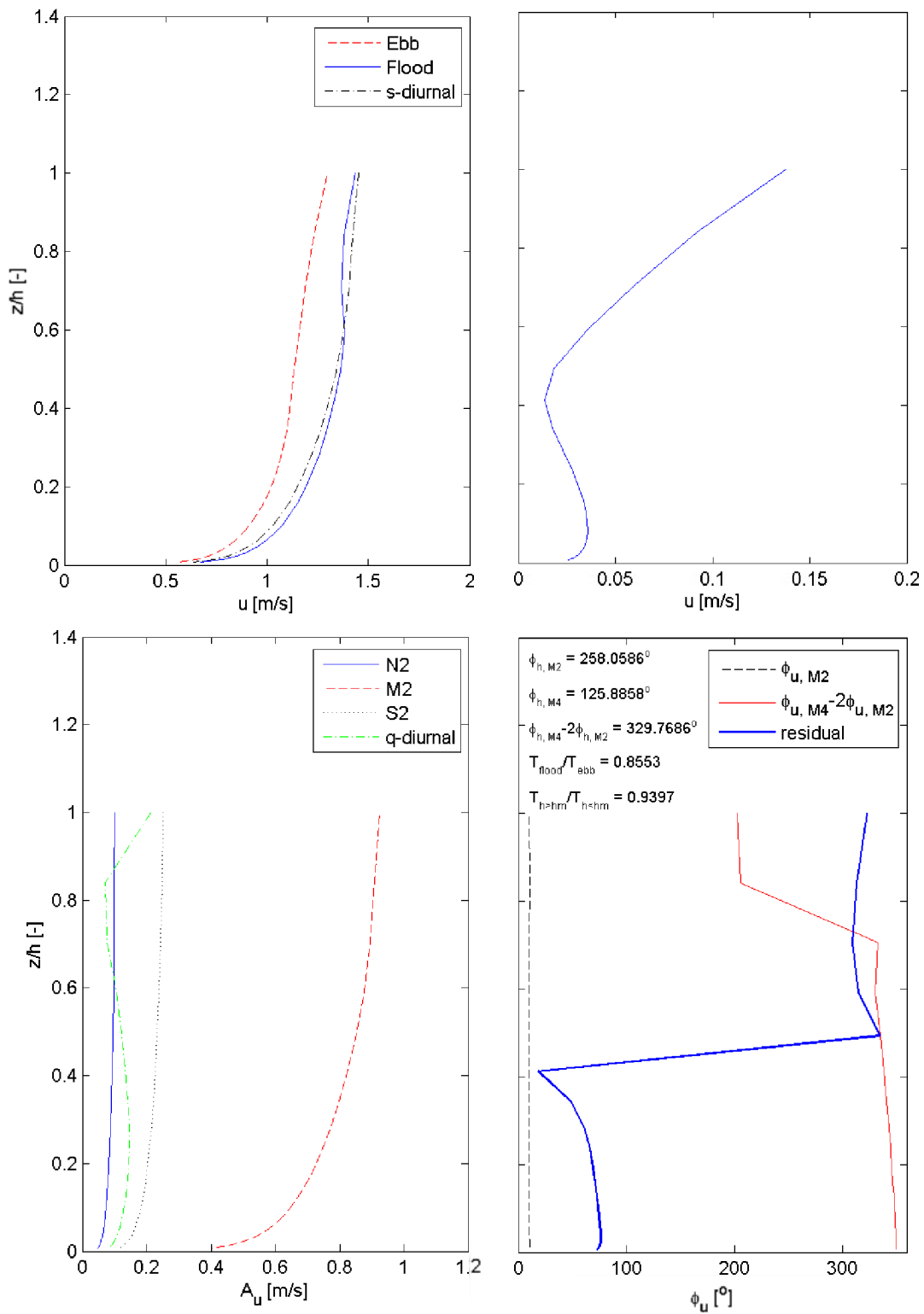
Annex-Figure B-5: Water levels and flow velocity parameters at station Kb. See page C9 for a description
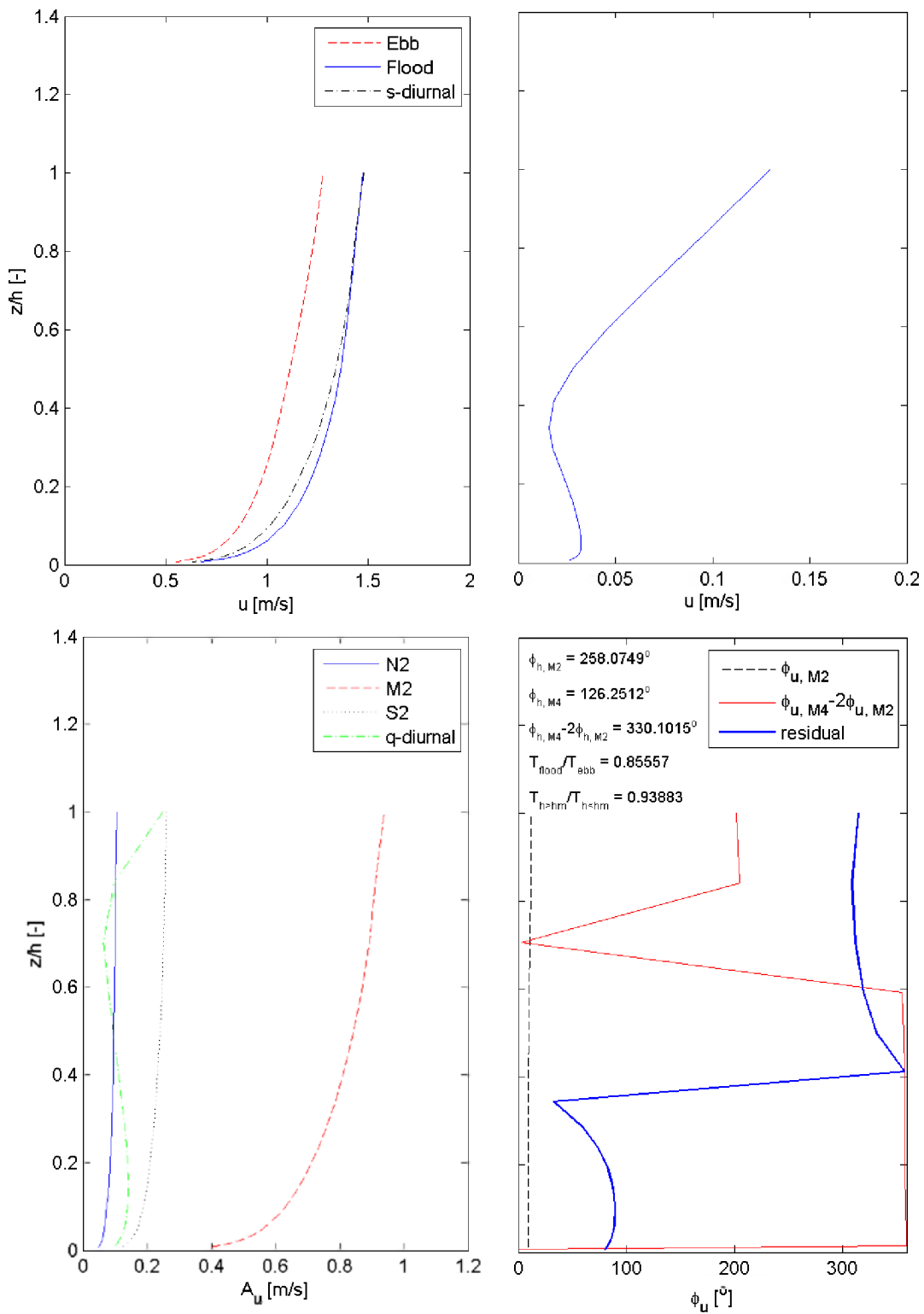
Annex-Figure B-6: Water levels and flow velocity parameters at station Kc. See page C9 for a description
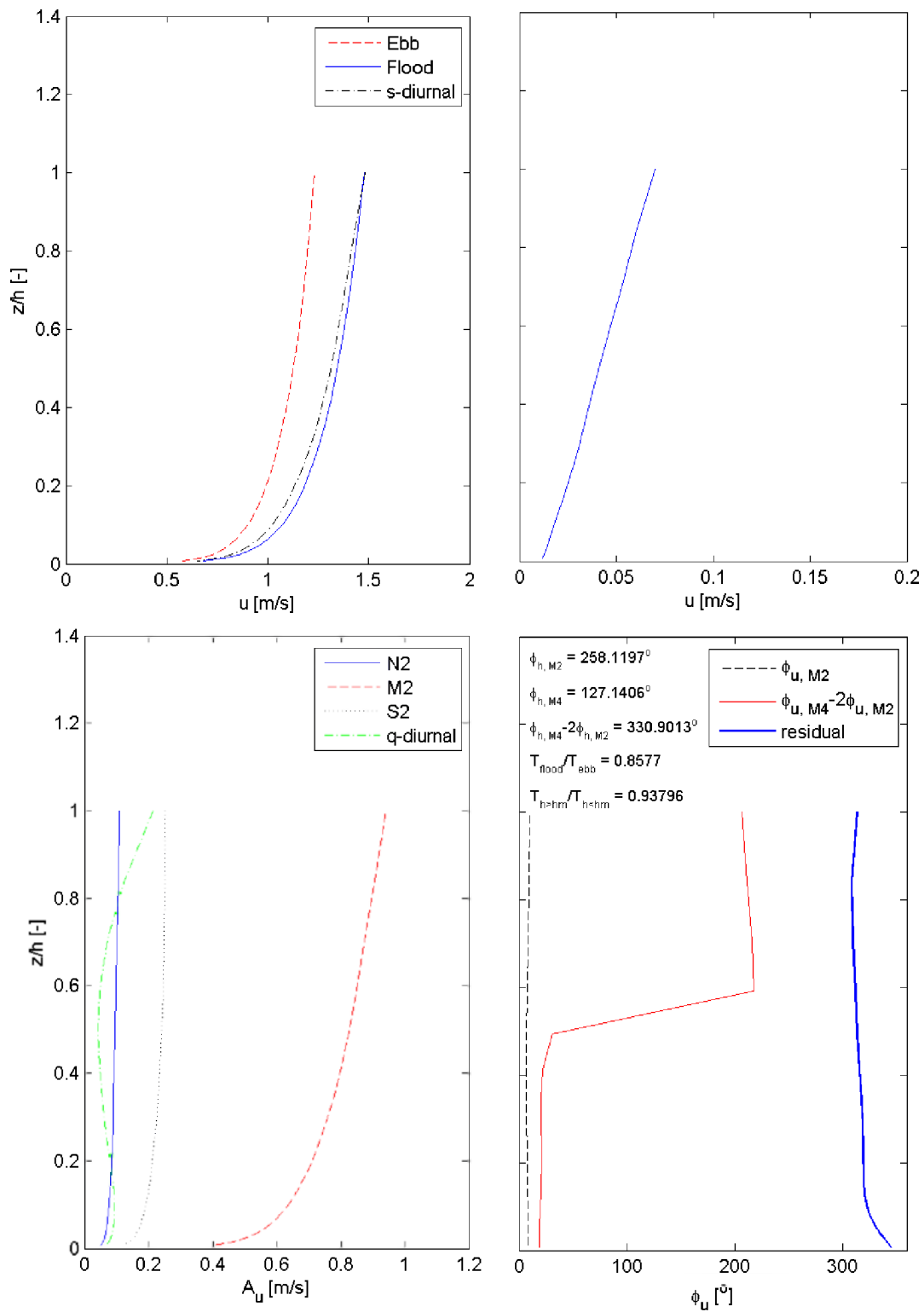
Annex-Figure B-7: Water levels and flow velocity parameters at station Kd. See page C9 for a description
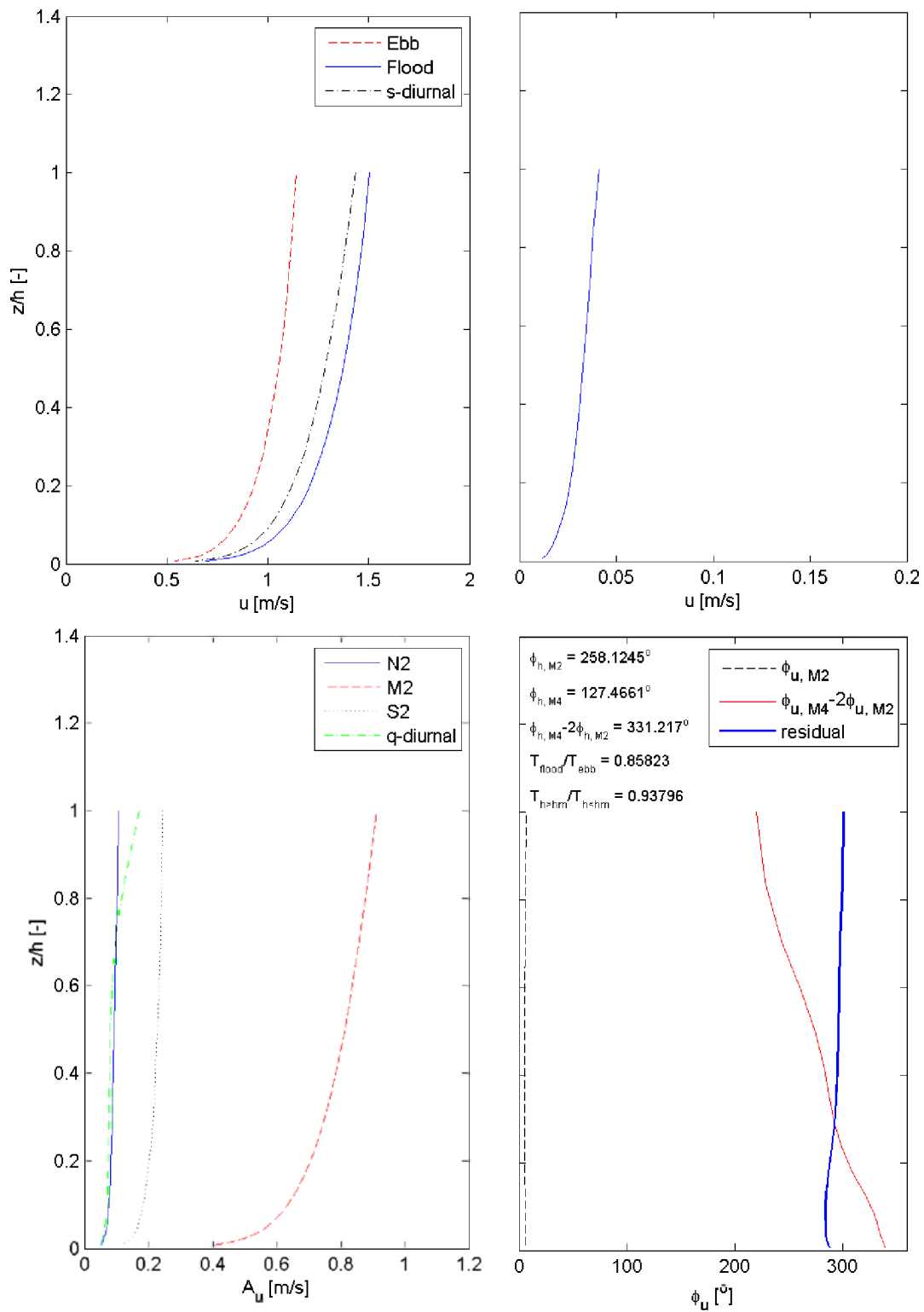
Annex-Figure B-8: Water levels and flow velocity parameters at station Ke. See page C9 for a description
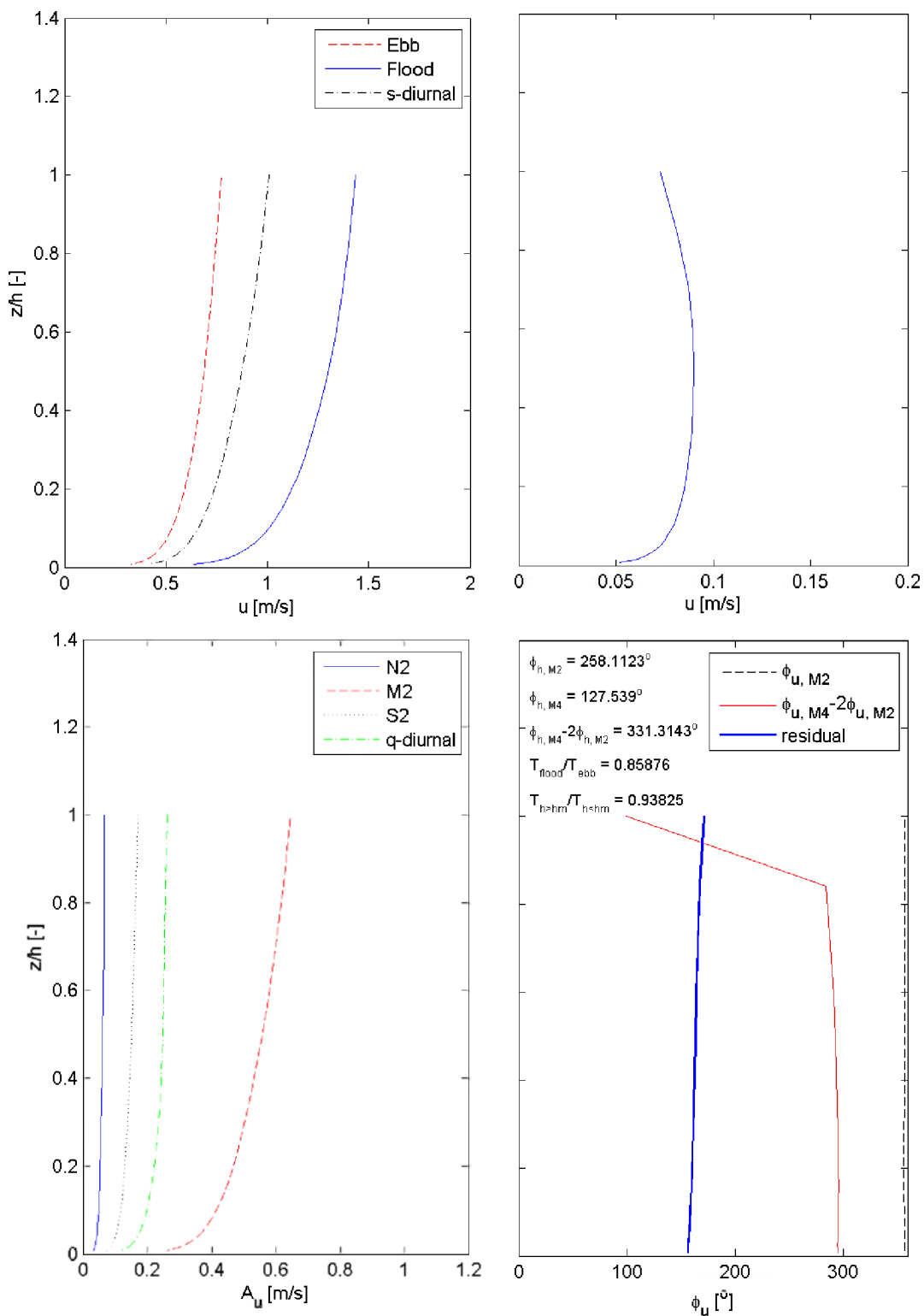
Annex-Figure B-9: Water levels and flow velocity parameters at station Kf. See page C9 for a description
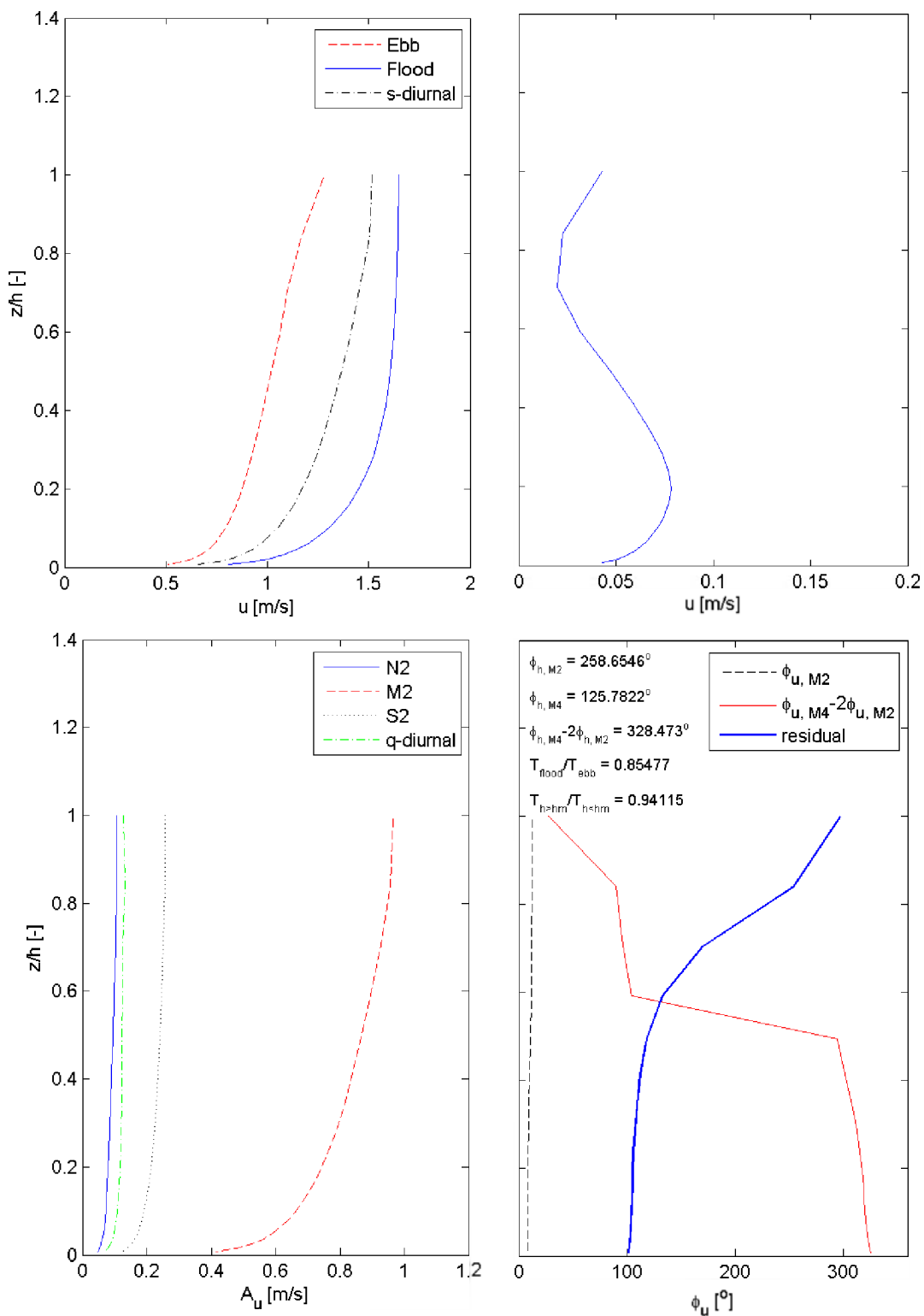
Annex-Figure B-10: Water levels and flow velocity parameters at station Liefkenshoek. See page C9 for a description
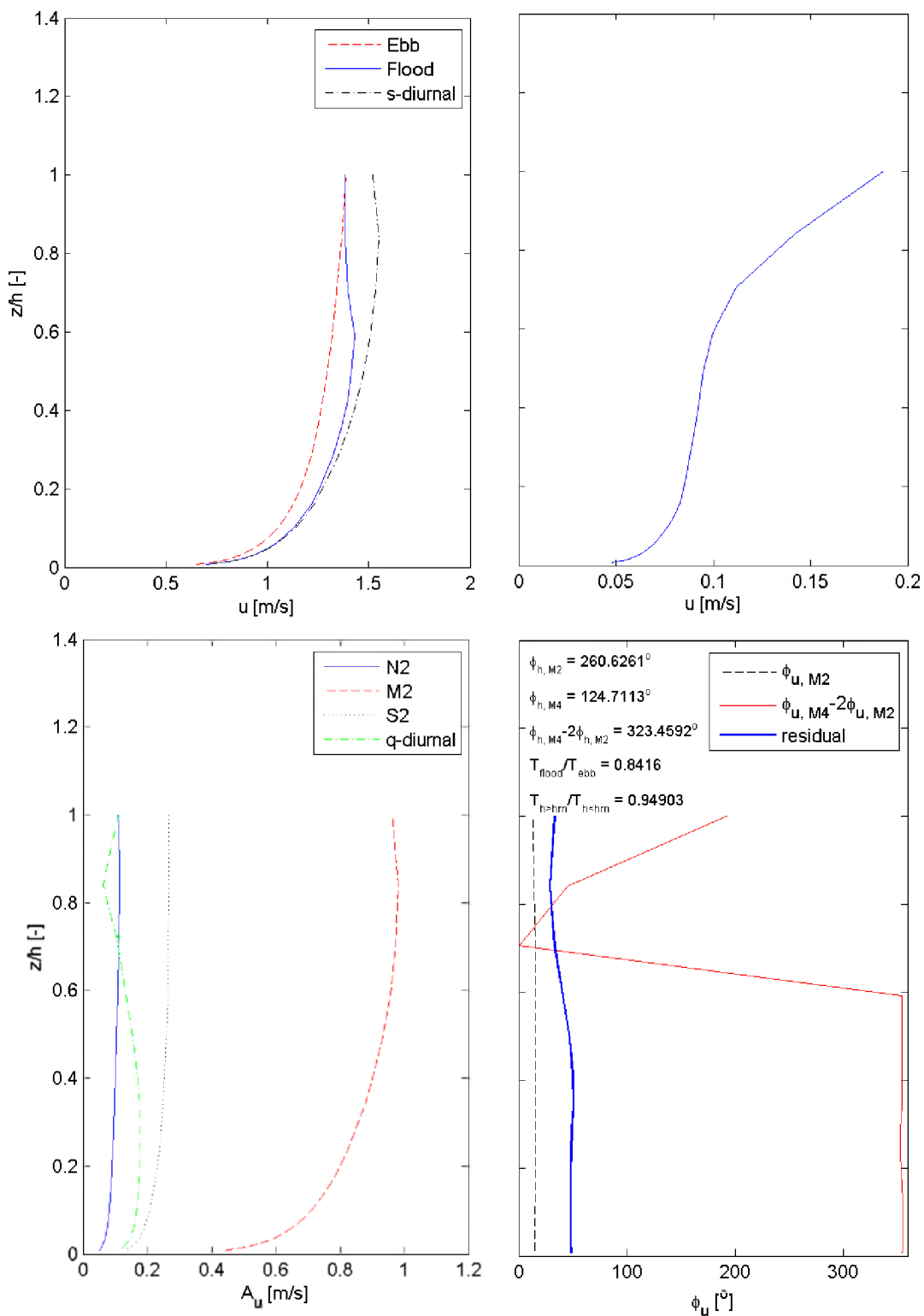
Annex-Figure B-11: Water levels and flow velocity parameters at station Kallo. See page C9 for a description
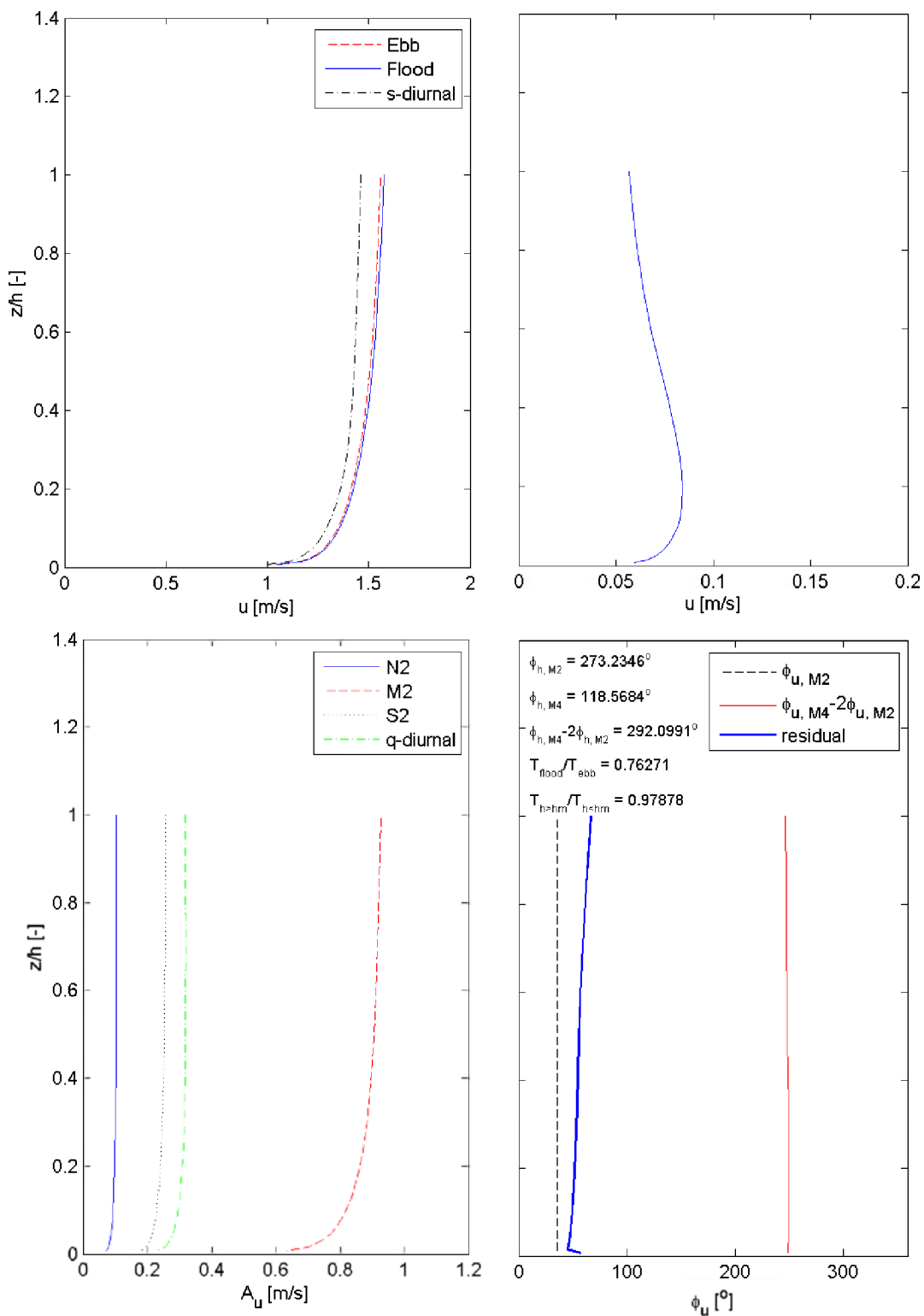
Annex-Figure B-12: Water levels and flow velocity parameters at station Schelle. See page C9 for a description

APPENDIX C.   TIMESERIES

Timeseries of surface flow velocity (blue, dashed line), near bed flow velocity (blue, solid line), and water level (black line), during neap tide (top) and spring tide (bottom).
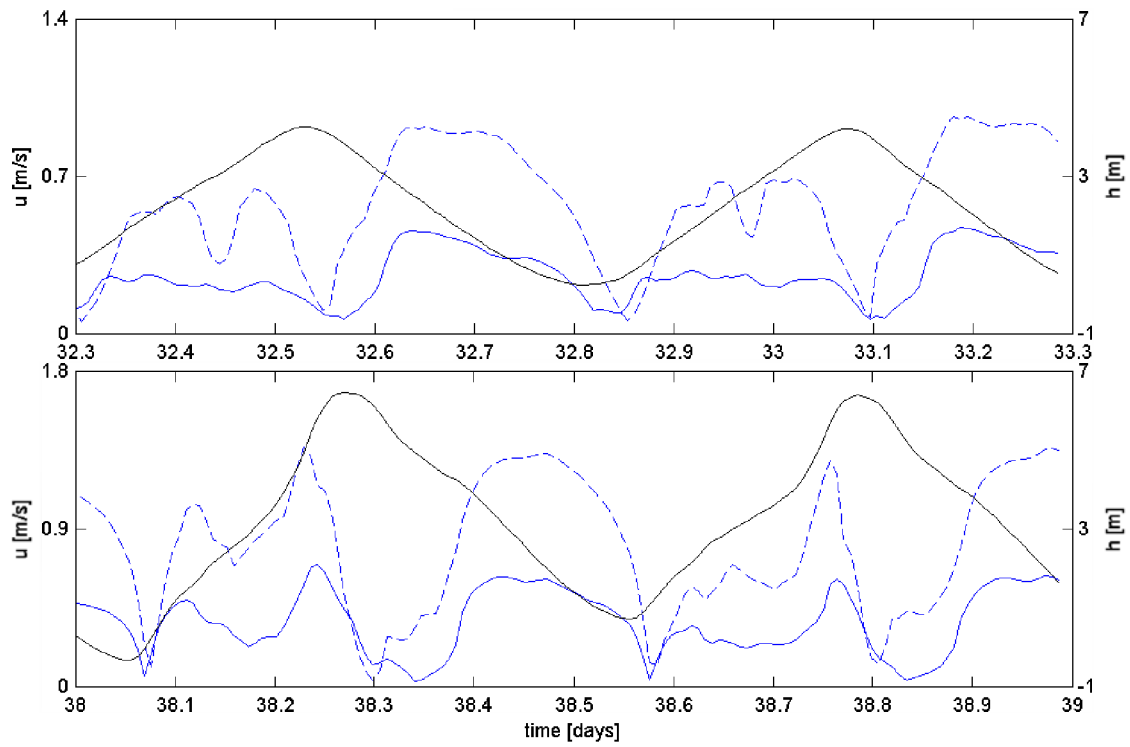
Annex-Figure C-1: Water levels and flow velocity at station lvs2.

Annex-Figure C-2: Water levels and flow velocity at station sta 5

Annex-Figure C-3: Water levels and flow velocity at station Leidam
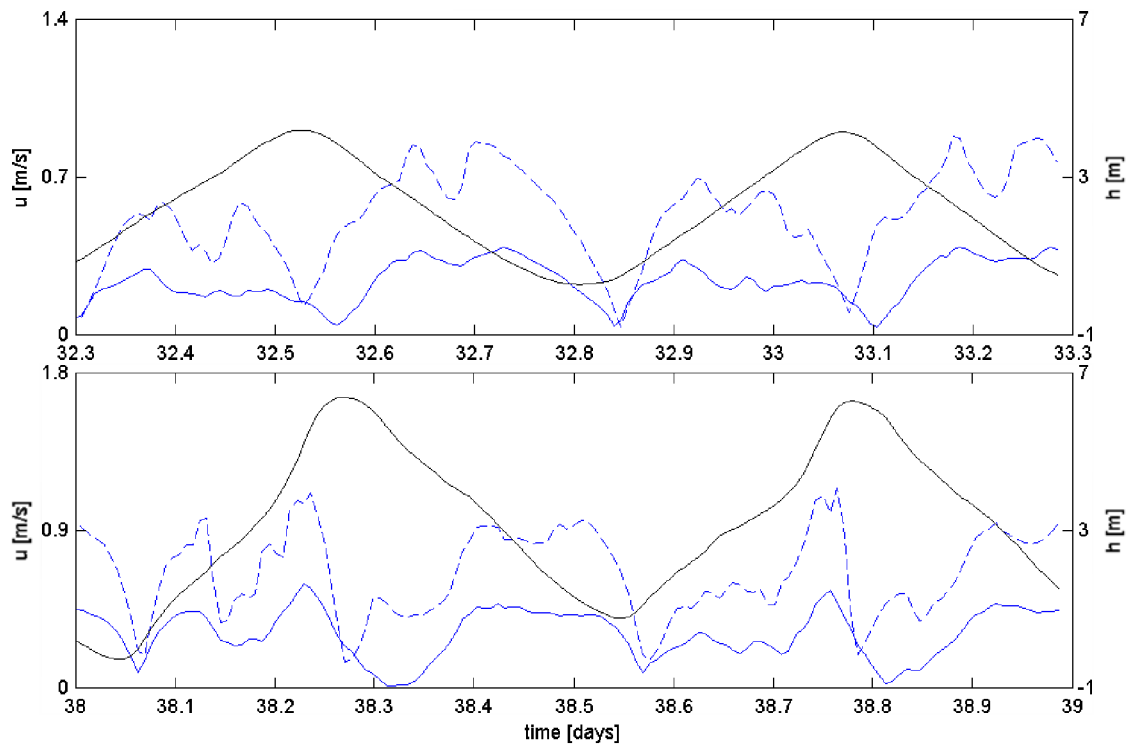
Annex-Figure C-4: Water levels and flow velocity at station Ka
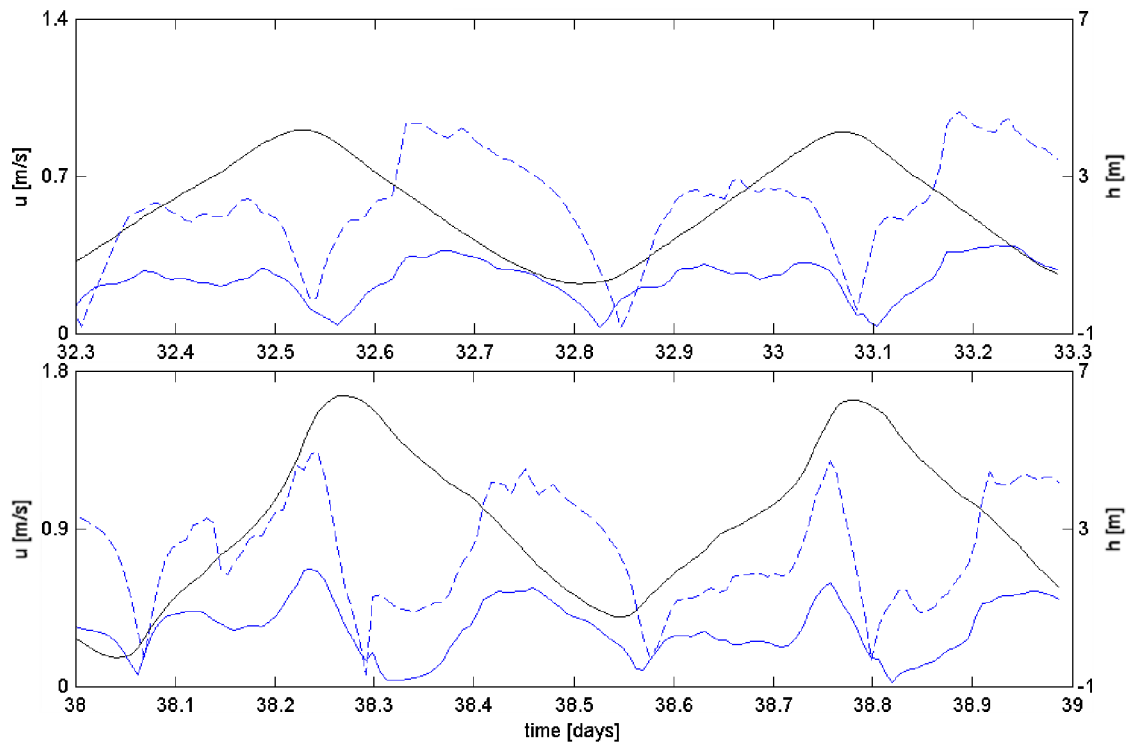
Annex-Figure C-5: Water levels and flow velocity at station Kb
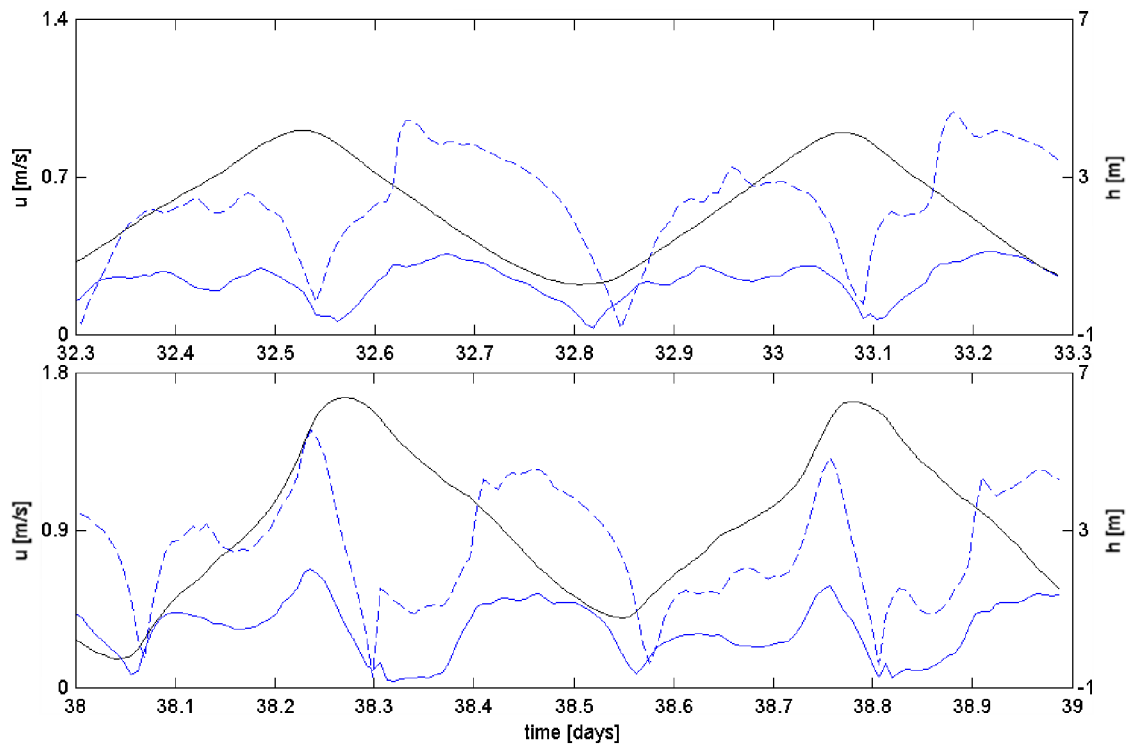
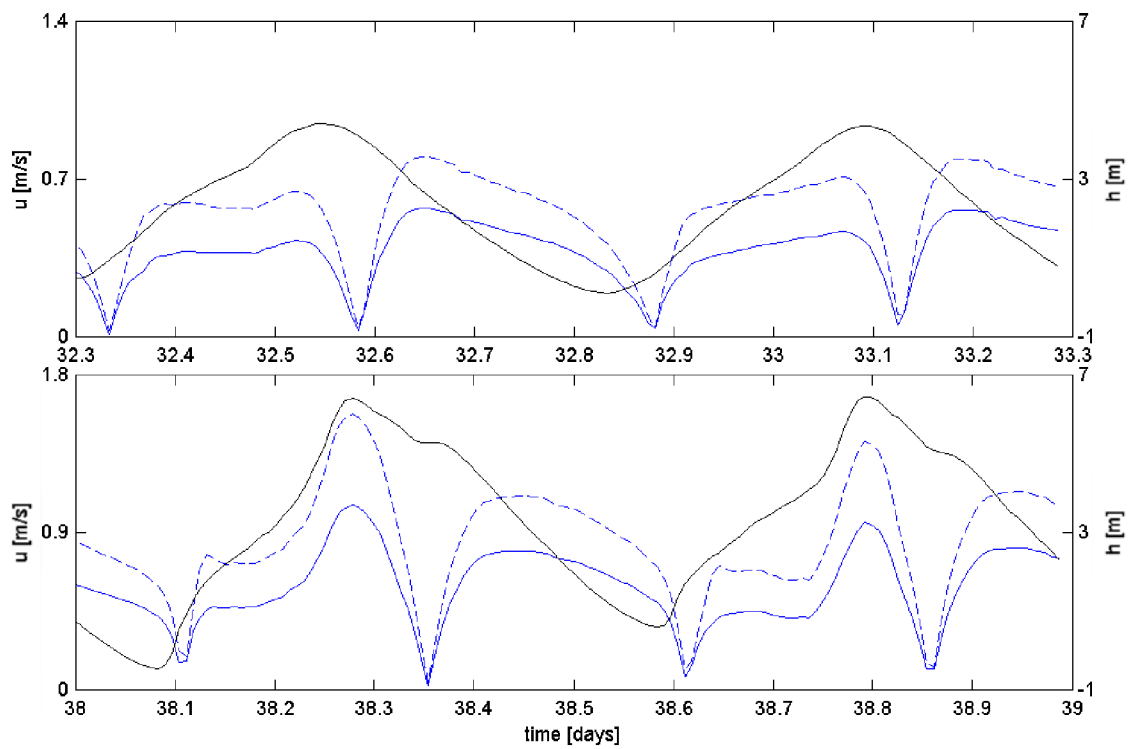*Annex-Figure C-6: Water levels and flow velocity at station Kc*
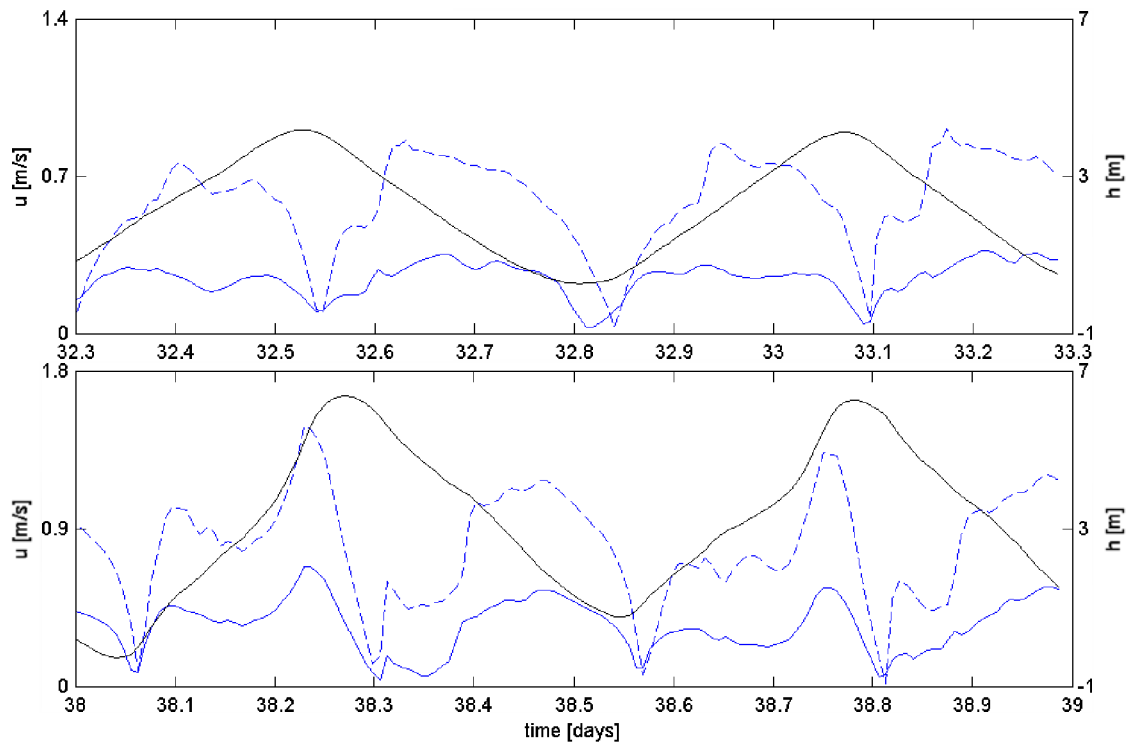
Annex-Figure C-7: Water levels and flow velocity at station Kd
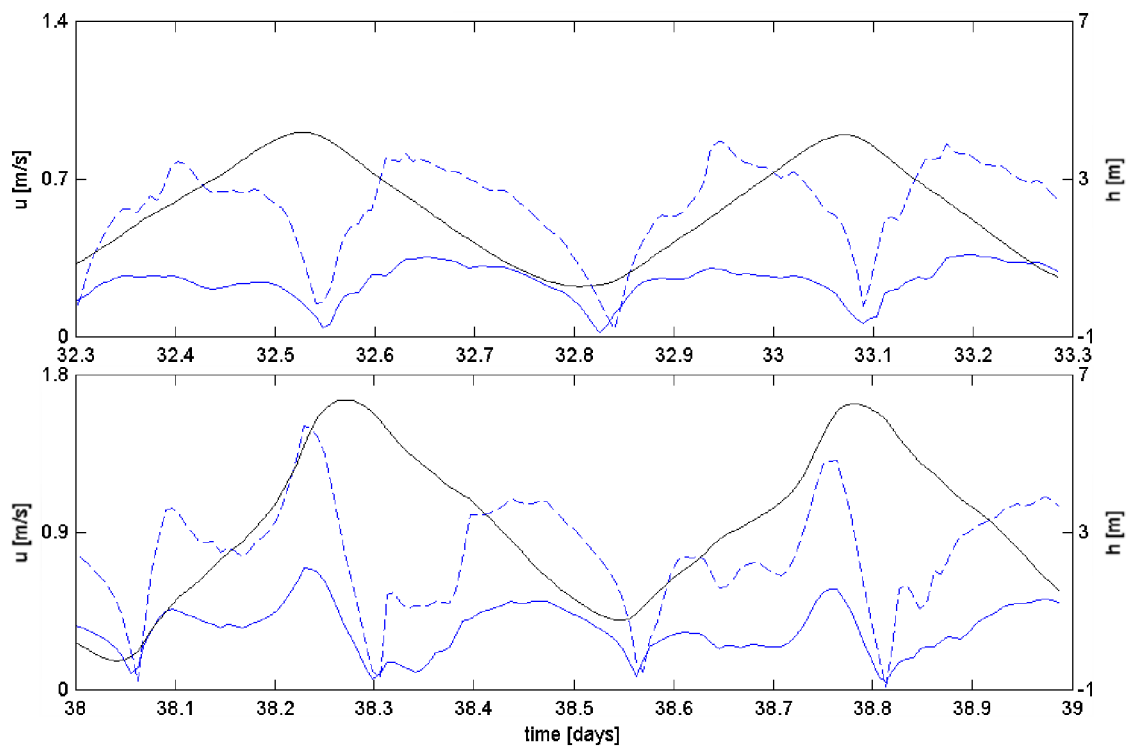
Annex-Figure C-8: Water levels and flow velocity at station Ke
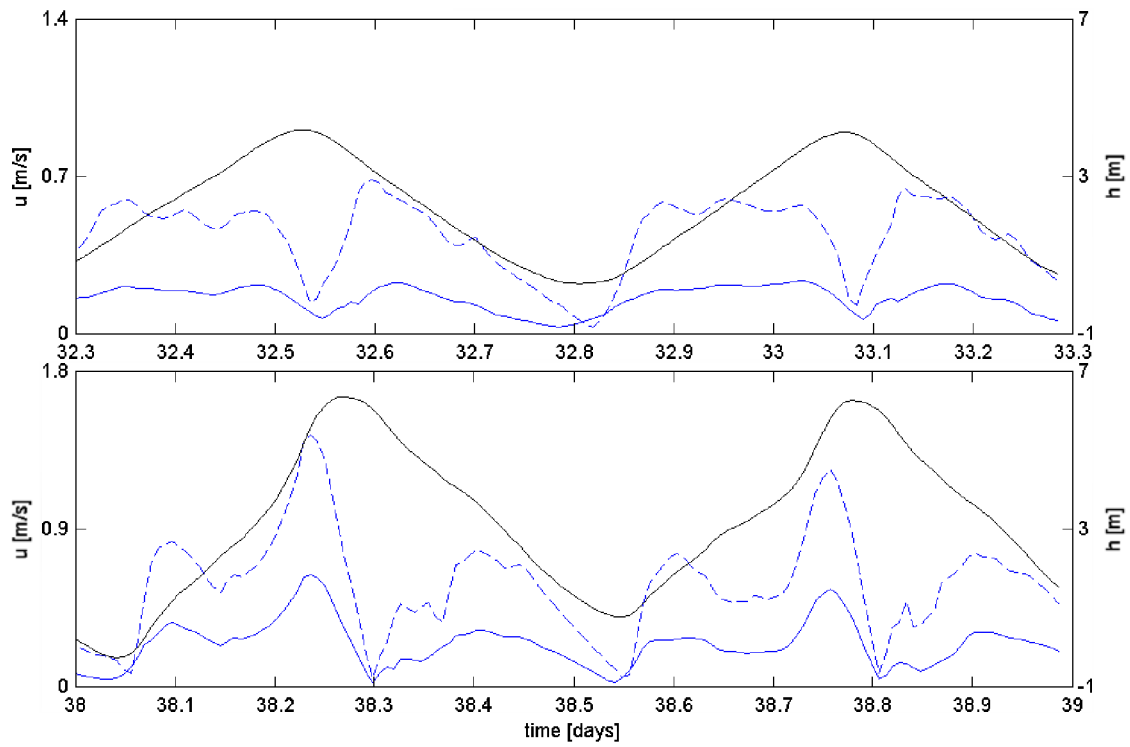
Annex-Figure C-9: Water levels and flow velocity at station Kf
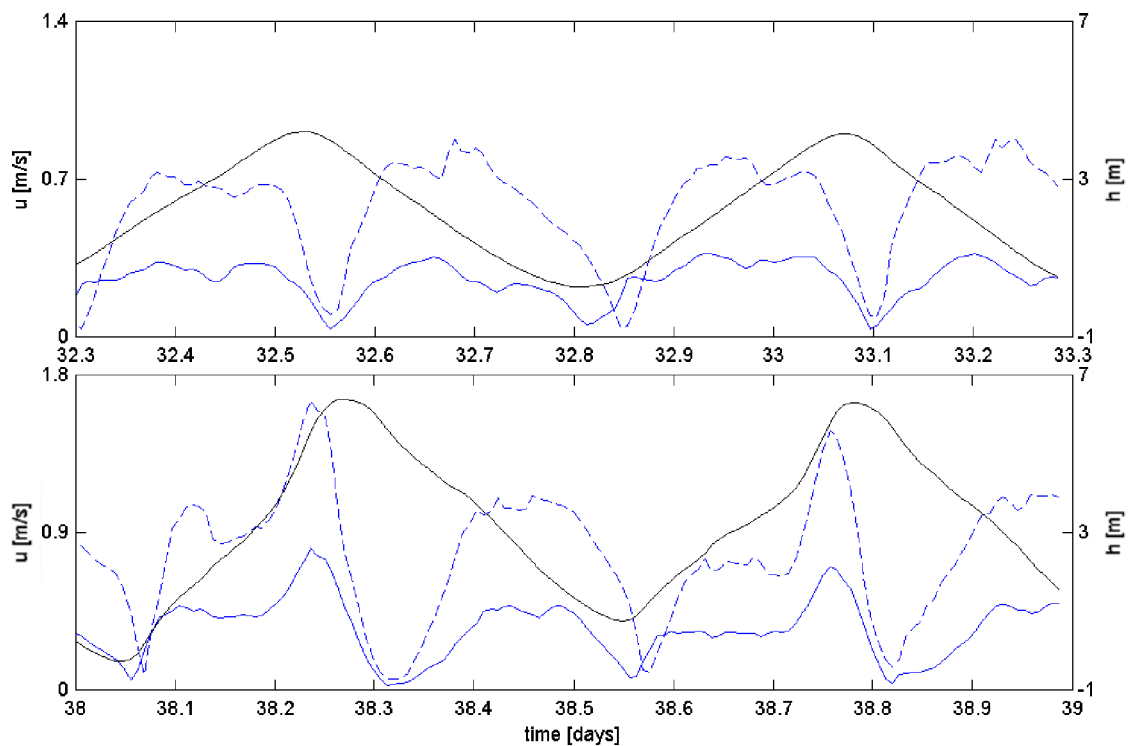
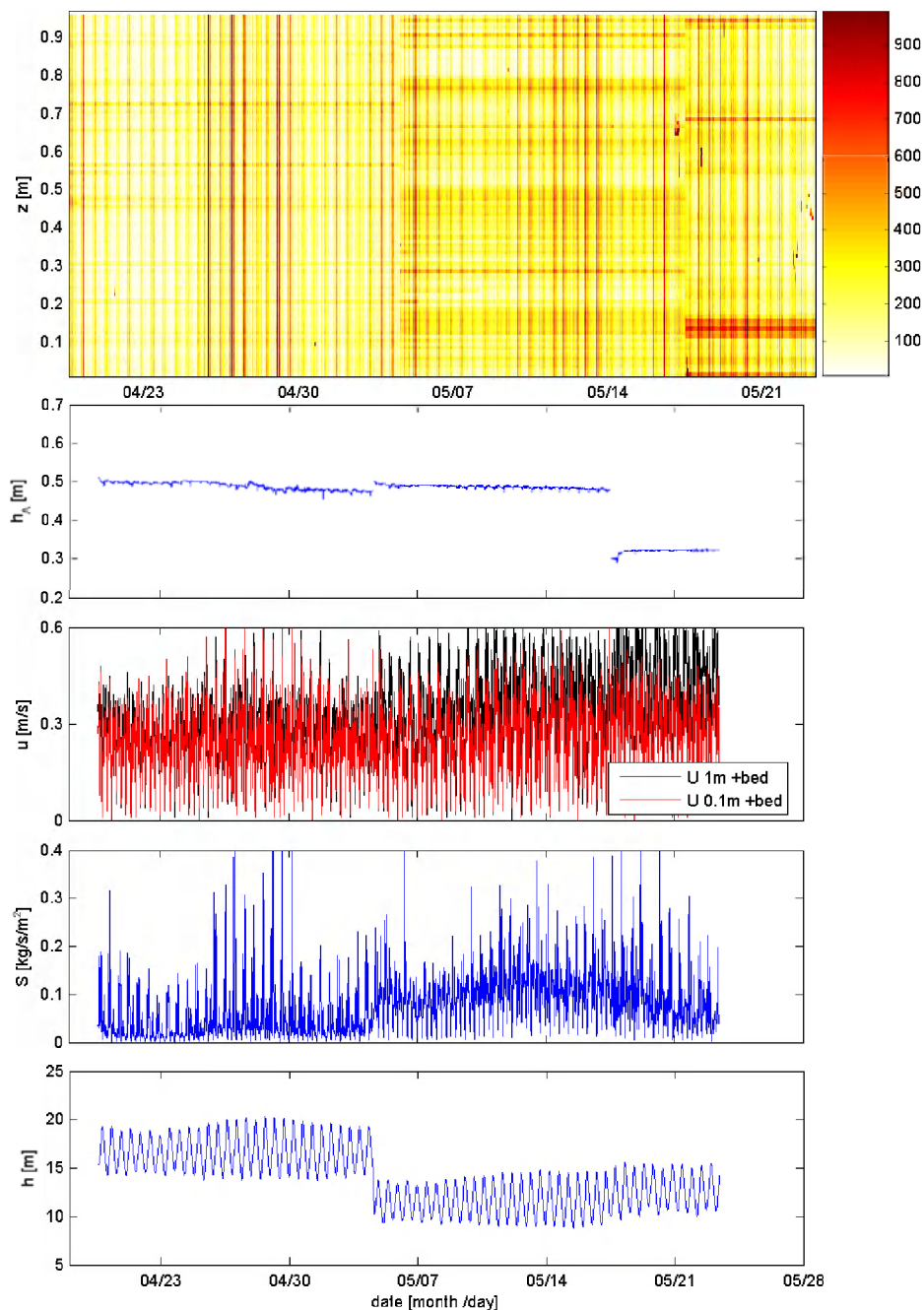*Annex-Figure C-10: Water levels and flow velocity at station Liefkenshoek*

Annex-Figure C-11: Water levels and flow velocity at station Kallo


Annex-Figure C-12: Water levels and flow velocity at station Schelle

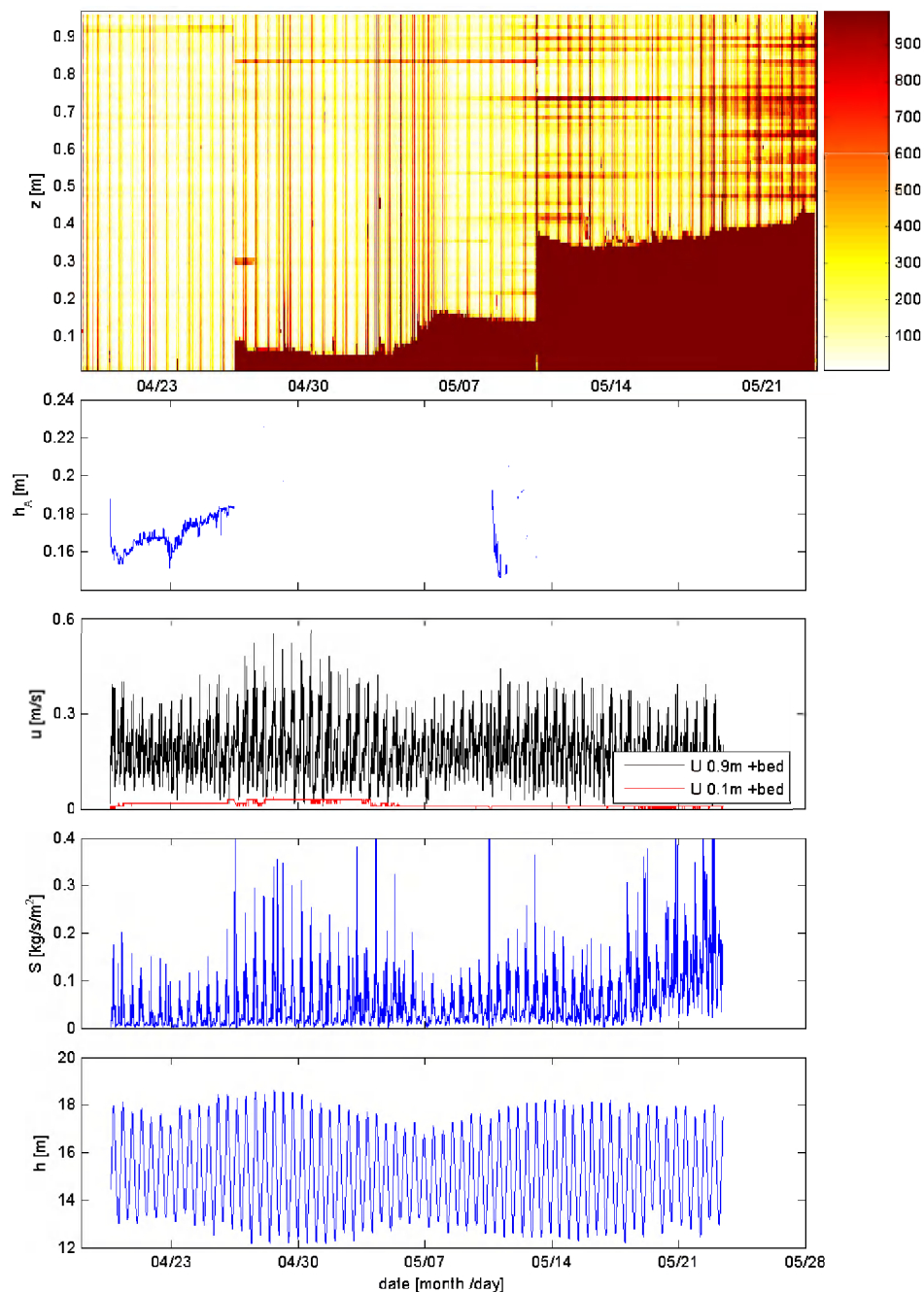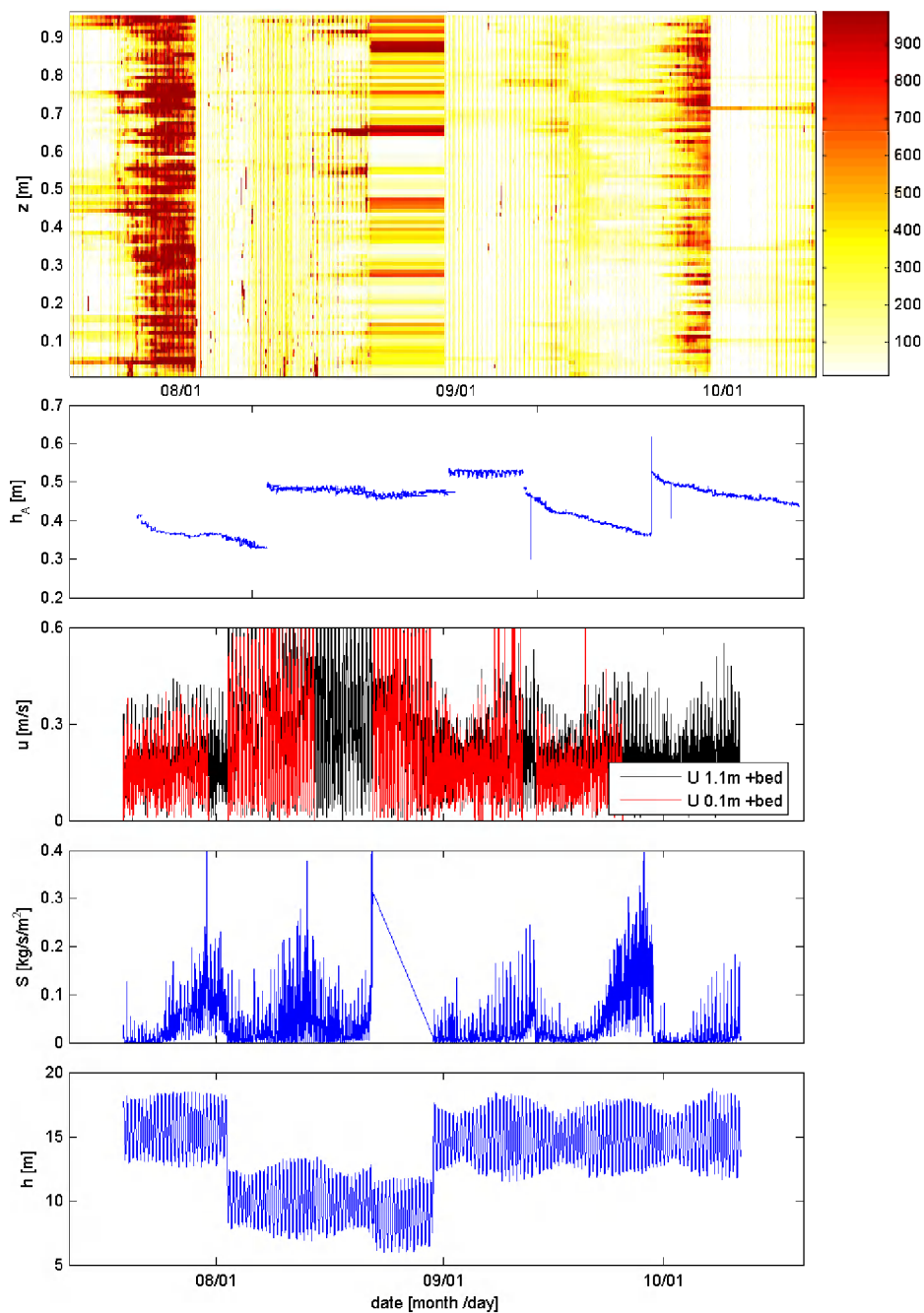# APPENDIX D. TIME-SERIES CDW FRAME AND SILL FRAME OF THE DEURGANCKDOK CAMPAIGNS (2006-2007)

Annex-Figure D-1: Sediment concentration (mg/l), measured with the ARGUS (top), depth hA measured with the ALTUS (average of 4 beams, with a positive hA being erosion), flow velocity measured with both currents meters, sediment flux S computed with the upper EMF and ARGUS sensor at 90 cm above the bed, and the local water depth h, at the location of the future CDW, downstream of the Deurganckdok, in April and May 2006.
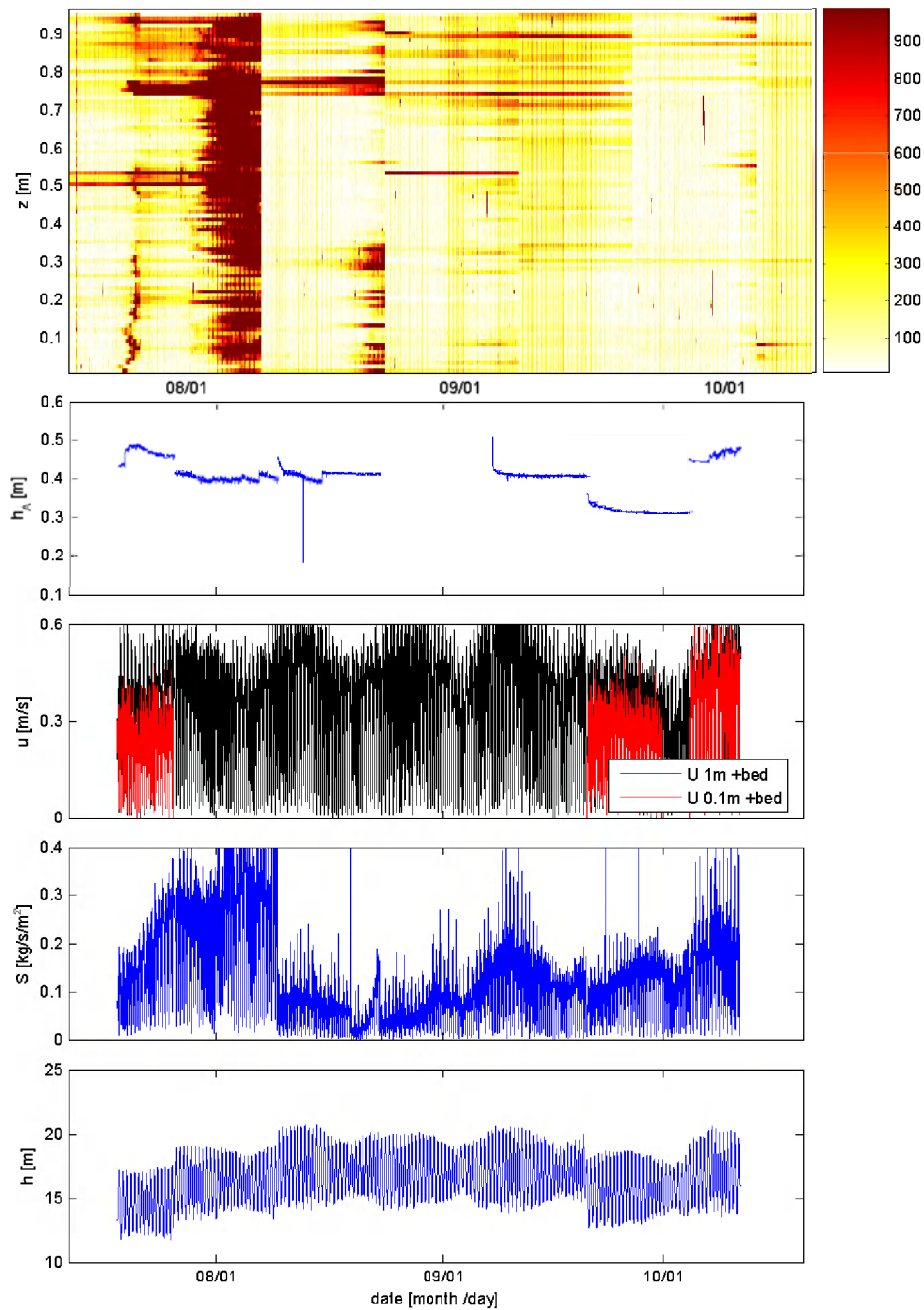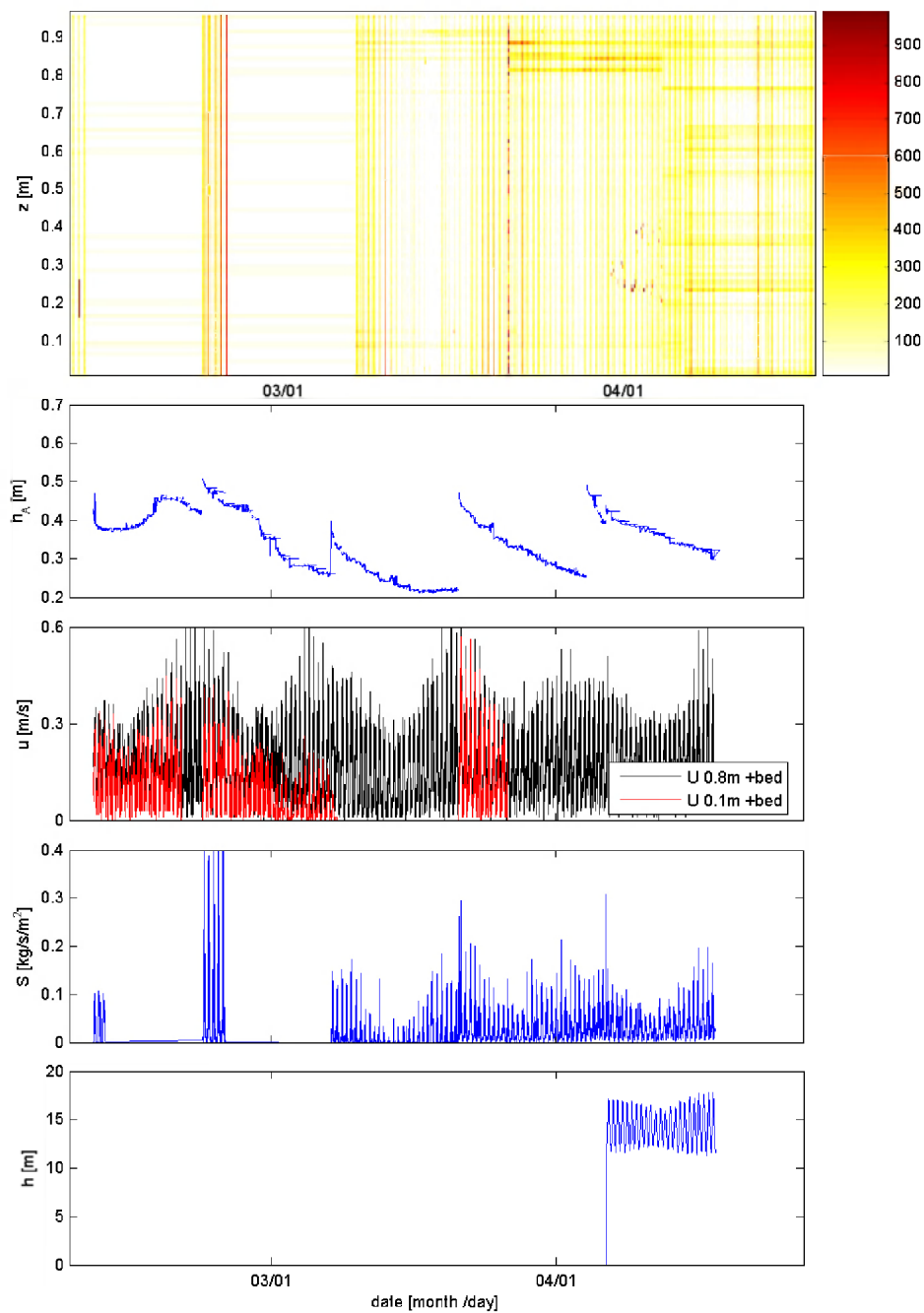
Annex-Figure D-2: Sediment concentration (mg/l), measured with the ARGUS (top), depth hA measured with the ALTUS (average of 4 beams, with a positive hA being erosion), flow velocity measured with both currents meters, sediment flux S computed with the upper EMF and ARGUS sensor at 90 cm above the bed, at the location of the future CDW, downstream of the Deurganckdok, from July through October 2006.

Annex-Figure D-3: Sediment concentration (mg/l), measured with the ARGUS (top), depth hA measured with the ALTUS (average of 4 beams, with a positive hA being erosion), flow velocity measured with both currents meters, sediment flux S computed with the upper EMF and ARGUS sensor at 90 cm above the bed, on the sill of the Deurganckdok, in April and May 2006.

Annex-Figure D-4: Sediment concentration (mg/l), measured with the ARGUS (top), depth hA measured with the ALTUS (average of 4 beams, with a positive hA being erosion), flow velocity measured with both currents meters, sediment flux S computed with the upper EMF and ARGUS sensor at 90 cm above the bed, on the sill of the Deurganckdok, from July through October 2006.

Annex-Figure D-5: Sediment concentration (mg/l), measured with the ARGUS (top), depth hA measured with the ALTUS (average of 4 beams, with a positive hA being erosion), flow velocity measured with both currents meters, sediment flux S computed with the upper EMF and ARGUS sensor at 90 cm above the bed, on the sill of the Deurganckdok, in March and April 2007.